THE DESIGN OF SEMI-SUBMERSIBLES FOR MINIMUM VERTICAL MOTION

KHIN MAUNG OO, B.E.

Submitted as a Thesis for the Degree of

Doctor of Philosophy

University of Glasgow

1974

SUMMARY

A survey is made of various semi-submersible platforms in operation and under construction. They are divided into two categories, viz. multi-hull and multi-leg, and descriptions of the current designs of platforms in each category are given. Some of single column platforms are also described.

A theoretical method for calculating the heave response of a semi-submersible platform in regular waves is described. In the calculation of the heave response it is assumed that the natural heave frequency of the platform is smaller than the frequencies of maximum wave energy encountered in practice. Thus the heave response outside the resonance region is obtained by neglecting the damping coefficient which is significant only in the resonance region.

An approximate method for calculating vertical and horizontal wave excited forces acting on both multi-hull and multi-leg platforms is described. This involves splitting up the exciting forces into the pressure, inertia and damping forces. Since the damping force is small compared to the other forces it is neglected in the calculation of heave response for frequencies outside the resonance region. But, in the resonance region, the damping force must be taken into account in the calculation. The validity of the approximations involved is checked by a number of comparisons, using the results of computer programmes developed for the different types of design, against model tests carried out in the department experiment tank and also published model tests and some full scale data. The agreement between the theory and experimental result is shown to be acceptable for design purposes.

The theoretical method is then used to investigate the effects of changing the dimensions or geometry of a multi-hull platform on the heave response. The effects of each change in dimensions are given in detail. From the results of this investigation it is concluded that the heave response can be reduced by increasing the number of vertical columns, increasing the volume ratio, increasing the displacement volume, decreasing the length and by increasing the natural heave frequency of the platform.

The theoretical method is also used to compare the heave response of a multi-hull and of a multi-leg platform with variable number of legs. From the comparison it is concluded that the heave response of the multi-leg platform is smaller than that of the multi-hull platform in the wave frequency range of 0.38 to 0.75 radian per second.

The computer printouts of some of the calculations in this thesis are given in separate folder.

CONTENTS

ACKNOWLEDGEMENTS

This thesis is based on research carried out in the Department of Naval Architecture at Glasgow University.

The author is grateful for the help and encouragement given to him by Professor J.F.C. Conn, Professor D. Faulkner and members of staff in the department, especially Mr. N.S. Miller.

The author wishes to express his gratitude to the Colombo Plan Authority for awarding a scholarship and to the Inland Water Transport Corporation (Ministry of Transport and Communication, Union of Socialist Republic of Burma) for granting a study leave.

NOMENCLATURE

A_w	waterplane area
$A(\omega)$	response amplitude operator
d	water depth
e	2.718
F_X	longitudinal wave excited force
F_Y	lateral wave excited force
F_Z	vertical wave excited force
F_o	amplitude of vertical wave excited force
g	acceleration due to gravity
J	0.635
K	wave number = $\frac{2\pi}{\lambda}$
m	mass of platform
m_z	added mass of platform
m_o	area under wave energy spectrum
N_z	equivalent damping coefficient assuming damping proportional to velocity
p	pressure
q_a	amplitude of motion
$S_w(\omega)$	wave energy spectrum
$S_q(\omega)$	motion energy spectrum
T_z	natural heave period = $\frac{2\pi}{\omega_n}$
T_w	wave period
t	time
x	longitudinal displacement
y	lateral displacement
z	vertical displacement
z_a	amplitude of heaving
∇	displacement volume
γ	ratio of actual damping to critical damping
ϵ	phase angle between motion and wave
ζ	distance from origin along ζ-axis
ζ_a	surface-wave amplitude

η distance from origin along η-axis

λ wave length

ξ distance from origin along ξ-axis

ξ, η, ζ coordinate system to describe the motion of water particles

π 3.142

ρ mass density

σ phase angle between force and wave

τ phase angle between force and motion

ϕ velocity potential

ω circular frequency of wave

ω_{max} frequency (greater than natural heave frequency) at which maximum heave response occurs

ω_n natural heave frequency

The following symbols are used for multi-hull platforms:-

b centre distance between two parallel horizontal cylinders

C_{V4} added mass coefficient for a mean aspect ratio $\frac{\pi d_2/4}{\ell_2}$

d_1 diameter of vertical column

d_2 diameter of horizontal cylinder

h_1 submerged height of vertical column

ℓ centre distance between two extreme columns on a horizontal cylinder

ℓ_2 overall length of horizontal cylinder

n number of vertical columns on each horizontal cylinder

V_1 total volume of vertical columns

V_2 total volume of horizontal cylinders

$\alpha = \frac{V_2}{V_1}$

The following symbols are used for multi-leg platforms:-

C_{V1} added mass coefficient for a mean aspect ratio $\frac{\pi R_2/2}{h_2}$

C_{V2} added mass coefficient for a mean aspect ratio $\frac{\pi R_1/2}{h_2}$

C_{V3} added mass coefficient for a mean aspect ratio $\frac{\pi R_1/2}{2(h_1+h_2)}$

h_1	submerged height of vertical column
h_2	height of caisson
n	total number of legs
R_1	radius of vertical column
R_2	radius of caisson
R_c	radius of circle passing through the centre of legs
ϕ	angle between wave direction and X-axis of platform

CHAPTER 1

VARIOUS TYPES OF SEMI-SUBMERSIBLES

1.1 Introduction

Rapid growth in world oil consumption has made the offshore oil industry speed up its offshore operations. Most predictions indicate that world consumption will increase from its present 52 million barrels per day to 100 million bpd in the early 1980's (Ref. 1.1). At present offshore oil provides 17% of total daily output and is anticipated to provide 33.3% in ten years.

The number of offshore mobile drilling rigs has increased from one in 1949 to 273 in 1973, in which 214 are in operation and 59 are under construction or planned (Ref. 1.2). Four main types of drilling rigs, viz., jack-ups, submersibles, semi-submersibles and drill ships/barges are being used world-wide for offshore drilling. Of the 214 rigs in operation, 108 (50.4%) are jack-ups, 22 (10.3%) are submersibles, 28 (13.1%) are semi-submersibles and 56 (26.2%) are drill ships/barges. The important steps in the development of each type of rig are discussed in (Ref. 1.3).

There are two significant trends in offshore drilling. The first is the move towards deeper waters. The second is the move into hostile environmental areas such as the North Sea, waters off the eastern coast of Canada, etc. As a result of these trends most of the rigs under construction are designed to be able to operate in deeper and rougher waters. In deeper waters semi-submersibles seem to be most suitable since they can be designed to have natural periods longer than the periods of waves most likely to be experienced and thus avoid resonance conditions (Ref. 1.4). At present 37 (63%) out of 59 rigs under construction or planned are semi-submersibles.

Since an increasing number of semi-submersibles will be used in the future, this chapter is devoted to the general description of the semi-submersibles in operation and under construction. The semi-submersibles have been divided into two categories and each category is described.

One of the many problems facing the offshore oil industry is the deep sea oil storage problem. As the drilling and production of oil move to deeper waters, the storage of oil must also be accomplished in deeper waters. One of the solutions to this problem is the use of the large single column platform (spar buoy). This type of platform can be regarded as special type of semi-submersibles for it can also be designed to have large natural period longer than the maximum expected wave period. Therefore, the general description of this type of platform is also included in this chapter.

From the study of existing semi-submersibles a trend toward bigger size, greater mobility and capability in deeper waters has been found.

1.2 Two Categories of Semi-Submersibles

The number of semi-submersibles has increased from one in 1962 to 65 in 1972 including 34 new rigs under construction. 26 out of 34 rigs under construction are scheduled to be completed during 1973. Therefore, by the end of 1973 there will be 57 rigs in operation (Ref. 1.2).

Since 1962 the design of semi-submersibles has been refined and innovated. There are two factors involved in the design. The first is to fulfil the required assignments at sea and the second is the feasibility from economical point of view such as operating costs, rig maintenance, probable life, insurance, interest on investment etc. Because these factors are widely varied throughout the world, most rigs are custom designed. This is reflected in the wide variety of rigs which are in operation and under construction. Therefore it would be difficult to arrive at a single optimum design of the rig which would fulfil the two factors mentioned above.

Although the design of semi-submersibles varies greatly, they can be generalised into two categories as follows:-

(i) Multi-hull semi-submersibles, and

(ii) Multi-leg semi-submersibles.

1.2.1 Multi-hull Semi-Submersibles

Semi-submersibles consisting two or more submerged longitudinal pontoon (lower hulls) and a water-tight rectangular or square main deck (upper hull) connected by a number of straight or tapered vertical columns (stability columns) fall under the first category. The world's first semi-submersible Blue Water Drilling Co., "Blue Water No. 1" (1962) and the world's first self-propelled semi-submersible Ocean Drilling and Exploration Co., (ODECO) "Ocean Prospector" (1971) belong to this category.

The five-year-old "Rig No. 1" of the Blue Water Drilling Co., was converted to semi-submersible in 1962 and became the world's first semi-submersible (Fig. 1.1). It should be noted that the large vertical columns are of bottle-type and the derrick is cantilevered over the side.

In 1963, the ODECO's V-shaped "Ocean Driller" was developed. It has the special features of locating the derrick closer to the centre of floatation to reduce trimming, towing and mooring problems and of using vertical columns enlarged at the water line to increase the water plane area and its moment of inertia. Itstwo lower hulls are connected at one end to form a V-shape (Fig. 1.2). The ODECO's other V-shaped semi-submersible "Ocean Explorer" was completed in 1964.

The ODECO's "Ocean Queen" (Fig. 1.3) was developed in 1965. It has the special features of using four parallel lower hulls of same diameter and two outriggers at one end. The outriggers contain cylinders at the normal operating draft which provide additional water plane area at a considerable lever arm in both directions. It also has enlargements on some of the secondary structural support columns at the operating draft to provide an increase in water plane area and in an event of severe motions or synchronism the water plane area could be changed by ballasting or deballasting the vessel and therefore change the heaving period. The ODECO's "Ocean Prince", "Ocean Viking" and "Ocean Digger" are of this design and the first two were completed in 1966 and the last two in 1967. But the "Ocean Prince" was destroyed in the North Sea in 1969 - and could not be salvaged.

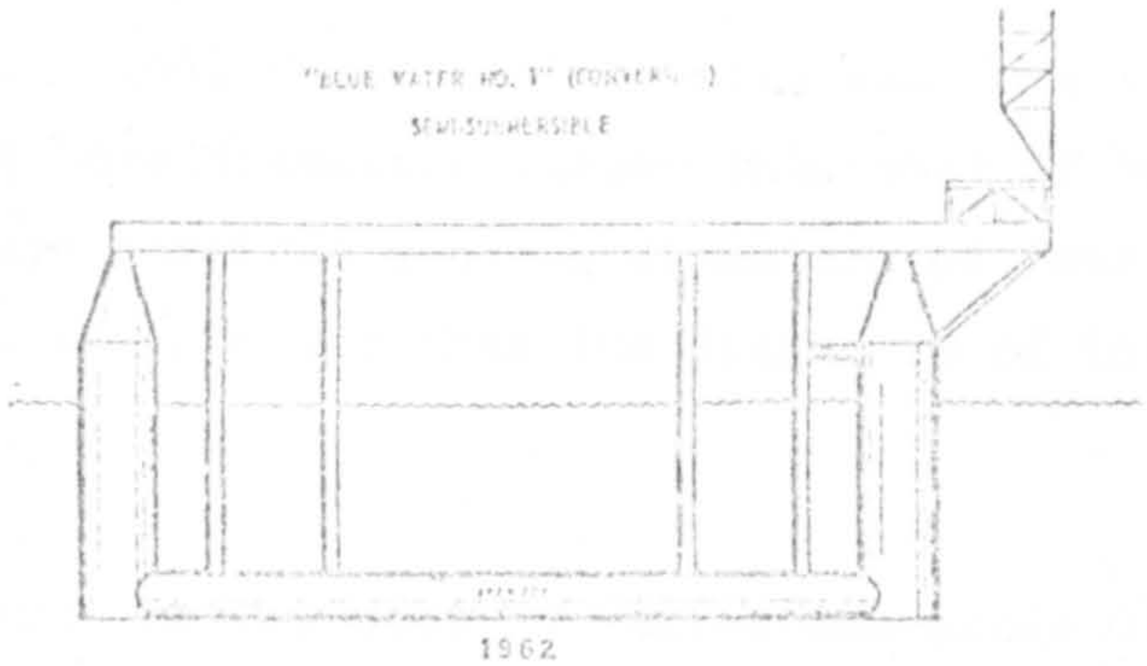

1962

Fig. 1.1 Blue Water No. 1

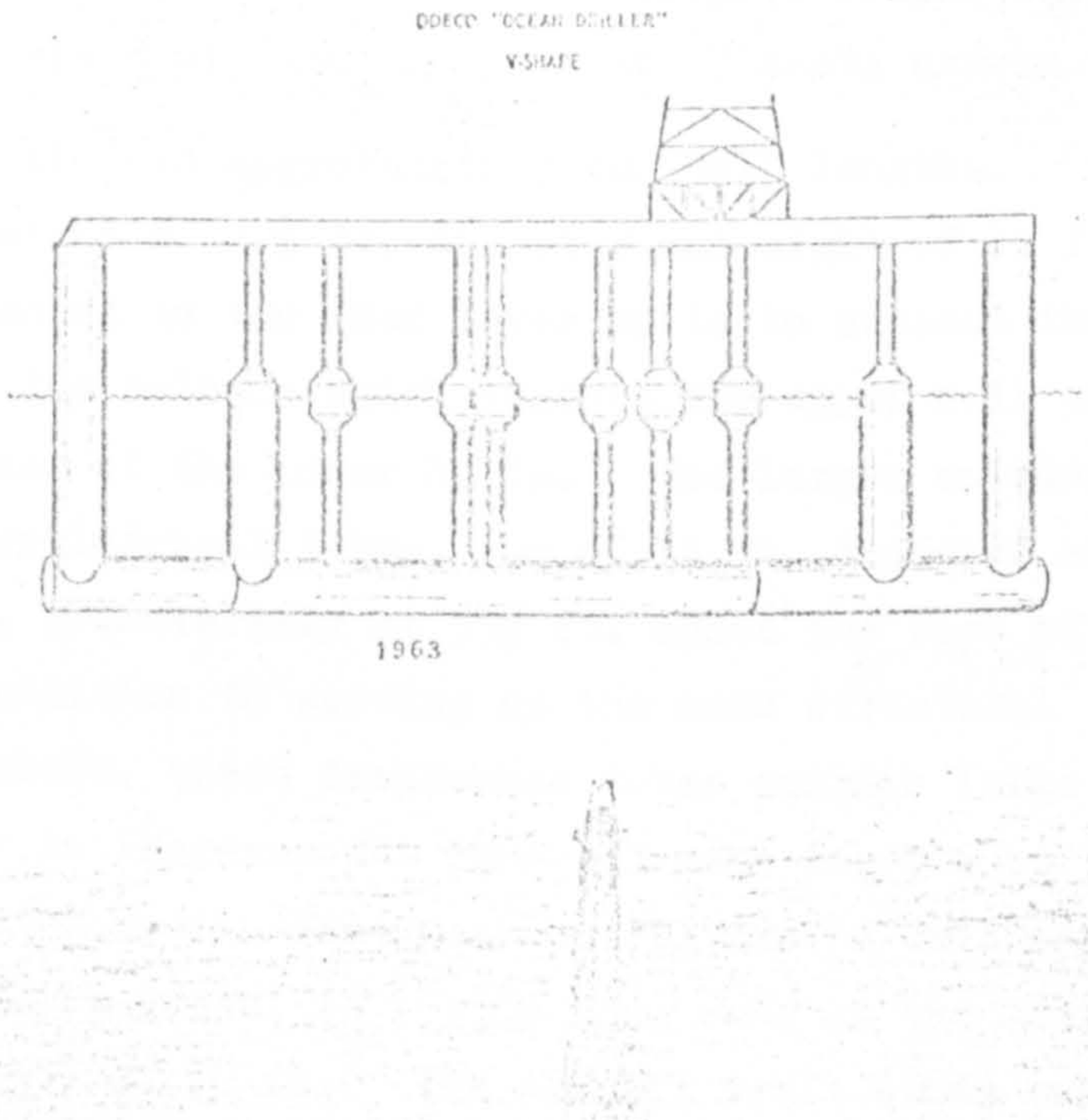

1963

Fig. 1.2 Ocean Driller

The Royal/Dutch Shell Co., "Staflo" also has four parallel lower hulls, the outer two have diameters larger than that of the inner two. All of its columns are straight and the diameters of four corner columns are the same and greater than the diameters of intermediate columns (Fig. 1.4).

The world's first self-propelled semi-submersible ODECO's "Ocean Prospector" (Fig. 1.5) was completed in February 1971. It is 344 ft. long, 263½ ft. wide and 125 ft. from keel to main deck. It has four parallel lower hulls of 25½ ft. diameter, the inner two of which are torpedo-shaped and are longer than the outer two. The twin kort nozzle propulsion system, installed in the torpedo-shaped hulls, gives the vessel a speed of 7 knots ahead and 3 knots astern and permits it to turn 180° in approximately two hull lengths. Sixteen vertical columns, eight of 22½ ft. diameter and eight of 12 ft. diameter, are connected to the four lower hulls to support the upper hull. The top of the columns which support the upper hull are 120 ft. from the base of the lower hulls. The larger columns are connected by four cylindrical tubes, two of 18 ft. diameter and two of 12 ft. diameter, transversely at 39½ ft. above the base of the lower hulls. In addition to serving as the main structural interconnecting members, these transverse tubes entrain large quantities of water to increase the immersed mass inertia of the vessel and give better motion-free characteristics in drilling mode. The displacement of the vessel is 19,300 long tons at the operating draft (when ballasted) of 70 ft. The transit draft (when completely deballasted) is approximately 20 ft. According to the (Ref. 1.2), other semi-submersibles of this basic design are ODECO's "Ocean Victory", "Ocean Kukuei", "Ocean Rover" and "Ocean Voyager", Oslo Drilling Co., "Odin", Gotaas-Larsen/Rowan Co., "NOR 101", and Waage Drilling Co., "Waage Drill 1" and "Waage Drill 2". The "Ocean Victory" is scheduled to be completed in 1972 while the othersin 1973.

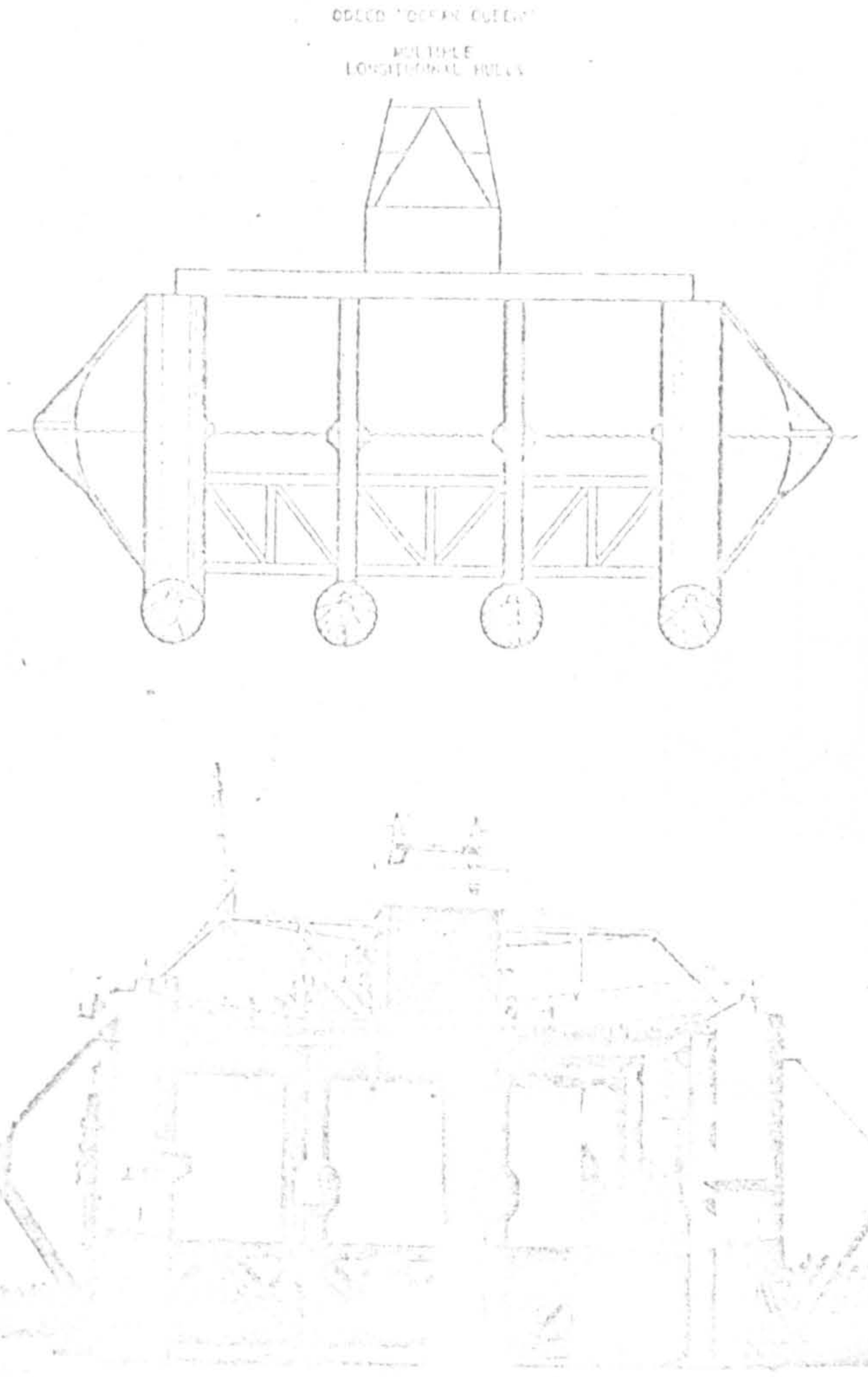

Fig. 1.3 Ocean Queen

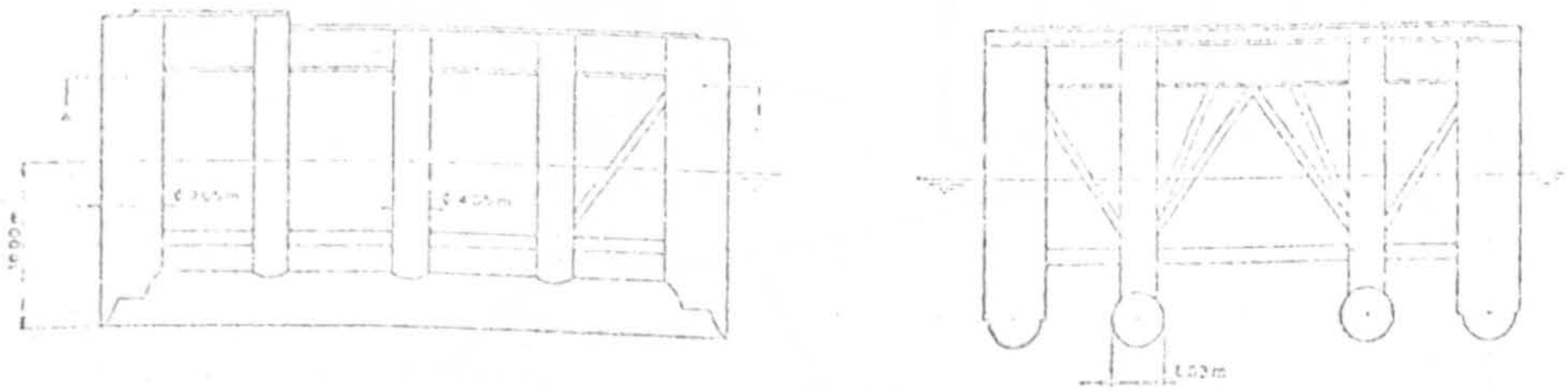

Fig. 1.4 Staflo

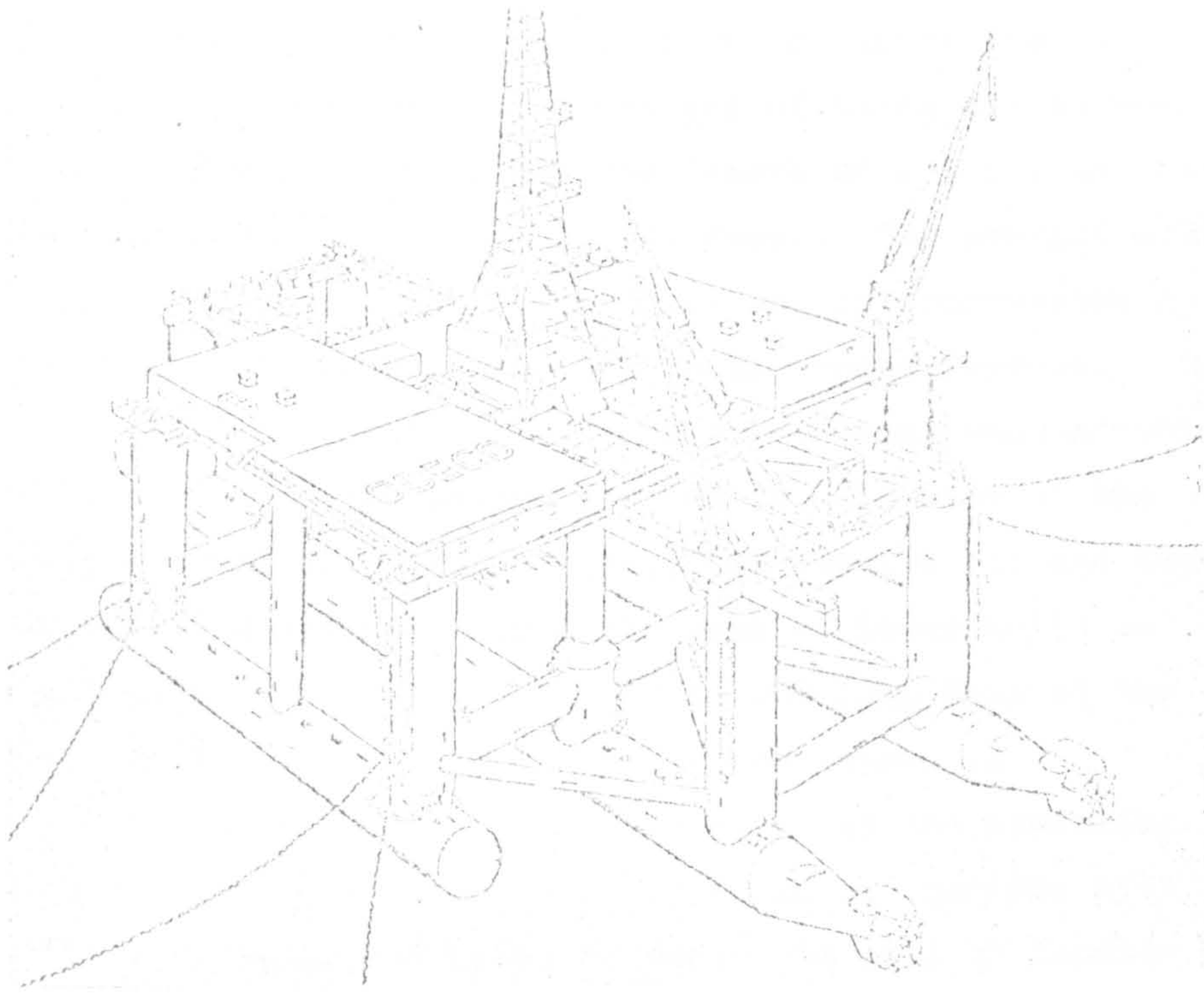

Fig. 1.5 Ocean Prospector

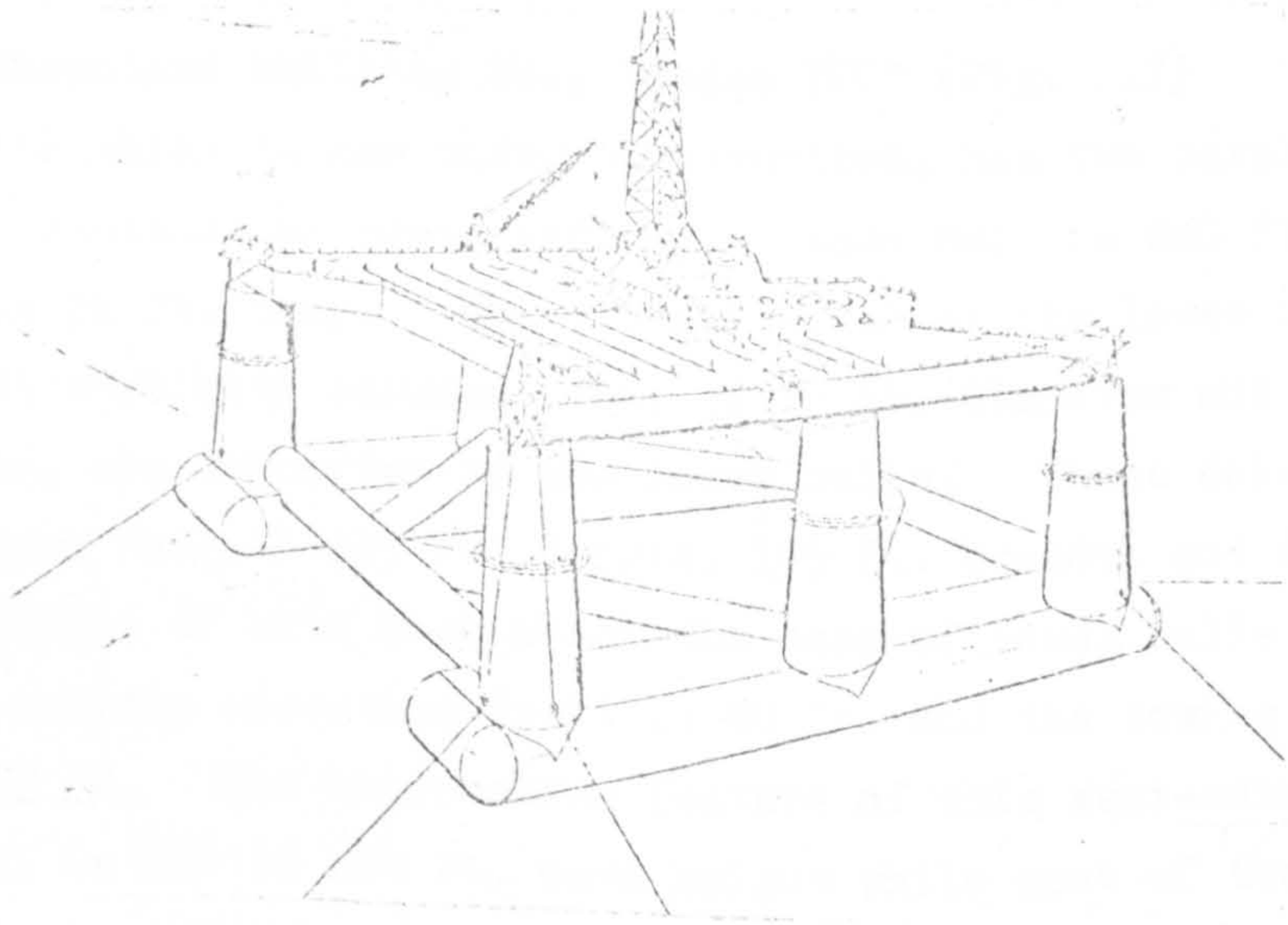

Fig. 1.6 Penrod 71

The Penrod Drilling Co., "Penrod 71" (Fig. 1.6) semi-submersible, now under construction, has interesting features of using the two wide parallel lower hulls with cylindrical sides and of using six tapered stability columns. The lower hull has the length of 298 ft. and its cross section measures 70 ft. wide by 30 ft. deep. The overall width of the lower hull is 216 ft. The lower hulls are interconnected by two parallel transverse tubes and four horizontal cross members. On top of the lower hulls are six tapered stability columns each of which measures 33 ft. diameter at the bottom and 28½ ft. diameter at the top, supporting the upper hull of length 233 ft., breadth 196 ft. and depth 18 ft. The height of upper hull above the base of lower hulls is 138 ft. The displacement of the vessel is 42,000 long tons at the 70 ft. operating draft. The towing draft of the vessel is approximately 15 ft. The dynamic characteristics at the operating draft for conducting drilling operations during normal periods are: Roll 35 sec., Pitch 37 sec., and Heave 38 sec. It will be capable of working in water depths in excess of 1,000 ft. from a moored position. The other semi-submersibles of this basic design are Penrod Drilling Co., "Penrod 70", "Penrod 72", "Penrod 73", "Penrod 74", and "Penrod 75". The "Penrod 70" is scheduled to be completed in 1972 while the others in 1973.

The Southeastern Drilling Co., "Sedco 700" (Fig. 1.7) semi-submersible which is now under construction, has two parallel lower hulls of rectangular cross section. Each hull is 280 ft. long, 50 ft. wide and 21 ft. deep. The overall width of the lower hull is 245 ft. Eight stability columns, four of 30 ft. diameter and four of 18 ft. diameter, are supported by the lower hulls. These columns support the upper hull of 225 ft. length, 195 ft. breadth and 6 ft. depth. The height of main deck above the base of lower hulls is 130 ft. The maximum operating draft is 80 ft. and the towing draft is 17 ft. to 19 ft. One interesting feature of this semi-submersible is the survival in 100 to 120 ft. wave height while most of the other multi-hull semi-submersibles are designed for survival in 85 ft. wave, once in 100-year storm. At a draft of 70 ft., the unit will be able to pass wave heights of 80 ft. and for survival in 100-120 ft. wave heights the vessel is deballasted to a draft of 60 ft. and pass the wave without any danger to the deck substructure (Fig. 1.8).

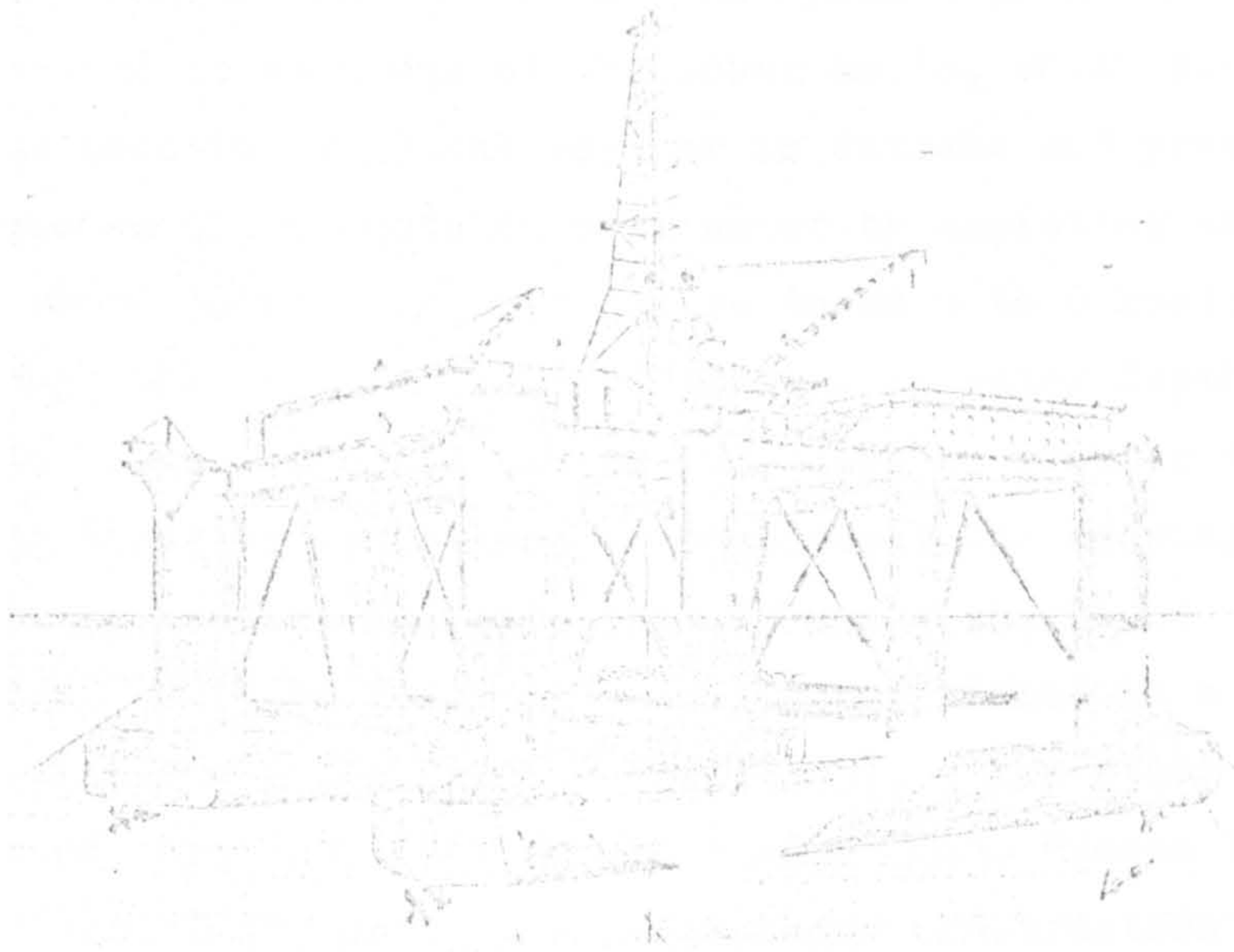

Fig. 1.7 Sedco 700

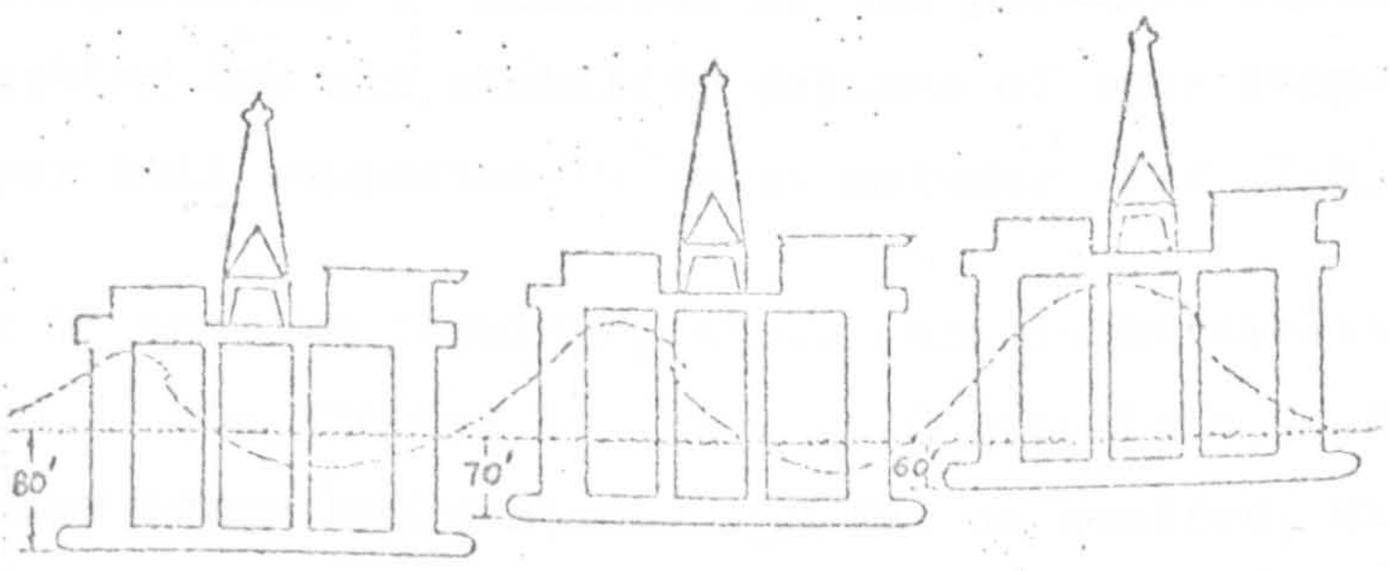

Fig. 1.8 Sedco 700 (storm survival)

Another interesting feature is the use of the dynamic positioning thrusters, one located at each end of the lower hulls, which assist to keep the vessel on location when the weather is extreme and provide a towing speed in excess of 10 knots in calm water by assisting an ocean going tug. For short moves, the unit can be towed 6 to 8 knots by a workboat. Although the unit is designed to work in water depth of 1,000 ft. the water depth capacity can be increased to greater than 2,000 ft. by using thruster assistance to supplement the mooring system. Theoretical studies indicate that by using the eight thrusters the vessel could be fully dynamically positioned in a 2-knot current, 50-knot wind and a Sea State 6 (Ref. 1.5). The other semi-submersibles of this basic design are "Sedco 701", "Sedco 702", "Sedco 703" and "Sedco 704", which are still under construction and scheduled to be completed in 1973.

The semi-submersibles of similar design to the "Sedco 700" are the Wester Oceanic Co., "Western Pacesetter 1", the Storm Drilling Co., "Zephyr 1" and "Zephyr 2", the Atwood Oceanic Co., "Margie" and the ODECO's "Ocean Scout".

The"Western Pacesetter 1" consists of two parallel rectangular lower hulls supporting the six stability columns of same diameter and a rectangular upper hull supported by these columns (Fig. 1.9).

The "Zephyr 1" and the remaining three semi-submersibles are identical in shape. The "Zephyr 1" (Fig. 1.10) consists of two parallel rectangular lower hulls spaced 150 ft. on centres, with four large stability corner columns of 32 ft. diameter and four small intermediate columns supporting a rectangular water-tight upper hull. The height of the main deck above the base of lower hulls is 108 ft. The length of lower hull is 202 ft. and the overall width is 182 ft. The operating draft and the towing draft are approximately 50 ft. and 20 ft. respectively.

The self-propelled semi-submersibles Zapata Corp. "SS-3000", Deep Sea Drilling Co., "Bergen Rig 1" and Gotaas-Larsen/Rowan Co., "NOR 102", which are under construction, also have two parallel rectangular lower hulls. The Zapata Corp. "SS 3000" (Fig. 1.11)

Fig. 1.9 Western Pacesetter 1

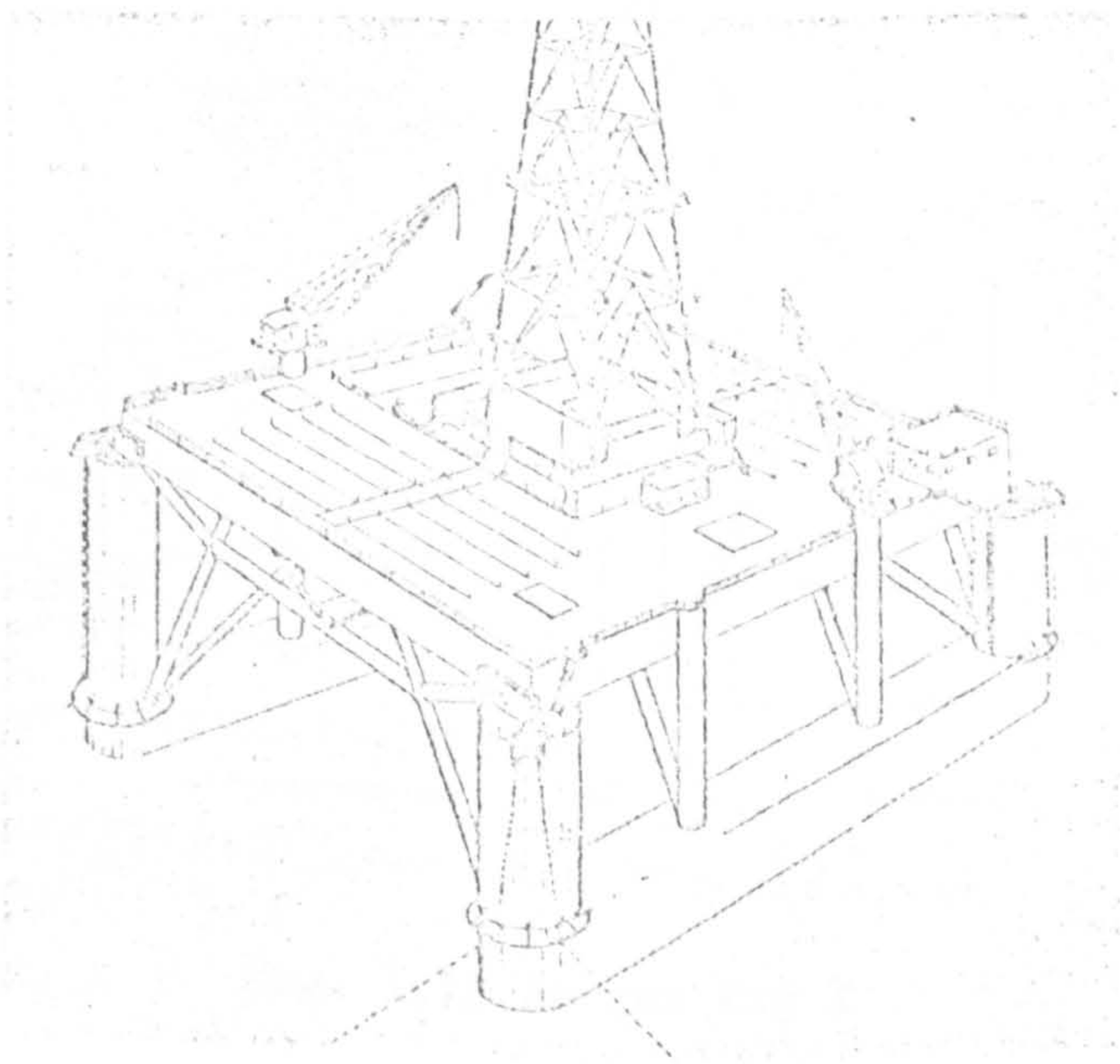

Fig. 1.10 Zephyr I

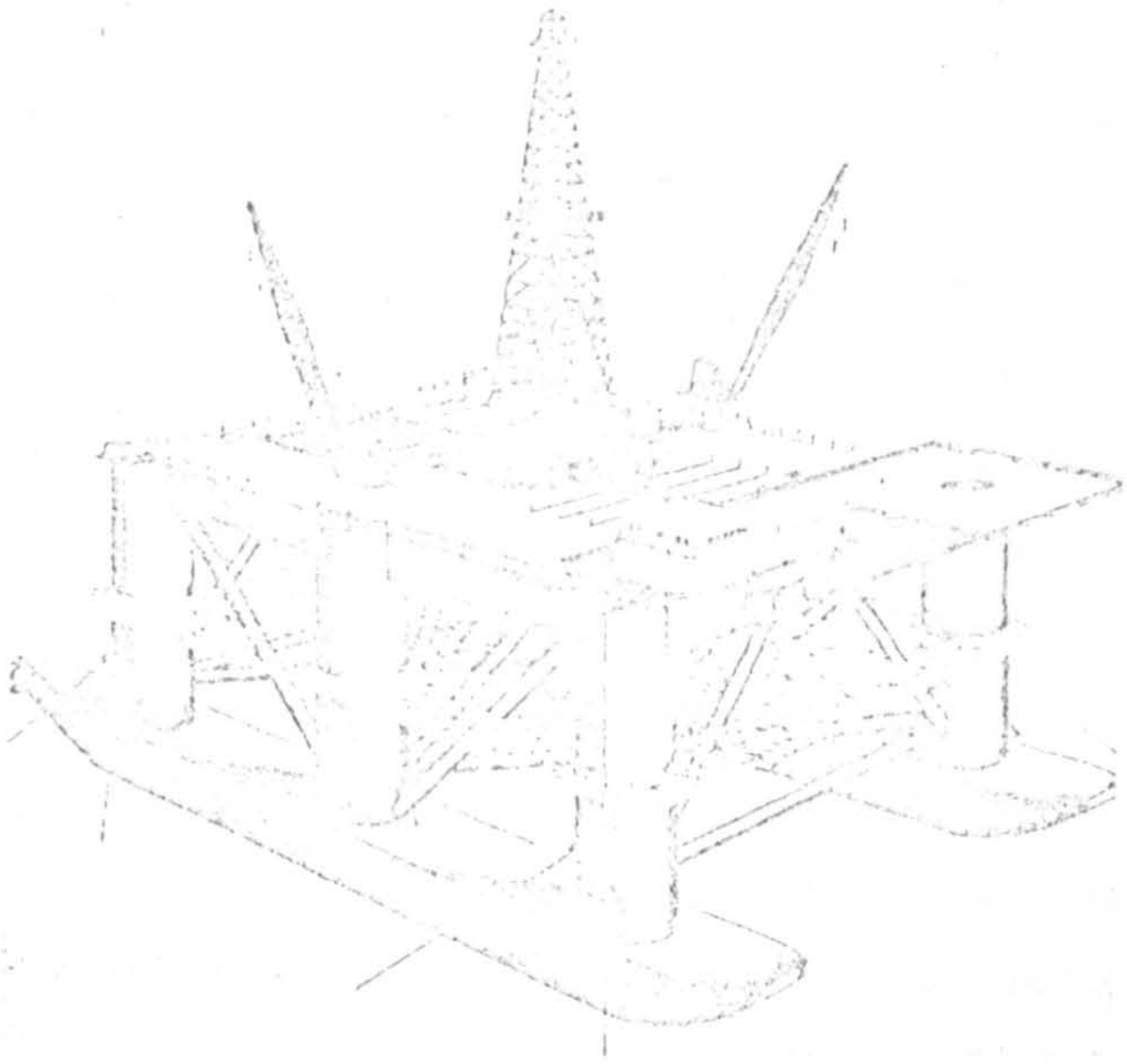

Fig. 1.11 SS 3000

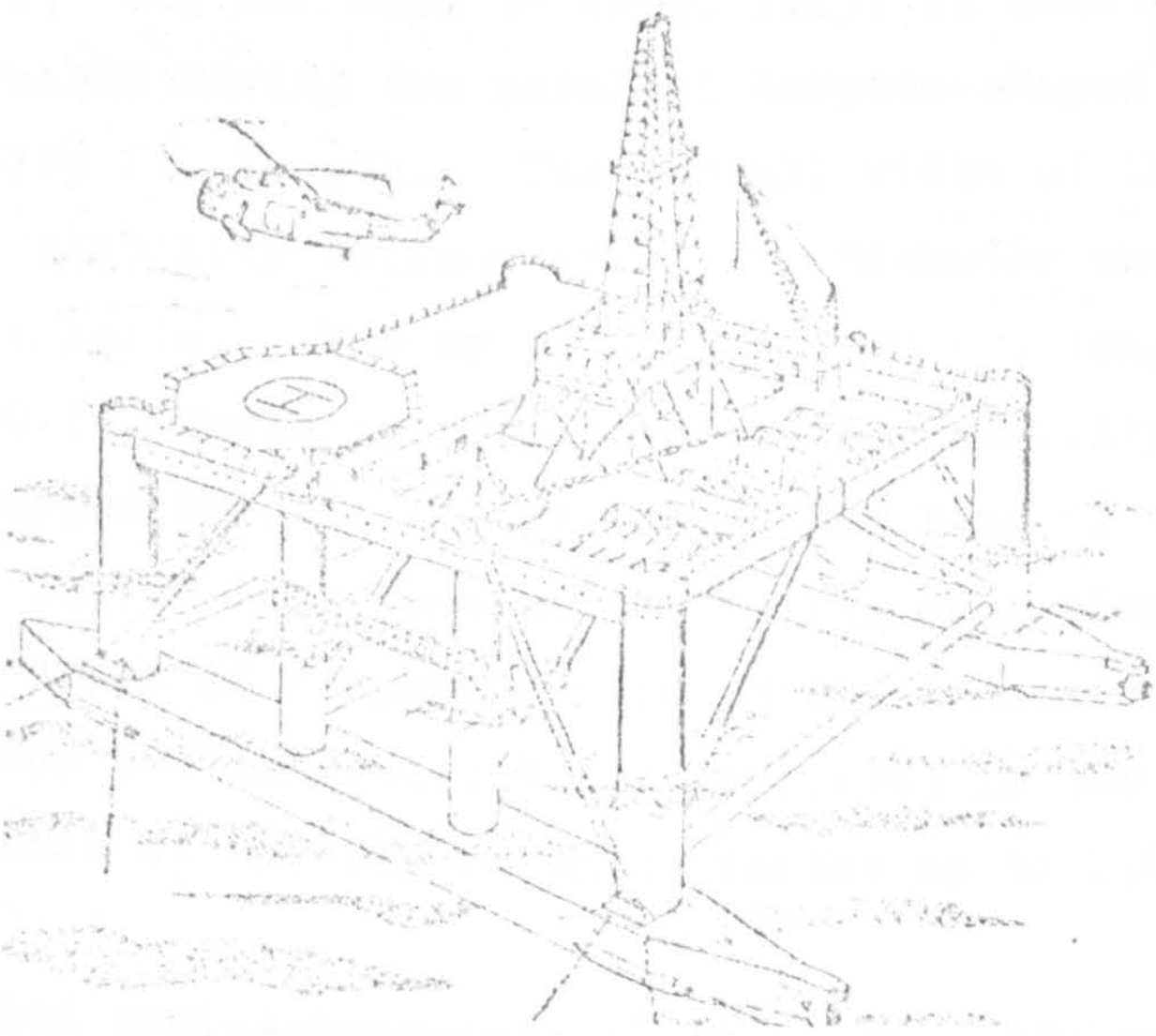

Fig. 1.12 Bergen Rig 1

has six stability columns of equal diameters supporting the upper hull. The vessel is 350 ft. long, 210 ft. wide and 125 ft. high from the keel to the underside of the upper hull and has a displacement of 26,600 long tons at the operating draft of 80 ft. The Deep Sea Drilling Co., "Bergen Rig 1" (Fig. 1.12) has four large stability corner columns of 26 ft. diameter and four small intermediate columns supporting the upper hull of 226 ft. length and 200 ft. width. The columns have a transition from circular to rectangular cross section at the lower end. This has been done to obtain a simple and strong structural connection between columns and internal bulkheads of lower hull and to match the column shell nicely in line with lower hull bulkheads and frames. The height of main deck above the base of lower hulls is 120 ft. and each lower hull is 355 ft. long, 36 ft. wide and 22 ft. deep. The overall width of the hull is 221 ft. It has a displacement of 19,000 long tons at the 70 ft. operating draft. The propeller propulsion system gives the vessel an estimated speed of 6 knots. The natural periods of the vessel are heave 22 sec., roll 34 sec. and pitch 30 sec. The "NOR 102" semi-submersible has the same design as the "Bergen Rig 1".

The Offshore Co., "SCP III Mark 2" (Fig. 1.13) is also a self-propelled semi-submersible having two parallel torpedo-shaped hulls of 35 ft. diameter and 378½ ft. length. The overall width of the lower hull is 242 ft. Six stability columns of 27 ft. diameter are supported by the lower hulls. The upper hull of 270 ft. length, 223 ft. breadth and 20 ft. depth is supported by the stability columns. The main deck of the upper hull is 140 ft. above the base of the lower hulls. It displaces 22,780 long tons at the 70 ft. operating draft and has a still water speed of 7 knots at the 28 ft. transit draft. It is under construction and scheduled to be completed in the early 1974. This unit will be capable of working in water depths up to 1,000 ft.

The self-propelled semi-submersible Amoshore Co., "Colonel Drake" (Fig. 1.14) has two parallel lower hulls with rounded sides. The overall length of the lower hull is 333 ft. Six stability columns of 28 ft. in diameter are connected to the lower hulls and the water-tight rectangular upper hull is supported by these columns. The propulsion system will give the vessel a speed of 6 knots ahead. This unit will be capable of drilling in water depths up to 600 ft. It is scheduled to be completed in the early 1974.

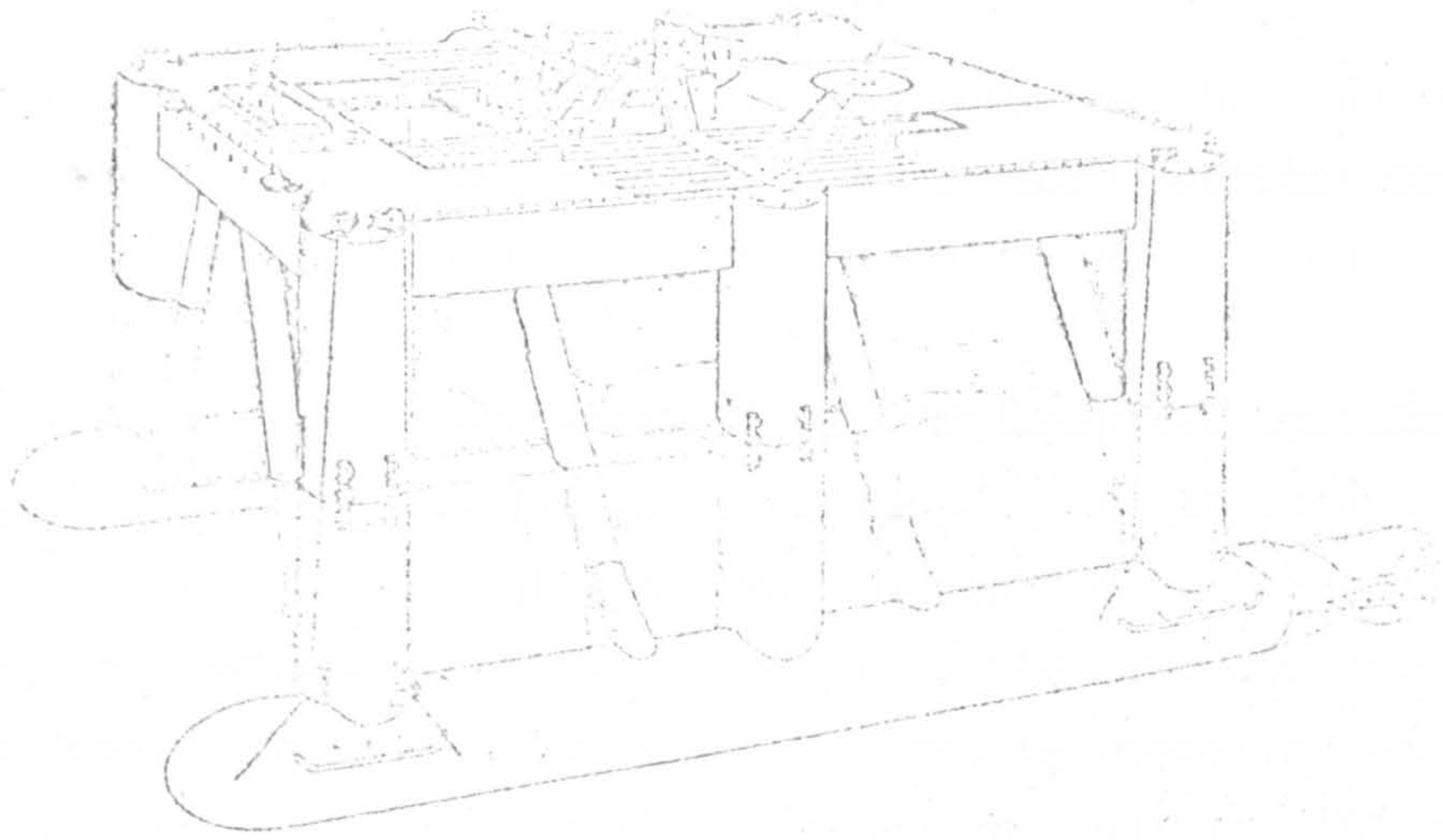

Fig. 1.13 SCP III Mark 2

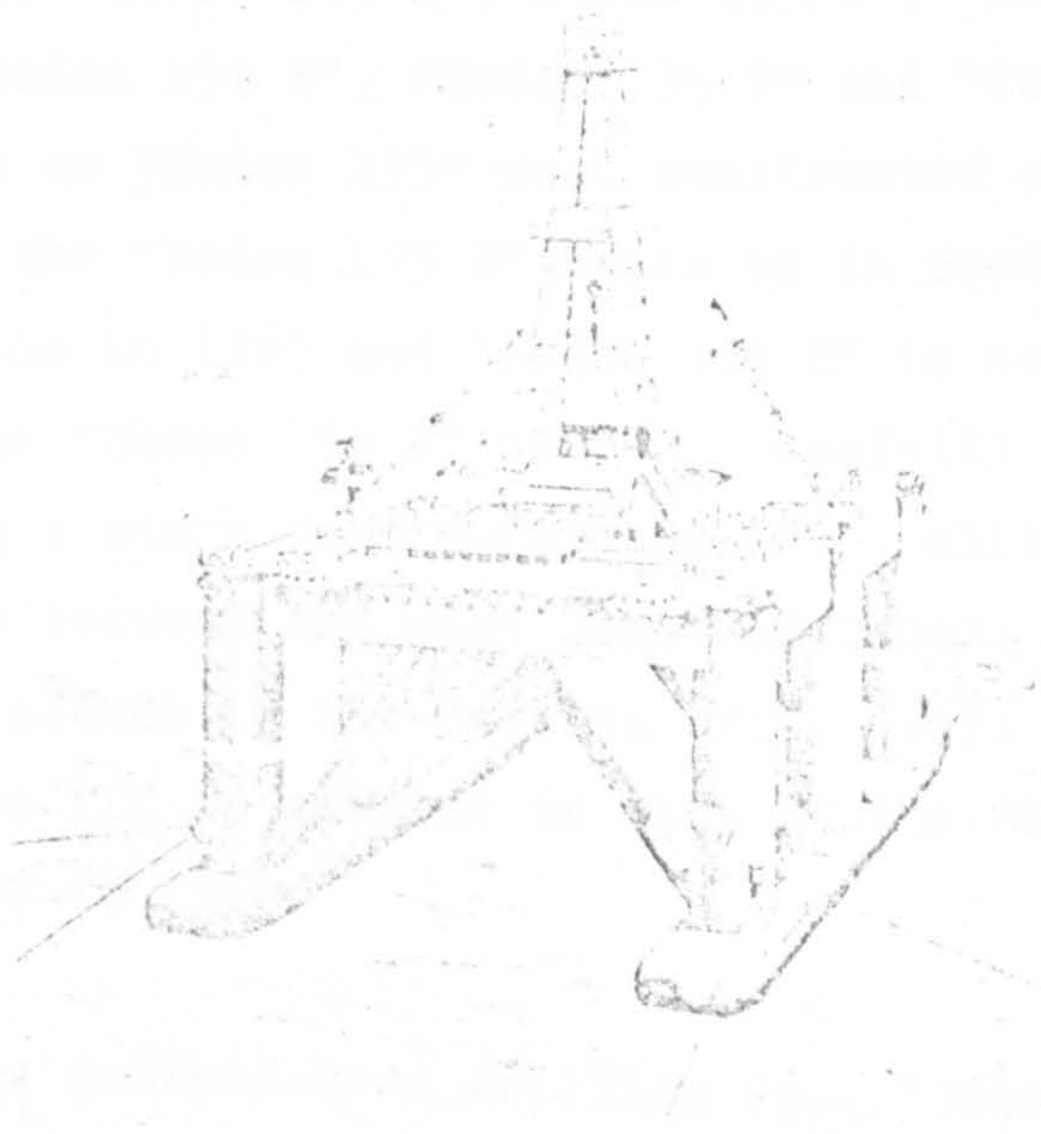

Fig. 1.14 Colonel Drake

1.2.2 Multi-leg Semi-Submersibles

Semi-submersibles fall under this category are those which have a water-tight upper hull supported by three of more vertical columns (or legs) having a large footing at the lower end of each column.

The first multi-leg semi-submersible Southeastern Drilling Co., "Sedco 135" (Fig. 1.15) was developed in 1965. It consists of a 280 x 280 x 280 ft. triangular upper hull supported by three bottle-shaped vertical columns of 35 ft. diameter and 141 ft. height. An elliptical footing measuring 100 x 60 x 25 ft. is connected to the lower end of each column. The top of the upper hull is 166 ft. above the base of footings. It has a displacement of 16,800 tons at the 80 ft. operating draft. The towing draft is 35 ft. It can work while sitting on the bottom in 135 foot water or while afloat in 600 foot water. It should be noted that drilling is done through the aft-vee (drilling slot) and not through the centre of the vessel. During the period between 1965 and 1968, seven multi-leg semi-submersibles, viz. "Sedco 135 A","Sedco 135 B", "Sedco 135 C", "Sedco 135 D", "Sedco 135 E", "Sedco 135 F" and "Sedco 135 G" of the same basic design as "Sedco 135" were constructed and put into operation. But the "Sedco 135 B" broke up in South China Sea while under tow to Borneo in 1965 and "Sedco 135 C" is now known as the "Sea Quest". The "Sedco 135 F" once successfully withstood 95 ft. high waves during a storm in mid-October 1968, while it was anchored in the Hecate Strait between the west coast of Canada and the remote Queen Charlotte Islands in the Pacific (Ref. 1.6). The design of Saipem's "Scarabeo II" is similar to that of the "Sedco 135" and the unit was completed in 1968.

In 1969, the Southeastern Drilling Co., "Sedco H" (Fig. 1.16) was completed. It is also a triangular semi-submersible with three legs and circular footings, but it varies greatly with the "Sedco 135" design. The main variations in the configuration are:- lowering the main deck by 20 ft. to 146 ft., replacing the bottle-shaped vertical columns with the straight vertical columns, replacing the elliptical footing with 80 ft. diameter x 30 ft. footings, eliminating the aft-vee (drilling slot) and locating the substructure forward to

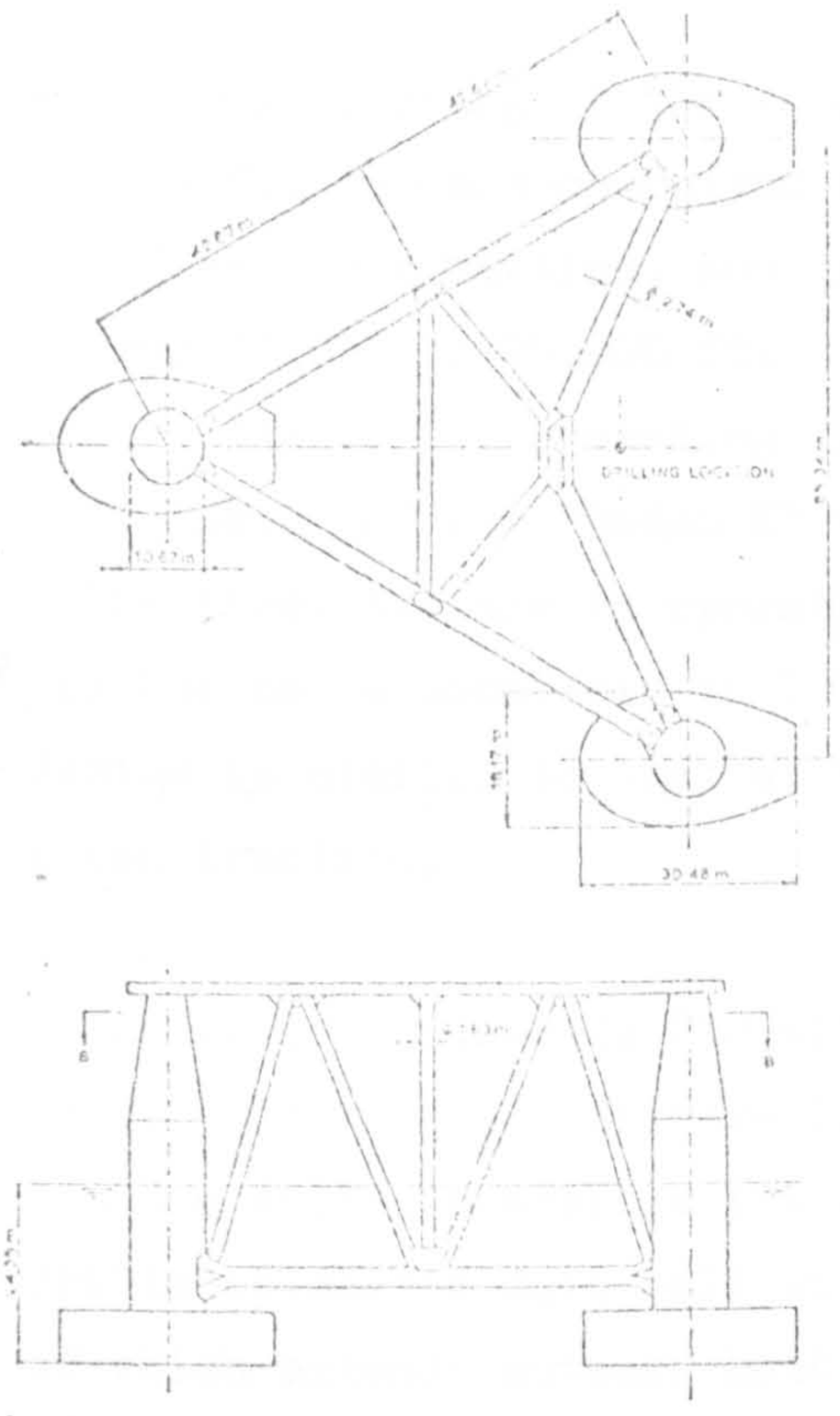

Fig. 1.15 Sedco 135

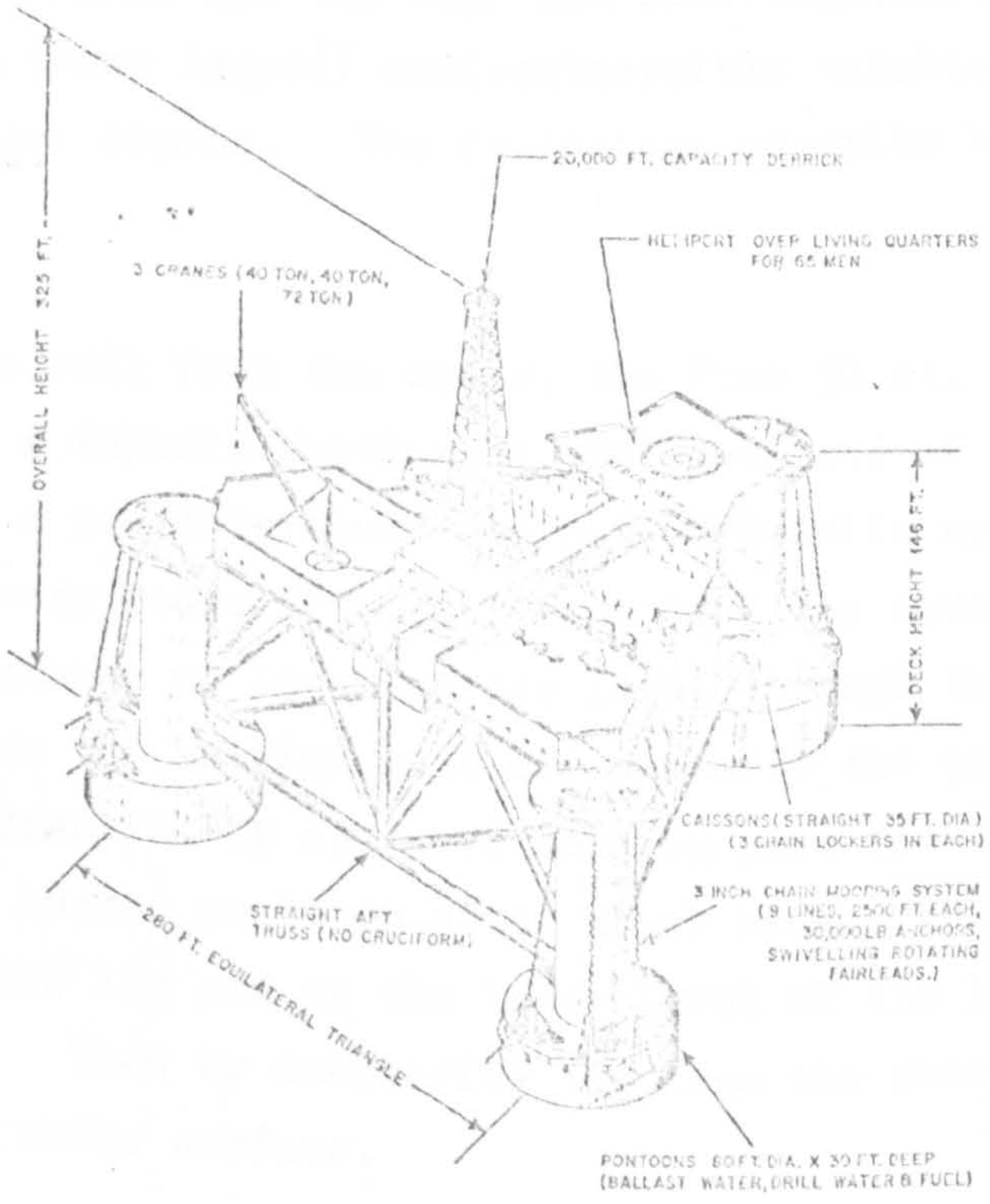

Fig. 1.16 Sedco H

permit through-the centre- drilling, changing the water depth capability from 135 ft. to 100 ft. for sit-on-bottom condition and from 600 ft. to 800 ft. for floating condition, and increasing the drilling depth capability from 20,000 to 25,000 ft. It has a displacement of 19,700 tons at the 80 ft. operating draft. The semi-submersibles "Sedco I", "Sedco J" and "Sedco K" are the sister units of the "Sedco H". The first two are in operation and the last under construction which is due to be completed in 1973. The Saipem's "Scarabeo III" design is similar to that of the "Sedco H" and the unit is now under construction.

The Transworld Drilling Co., "Transworld Rig 61" of most unusual design was completed in 1970. The special feature is the combination of a drillship, a jack-up and a semi-submersible (Fig. 1.17). It has a 400 x 58 x 23 ft. drillship-shaped main hull with a pair of outrigger trusses, each of which extends outward both right and left from the centre of the main hull. There are four spud wells, each located 135 ft. forward, aft, port and starboard of midships centre. The unit moves to a drillsite as a conventional drillship. Once there, it becomes a self-elevating rig. But after the main hull is raised from the water surface and the legs are semi-submerged, the unit becomes multi-leg (four legged) semi-submersible capable of drilling in 600 ft. water depths. The followings describe how the unit works:-

(a) To raise the main hull from the water, the four 30 ft. diameter x 148 ft. legs and a rhombic footing at the lower end of each leg are ballasted to a pre-determined depth. Hydraulic cylinders in the leg machinery rooms are used to control the movement of the legs (i.e. raising or lowering the legs) through the four spud wells. When the holding pins are opposite the pinholes of the legs, the hydraulically operated holding pins fix the hull to the legs in a locked position after which wedges are set at both the top of the leg and at the lower level of the leg machinery rooms. Then by dewatering the legs the main hull is raised above the water surface.

(b) To lower the main hull, the wedges are removed and the legs and their footings are ballasted through the sea chest at the sides

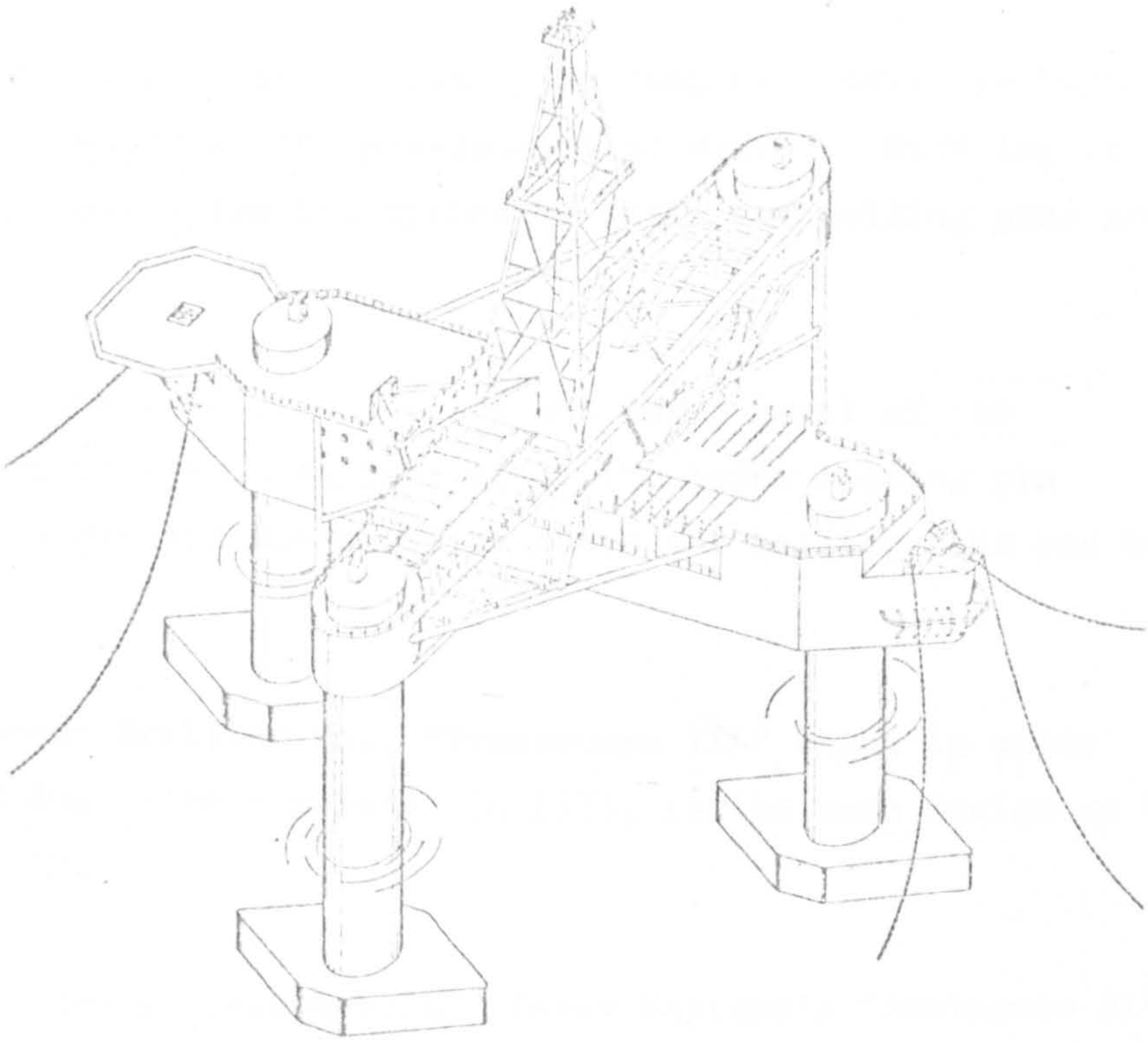

Fig. 1.17 Transworld Rig 61

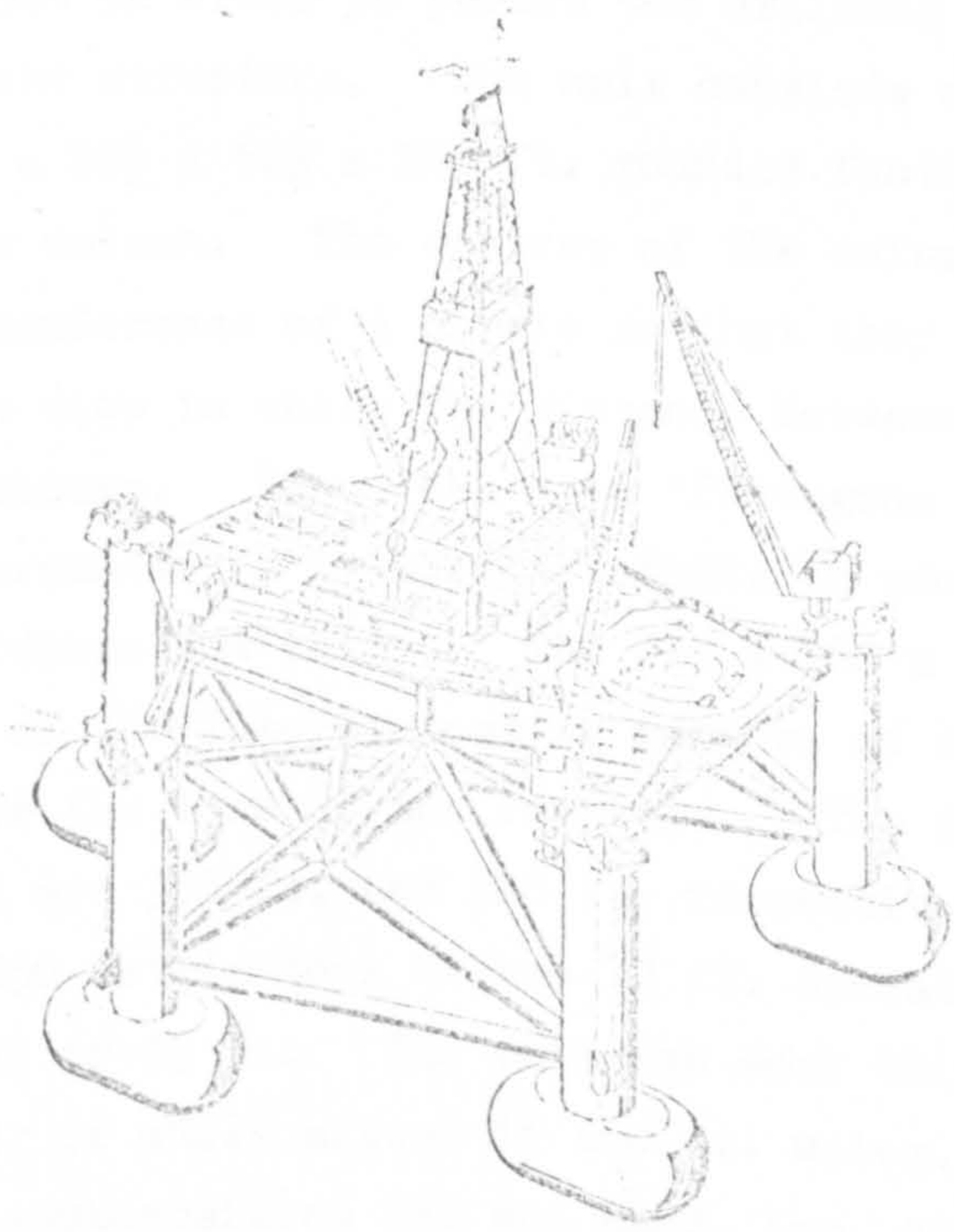

Fig. 1.18 Pentagone 81

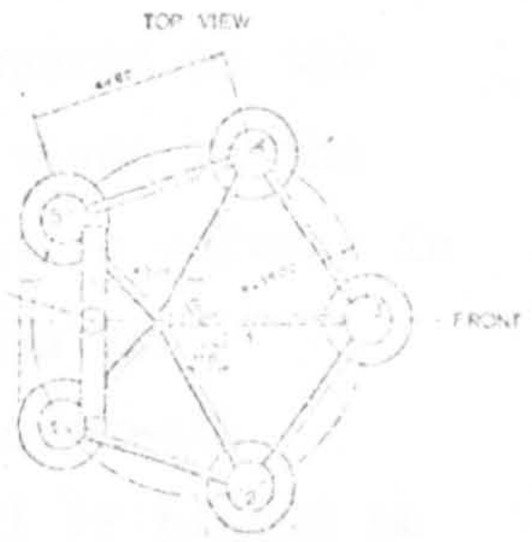

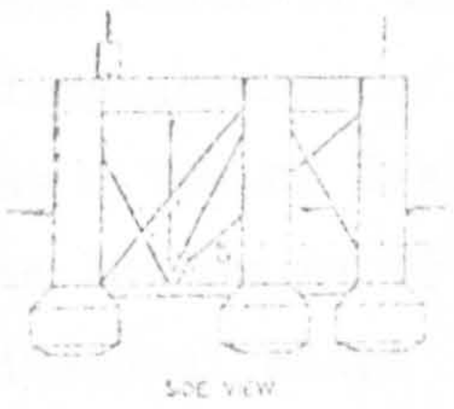

Fig. 1.19 Norrig 5

of the footings (either by gravity or pumping) until the hull sits in the water at the pre-determined draft. Each leg is held by the four hydraulic cylinders until the holding pins are retracted.

(c) For towing, the wedges at the top and lower level of the machinery rooms are installed, after the lower holding pin location has reached the position where the holding pins can be engaged.

The Transocean Drilling Co., "Transocean III" which is under construction and due to be completed in 1973, is the same design as the "Transworld Rig 61".

The five-legged semi-submersible Forex Neptune's "Pentagone 81" (also known as "Neptune 7") was completed in 1968. This pentagonal shape unit (Fig. 1.18) is especially designed to work in the rugged conditions found in the North Sea and Bay of Biscay. It can operate in 60 mph wind and 33 ft. wave height. The pentagonal shape was chosen in order to permit the drilling axis to be located in the centre of the structure. The unit consists of five $31\frac{1}{4}$ ft. diameter columns and a $80\frac{1}{2}$ x $52\frac{1}{2}$ x $24\frac{1}{2}$ ft. rounded footing connected to the lower end of each column. The centres of the columns are equally spaced on the circumference of a circle so that they form a pentagon shape in the plan view in which the distance between two non-consecutive columns is 81 meters. Hence the name "Pentagone 81". The columns are interconnected by tubular struts to provide sufficient over-all rigidness and unity. The 213 x 108 x $2\frac{1}{4}$ ft. upper hull is placed on top of the interconnecting members so that its main deck is 134 ft. above the base of the footings. The over-all length and width of the unit are 333 ft. and 318 ft. respectively. It has a displacement of 16,050 metric tons at the 72 ft. operating draft and has a towing draft of 21 to 25 ft. The unit can work while sitting on the bottom in 95 ft. water or while afloat in 600 ft. water. The other pentagonal shape semi-submersibles Sea and Land, Inc. "Pentagone 82" and "Pentagone 84" and Herlofson Group "S/S Pentagone 83" are now under construction.

The Peter Smedvig "Norrig 5" (Fig. 1.19) is also a five-legged semi-submersible and has a pentagonal shape in the plan view.

The features different from the "Pentagone 81" are its circular footings and the location of the drilling axis which is on one side of the pentagone. The upper hull is supported by the interconnecting structural members of the columns and its main deck is 187 ft. above the base of the footings. The lower end of each $33\frac{1}{2}$ ft. diameter column is connected to a $62\frac{1}{2}$ ft. diameter footing by a transition piece. The over-all length and width of the unit are 288 ft. and 299 ft. respectively. The unit can work in 118 ft. water while sitting on the bottom or 1,000 ft. water while floating. The displacements at the 98 ft. operating draft and 26 ft. towing draft are 25,410 and 11,620 metric tons respectively. The unique feature of this unit is its capability of self-docking which means that any of the five footings can be lifted above the light water line by proper ballasting. The unit is under construction and due to be completed in 1973.

The semi-submersibles in operation and under construction are given in Tables (1.1), (1.2) and (1.3). The lists of the semi-submersibles in Table (1.1) and (1.2) are based on the (Ref.1.2) and the new rigs which are not included in the (Ref. 1.2) are shown in Table (1.3).

Table (1.1) Semi-Submersibles in Operation

Sr. No.	Owner	Rig Name	Year Completed	Dimensions (ft)	Water Depth (ft)	Category
1	British Petroleum	Sea Quest	1966	342 x 340 x 166	600	Multi-leg; Triangular
2	Japan Drilling Co.	Hakuryu II	1971	275½ x 200	656	- - -
3	Forex Neptune	Pentagone 81	1968	333 x 318 x 134	600	Multi-leg; Pentagonal
4	Ocean Drilling and Exploration Co.	Ocean Digger	1967	365½ x 217½	600	Multi-hull
5	Ocean Drilling and Exploration Co.	Ocean Driller	1963	377 on a side	600	Multi-hull, V-shaped
6	Ocean Drilling and Exploration Co.	Ocean Explorer	1964	377 on a side	600	Multi-hull, V-shaped
7	Ocean Drilling and Exploration Co.	Ocean Prospector	1971	344 x 263½ x 125	600	Multi-hull; Self-propelled
8	Ocean Drilling and Exploration Co.	Ocean Queen	1965	365½ x 217½	600	Multi-hull
9	Ocean Drilling and Exploration Co.	Ocean Traveller	1966	365½ x 217½	600	Multi-hull
10	Ocean Drilling and Exploration Co.	Ocean Viking	1967	365½ x 217½	600	Multi-hull
11	Saipem	Scarabeo II	1968	348 x 300 x 156	600	Multi-leg; Triangular
12	Santa Fe International Corp.	Blue Water 2	1964	205 x 204	1000	Multi-hull
13	Santa Fe International Corp.	Blue Water 3	1966	220 x 198	1000	Multi-hull
14	Santa Fe International Corp.	Mariner I	1968	270 x 106	600	Multi-hull
15	Southeastern Drilling Co.	Sedco 135	1965	342 x 340 x 166	600	Multi-leg; Triangular
16	Southeastern Drilling Co.	Sedco 135 A	1965	342 x 340 x 166	600	Multi-leg; Triangular
17	Southeastern Drilling Co.	Sedco 135 D	1966	342 x 340 x 166	600	Multi-leg; Triangular
18	Southeastern Drilling Co.	Sedco 135 E	1966	342 x 340 x 166	600	Multi-leg; Triangular
19	Southeastern Drilling Co.	Sedco 135 F	1967	342 x 340 x 166	600	Multi-leg; Triangular

Cont'd/...

Cont'd/... Table (1.1)

Sr. No.	Owner	Rig Name	Year Completed	Dimensions (ft)	Water Depth (ft)	Category
20	Southeastern Drilling Co.	Sedco 135 G	1968	342 x 340 x 166	600	Multi-leg; Triangular
21	Southeastern Drilling Co.	Sedco H	1969	382 x 347 x 146	800	Multi-leg; Triangular
22	Southeastern Drilling Co.	Sedco I	1970	382 x 347 x 146	800	Multi-leg; Triangular
23	Southeastern Drilling Co.	Sedco J	1972	382 x 347 x 146	800	Multi-leg; Triangular
24	Sea Drilling Netherlands	Sedneth I	1967	272 x 239	650	Multi-hull
25	Royal Dutch/Shell	Staflo	1967	251 x 218	600	Multi-hull
26	Transworld Drilling Co.	Rig 58	1966	226½ x 200	600	Multi-hull
27	Transworld Drilling Co.	Rig 61	1970	Hull: 400 x 58 x 23	600	Multi-leg
28	Zapata Corp.	Louisiana	1957	180 x 151	600	Multi-hull

Table (1.2) Semi-Submersibles Under Construction

Sr. No.	Owner	Rig Name	Completion Date	Dimensions (ft)	Water Depth (ft)	Category
1	Atwood Oceanics, Inc.	Margie	June 1973	202 x 182 x 110	600	Multi-hull
2	Deep Sea Drilling Co.	Bergen Rig 1	Dec. 1973	355 x 221 x 120	1000	Multi-hull; Self-propelled
3	Diamond M Drilling Co.	Unknown	Sept. 1973	270 x 173	600	Multi-hull
4	Gotaas Larsen/Rowan Co.	Nor 101	Late 1973	320 x 266 x 128	600	Multi-hull; Self-propelled
5	Gotaas Larsen/Rowan Co.	Nor 102	June 1974	355 x 221 x 120	600	Multi-hull; Self-propelled
6	Herlofson Group	S/S Pentagone 83	Late 1973	338 x 325 x 134	660	Multi-leg; Pentagonal
7	Ocean Drilling and Exploration Co.	Ocean Kukuei	Mid. 1973	320 x 262	600	Multi-hull; Self-propelled
8	Ocean Drilling and Exploration Co.	Ocean Rover	Early 1973	320 x 262	600	Multi-hull; Self-propelled
9	Ocean Drilling and Exploration Co.	Ocean Scout	Spring 1973	202 x 182	600	Multi-hull
10	Ocean Drilling and Exploration Co.	Ocean Victory	Fall 1972	320 x 262	600	Multi-hull; Self-propelled
11	Ocean Drilling and Exploration Co.	Ocean Voyager	1973	320 x 262	600	Multi-hull; Self-propelled
12	The Offshore Co.	SCP III Mark II	-	378½ x 242 x 140	1000	Multi-hull; Self-propelled
13	Oslo Drilling Co.	Odin	Jan.1974	326 x 283	600	Multi-hull; Self-propelled
14	Penrod Drilling Co.	Penrod 70	Jan.1973	245 x 145	800	Multi-hull
15	Penrod Drilling Co.	Penrod 71	Mar. 1973	298 x 216 x 138	1000	Multi-hull
16	Penrod Drilling Co.	Penrod 72	July 1973	298 x 216 x 138	1000	Multi-hull
17	Penrod Drilling Co.	Penrod 73	Nov. 1973	255 x 191 x 128	1000	Multi-hull
18	Penrod Drilling Co.	Penrod 74	July 1973	255 x 191 x 128	1000	Multi-hull
19	Saipem	Scarabeo III	April 1974	358 x 329 x 146	1000	Multi-leg; Triangular

Cont'd/....

Cont'd/.... Table (1.2)

Sr. No.	Owner	Rig Name	Completion Date	Dimensions (ft)	Water Depth (ft)	Category
20	Santa Fe International Corp.	Mariner II	Early 1973	270 x 106	1000	Multi-hull
21	Sea and Land, Inc.	Pentagone 82	late 1972	338 x 325 x 134	660	Multi-leg; Pentagonal
22	Sea and Land, Inc.	Pentagone 84	-	336 x 323 x 134	650	Multi-leg; Pentagonal
23	Southeastern Drilling Co.	Sedco K	1973	382 x 347 x 146	800	Multi-leg; Triangular
24	Southeastern Drilling Co.	Sedco 700	Spring 1973	280 x 245 x 130	1000	Multi-hull
25	Southeastern Drilling Co.	Sedco 702	Spring 1973	280 x 245 x 130	1000	Multi-hull
26	Southeastern Drilling Co.	Sedco 703	Fall 1973	280 x 245 x 130	1000	Multi-hull
27	Southeastern Drilling Co.,	Sedco 704	Spring 1974	280 x 245 x 130	1000	Multi-hull
28	Sea Drilling Netherlands	Sedco/Sedneth 701	Fall 1973	280 x 245 x 130	1000	Multi-hull
29	Peter Smedvig	Norrig 5	May 1973	335 x 349 x 153	1000	Multi-leg; Pentagonal
30	Storm Drilling Co.	Zephyr I	Dec. 1972	202 x 182 x 108	600	Multi-hull
31	Storm Drilling Co.	Zephyr II	Sept.1973	202 x 182 x 108	600	Multi-hull
32	Transocean Drilling Co.	Transocean III	1973	Hull: 400 x 58 x 23	600	Multi-leg
33	Waage Drilling Co.	Waage Drill I	May 1973	320 x 293	600	Multi-hull; Self-propelled
34	Waage Drilling Co.	Waage Drill II	Dec. 1973	320 x 293	600	Multi-hull; Self-propelled
35	Western Oceanic	Western Pacesetter I	Mar. 1973	260 x 200	600	Multi-hull
36	Zapata Corp.	SS - 3000	Aug. 1973	350 x 210 x 130	1500	Multi-hull; Self-propelled
37	Zapata Corp.	Zapata Ugland	Aug. 1973	350 x 210	1000	- ; Self-propelled

Table (1.3) Semi-Submersibles Under Construction

Sr. No.	Owner	Rig Name	Completion Date	Dimensions (ft)	Water Depth (ft)	Category
1	Amoshore Drilling Co.	Colonel Drake	Early 1974	-	600	Multi-hull; Self-propelled
2	Field Int'l Drilling Co.	Pat Rutherford Sr.	Early 1974	222 x 177	600	Multi-hull
3	Penrod Drilling Co.	Penrod 75	late 1973	298 x 216 x 138	1000	Multi-hull
4	Western Oceanic	Western Pacesetter II	late 1973	260 x 200	600	Multi-hull

1.3 Single-Column Semi-Submersible Platforms (Spar Platforms)

Due to the soaring world's energy demand, exploration of undersea oil wells have moved into deeper and rougher waters. With the present technology, drilling in 1,000 ft. water is possible and in near future drilling in 2,000 to 3,000 ft. water is expected. When an oil well has been found in deep water, problems of production and storage of oil arise. Although fixed production platforms have been used successfully in shallow water, they would not be suitable for deep water production because of their high costs of construction and installation. Therefore, other types of production and storage units suitable for using in deep water should be considered. At present three types of production and storage units, viz. submerged, semi-submerged and floating units, can be found. Of the three types, the semi-submerged type seems to be most suitable because it is better than the submerged unit with regard to mobility and is better than the floating unit with regard to good seakeeping characteristics. Due to these considerations, single-column semi-submersible platforms have been proposed to use as production and storage units in deep water.

The description of two different designs of single-column platforms are given below:

(1) Single-Column Production/Storage Platform (Hydronautics, Inc.)

This single-column platform which has an oil storage capacity of 66,500 long tons was proposed by Hydronautics, Inc. of Laurel, Md., in 1969 (Ref. 1.7). The principal characteristics of the platform are shown in Table 1.4.

Table 1.4

Depth	480 ft
Diameter	100 ft
Draught (oil filled)	392 ft
Draught (salt water)	435 ft
Light displacement	21,500 long tons
Loaded displacement (full load oil)	88,000 long tons
Loaded displacement (full load salt water)	97,500 long tons
GM at 392 ft. draught	11 ft
GM at 435 ft. draught	34 ft

The platform can also be used as a production unit from wells in 1000 ft. water. It will have a natural heave period of 30 sec. and will survive in a sea condition with a significant wave height of 62 ft. and a period of maximum wave energy of about 20 sec.

The storage section is divided into several vertical tanks with flooding channels located at the top and bottom to admit oil or salt water. Two sets of damping plates, one at the bottom and the other below the load water-line, are fixed to the platform. The lower damping plates are folded to form a pyramid shaped bow while the platform is being towed to location in a horizontal mode. At the site, the platform is temporarily connected to the previously placed moorings by light wire pennants and is up-ended by pumping the ballast from the upper void space and then filling the main storage tanks via a water inlet manifold system. When the platform reaches the vertical position the mooring cables are winched into position via the light wire pennants. The tanks are always full of liquid when the platform is on station, resulting in small pressure differential between the pressure inside the tank and the surrounding sea.

(2) <u>Single-Column Production/Storage Platform (I.H.C. Holland)</u>

A single-column production and storage platform has been recently developed by I.H.C. Holland in collaboration with S.I.P.M. (Ref. 1.8).

The platform consists of three vertical cylinders, mounted one on top of the other (Fig. 1.20). The top cylinder which is above the water surface is the superstructure, in which production and control equipment and the crew's quarter are situated. A helideck and single point mooring facilities are located on top of the superstructure. The middle cylinder, or vertical column, is situated in the area subjected to surface wave forces. The bottom cylinder, or the body, which is below the water surface gives the storage capacity.

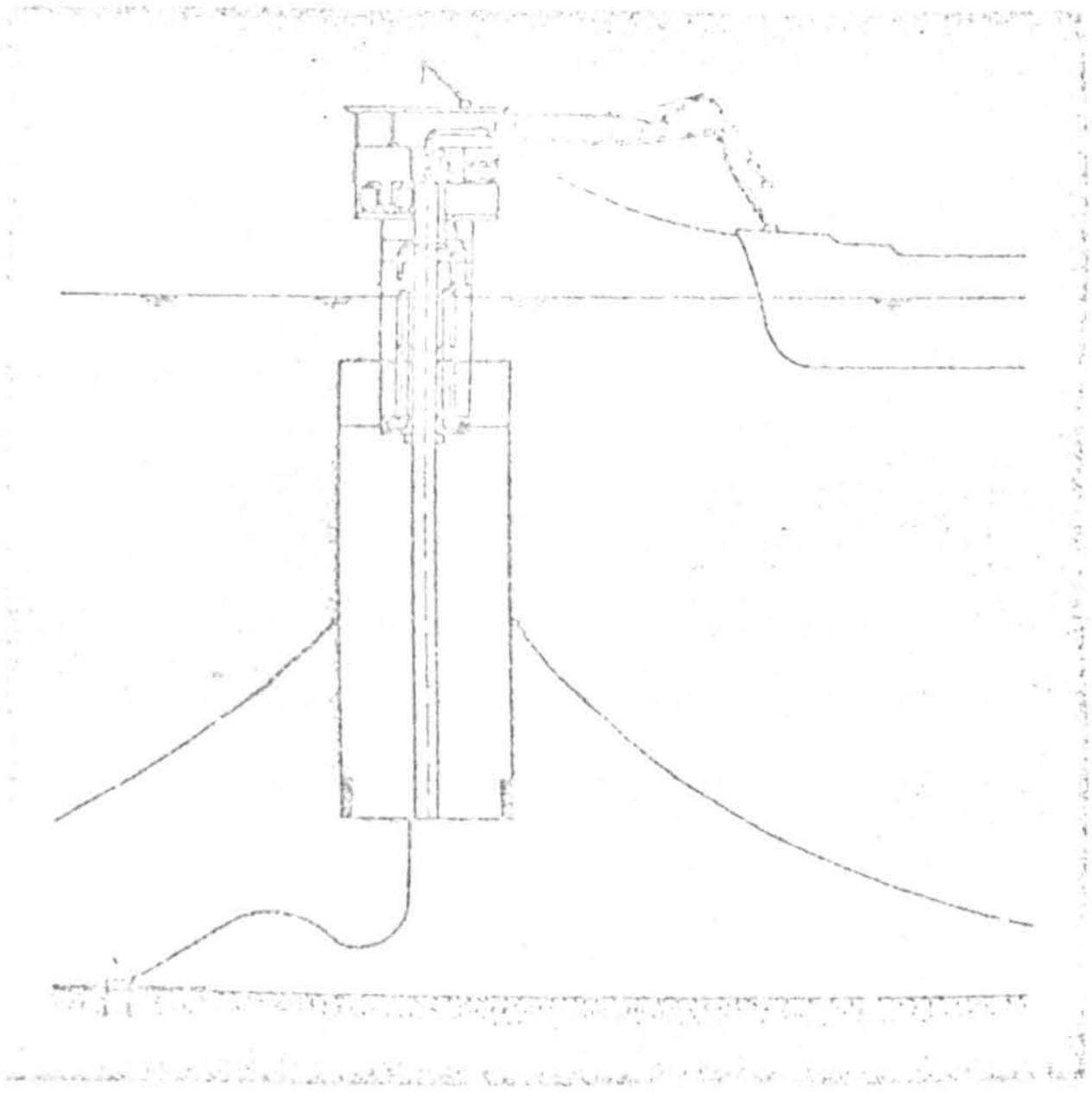

Fig. 1.20 Sectional view of the single-column platform.

The lower two cylinders are divided by radial bulkheads to form six oil-tight compartments and further subdivision into longitudinal compartments is required for strength during towing and up-ending operations.

The platform is designed to fulfil the two main conditions, which are

(i) The tanker must be able to moor and to remain connected to the platform in a given operational weather condition.

(ii) In severe weather conditions (normally 100 year storm conditions are taken), the platform must remain safely anchored on location without tanker.

In addition, it is also designed to meet stability requirements in both the loaded and ballasted conditions.

Main dimensions of the platform are determined on the basis of water depth, bottom clearance, maximum expected wave height, heave criterion and maximum oil storage capacity.

Model tests indicate that the platform which has a natural heave period in excess of 30 sec. behaves well in waves and the maximum angle of tilt is less than 10 degrees.

The platform has a constant draught in both the loaded and ballasted conditions, which implies that the compartments destined to hold oil may not be completely filled with seawater in the ballasted condition because of a difference between specific gravities of oil and water.

From the foregoing it can be seen there is a wide range of designs with a range of claims regarding the performance. At present there exists no ready means of comparing their performance either technically or economically.

The following work attempts to provide a method by which the dimensions of the multi-hull platform with minimum heaving motion in regular waves can be obtained and to show the comparison of the heaving motions of the multi-hull and the multi-leg platforms. From the results presented it is believed that it is possible to make a fairly quick assessment of the heaving motion characteristics of any particular design of the above two types.

CHAPTER 2

HEAVING OF A SEMI-SUBMERSIBLE PLATFORM IN REGULAR WAVES

2.1 Introduction

In this chapter the equation of heaving motion of a semi-submersible platform is derived and the effect of frequency of exciting force on the heaving motion is discussed. The acceptable motion limits from the practical point of view are briefly discussed.

The response amplitude operator which is the ratio of motion amplitude to wave amplitude is obtained both from calculations and from experimentally measured motions of a model in regular waves. No attempt is made to calculate the motion of the platform in irregular waves but the method of determining the motion of the platform in a given seaway by using the response amplitude operator and the energy spectrum of the seaway is described. Considerable attention is given to methods of reducing the response amplitude operator. The work makes clear the need for selecting the natural frequency of heaving below the frequency of the predominant wave in the system.

2.2 Equation of Heaving Motion of a Semi-Submersible Platform

The equation of heaving motion of a semi-submersible platform in regular waves can be written as: (See Appendix 1)

$$(m + m_z)\,\ddot{z} + N_z\,\dot{z} + (\rho g A_w)\,z = F_o \cos(\omega t + \sigma) \qquad (2.1)$$

where m = mass of the platform

m_z = added mass of entrained water of the platform

N_z = equivalent damping coefficient assuming damping proportional to velocity

$(\rho g A_w)$ = restoring coefficient or spring constant, A_w being water plane area

z = linear vertical displacement of the platform from its calm-water position

$\dot{z}$ = dz/dt = heaving velocity of the platform

$\ddot{z}$ = d^2z/dt^2 = heaving acceleration of the platform

F_o = amplitude of wave exciting force

ω = circular frequency of wave

t = time

σ = phase angle by which exciting force leads wave elevation when its value is positive

The solution to the equation of heaving motion is given by:

$$z = z_a \cos(\omega t - \epsilon) \tag{2.2}$$

where

$$z_a = \frac{F_o}{\sqrt{\{\rho g A_w - (m + m_z)\omega^2\}^2 + (N_z\omega)^2}} \tag{2.3}$$

ϵ = phase angle by which heaving motion lags wave elevation when its value is positive.

Since the natural frequency of heaving motion of the platform is given by:

$$\omega_n = \sqrt{\frac{\rho g A_w}{m + m_z}} \tag{2.4}$$

the amplitude of heaving motion of the platform can be rewritten as:

$$z_a = \frac{F_o/\rho g A_w}{\sqrt{\{1 - (\frac{\omega}{\omega_n})^2\}^2 + (2\gamma)^2 (\frac{\omega}{\omega_n})^2}} \tag{2.5}$$

where

$$\gamma = \frac{\text{actual damping}}{\text{critical damping}} = \frac{N_z}{2(m + m_z)\omega_n} \tag{2.6}$$

It can be seen from equation (2.5) that the heave amplitude is directly proportional to the amplitude of exciting force F_o and to

the magnification factor, which is

$$\frac{1}{\sqrt{\left\{1 - \left(\frac{\omega}{\omega_n}\right)^2\right\}^2 + (2\gamma)^2 \left(\frac{\omega}{\omega_n}\right)^2}} \qquad (2.7)$$

but is inversely proportional to the water plane area A_w.

In general, the heave amplitude can be minimised by reducing the exciting force so long as the frequency of exciting force is very much smaller than or greater than the natural frequency of heaving of the platform because when ω is very much less than ω_n, the magnification factor tends to unityand when ω is very much greater than ω_n, the magnification factor has small value. In such cases the effect of γ (or damping) on the heave amplitude is of little practical importance and heave amplitude can be calculated with sufficient accuracy by neglecting damping.

At resonance (i.e. when $\omega = \omega_n$), the magnification factor depends only on γ and attains its maximum value. In such a case the effect of damping on the ~~heave~~ amplitude is very significant and even a very small exciting force can produce ~~heave~~ large amplitude owing to relatively small amount of damping present. The heave amplitude of the platform can be calculated fairly accurately provided the damping is known. Unfortunately, the existing knowledge on hydrodynamic damping is relatively poor, so that it is not possible to calculate the motion accurately near the natural frequency. Thus it is desirable to make the natural frequencies in heave, pitch and roll, very low so that they correspond to range of wave lengths greater than 350 m or 1150 ft. i.e. they lie below the frequency of the predominant waves in all except the most severe storms. Natural periods of semi-submersible platforms are in general greater than 15 sec and frequently of the order of 25 sec. Thus the general practice would be to select a natural frequency which is well below the frequency of maximum wave energy which has been obtained from the measured energy spectrum of the seaway where the platform is to be operated.

The method of determining the motion of the platform from the energy spectrum and the response amplitude operator (i.e. the ratio of heave amplitude to wave amplitude) will be discussed later.

In practice, the most important criterion for the behaviour of the platform is that the motions may not exceed a predetermined value or a limit which has been chosen by considerations of safety and workability. But there are no universally accepted specifications for the limits of platform motion. At present it appears that a heave of approximately 2 m or 7 ft. is the maximum acceptable for drilling and roll and pitch should be kept to less than 3 deg. As the water depth increases to a region where the use of pile-supported fixed platform is not economical, the drill string of semi-submersible platforms can tolerate larger horizontal movements at the sea surface and these can be of the order of 4.5 m or 15 ft. in depths of water greater than 200 m.

From equation (2.5), the motion of the platform in any long-crested regular waves can be calculated when all hydrodynamic coefficients of the platform, i.e. $(m + m_z)$, N_z and $(\rho g A_w)$, and the wave exciting force are known. This result is of importance because it enables us to answer the question whether the motion of the platform will be satisfactory in a given seaway where drilling is to be done.

In nature, regular long-crested waves do not exist and the actual seaway is found to be highly irregular in pattern. A brief note will be given here, on the method of determining the motion of the platform in a desired seaway. The irregular sea surface can be described by superimposing a large number of regular sine waves, the so-called component waves, each with its own direction and period and each of small height/length ratio. The phase relationships among these various component waves are considered to be completely random. Since methods for the treatment of the variability of the direction of sea waves and the observational data on this variability are not yet sufficiently developed, it is usually assumed that the component waves are unidirectional. The spectrum of sea obtained from this

assumption is known as one-dimensional spectrum. By using the statistical theory any seaway can be completely described by its energy spectrum.

The energy spectrum $S_w(\omega)$ is a continuous function (see Fig. 2.1) such that any increment of area under its graph, when multiplied by a suitable constant, represents the wave energy in that incremental band of frequencies (Ref. 2.2).

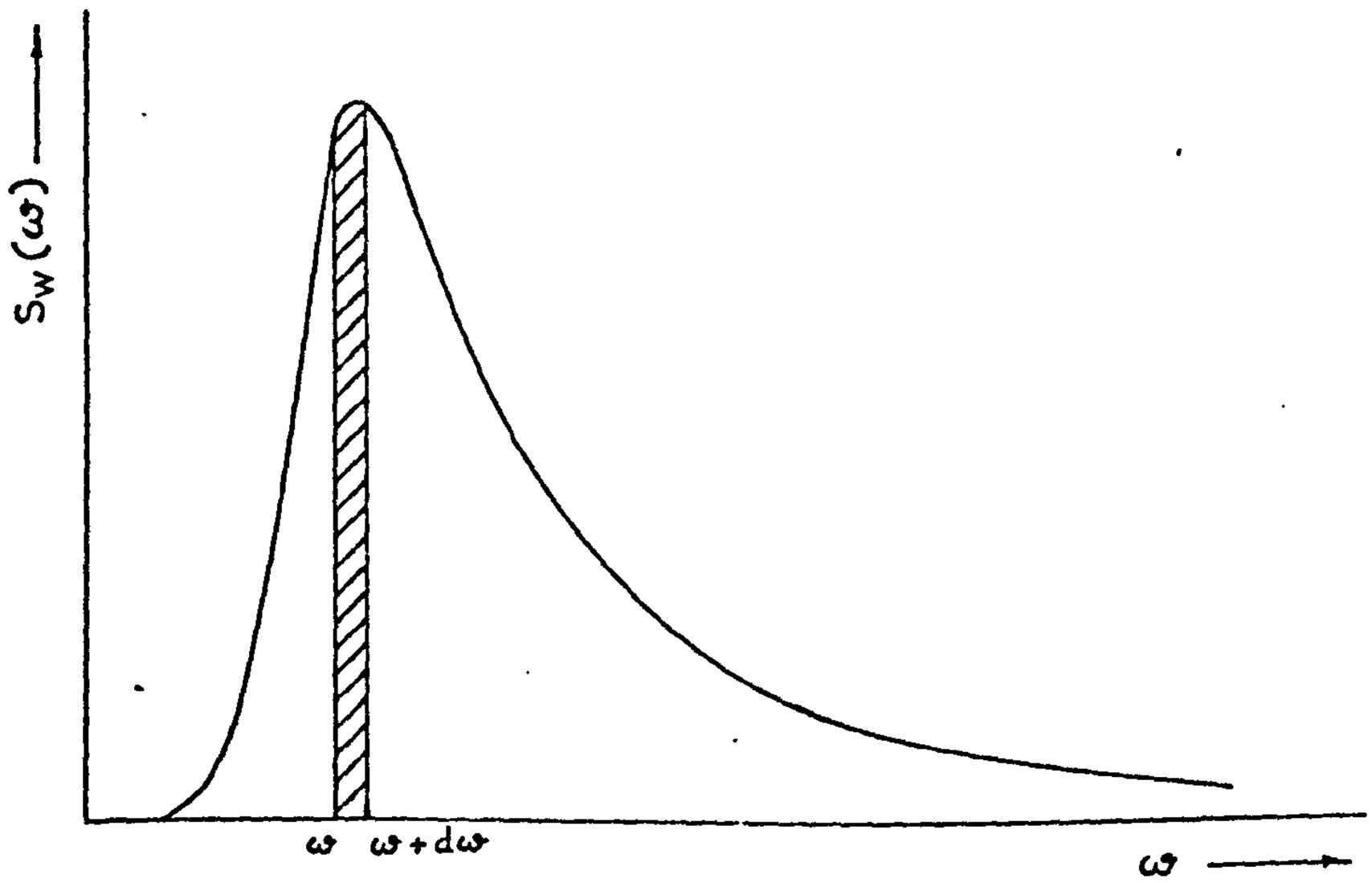

Fig. 2.1 Wave Energy Spectrum

The energy per unit surface area of each component wave is given by

$$\frac{1}{2} \rho g \left[\zeta_a (\omega) \right]^2$$

where ρ is mass density, g is acceleration of gravity and $\zeta_a (\omega)$ is the wave amplitude which is a function of wave frequency. The total energy of component waves present in the frequency interval from ω to $(\omega + d\omega)$, must be equal to the product of the area $S_w (\omega)\, d\omega$ and a constant quantity (ρg). That is

$$\rho g \times S_w (\omega)\, d\omega = \sum_{\omega}^{\omega + d\omega} \frac{1}{2} \rho g \left[\zeta_a (\omega) \right]^2 \qquad (2.8)$$

or simply,

$$S_w(\omega)\ d\omega = \frac{1}{2} \zeta_a^2 \qquad (2.9)$$

In other words the area $S_w(\omega)\ d\omega$ is equal to the mean-square value or 'variance' $\sum \frac{1}{2} \left[\zeta_a(\omega)\right]^2$ of all those component waves whose frequency lies between ω and $(\omega + d\omega)$, and therefore the total area is equal to the total variance (m_o) of an infinite number of waves. Thus

$$\int_0^\infty S_w(\omega)\ d\omega = m_o \qquad (2.10)$$

from which the following statistical properties of apparent (visible) waves are obtained.

Average apparent wave height, crest to trough	$\bar{\bar{h}}_w = 2.5 \sqrt{m_o}$
or average amplitude	$\bar{\bar{\zeta}}_a = 1.25 \sqrt{m_o}$
Average of the 1/3 highest waves, or 'significant' height	$(\bar{\bar{h}}_w)1/3 = 4.0 \sqrt{m_o}$
Average of the 1/10 highest waves	$(\bar{\bar{h}}_w)1/10 = 5.1 \sqrt{m_o}$

In a dynamic problem, it is important that the system is linear, i.e. any response considered is linearly related to the wave amplitude. Then the separate response of the platform to each component wave whose frequency lies between ω and $(\omega + d\omega)$, can be superimposed and represented by the energy spectrum of the platform motion

$$S_q(\omega)\ d\omega = \frac{1}{2} q_a^2 \qquad (2.11)$$

From equations (2.9) and (2.11), the following relations

$$S_q(\omega) = \left(\frac{q_a}{\zeta_a}\right)^2 S_w(\omega) \qquad (2.12)$$

or

$$S_q(\omega) = \left[A(\omega)\right]^2 S_w(\omega) \qquad (2.13)$$

are obtained. The function $\left[A(\omega)\right] = \left(\frac{q_a}{\zeta_a}\right)$ is called the response amplitude operator. The response amplitude operator can be obtained (a) by calculation of responses of the platform in regular waves, using equation (2.5) or from experimentally measured responses of a model to a series of regular waves and (b) by the statistical analysis of platform motion and wave height records taken at sea (Ref. 2.3).

The energy spectrum of the wave can be obtained from an analysis of a wave height record. This analysis can be performed numerically, using an automatic digital computing machine (Digital method) or by using an electro-mechanical device (Analogue method), (Ref. 2.4).

It is evident from equation (2.13) that any two of the three items: energy spectrum of wave, response amplitude operator and energy spectrum of motion being known, the third is immediately derived. Therefore the energy spectrum of the platform motion can be obtained when the response amplitude operator and the energy spectrum of the wave are known. From the energy spectrum of the motion,

various statistical averages of the motion such as $\overline{q}_a$, $(\overline{q}_a)_{1/3}$ and $(\overline{q}_a)_{1/10}$ can be obtained by using the same statistical theory as for sea waves. The relationship between the three items mentioned above is shown in Fig. (2.2).

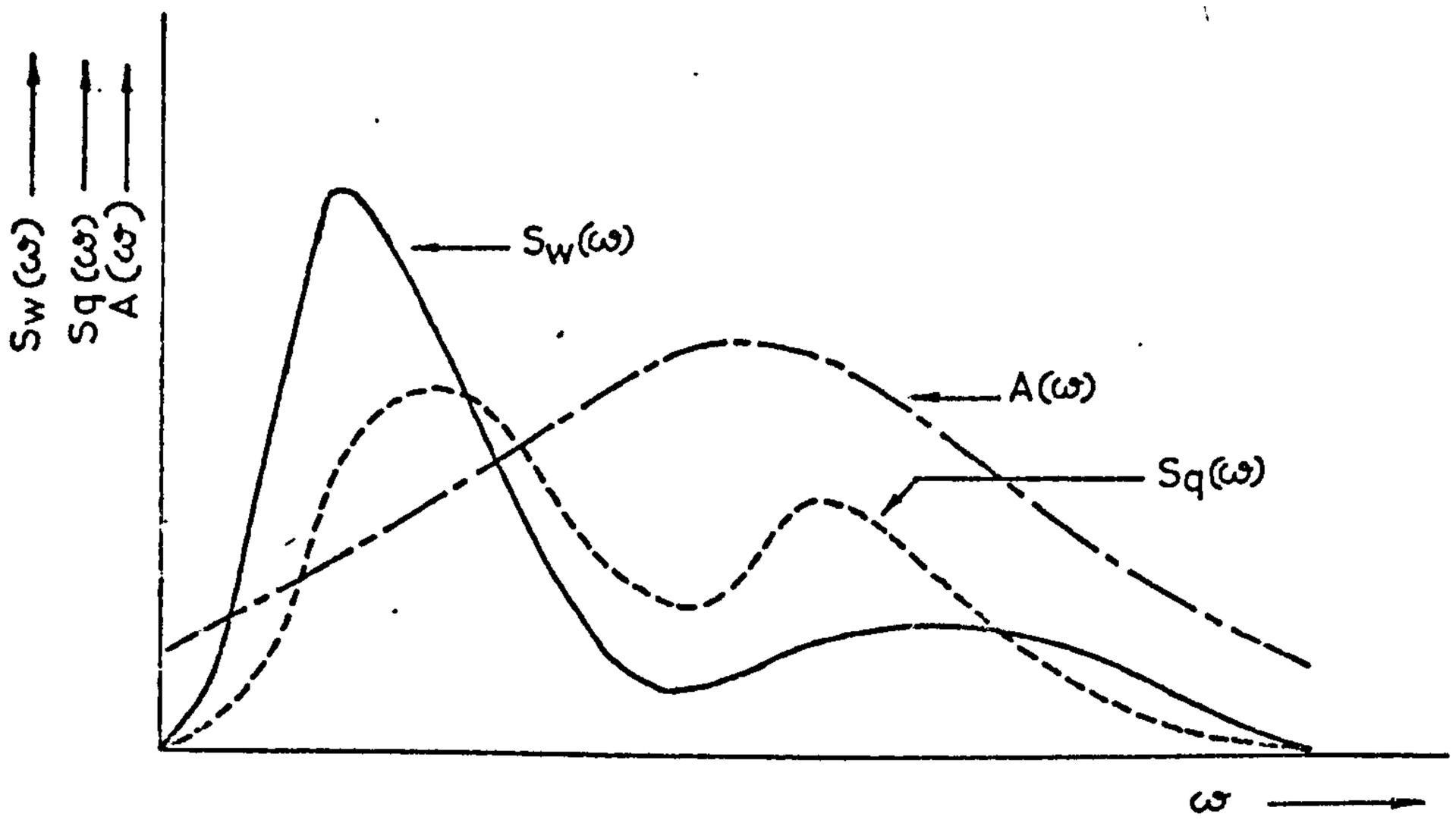

Fig. 2.2 Relationship between wave energy spectrum, response amplitude operator and motion energy spectrum.

The method of obtaining the energy spectrum of the motion from the response amplitude operator and the energy spectrum of the wave has been described above. However, in this thesis no attempt is made to determine the energy spectrum of the motion, but attention is confined to determining the response amplitude operator which can be used in conjunction with the energy spectrum of the wave in any sea area. Since the energy spectrum of the motion is directly proportional to the square of the response amplitude operator for a given energy spectrum of the wave, a reduction in the value of the response amplitude operator will reduce the motion spectrum. Thus in order to obtain the minimum motion of the platform, a detail study on the reduction of the response amplitude operator is made in this work.

CHAPTER 3

DETERMINATION OF WAVE EXCITED FORCES ON A MULTI-HULL AND ON A MULTI-LEG SEMI-SUBMERSIBLE PLATFORMS

3.1 Wave Excited Forces

The wave excited forces on a semi-submersible platform can be approximated by the sum of the following three forces:

(i) The undisturbed pressure force F_{Z1} arising from the pressure change over the hull in a wave that is not disturbed by the presence of the hull (Froude-Kriloff force).

(ii) The inertia force F_{Z2} arising from the acceleration of the water particles in a wave, which is not disturbed by the presence of the hull, acting on the added mass of the hull.

(iii) The damping force F_{Z3} arising from the damping due to hull, of the velocity of the water particles in a wave that is not disturbed by the presence of the hull.

The inertia force and the damping force are 180 deg. and 90 deg. respectively in advance of the undisturbed pressure force.

It will be assumed for the vertical columns and the horizontal cylinders that their dimensions are small compared to the wave length. This assumption has been investigated by Hooft (Ref. 3.1) and he has found that the approximation holds true for a body of which the dimension parallel to the direction of wave travel is equal to or less than one fifth of the wave length. In such a case the maximum difference between the approximation (which is an overestimation) and the exact theory is 5%.

The total wave excited force is obtained by adding the forces on subelements of the semi-submersible platform. In the present work, the subelements are found to be fully submerged cylinders, fully submerged right circular caisson (or footing) and surface piercing vertical columns. The forces on the subelements are computed by the strip theory (Ref. 3.2) which is usually used in the calculation of ship motions. The effect of interference between the subelements is neglected.

Now, the total wave excited force F_Z on the semi-submersible platform can be expressed as:

$$F_Z = \sqrt{(F_{Z1} + F_{Z2})^2 + (F_{Z3})^2} \tag{3.1}$$

The damping force F_{Z3} can be due to potential effects (i.e. dissipation of energy through wave generation) and viscous effects (i.e. dissipation of energy through the action of viscosity). The potential damping is proportional to the velocity of the water particles while the viscous damping is proportional to the square of the velocity. When the nonlinear viscous damping is present in the system, the method of equivalent linearization can be used. The nonlinear damping term is replaced by a linear term such that the work dissipated per cycle by each term is the same (Ref. 3.3).

The damping force is most important in the evaluation of motion amplitudes near resonance, but outside the region of resonance the damping has relatively little effect on the amplitude. Since the damping force on a semi-submersible platform is much less than the undisturbed pressure force and the inertia force, it can be treated as small except near resonance (Ref. 3.4). Also, since the semi-submersible platforms considered in the present work have very low natural frequencies (of the order of 0.314 radian per sec. or a natural period of 20 sec.), the frequencies of most waves will be much greater than the natural frequencies and will be outside the region of resonance. Hence the total wave excited force can be calculated by neglecting the damping force and can be expressed as:

$$F_Z = F_{Z1} + F_{Z2} \tag{3.2}$$

3.2 Wave Excited Forces on a Multi-hull Semi-Submersible Platform

3.2.1 Description of a Multi-hull Semi-Submersible Platform

The multi-hull semi-submersible platform considered has two parallel horizontal cylinders, a variable number of vertical columns on each cylinder and a main deck on top of these columns (Fig. 3.1). The vertical columns are equally spaced on each of the cylinder and the diameter of the column is not to be greater than that of the cylinder. The general shape of the platform shown in Fig. 3.1 is maintained throughout the present work.

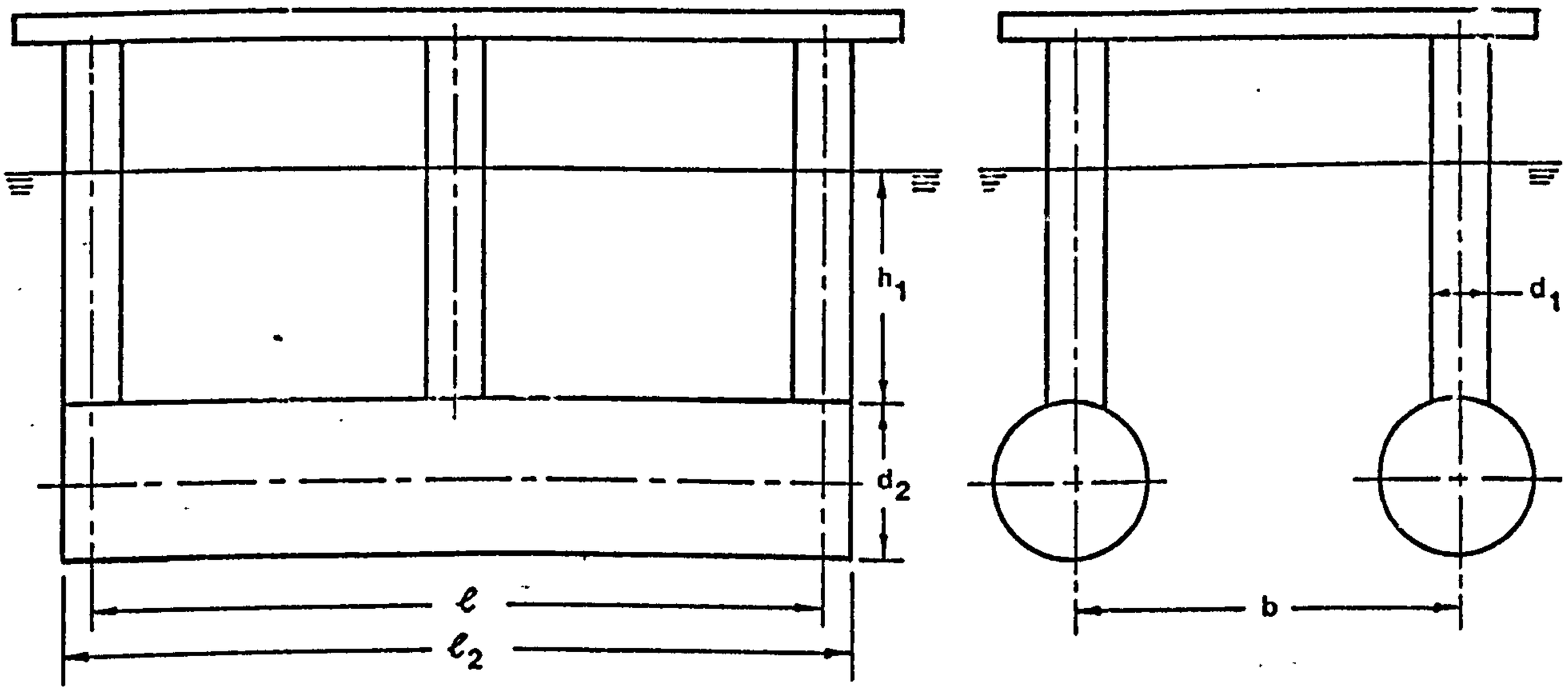

Fig. 3.1 The Multi-hull Semi-Submersible Platform.

It is desirable to have approximately the same period for pitch and roll, and this could be achieved by having the same moment of inertia of the waterplane area about both longitudinal and transverse axes. Thus the beam-length ratio of the platform as a function of the number of columns on each cylinder is derived (see Appendix 2), so that the platform will have the same moment of inertia about the two axes. The beam b is taken as the centre distance between two parallel horizontal cylinders and the length ℓ as the centre distance between two extreme vertical columns which are on one cylinder.

The beam-length ratio as a function of the number of columns on each cylinder n can be expressed in the form:

$$\frac{b}{\ell} = f(n) = \sqrt{\frac{(n+1)}{3(n-1)}} \qquad (3.3)$$

from which the values of (b/ℓ) for different values of n, as shown in Table (3.1), are obtained.

Table (3.1)

n	$\frac{b}{\ell}$
3	0.82
4	0.75
5	0.71
6	0.68

All the multi-hull platforms considered in this work have the same moment of inertia about the two axes.

3.2.2 Calculation of Vertical Wave Excited Forces in Beam-Sea Condition

The space-fixed coordinate system O_1- $\xi\eta\zeta$ and the body-fixed coordinate system O-XYZ are introducted as shown in Fig. 3.2. In calm water, the XOY plane coincides with the $\xi O_1\eta$ plane and the origins of the coordinates lie in the still water level.

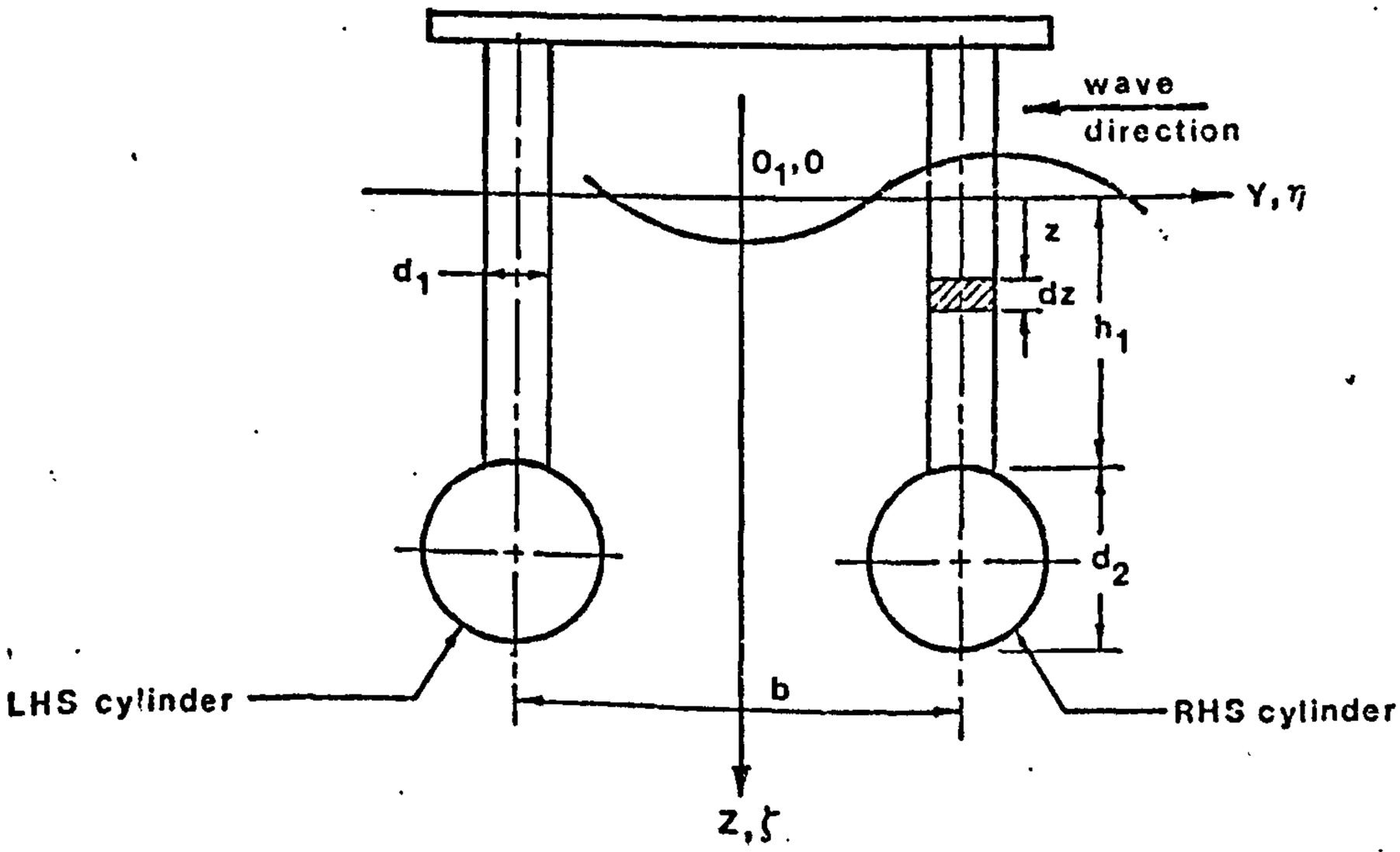

Fig. 3.2 Coordinate System in Beam-Sea Condition.

The motions of the water particles in waves are defined relative to the $O_1 - \xi\eta\zeta$ coordinate system.

The characteristics of a regular long-crested wave progressing in the opposite direction of η in a fluid of infinite depth can be deduced from the velocity potential,

$$\phi = \frac{\omega}{K} \zeta_a e^{-K\zeta} \sin (K\eta + \omega t) \qquad (3.4)$$

where ω = wave frequency = $\frac{2\pi}{T_w} = \sqrt{gK}$

T_w = wave period

K = wave number = $\frac{2\pi}{\lambda} = \frac{\omega^2}{g}$

λ = wave length

g = acceleration due to gravity

ζ_a = wave amplitude

t = time

From equation (3.4) the motion of the water surface, the orbital velocity and acceleration of the water particles, and the pressure variation in waves can be deduced (Ref. 3.5)

The equation of subsurface of waves is given by:

$$\zeta_w = \frac{1}{g} \frac{\partial \phi}{\partial t} = \zeta_a e^{-K\zeta} \cos (K\eta + \omega t), \qquad (3.5)$$

from which the equation of surface elevation is obtained when ζ becomes zero.

The vertical components of orbital velocity and acceleration of the water particles in waves are given by:

$$\dot{\zeta}_w = \frac{d\zeta_w}{dt} = \frac{\partial \phi}{\partial \zeta} = -\omega \zeta_a e^{-K\zeta} \sin (K\eta + \omega t) \qquad (3.6)$$

$$\ddot{\zeta}_w = \frac{d^2\zeta_w}{dt^2} = \frac{d\dot{\zeta}_w}{dt} = -\omega^2 \zeta_a e^{-K\zeta} \cos(K\eta + \omega t) \qquad (3.7)$$

The horizontal components of velocity and acceleration of water particles are given by:

$$\dot{\eta}_w = \frac{\partial\phi}{\partial\eta} = \omega \zeta_a e^{-K\zeta} \cos(K\eta + \omega t) \qquad (3.8)$$

$$\ddot{\eta}_w = \frac{d\dot{\eta}_w}{dt} = -\omega^2 \zeta_a e^{-K\zeta} \sin(K\eta + \omega t) \qquad (3.9)$$

The pressure (due to wave formation only) acting at any point in water is given by:

$$p = -\rho \frac{\partial\phi}{\partial t} = -\rho g \zeta_a e^{-K\zeta} \cos(K\eta + \omega t) \qquad (3.10)$$

where ρ is the mass density of fluid.

The Froude-Kriloff Force (F_{Zl})

The Froude-Kriloff force can be obtained by integrating the pressure acting on the surface of the hull. The multi-hull platform is divided into the subelements (a) fully submerged horizontal cylinders and (b) surface piercing vertical columns.

The Froude-Kriloff force can be written as:

$$F_{Zl} = (F_{Zl})_{cyl.} - (F_{Zl})_{col.} \qquad (3.11)$$

in which

$(F_{Zl})_{cyl.}$ = pressure force acting on the horizontal cylinders with no vertical columns.

$(F_{Zl})_{col.}$ = pressure force acting on the bottom ends of the vertical columns.

The Froude-Kriloff force on the horizontal cylinders $(F_{Z1})_{cyl.}$

From equation (3.10) the vertical pressure force acting on the right hand side (RHS) cylinder is given by: (see Fig. 3.2)

$$(F_{Z1})_{RHS\ cyl.} = -\int_{\theta=0}^{2\pi}\int_{x=-\ell_2/2}^{+\ell_2/2} \rho g\ \zeta_a\ e^{-K\ (h_1 + \frac{d_2}{2} - \frac{d_2}{2}\sin\theta)}$$

$$\cos\left\{K\ (\frac{b}{2} + \frac{d_2}{2}\cos\theta) + \omega t\right\}(\frac{d_2}{2}\ d\theta.dx)\ \sin\theta$$

$$= -\rho g\ \zeta_a\ e^{-K\ (h_1 + \frac{d_2}{2})} \cos\left\{K(\frac{b}{2} + \frac{d_2}{2}\cos\theta) + \omega t\right\}\ \frac{d_2}{2}$$

$$\int_{-\ell_2/2}^{+\ell_2/2} dx \int_0^{2\pi} e^{K\ \frac{d_2}{2}\sin\theta}\ \sin\theta.d\theta.$$

The distance $(\frac{d_2}{2}\cos\theta)$ from the cosine term can be neglected since it is small compared to the distance $\frac{b}{2}$. Also expanding the term $e^{K\ \frac{d_2}{2}\sin\theta}$ into a power series and taking only the first two terms of the series (i.e. $1 + K\ \frac{d_2}{2}\sin\theta$) since the values of $(K\ \frac{d_2}{2}\sin\theta)^2$ and higher powers are negligible due to the smallness of $\frac{d_2}{2}$ compared to the wave length λ, we obtain

$$(F_{Z1})_{RHS\ cyl.} = -\rho g\ \zeta_a \pi\ (\frac{d_2}{2})^2\ e^{-K(h_1 + \frac{d_2}{2})} K\ell_2 \cos\ (K\ \frac{b}{2} + \omega t) \qquad (3.12)$$

The vertical pressure force on the left hand side cylinder is the same as equation (3.12) except $(-K\ \frac{b}{2})$ instead of $(K\ \frac{b}{2})$ in the cosine term. Then the vertical pressure force on both cylinders can

be written as follows:

$$(F_{Z1})_{cyl.} = -2\rho g\, \zeta_a \frac{\pi}{4} d_2^2\, K\ell_2 e^{-K\left(h_1 + \frac{d_2}{2}\right)} \cos K\frac{b}{2} \cos \omega t \qquad (3.13)$$

<u>The Froude-Kriloff force on the bottom of the vertical columns</u> $(F_{Z1})_{col.}$

In calculating the vertical pressure force on the bottom of the columns the pressure variation across the diameter of the column is assumed to be very small since the column diameter is small compared to the wave length and thus the mean pressure at the centre of the bottom surface of the column is taken.

The vertical pressure force on the RHS columns can be expressed as the product of the mean pressure, the area of bottom surface of each column and the number of columns. That is

$$(F_{Z1})_{RHS\ col.} = -\rho g\, \zeta_a \frac{\pi}{4} d_1^2\, n\, e^{-Kh_1} \cos\left(K\frac{b}{2} + \omega t\right) \qquad (3.14)$$

The vertical pressure force on the left hand side columns is the same as equation (3.14) except $\left(-K\frac{b}{2}\right)$ instead of $\left(K\frac{b}{2}\right)$ in the cosine term. Then the force on both RHS and LHS columns can be written as follows:

$$(F_{Z1})_{col.} = -2\rho g\, \zeta_a \frac{\pi}{4} d_1^2\, n\, e^{-Kh_1} \cos K\frac{b}{2} \cos \omega t \qquad (3.15)$$

The Froude-Kriloff force on the platform is obtained by substituting equations (3.13) and (3.15) in equation (3.11) and is expressed in the form:

$$F_{Z1} = 2\rho g\, \zeta_a e^{-Kh_1} \left(\frac{\pi}{4} d_1^2 n - e^{-K\frac{d_2}{2}} \frac{\pi}{4} d_2^2 \times K\ell_2\right) \cos K\frac{b}{2} \cos \omega t \qquad (3.16)$$

From the equation (3.16) it can be seen that the vertical pressure forces on the horizontal cylinder and on the vertical column are acting in opposite directions. The vertical pressure force on the cylinder is acting upward under the wave trough and is downward under the wave crest (Ref. 3.6).

The Inertia Force (F_{Z2})

The inertia force acting in the vertical direction can be expressed as the product of the added mass of the body in the vertical direction and the vertical component of the orbital acceleration of the water particles in a wave that is not disturbed by the presence of the body.

Neglecting the free surface effect, the added mass of a submerged horizontal cylinder oscillating in an infinite fluid is equal to the mass of the displaced volume of the cylinder since the influence of the frequency of oscillation on the added mass can be neglected for the low frequencies which we are concerned, i.e. for frequencies

$$\omega \sqrt{\frac{d_2/2}{g}} < 0.8$$

where ω is the frequency of oscillation (Ref. 4.1). For a semi-submersible platform consisting of submerged horizontal cylinders and surface piercing vertical columns, it is sufficient to consider the added mass of the cylinders only (Ref. 3.4). Thus the added mass, in the vertical direction, of a horizontal cylinder of diameter d_2 and length ℓ_2 is given by:

$$m'_z = \rho \frac{\pi}{4} (d_2)^2 \ell_2 \qquad (3.17)$$

The vertical component of the mean orbital acceleration of the water particles at the centre of the RHS cylinder (see Fig. 3.2) is obtained by substituting $\zeta = (h_1 + \frac{d_2}{2})$ and $\eta = \frac{b}{2}$ in equation (3.7) and is given by:

$$\ddot{\zeta}_w = -\omega^2 \zeta_a e^{-K (h_1 + \frac{d_2}{2})} \cos (K \frac{b}{2} + \omega t) \qquad (3.18)$$

From equations (3.17) and (3.18), the inertia force acting on the RHS cylinder can be expressed as follows:

$$(F_{Z2})_{RHS\ cyl.} = -\rho g\, \zeta_a \frac{\pi}{4} d_2^2\, K\ell_2 e^{-K(h_1 + \frac{d_2}{2})} \cos\,(K\frac{b}{2} + \omega t) \qquad (3.19)$$

The inertia force on the LHS cylinder is the same as equation (3.19) except $(-K\frac{b}{2})$ instead of $(K\frac{b}{2})$ in the cosine term. Then the inertia force on both cylinders can be expressed as follows:

$$F_{Z2} = -2\rho g\, \zeta_a \frac{\pi}{4} d_2^2\, K\ell_2 e^{-K(h_1 + \frac{d_2}{2})} \cos K\frac{b}{2} \cos \omega t \qquad (3.20)$$

By comparing equations (3.13) and (3.20), it can be seen that the Froude-Kriloff force on the submerged horizontal circular cylinders is equal to the inertia force. Therefore, it should be noted that for a submerged horizontal circular cylinder the Froude-Kriloff force can be approximated by the product of the mass of water displaced by the cylinder and the mean value of the orbital acceleration of the water particles at the centre of the cylinder. This is only generally true for circular sections and in other shapes of cross-section the pressure and inertia forces are unlikely to be equal.

The vertical wave excited force on the multi-hull platform in the beam-sea condition is obtained by substituting equations (3.16) and (3.20) in equation (3.2) and is written in the form:

$$F_Z = 2\rho g\, \zeta_a e^{-Kh_1} (\frac{\pi}{4} d_1^2\, n - 2e^{-K\frac{d_2}{2}} \frac{\pi}{4} d_2^2\, K\ell_2) \cos K\frac{b}{2} \cos \omega t \qquad (3.21)$$

The above equation can be written in terms of the total column volume and the total cylinder volume as follows:

$$F_Z = \rho g\, \zeta_a \frac{V_1}{h_1} e^{-Kh_1} (1 - e^{-K\frac{d_2}{2}} 2Kh_1\alpha) \cos K\frac{b}{2} \cos \omega t \qquad (3.22)$$

in which

V_1 = total volume of the vertical columns = $2(\frac{\pi}{4} d_1^2\, h_1\, n)$

V_2 = total volume of the horizontal cylinders = $2(\frac{\pi}{4} d_2^2\, \ell_2)$

$\alpha = \frac{V_2}{V_1}$.

3.2.3 Calculation of Vertical Wave Excited Forces in Head-Sea Condition

The multi-hull platform is considered to heave in the head-sea condition as shown in Fig. 3.3.

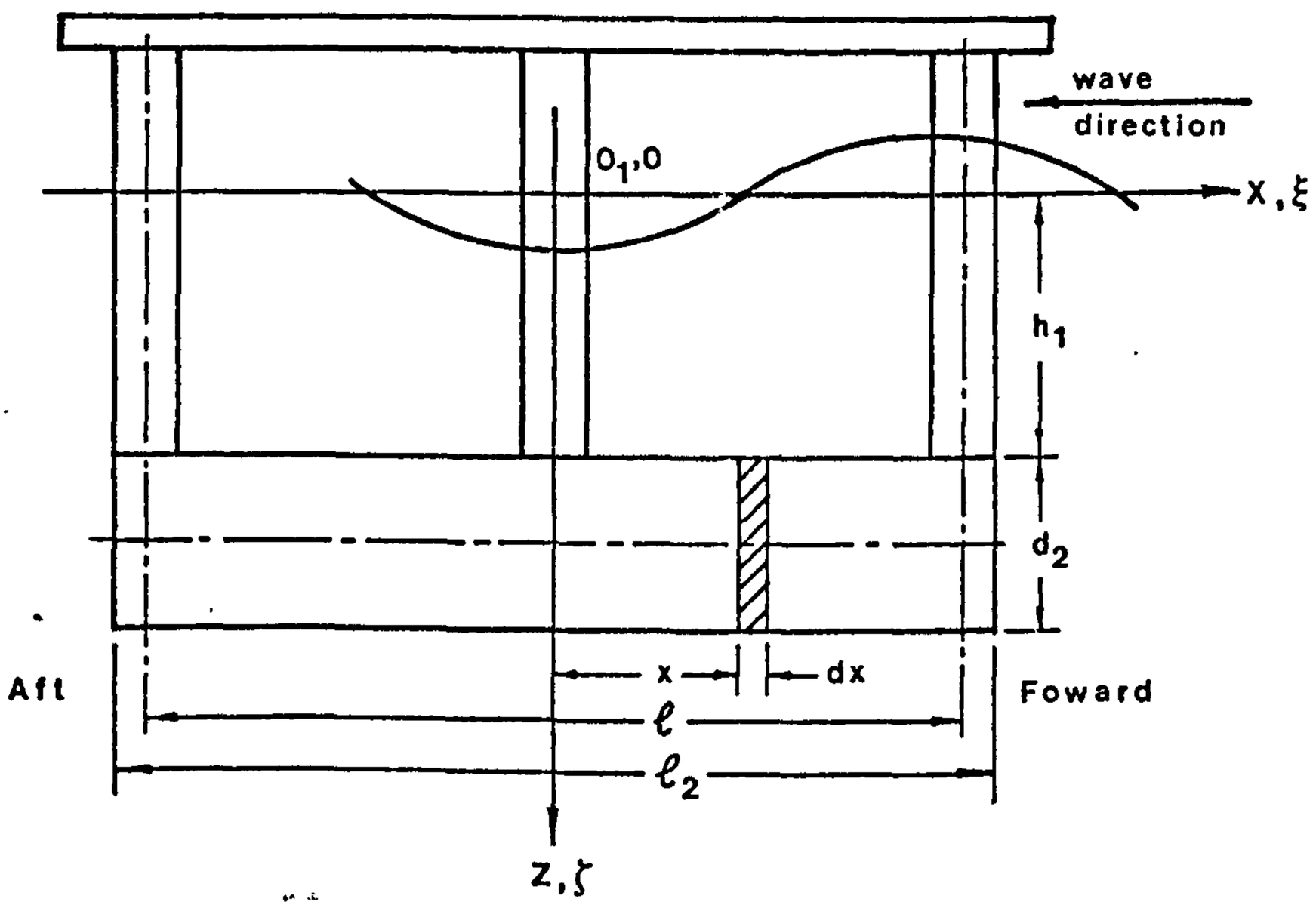

Fig. 3.3 Coordinate System in Head-Sea Condition

The Froude Kriloff Force (F_{Z1})

As in the case of the beam-sea condition, the Froude-Kriloff force on the platform in the head-sea condition can be written as follows:

$$F_{Z1} = (F_{Z1})_{cyl.} - (F_{Z1})_{col.} \tag{3.23}$$

The Froude-Kriloff force on the horizontal cylinders $(F_{Z1})_{cyl.}$

The Froude-Kriloff force on the horizontal cylinders is approximated by using the strip theory. The cylinder is divided into a number of small sections of length dx and the force due to pressure acting on each section is evaluated. The force on the entire length of the cylinder is obtained by integrating the force on the individual section over the length ℓ_2.

For head-sea condition, the equations for subsurface waves, for orbital velocity and acceleration of the water particles and for pressure due to wave are obtained by substituting ξ instead of η in equation (3.5) to equation (3.10).

The vertical pressure force on a section of length dx and at a distance x from the Z-axis (see Fig. 3.3) can be written as:

$$df_z = -\rho g \zeta_a \frac{d_2}{2} e^{-K(h_1 + \frac{d_2}{2})} \cos(Kx + \omega t)dx \int_0^{2\pi} e^{-K\frac{d_2}{2}\sin\theta} \sin\theta . d\theta \quad (3.24)$$

from which the force on two horizontal cylinders can be deduced as follows:

$$(F_{Z1})_{cyl.} = -2\rho g \zeta_a \frac{d_2}{2} e^{-K(h_1 + \frac{d_2}{2})} \int_0^{2\pi} e^{-K\frac{d_2}{2}\sin\theta} \sin\theta . d\theta \int_{-\ell_2/2}^{+\ell_2/2} \cos(Kx + \omega t)dx \quad (3.25)$$

In the above equation, the exponential $e^{K\frac{d_2}{2}\sin\theta}$ is expanded into a power series and only the first two terms (i.e. $1 + K\frac{d_2}{2}\sin\theta$) are taken since the values of $(K\frac{d_2}{2}\sin\theta)^2$ and higher powers are negligible due to the smallness of $\frac{d_2}{2}$ compared to the wave length λ, and when the integrals are evaluated we obtain

$$(F_{Z1})_{cyl.} = -4\rho g\, \zeta_a \frac{\pi}{4} d_2^2\, e^{-K(h_1 + \frac{d_2}{2})} \sin\frac{K\ell_2}{2} \cos\omega t \qquad (3.26)$$

<u>The Froude-Kriloff force on the bottom of the vertical columns</u> $(F_{Z1})_{col.}$

The Froude-Kriloff force on the bottom of the vertical columns in the head-sea condition can be calculated as in the case of the beam-sea condition. The force on the bottom of the columns is expressed in the form:

$$(F_{Z1})_{col.} = -2\rho g\, \zeta_a \frac{\pi}{4} d_1^2\, e^{-Kh_1} (Q_o) \cos\omega t \qquad (3.27)$$

in which

$$Q_o = (1 + \sum_{i=1}^{(n-1)/2} 2\cos Kx_i); \quad x_i = \frac{\ell}{(n-1)} i, \text{for } n = \text{odd} \qquad (3.28)$$

$$Q_o = (\sum_{i=1}^{n/2} 2\cos Kx_i); \quad x_i = \frac{\ell}{(n-1)} \frac{(2i-1)}{2}, \text{ for } n = \text{even} \qquad (3.29)$$

The Froude-Kriloff force on the multi-hull platform in the head-sea condition is obtained by substituting equations (3.26) and (3.27) in equation (3.23) and is expressed as follows:

$$F_{Z1} = 2\rho g\, \zeta_a \frac{\pi}{4} d_1^2\, e^{-Kh_1} \left\{ Q_o - 2\left(\frac{d_2}{d_1}\right)^2 e^{-K\frac{d_2}{2}} \sin\frac{K\ell_2}{2} \right\} \cos\omega t \qquad (3.30)$$

<u>The Inertia Force</u> (F_{Z2})

The inertia force on the submerged horizontal cylinders is obtained, as in the case of the beam-sea condition.

The inertia force acting on a small section of length dx and at a distance x from the Z-axis (see Fig. 3.3) is obtained by the product of the added mass of the section and the mean orbital acceleration of the water particles at the centre of the section.

The added mass of the section being $\rho \frac{\pi}{4} d_2^2 \, dx$ and by using equation (3.7), the force on the section is given by:

$$df_z = -\rho \frac{\pi}{4} d_2^2 \omega^2 \zeta_a e^{-K(h_1 + \frac{d_2}{2})} \cos (Kx + \omega t) \, dx \qquad (3.31)$$

from which the inertia force on the two horizontal cylinders can be deduced as follows:

$$F_{Z2} = -2\rho \frac{\pi}{4} d_2^2 \omega^2 \zeta_a e^{-K(h_1 + \frac{d_2}{2})} \int_{-\ell_2/2}^{+\ell_2/2} \cos (Kx + \omega t) \, dx$$

$$= -4\rho g \zeta_a \frac{\pi}{4} d_2^2 e^{-K(h_1 + \frac{d_2}{2})} \sin \frac{K\ell_2}{2} \cos \omega t \qquad (3.32)$$

When comparing equations (3.32) and (3.26) it is found that, as in the case of the beam-sea condition, the Froude-Kriloff force and the inertia force acting on the submerged horizontal cylinders are equal.

The vertical wave excited force on the multi-hull platform in the head-sea condition is obtained by substituting equations (3.30) and (3.32) in equation (3.2) and is expressed as follows:

$$F_Z = 2\rho g \zeta_a \frac{\pi}{4} d_1^2 e^{-Kh_1} \left\{ Q_o - 4\left(\frac{d_2}{d_1}\right)^2 e^{-K\frac{d_2}{2}} \sin \frac{K\ell_2}{2} \right\} \cos \omega t \qquad (3.33)$$

The above equation can be written in terms of the total column volume and the total cylinder volume as follows:

$$F_Z = \rho g \zeta_a \frac{V_1}{h_1} e^{-Kh_1} \left\{ \frac{Q_o}{n} - e^{-K\frac{d_2}{2}} \frac{4a}{(\ell_2/h_1)} \sin \frac{K\ell_2}{2} \right\} \cos \omega t \qquad (3.34)$$

3.2.4 Calculation of Horizontal Wave Excited Forces in Beam-Sea Condition

The Froude-Kriloff Force (F_{Y1})

The Froude-Kriloff force F_{Y1} acting on the multi-hull platform in the beam-sea condition is obtained by the sum of the horizontal pressure forces on the horizontal cylinders and on the vertical columns.

The Froude-Kriloff force on the horizontal cylinders $(F_{Y1})_{cyl.}$

The horizontal pressure force acting on a small section of length dx of the RHS cylinder (see Fig. 3.2) can be expressed as follows:

$$df_y = -\rho g \zeta_a e^{-K(h_1 + \frac{d_2}{2})} \cos(K\frac{b}{2} + \omega t - K\frac{d_2}{2}\cos\theta)(\frac{d_2}{2} d\theta.dx)\cos\theta \quad (3.35)$$

From equation (3.35), the horizontal pressure force on the whole length of the RHS cylinder can be deduced as follows:

$$(F_{Y1})_{RHS\ cyl.} = -\rho g \zeta_a e^{-K(h_1 + \frac{d_2}{2})} \frac{d_2}{2} \int_{-\ell_2/2}^{+\ell_2/2} dx \int_0^{2\pi} \cos(K\frac{b}{2} + \omega t - K\frac{d_2}{2}\cos\theta) \cos\theta.d\theta$$

$$= -\rho g \zeta_a e^{-K(h_1 + \frac{d_2}{2})} \frac{d_2}{2} \ell_2 \, 2\pi J_1(K\frac{d_2}{2}) \sin(K\frac{b}{2} + \omega t) \quad (3.36)$$

in which $J_1(K\frac{d_2}{2})$ is the Bessel function of the first kind.

The horizontal pressure force on the LHS cylinder is the same as equation (3.36) except $(-K\frac{b}{2})$ instead of $(K\frac{b}{2})$ in the sine term. Then the horizontal force on both RHS and LHS can be written in the form:

$$(F_{Y1})_{cyl.} = -2\rho g \zeta_a e^{-K(h_1 + \frac{d_2}{2})} \frac{d_2}{2} \ell_2 2\pi J_1(K\frac{d_2}{2}) \cos K\frac{b}{2} \sin \omega t \quad (3.37)$$

Since $\frac{d_2}{2}$ is small compared to the wave length λ,

$J_1(K\frac{d_2}{2}) \approx \frac{1}{2}(K\frac{d_2}{2})$ and when this value is substituted in equation (3.37), we obtain

$$(F_{Y1})_{cyl.} = -2\rho g\ \zeta_a \frac{\pi}{4} d_2^2\ e^{-K(h_1 + \frac{d_2}{2})}\ K\ell_2 \cos K\frac{b}{2} \sin \omega t \qquad (3.38)$$

The Froude-Kriloff force on the vertical columns $(F_{Y1})_{col.}$

The horizontal pressure force acting on a small section (of the RHS column) of length dz and at a distance z from the still water level (see Fig. 3.2) can be expressed as:

$$df_y = -\rho g\ \zeta_a\ e^{-Kz} \cos\ (\overline{K\frac{b}{2} + \omega t} - K\frac{d_1}{2}\cos\theta)(\frac{d_1}{2} d\theta.dz)\cos\theta \qquad (3.39)$$

From equation (3.39) the horizontal force on n number of RHS columns can be deduced as follows:

$$(F_{Y1})_{RHS\ col.} = -n\rho g\ \zeta_a \frac{d_1}{2} \int_0^{h_1} e^{-Kz}\, dz \int_0^{2\pi} \cos(\overline{K\frac{b}{2} + \omega t} - K\frac{d_1}{2}\cos\theta)\ \cos\theta.d\theta$$

$$= -n\rho g\ \zeta_a \frac{d_1}{2}\frac{1}{K}(1 - e^{-Kh_1})2\pi J_1(K\frac{d_1}{2})\sin(K\frac{b}{2} + \omega t) \qquad (3.40)$$

where $J_1(K\frac{d_1}{2})$ is the Bessel function of first kind.

The horizontal pressure force on n number of LHS columns is the same as equation (3.40) except $(-K\frac{b}{2})$ instead of $(K\frac{b}{2})$ in the sine term. Then the horizontal force on both RHS and LHS columns can be written in the form:

$$(F_{Y1})_{col.} = -n\rho g\ \zeta_a \frac{d_1}{2}\frac{1}{K}(1 - e^{-Kh_1})2\pi J_1(K\frac{d_1}{2})2\ \cos K\frac{b}{2} \sin \omega t \qquad (3.41)$$

Since $\frac{d_1}{2}$ is small compared to the wave length λ,

$J_1(K\frac{d_1}{2}) \approx \frac{1}{2}(K\frac{d_1}{2})$ and when this value is substituted in equation (3.41), we obtain

$$(F_{Y1})_{col.} = -2n\rho g\, \zeta_a \frac{\pi}{4} d_1^2 (1 - e^{-Kh_1}) \cos K\frac{b}{2} \sin \omega t \qquad (3.42)$$

From equations (3.38) and (3.42) the Froude-Kriloff force on the platform is obtained and is given by:

$$F_{Y1} = -2n\rho g\, \zeta_a \frac{\pi}{4} d_1^2 \left\{(\frac{d_2}{d_1})^2 \frac{K\ell_2}{n} e^{-K(h_1 + \frac{d_2}{2})} + (1 - e^{-Kh_1})\right\} \cos K\frac{b}{2} \sin \omega t \qquad (3.43)$$

<u>The Inertia Force</u> (F_{Y2})

The inertia force F_{Y2} acting on the multi-hull platform in the beam-sea condition is obtained by the sum of the inertia forces on the horizontal cylinders and on the vertical columns.

<u>The Inertia force on the horizontal cylinders</u> $(F_{Y2})_{cyl.}$

The inertia force on the RHS cylinder (see Fig. 3.2) is obtained by the product of the added virtual mass of the cylinder in the horizontal direction and the mean horizontal acceleration of the water particles at the centre of the cylinder. Thus the inertia force on the RHS cylinder is given by:

$$(F_{Y2})_{RHS\ cyl.} = -\rho g\, \zeta_a \frac{\pi}{4} d_2^2\, K\ell_2\, e^{-K(h_1 + \frac{d_2}{2})} \sin (K\frac{b}{2} + \omega t) \qquad (3.44)$$

The inertia force on the LHS cylinder is the same as equation (3.44) except $(-K\frac{b}{2})$ instead of $(K\frac{b}{2})$ in the sine term. Then the force on both RHS and LHS cylinders can be expressed as follows:

$$(F_{Y2})_{cyl.} = -2\rho g\, \zeta_a \frac{\pi}{4} d_2^2\, K\ell_2\, e^{-K(h_1 + \frac{d_2}{2})} \cos K\frac{b}{2} \sin \omega t \qquad (3.45)$$

The inertia force on the vertical columns $(F_{Y1})_{col.}$

The inertia force acting on a small section (of the RHS column) of length dz and at a distance z from the still water level (see Fig. 3.2) can be expressed as:

$$df_y = -\rho g \sum_a \frac{\pi}{4} d_1^2 K e^{-Kz} dz \sin\left(K\frac{b}{2} + \omega t\right) \tag{3.46}$$

From equation (3.46) the inertia force on n number of RHS columns can be deduced as follows:

$$(F_{Y2})_{RHS\ col.} = -n\rho g \sum_a \frac{\pi}{4} d_1^2 K \sin\left(K\frac{b}{2} + \omega t\right) \int_0^{h_1} e^{-Kz} dz$$

$$= -n\rho g \sum_a \frac{\pi}{4} d_1^2 (1 - e^{-Kh_1}) \sin\left(K\frac{b}{2} + \omega t\right) \tag{3.47}$$

The inertia force on n number of LHS columns is the same as equation (3.47) except $\left(-K\frac{b}{2}\right)$ instead of $\left(K\frac{b}{2}\right)$ in the sine term. Then the force on both RHS and LHS columns can be expressed as:

$$(F_{Y2})_{col.} = -2n\rho g \sum_a \frac{\pi}{4} d_1^2 (1 - e^{-Kh_1}) \cos K\frac{b}{2} \sin \omega t \tag{3.48}$$

The inertia force on the platform is obtained from equations (3.45) and (3.48) and is given by:

$$F_{Y2} = -2n\rho g \sum_a \frac{\pi}{4} d_1^2 \left\{\left(\frac{d_2}{d_1}\right)^2 \frac{K\ell_2}{n} e^{-K\left(h_1 + \frac{d_2}{2}\right)} + (1 - e^{-Kh_1})\right\} \cos K\frac{b}{2} \sin \omega t \tag{3.49}$$

From equations (3.49) and (3.43) it can be seen that the inertia force is equal to the Froude-Kriloff force.

The horizontal wave excited force on the multi-hull platform in the beam-sea condition is obtained from equations (3.43) and (3.49) and is given by:

$$F_Y = -4n\rho g \sum_a \frac{\pi}{4} d_1^2 \left\{\left(\frac{d_2}{d_1}\right)^2 \frac{K\ell_2}{n} e^{-K\left(h_1 + \frac{d_2}{2}\right)} + (1 - e^{-Kh_1})\right\} \cos K\frac{b}{2} \sin \omega t \tag{3.50}$$

3.2.5 Calculation of Horizontal Wave Excited Forces in Head-Sea Condition

The Froude-Kriloff force (F_{X1})

As in the case of beam-sea condition, the Froude-Kriloff force F_{X1} on the multi-hull platform is obtained by the sum of the horizontal pressure forces on the horizontal cylinders and on the vertical columns.

The Froude-Kriloff force on the horizontal cylinders $(F_{X1})_{cyl.}$

The horizontal pressure force on the horizontal cylinders is obtained by the product of the cross-sectional area of the cylinder, the difference in the mean pressures between the forward and aft ends of the cylinders and the number of cylinders. Thus the horizontal pressure force can be written as:

$$(F_{X1})_{cyl.} = \frac{\pi}{4} d_2^2 \left[-\rho g \, \zeta_a e^{-K(h_1 + \frac{d_2}{2})} \left\{ \cos(-K \frac{\ell_2}{2} + \omega t) - \cos(K \frac{\ell_2}{2} + \omega t) \right\} \right] \times 2$$

$$= -4\rho g \, \zeta_a \frac{\pi}{4} d_2^2 \, e^{-K(h_1 + \frac{d_2}{2})} \sin \frac{K\ell_2}{2} \sin \omega t \qquad (3.51)$$

The Froude-Kriloff force on the vertical columns $(F_{X1})_{col.}$

The horizontal pressure force on the vertical columns in the head-sea condition is obtained by using the same method as in the case of the beam-sea condition and is expressed in the form:

$$(F_{X1})_{col.} = -2\rho g \, \zeta_a \frac{\pi}{4} d_1^2 \, (1 - e^{-Kh_1}) \, (Q_o) \sin \omega t \qquad (3.52)$$

where Q_o is given by the equations (3.28) and (3.29).

The Froude-Kriloff force on the platform is obtained from the equations (3.51) and (3.52) and is given by:

$$F_{X1} = -2\rho g \, \zeta_a \frac{\pi}{4} d_1^2 \left\{ (1 - e^{-Kh_1}) Q_o + 2(\frac{d_2}{d_1})^2 \, e^{-K(h_1 + \frac{d_2}{2})} \sin K \frac{\ell_2}{2} \right\} \sin \omega t \qquad (3.53)$$

The Inertia Force (F_{X2})

The inertia force on the platform is obtained as the sum of the inertia forces on the horizontal cylinders and on the vertical columns.

The inertia force on the horizontal cylinders $(F_{X2})_{cyl.}$

The inertia force on the horizontal cylinders is obtained as the sum of the inertia forces on the forward and aft ends of the cylinders.

The added virtual mass (A.V.M.) of the horizontal cylinder in the horizontal direction is given by:

$$\text{A.V.M.} = \frac{4}{3}\rho\pi\left(\frac{d_2}{2}\right)^3 J\, C_{V4} \quad \text{(see Appendix 4)} \tag{3.54}$$

where

$J = 0.635$

C_{V4} = added mass coefficient for a mean aspect ratio of $\dfrac{\pi d_2/4}{\ell_2}$

The inertia force on the forward ends (see Fig. 3.3) of the two cylinders can be written as follows:

$$(F_{X2})_{for'd.} = -2\rho g \int_a \frac{\pi}{4} d_2^2 \left(\frac{2}{3} C_{V4} JK \frac{d_2}{2}\right) e^{-K\left(h_1 + \frac{d_2}{2}\right)} \sin\left(K\frac{\ell_2}{2} + \omega t\right) \tag{3.55}$$

The inertia force on the aft ends of the two cylinders is the same as equation (3.55) except $(-K\frac{b}{2})$ instead of $(K\frac{b}{2})$ in the sine term.

Thus the inertia force on both ends of the horizontal cylinders can be written in the form:

$$(F_{X2})_{cyl.} = -4\rho g \int_a \frac{\pi}{4} d_2^2 \left(\frac{2}{3} C_{V4} JK \frac{d_2}{2}\right) e^{-K\left(h_1 + \frac{d_2}{2}\right)} \cos K\frac{\ell_2}{2} \sin \omega t \tag{3.56}$$

The inertia force on the vertical columns $(F_{X2})_{col.}$

It has been shown in the beam-sea condition that the inertia force on the vertical columns is equal to the horizontal pressure force. Therefore for the head-sea condition, it can also be shown that the inertia force on the columns is the same as that of the horizontal pressure force on the columns which is given by the equation (3.52). Thus the inertia force on the vertical columns can be written as:

$$(F_{X2})_{col.} = -2\rho g \; \zeta_a \frac{\pi}{4} d_1^2 \; (1 - e^{-Kh_1}) \; (Q_o) \sin \omega t \qquad (3.57)$$

The inertia force on the platform in the head-sea condition is obtained from equations (3.56) and (3.57) and is given by:

$$(F_{X2}) = -2\rho g \; \zeta_a \frac{\pi}{4} d_1^2 \left\{ (1-e^{-Kh_1}) Q_o + 2\left(\frac{d_2}{d_1}\right)^2 \left(\frac{2}{3} C_{V4} JK \frac{d_2}{2}\right) e^{-K\left(h_1 + \frac{d_2}{2}\right)} \cos K \frac{\ell_2}{2} \right\} \sin \omega t \qquad (3.58)$$

From equations (3.53) and (3.58) the horizontal wave excited force on the multi-hull platform in the head-sea condition is obtained and is expressed in the form:

$$F_X = -4\rho g \; \zeta_a \frac{\pi}{4} d_1^2 \left[(1-e^{-Kh_1}) Q_o + \left(\frac{d_2}{d_1}\right)^2 e^{-K\left(h_1 + \frac{d_2}{2}\right)} \left\{ \sin K \frac{\ell_2}{2} + \left(\frac{2}{3} C_{V4} JK \frac{d_2}{2}\right) \cos K \frac{\ell_2}{2} \right\} \right] \sin \omega t \qquad (3.59)$$

3.3 Wave Excited Forces on a Multi-leg Semi-Submersible Platform

3.3.1 Description of a Multi-leg Semi-submersible Platform

The multi-leg semi-submersible platform has a variable number of legs n and a main deck on top of these legs (Fig. 3.4). Each leg consists of an upright circular caisson (or footing) at the bottom of the leg and on top of the centre of the caisson is a vertical column having the diameter smaller than that of the caisson. The vertical

legs are equally spaced round a circle of radius R_c . This arrangement produces equal moment of inertia of waterplane area about any axes (see Appendix 3).

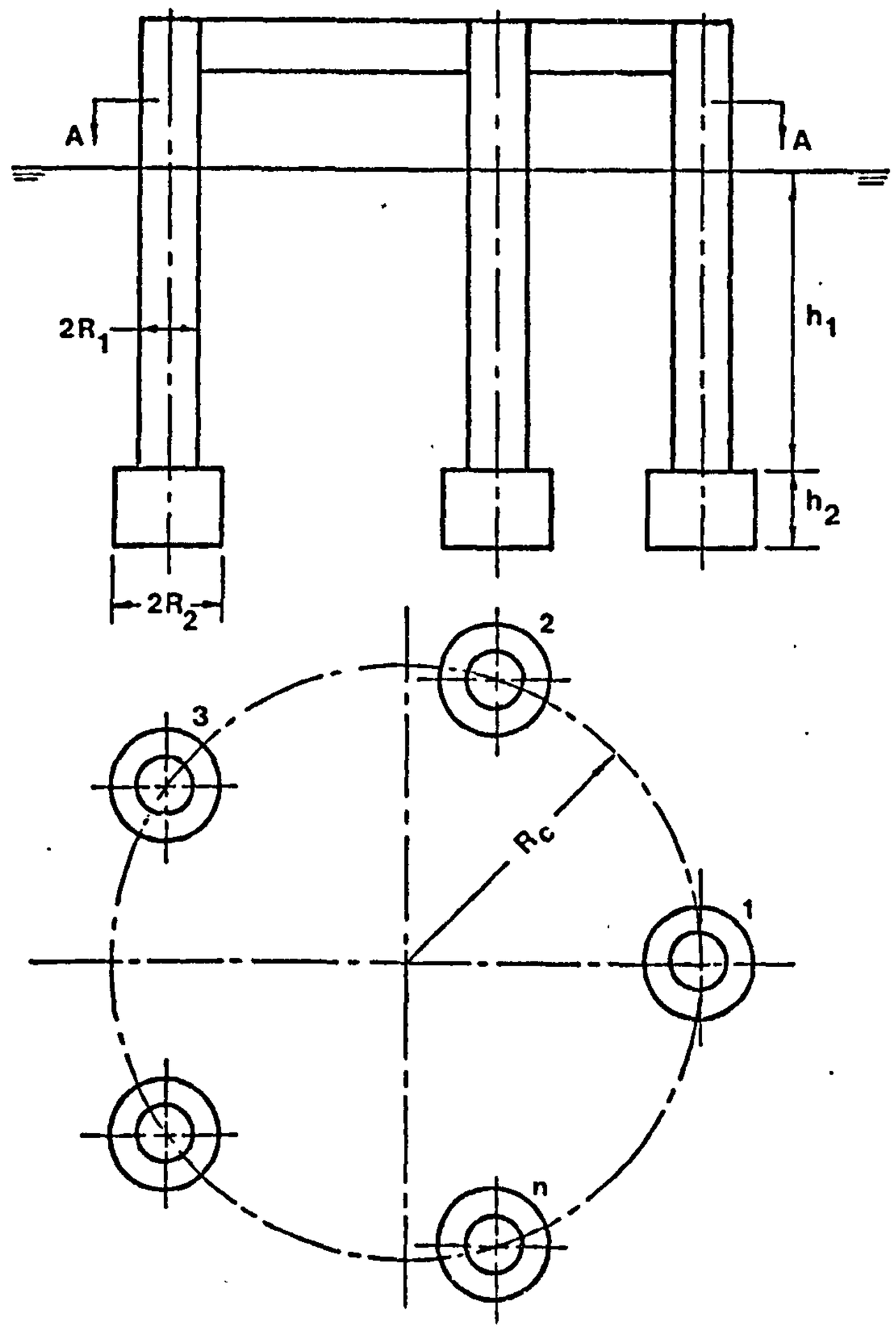

Fig. 3.4 The Multi-leg Semi-submersible Platform

3.3.2 Calculation of Vertical Wave Excited Forces in Beam-Sea and Head-Sea Conditions

The multi-leg platform with n number of vertical legs is assumed to be orientated to the wave direction as shown in Fig. 3.5. When the angle of orientation ϕ is equal to 90 deg. the platform will be

in the beam-sea condition and when ϕ is equal to zero, it will be in the head-sea condition.

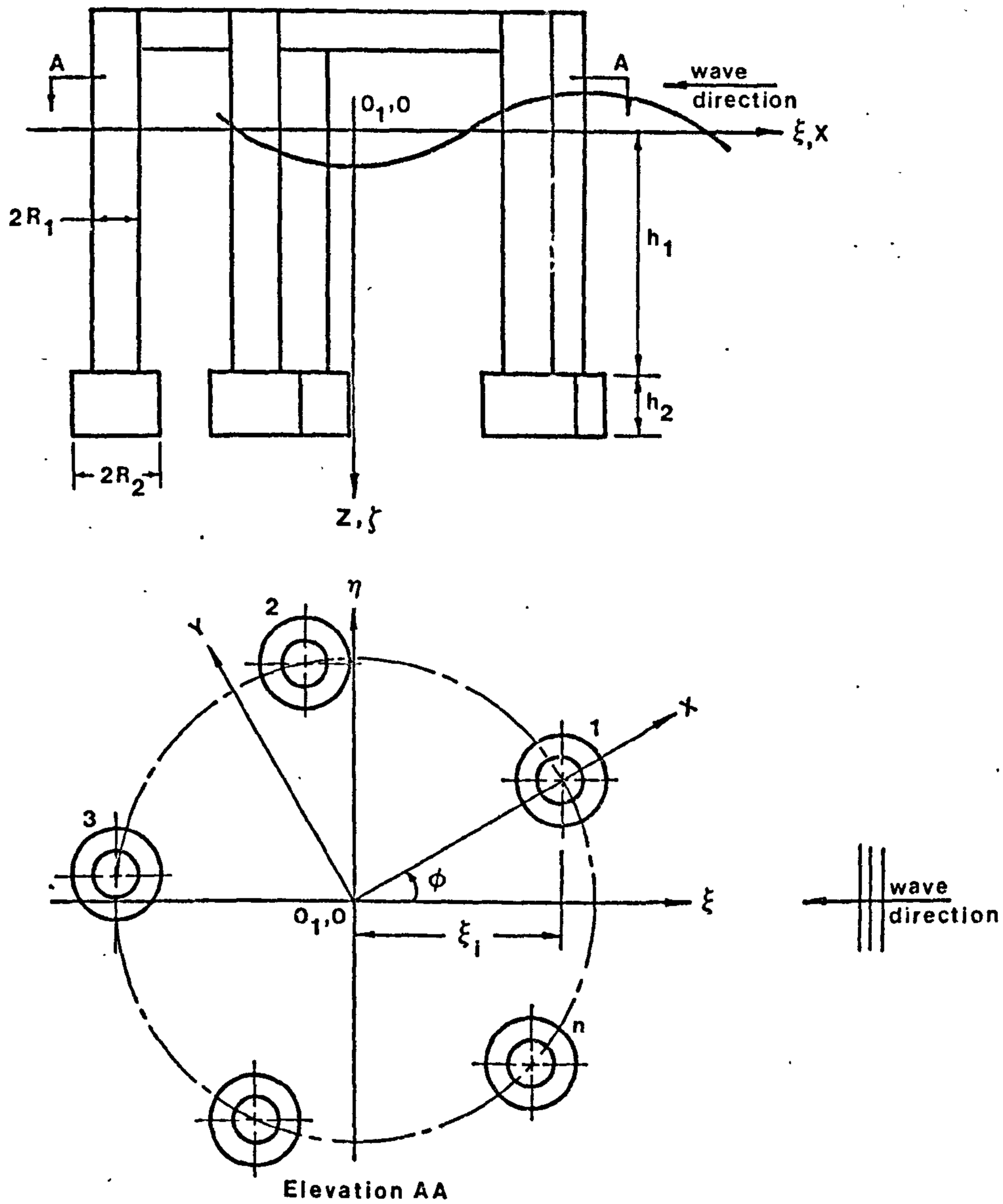

Fig. 3.5 Orientation of the Multi-leg Platform to the Wave Direction

The horizontal distances ξ_i (see Fig. 3.5) of the centres of the vertical legs on the ξ-axis from the origin is given by:

$$\xi_i = R_c \cos\left(\frac{2\pi}{n} i + \phi\right) \tag{3.60}$$

where $i = 0, 1, 2, 3, \ldots\ldots\ldots, (n-1)$

ϕ = angle of orientation of the platform to the wave direction, i.e. the angle between the X-axis which passes through the centre of one of the legs and the ξ - axis.

The Froude-Kriloff Force (F_{Z1})

The Froude-Kriloff force acting on the platform can be written in the form:

$$F_{Z1} = (F_{Z1})_{cais.} - (F_{Z1})_{col.} \qquad (3.61)$$

where

$(F_{Z1})_{cais.}$ = vertical pressure force on the caissons without vertical columns

$(F_{Z1})_{col.}$ = vertical pressure force on the bottom ends of the vertical columns

The vertical pressure force on the caissons without vertical columns can be written as follows:

$$(F_{Z1})_{cais.} = -2\rho g\, \zeta_a \pi R_2^2 \frac{J_1(KR_2)}{(KR_2)} e^{-Kh_1}(1 - e^{-Kh_2}) \sum_{i=0}^{n-1} \cos(K\xi_i + \omega t) \qquad (3.62)$$

where $J_1(KR_2)$ is the Bessel function of first kind.

The vertical pressure force on the bottom ends of the vertical columns is given by:

$$(F_{Z1})_{col.} = -2\rho g\, \zeta_a \pi R_1^2 \frac{J_1(KR_1)}{(KR_1)} e^{-Kh_1} \sum_{i=0}^{n-1} \cos(K\xi_i + \omega t) \qquad (3.63)$$

The Froude-Kriloff force on the platform is obtained by substituting equations (3.62) and (3.63) in equation (3.61) and is expressed as:

$$F_{Z1} = 2\rho g\, \zeta_a \pi R_1^2 e^{-Kh_1} \left[\frac{J_1(KR_1)}{(KR_1)} - \left(\frac{R_2}{R_1}\right)^2 \frac{J_1(KR_2)}{(KR_2)}(1-e^{-Kh_2})\right] \sum_{i=0}^{n-1} \cos(K\xi_i + \omega t) \qquad (3.64)$$

Since R_1 and R_2 are small compared to the wave length λ, the Bessel functions

$$J_1(KR_1) \approx \frac{1}{2}(KR_1)$$

$$J_1(KR_2) \approx \frac{1}{2}(KR_2) \qquad (3.65)$$

and when the above values are substituted in equation (3.64), we obtain

$$F_{Z1} = \rho g \zeta_a \pi R_1^2 e^{-Kh_1} \left[1 - \left(\frac{R_2}{R_1}\right)^2 (1 - e^{-Kh_2})\right] \sum_{i=0}^{n-1} \cos (K \xi_i + \omega t) \qquad (3.66)$$

When the value of ξ_i given by the equation (3.60) is substituted, the equation (3.66) becomes

$$F_{Z1} = \rho g \zeta_a \pi R_1^2 e^{-Kh_1} \left[1 - \left(\frac{R_2}{R_1}\right)^2 (1 - e^{-Kh_2})\right] \sum_{i=0}^{n-1} \cos\left\{KR_c \cos\left(\frac{2\pi}{n} i + \phi\right) + \omega t\right\} \qquad (3.67)$$

The Inertia Force (F_{Z2})

In calculating the inertia force, each leg of the platform is considered to be a combination of the circular caisson of radius R_2 with a hole of radius R_1 in the middle and the vertical columns of radius R_1 is fitted into the hole in such a way that the bottom surfaces of the caisson and of the vertical column are in the same horizontal plane.

The added virtual mass (A.V.M.) of the caisson and of the vertical column can be expressed as follows (see Appendix 4):

$$\text{A.V.M.} = \frac{4}{3} \rho \pi R_2^3 JC_{V1} \text{ , for the caisson of radius } R_2 \qquad (3.68)$$

$$\text{A.V.M.} = \frac{4}{3} \rho \pi R_1^3 JC_{V2} \text{ , for the caisson of radius } R_1 \qquad (3.69)$$

$$\text{A.V.M.} = \frac{2}{3} \rho \pi R_1^3 JC_{V3} \text{ , for the vertical column of radius } R_1 \qquad (3.70)$$

in which

J = 0.635; the correction factor to take account of the three dimensional effect

C_{V1} = added mass coefficient for a mean aspect ratio of $\frac{\pi R_2/2}{h_2}$

C_{V2} = added mass coefficient for a mean aspect ratio of $\frac{\pi R_1/2}{h_2}$

C_{V3} = added mass coefficient for a mean aspect ratio of $\frac{\pi R_1/2}{2(h_1 + h_2)}$

The inertia force on the platform is calculated as the sum of the forces on the caisson with a hole in the middle and on the bottom of the vertical columns and is written as:

$$F_{Z2} = (F_{Z2})_{cais.} + (F_{Z2})_{col.} \qquad (3.71)$$

The inertia force on the caissons with a hole in the middle is obtained as the sum of the forces on the lower and upper surfaces of the caissons and is given by:

$$(F_{Z2})_{cais.} = -\frac{1}{2}\rho\pi J g K \zeta_a e^{-Kh_1}(1+e^{-Kh_2})R_1^3 \frac{4}{3}\left(\frac{R_2^3}{R_1^3} C_{V1} I_F - C_{V2} I_C\right)\sum_{i=0}^{n-1}\cos(K\xi_i+\omega t) \qquad (3.72)$$

where

$$I_F = 1 - \frac{(KR_2)^2}{10} + \frac{(KR_2)^4}{280} - \frac{(KR_2)^6}{15120} + - - - -$$

$$I_C = 1 - \frac{(KR_1)^2}{10} + \frac{(KR_1)^4}{280} - \frac{(KR_1)^6}{15120} + - - - -$$

The inertia force on the bottom of the vertical columns of radius R_1 can be written as:

$$(F_{Z2})_{col.} = -\frac{1}{2}\rho\pi R_1^3 J C_{V3} g K \zeta_a e^{-K(h_1+h_2)} \frac{4}{3} I_C \sum_{i=0}^{n-1}\cos(K\xi_i+\omega t) \qquad (3.73)$$

The inertia force on the platform is obtained by substituting equations (3.72) and (3.73) in equation (3.71) and is expressed as:

$$F_{Z2} = -\rho g\ \zeta_a \pi R_1^2 \left(\frac{2}{3} JKR_1\right)\ e^{-Kh_1}\ \left[(1+e^{-Kh_2})\ \left(\frac{R_2^3}{R_1^3} C_{V1}\ I_F - C_{V2}\ I_C\right) + \right.$$

$$\left. + e^{-Kh_2}\ C_{V3}\ I_C\right]\ \sum_{i=0}^{n-1} \cos\ (K\ \xi_i + \omega t) \qquad (3.74)$$

Since the diameters of the caissons and of the vertical columns are assumed to be small compared to the wave length λ, the terms I_F and I_C in the equation (3.74) tend to unity and when the value of ξ_i is substituted in the above equation,, we obtain

$$F_{Z2} = -\rho g\ \zeta_a \pi R_1^2\ \left(\frac{2}{3} JKR_1\right) e^{-Kh_1}\ \left[(1+e^{-Kh_2})\ \left(\frac{R_2^3}{R_1^3} C_{V1} - C_{V2}\right) + \right.$$

$$\left. + e^{-Kh_2}\ C_{V3}\right] \sum_{i=0}^{n-1} \cos \left\{KR_C \cos\ \left(\frac{2\pi}{n} i+\phi\right) + \omega t\right\} \qquad (3.75)$$

The vertical wave excited force on the multi-leg platform is obtained from equations (3.67) and (3.75) and is given by:

$$F_Z = F_o \cos\ (\omega t + \sigma) \qquad (3.76)$$

where

$$F_o = \left|F_o'\right| \sqrt{Q_c^2 + Q_s^2} \qquad (3.77)$$

$$F_o' = \rho g\ \zeta_a \pi R_1^2\ e^{-Kh_1}\ \left[\left\{1 - \left(\frac{R_2}{R_1}\right)^2\ (1-e^{-Kh_2})\right\}\ - \right.$$

$$\left. - \frac{2}{3} JKR_1\ \left\{(1+e^{-Kh_2})\ \left(\frac{R_2^3}{R_1^3} C_{V1} - C_{V2}\right) + e^{-Kh_2}\ C_{V3}\right\}\right] \qquad (3.78)$$

$$Q_c = \sum_{i=0}^{n-1} \cos \left\{KR_c\ \cos\ \left(\frac{2\pi}{n} i + \phi\right)\right\} \qquad (3.79)$$

$$Q_s = \sum_{i=0}^{n-1} \sin \left\{ KR_c \cos \left(\frac{2\pi}{n} i + \phi \right) \right\} \tag{3.80}$$

$$\sigma = \tan^{-1} \frac{Q_s}{Q_c} \tag{3.81}$$

3.3.3 Calculation of Horizontal Wave Excited Forces in Beam-Sea and Head-Sea Conditions

In calculating the horizontal wave excited forces on the multi-leg platform, the platform is assumed to be orientated to the wave direction at angle ϕ as shown in Fig. 3.5. The horizontal forces on the vertical columns and on the caissons are calculated by using the strip theory.

The Froude-Kriloff Force (F_{X1})

The Froude-Kriloff force on the multi-leg platform can be obtained as the sum of the horizontal pressure forces on the legs of the platform.

The horizontal pressure force on the legs, which consists of the vertical columns and caissons, can be calculated in the same way as in the case of the calculation of the horizontal force on the vertical columns of the multi-hull platform in the beam-sea condition (see Section 3.2.4).

The horizontal pressure force on the vertical columns of the legs can be written as:

$$(F_{X1})_{col.} = -\rho g \, \zeta_a \pi R_1^2 \, (1-e^{-Kh_1}) \sum_{i=0}^{n-1} \sin (K \xi_i + \omega t) \tag{3.82}$$

where ξ_i is given by the equation (3.60).

The horizontal pressure force on the caissons of the legs can be written as:

$$(F_{X1})_{cais.} = -\rho g\ \zeta_a \pi R_2^2\ e^{-Kh_1}(1-e^{-Kh_2})\ \sum_{i=0}^{n-1} \sin\ (K\ \xi_i + \omega t) \qquad (3.83)$$

By adding the equations (3.82) and (3.83) the Froude-Kriloff force on the multi-leg platform is obtained and is expressed in the form:

$$F_{X1} = -\rho g\ \zeta_a \pi R_1^2 \left[(1-e^{-Kh_1})+\left(\frac{R_2}{R_1}\right)^2 e^{-Kh_1}(1-e^{-Kh_2})\right] \sum_{i=0}^{n-1} \sin(K\ \xi_i+\omega t) \qquad (3.84)$$

The Inertia Force(F_{X2})

In the case of the multi-hull platform, it has been shown that the horizontal pressure force and the inertia force acting on the vertical columns of the platform are equal in both beam-sea and head-sea conditions.

For the multi-leg platform, it can also be shown that the inertia force due to the horizontal acceleration of the water particles acting on the added mass of the legs of the platform is equal to the horizontal pressure force on the legs of the platform which is given by the equation (3.84). Hence the inertia force on the multi-leg platform can be written as:

$$F_{X2} = -\rho g\ \zeta_a \pi R_1^2 \left[(1-e^{-Kh_1})+\left(\frac{R_2}{R_1}\right)^2 e^{-Kh_1}(1-e^{-Kh_2})\right] \sum_{i=0}^{n-1} \sin(K\ \xi_i + \omega t) \quad (3.85)$$

The horizontal wave excited force on the multi-leg platform is obtained from equations (3.84) and (3.85) and is given by:

$$F_X = -2\rho g\ \zeta_a \pi R_1^2 \left[(1-e^{-Kh_1})+\left(\frac{R_2}{R_1}\right)^2 e^{-Kh_1}(1-e^{-Kh_2})\right] \sum_{i=0}^{n-1} \sin(K\ \xi_i+ \omega t) \quad (3.86)$$

Calculations of the vertical and horizontal wave excited forces on a single-leg platform whose diameter is small relative to the wave length is not shown separately because these forces can be obtained by using the equations given for the multi-leg platform and by putting the

number of legs n is equal to unity and the radius through the centres of the legs R_c equal to zero. When these values are substituted in the equations the forces on the single-leg platform situated at the wave trough are obtained. When the diameter of the single-leg platform is large relative to the wave length, the given approximate equations cannot be used and in the calculation of forces the variations of pressure and acceleration of the water particles across the diameter must take into account.

The approximate equations for the vertical wave excited forces on the platforms given in this chapter will be used later to determine the heaving motions of the platform in waves.

CHAPTER 4
VERIFICATION OF THEORY

4.1 Introduction

The theoretical method of predicting the heaving motion of a semi-submersible platform due to wave excited forces has been dealt with in the chapters 2 and 3. Before using this theory to investigate changes in geometry and dimensions it is necessary to verify its accuracy by comparison with model and full scale tests. At the beginning of this investigation no experimental data had been published for the range of designs for which the above theory holds. Thus in order to check its validity, tests were carried out in the Glasgow University Experimental Tank on a rig which incorporated many of the geometrical features of the multi-hull types. Subsequently model data were published (Ref. 4.2) on multi-leg design and full scale and model on a multi-hull design and all of them have been used to test the foregoing theory.

Having established the accuracy of the theory it is then proposed to investigate the effect of changing dimensions and geometrical features. The computer programmes enable these results to be established in a very short time and at much less cost than the equivalent model or full scale tests.

The maximum vertical wave excited forces and the maximum heave response will be referred to in the present chapter and in the chapter 5. It should be noted that the maximum forces and response referred to are those at frequencies greater than the natural frequency of platform since the actual maximum force occurs at zero frequency and the actual maximum heave response occurs at the natural frequency but neither of these conditions are of practical interest for the majority of designs.

4.2 Calculation of the Heaving Motions of the Staflo and the Norrig-5 Semi-Submersible Platforms in Regular Waves

The heaving motions of two existing platforms, i.e. the Staflo (Ref. 4.1) and the Norrig-5 (Ref. 4.2), were calculated using the theoretical method described in the chapters 2 and 3.

The Staflo platform is a multi-hull type platform while the Norrig-5 is a multi-leg type.

4.2.1 Calculation of the heaving motion of the Staflo platform in regular waves

The principal data for the platform are shown in Fig. 4.1

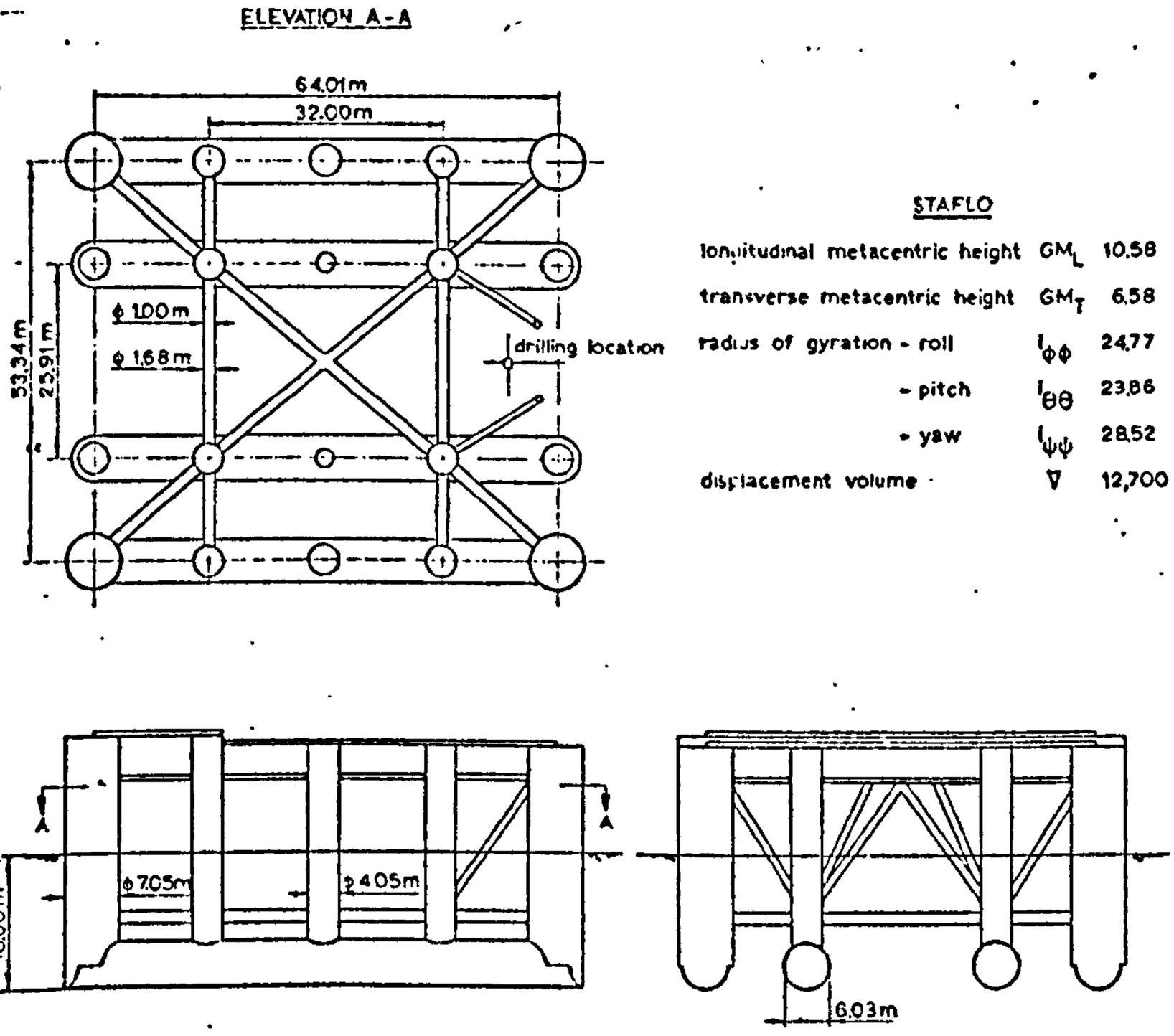

Fig. 4.1 The Staflo Semi-Submersible Platform.

The vertical wave excited force and the heaving motion of the platform in beam-sea and head-sea conditions for infinite water depth are calculated in Appendix 5. A comparison is made between the calculated force and the measured force (40 meters water depth) in Fig. 4.2 and Fig. 4.3. The measured force data were obtained from Fig. 11 of the (Ref. 4.1). The calculated motion in the beam-sea condition is shown in Fig. 4.4. The comparison between the calculated motion in the head-sea condition and the full scale measurements at 85 meters water depth (Ref. 2.9) is shown in Fig. 4.5.

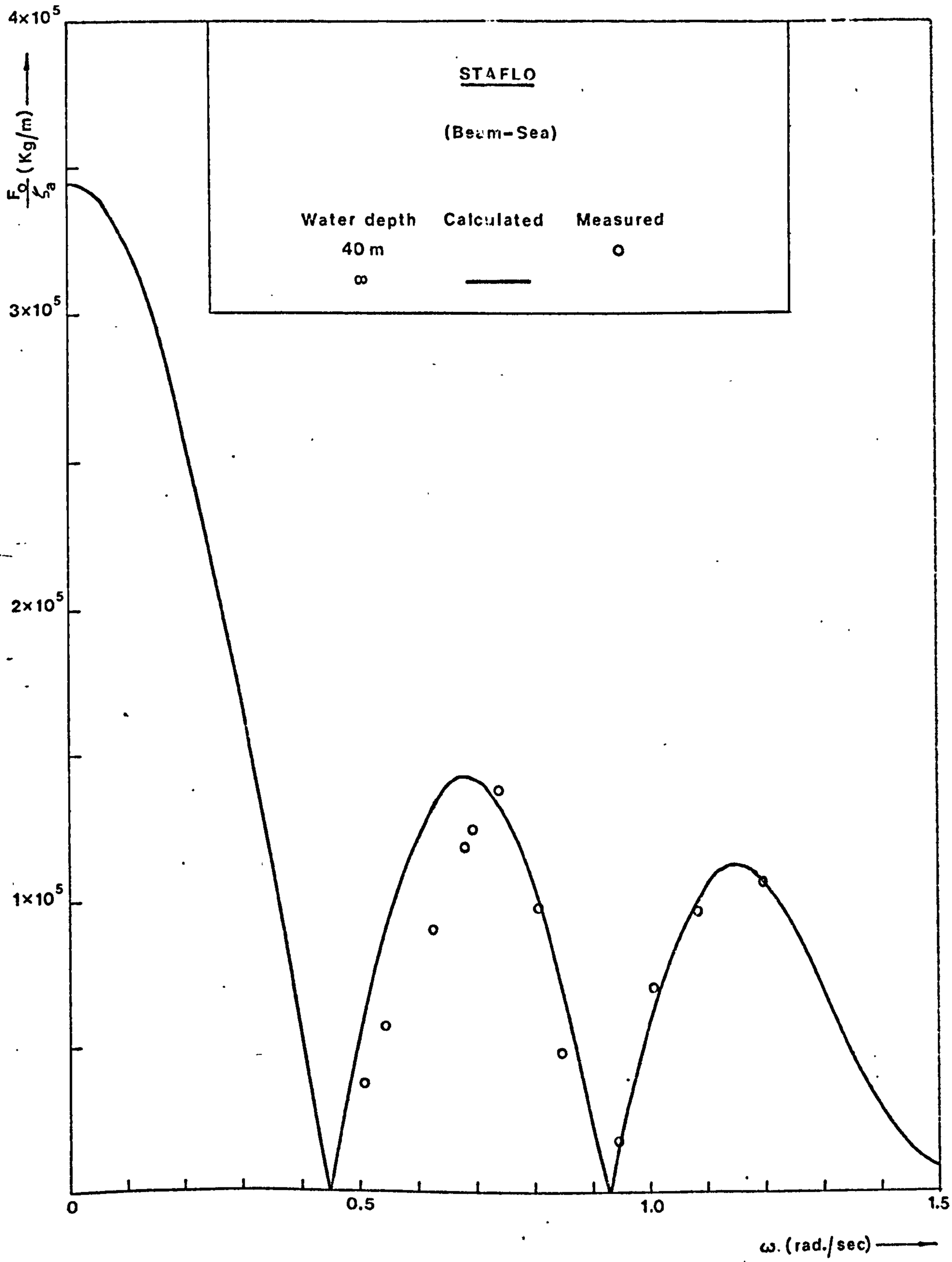

Fig. 4.2 Comparison between the calculated vertical wave-excited forces in deep water and the measured forces at 40-meter water depth in beam seas

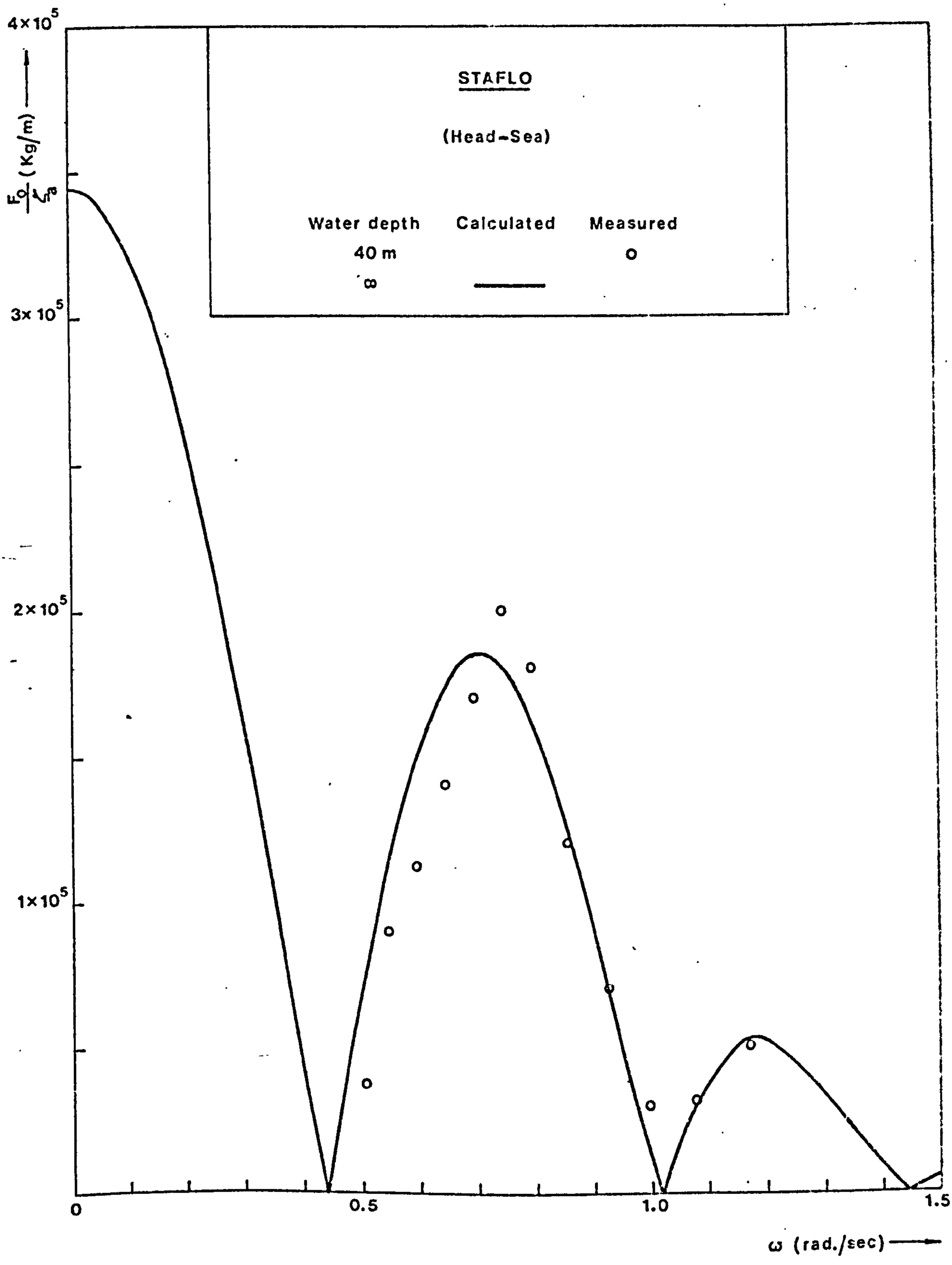

Fig. 4.3 Comparison between the calculated vertical wave-excited forces in deep water and the measured forces at 40-meter water depth in head seas

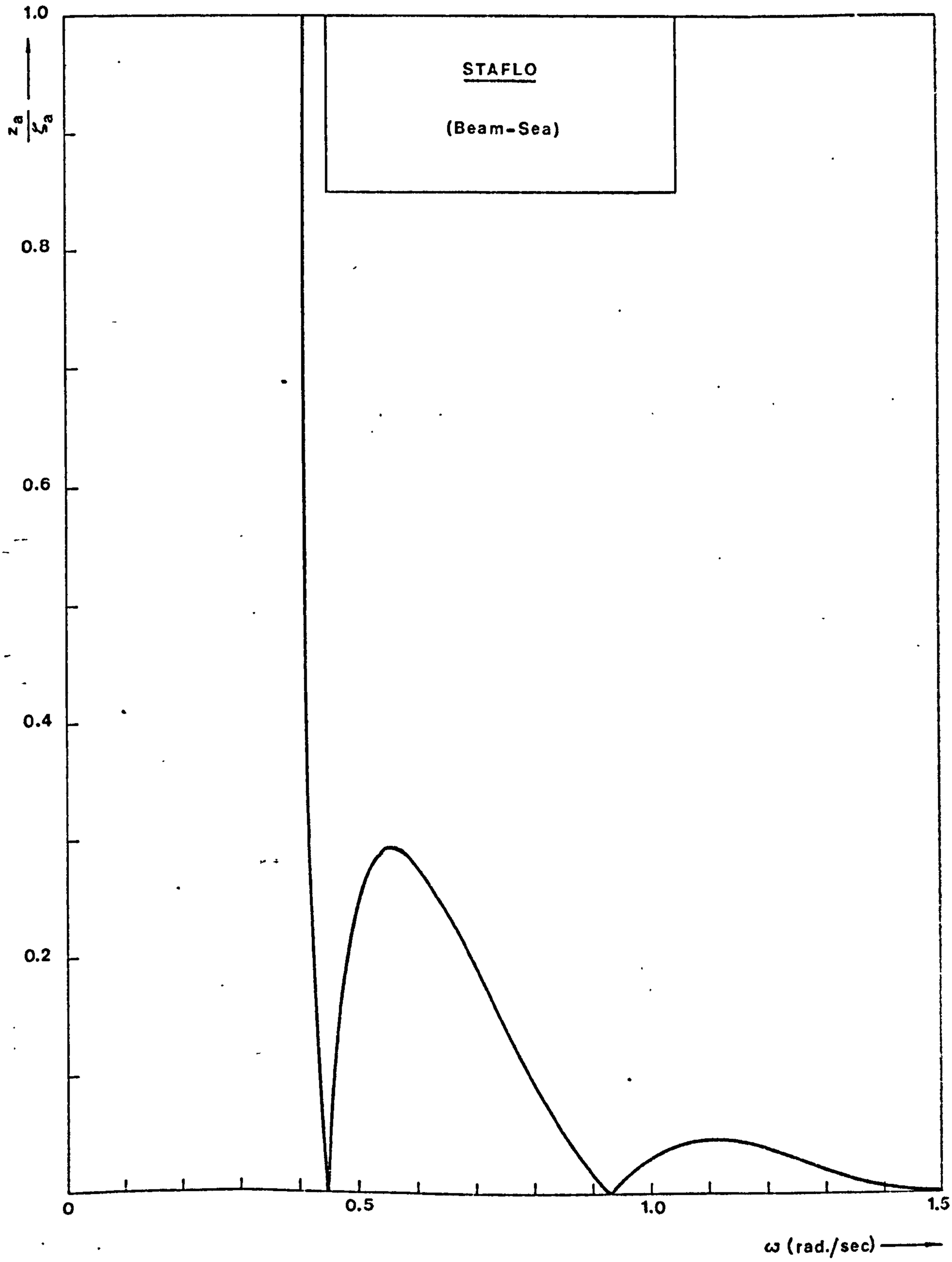

Fig. 4.4 The calculated heave response in deep water in beam seas

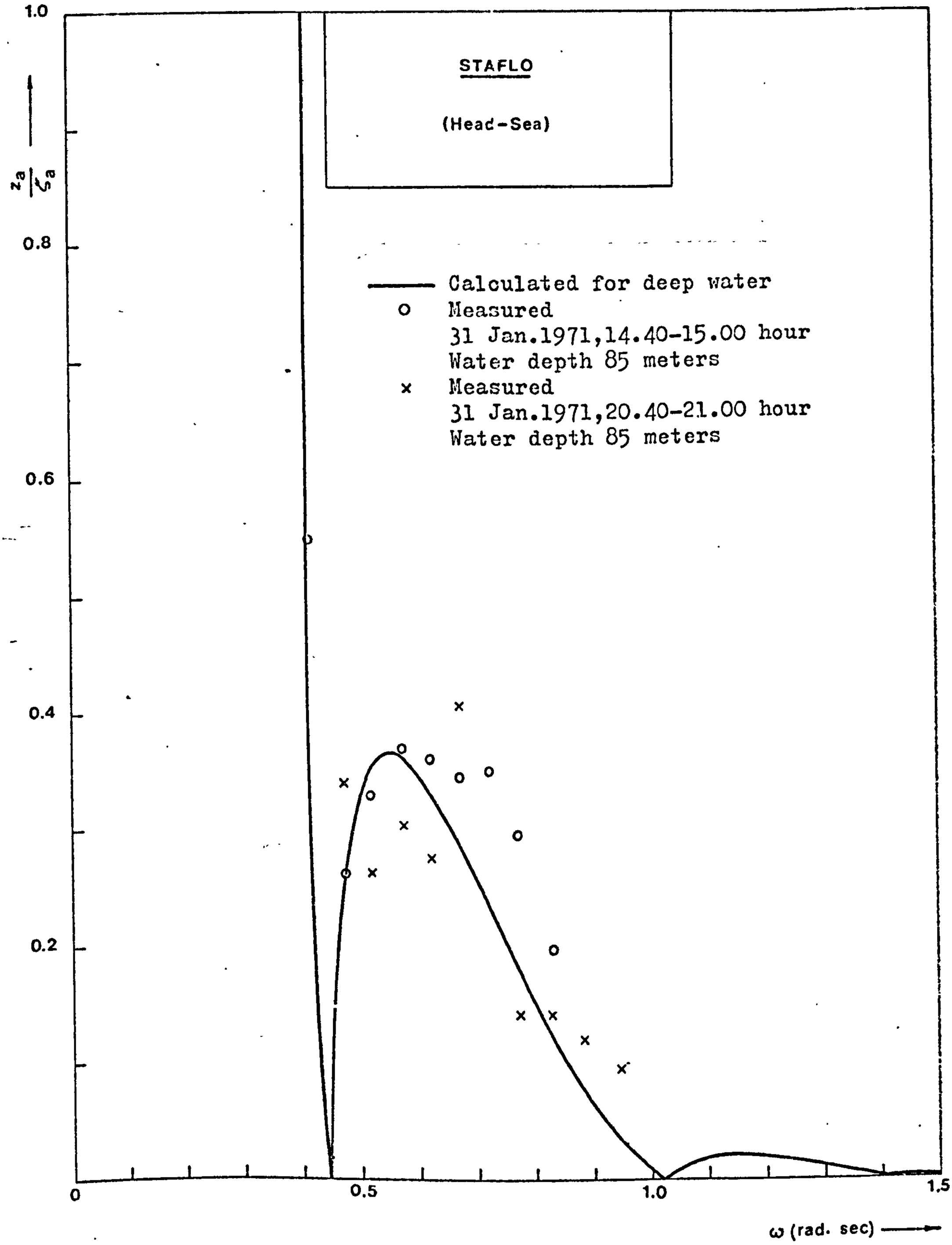

Fig. 4.5 Comparison between the calculated heave response in deep water and the full scale measurements at 85-meter water depth in head seas

The influence of water depth on the heaving motions of the Staflo platform is shown in Fig. 15 of the (Ref. 4.1). It shows that the frequency at which the maximum heave response occurs moves toward a lower frequency region and the magnitude of the maximum response increases as the water depth increases from 40 meters to 120 meters.

From Figs. 4.2 and 4.3 which give a comparison between model test data for heaving forces and theoretical calculations it can be seen that the trend of the theoretical results is substantiated by the model measurement. The maximum forces are of the same order to within a few percent. In Fig. 4.5 the calculated heave response is compared with full scale data derived from spectral analysis and again the general trend of the results is similar although there is a greater scatter than the model tests. This is to be expected in any full scale data.

In Figs. 4.2 and 4.3, it can be seen that the calculated maximum force in deep water occurs at a frequency lower than that of the measured maximum force (40 meters water depth). In Fig. 4.5, the calculated maximum heave response appears to occur at a frequency lower than the frequency of the measured maximum response (full scale - 85 meters water depth). The above observations agree with the influence of the water depth mentioned earlier.

However, in Fig. 4.5 the calculated maximum response is not found to be greater than that of the measured maximum response. This does not agree with the trend for shallow water and it is believed that the discrepancy may be due to either non-linear effects in the real wave system or some weakness in the measurement system.

No data exists to check the calculated heave response (beam-sea) shown in Fig. 4.4.

4.2.2 Calculation of the heaving motion of the Norrig-5 platform in regular waves

The principal data for the platform are shown in Fig. 4.6

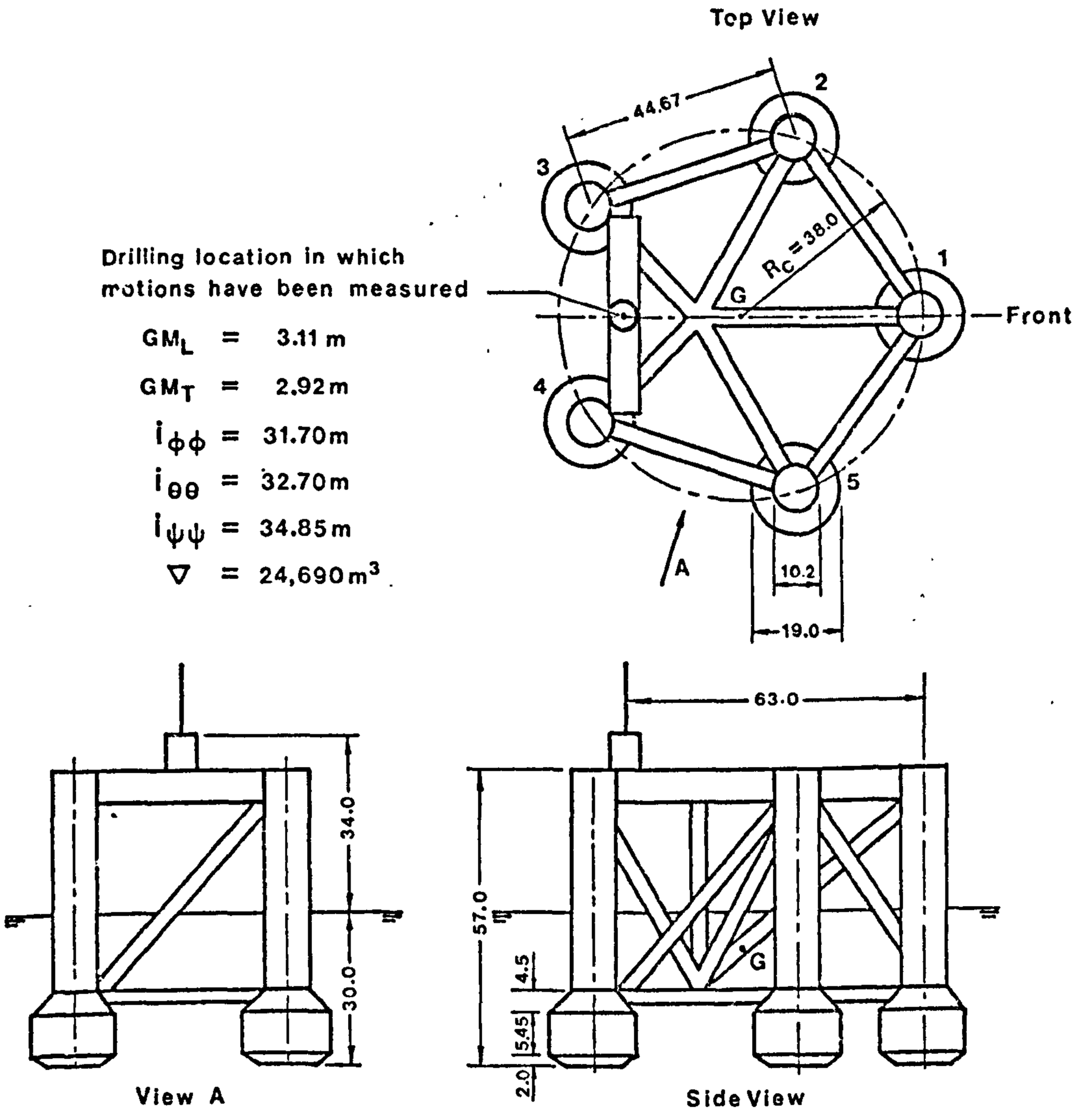

Fig. 4.6 The Norrig-5 Semi-Submersible Platform.
(Dimensions are in meters for the full size)

The rig dimensions and theory for vertical wave excited force and the heaving motion of the platform in beam-sea and head-sea conditions for water depths of 30, 40 and 50 meters are given in Appendix 6. The comparisons between the calculated forces and the measured forces (frommodel tests) are shown in Fig. 4.7 and 4.8. The measured force data were obtained from Fig. 12b of the (Ref.4.2). The calculated heaving motions of the platform are shown in Figs. 4.9 and 4.10, but no corresponding model data are available.

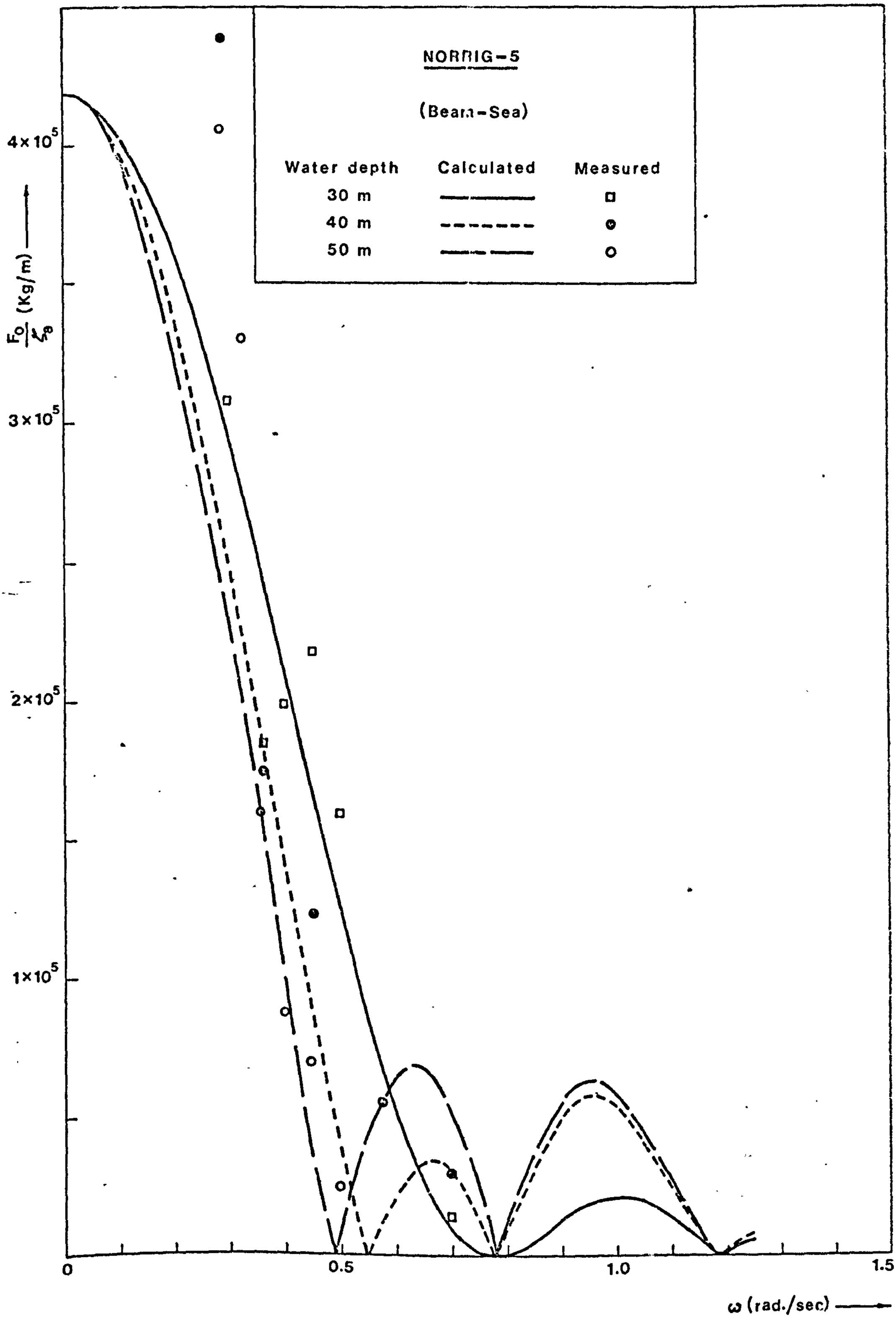

Fig. 4.7 Comparison between the calculated and the measured vertical wave-excited forces in beam seas

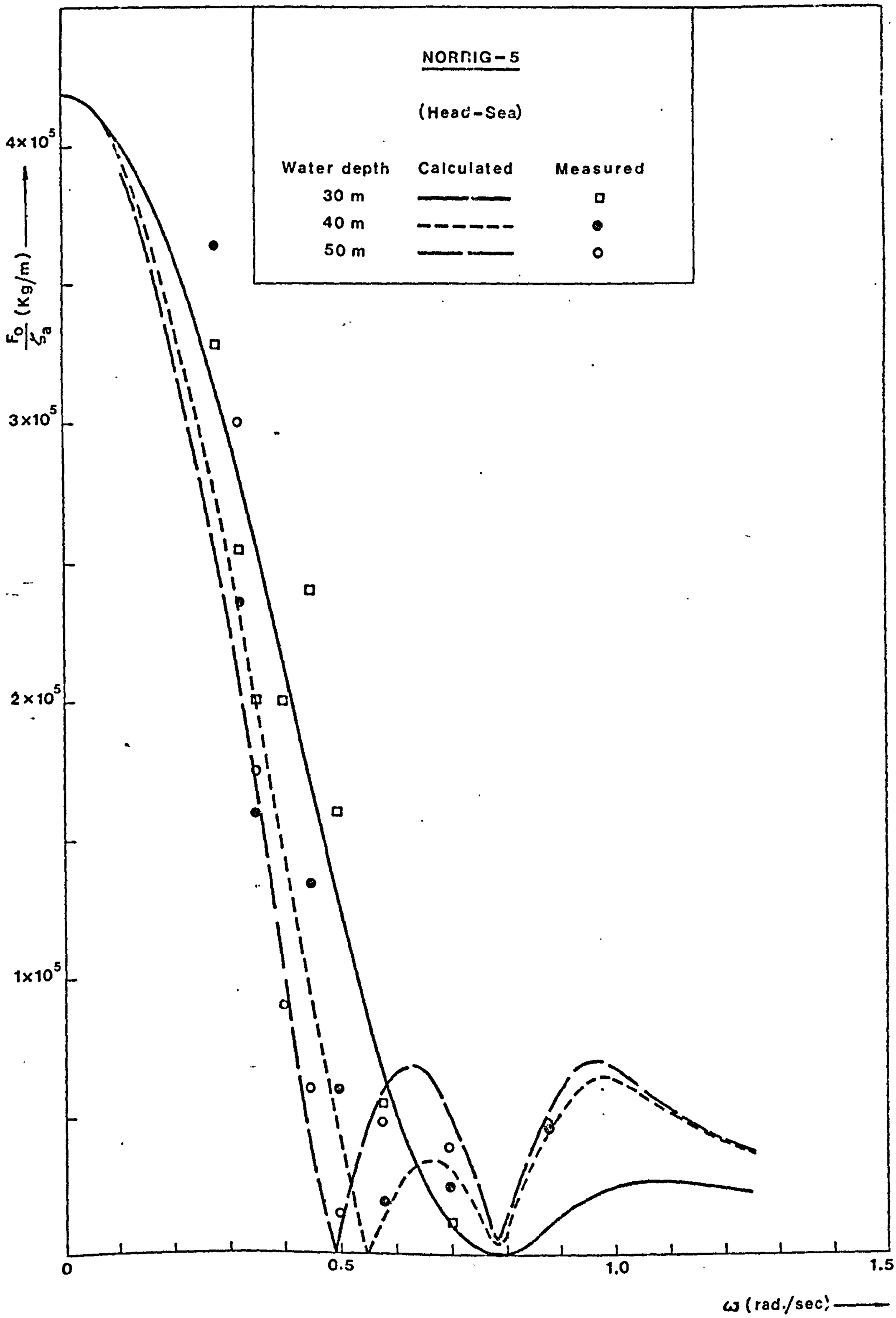

Fig. 4.8 Comparison between the calculated and the measured vertical wave-excited forces in head seas

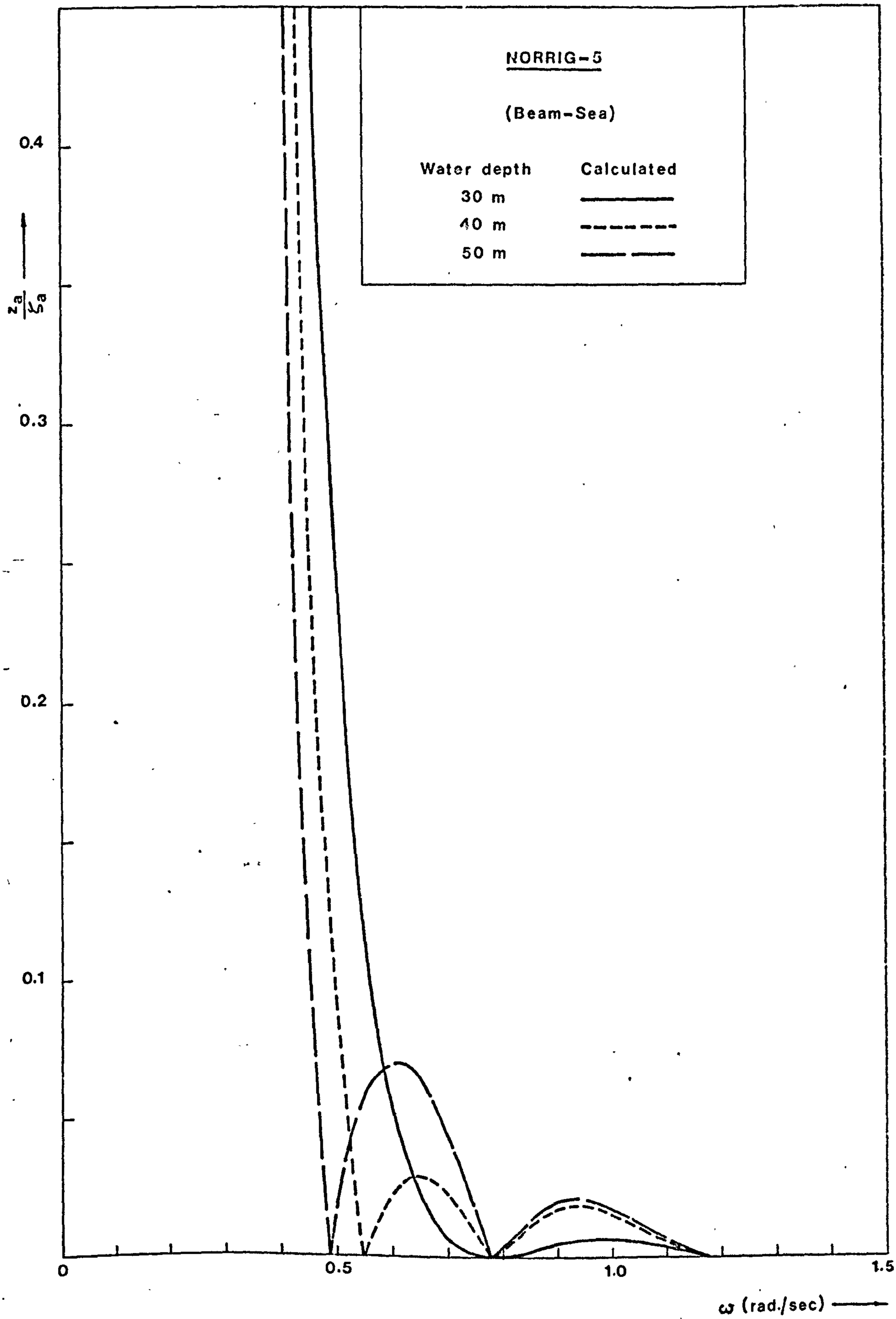

Fig. 4.9 The calculated heave response in beam seas

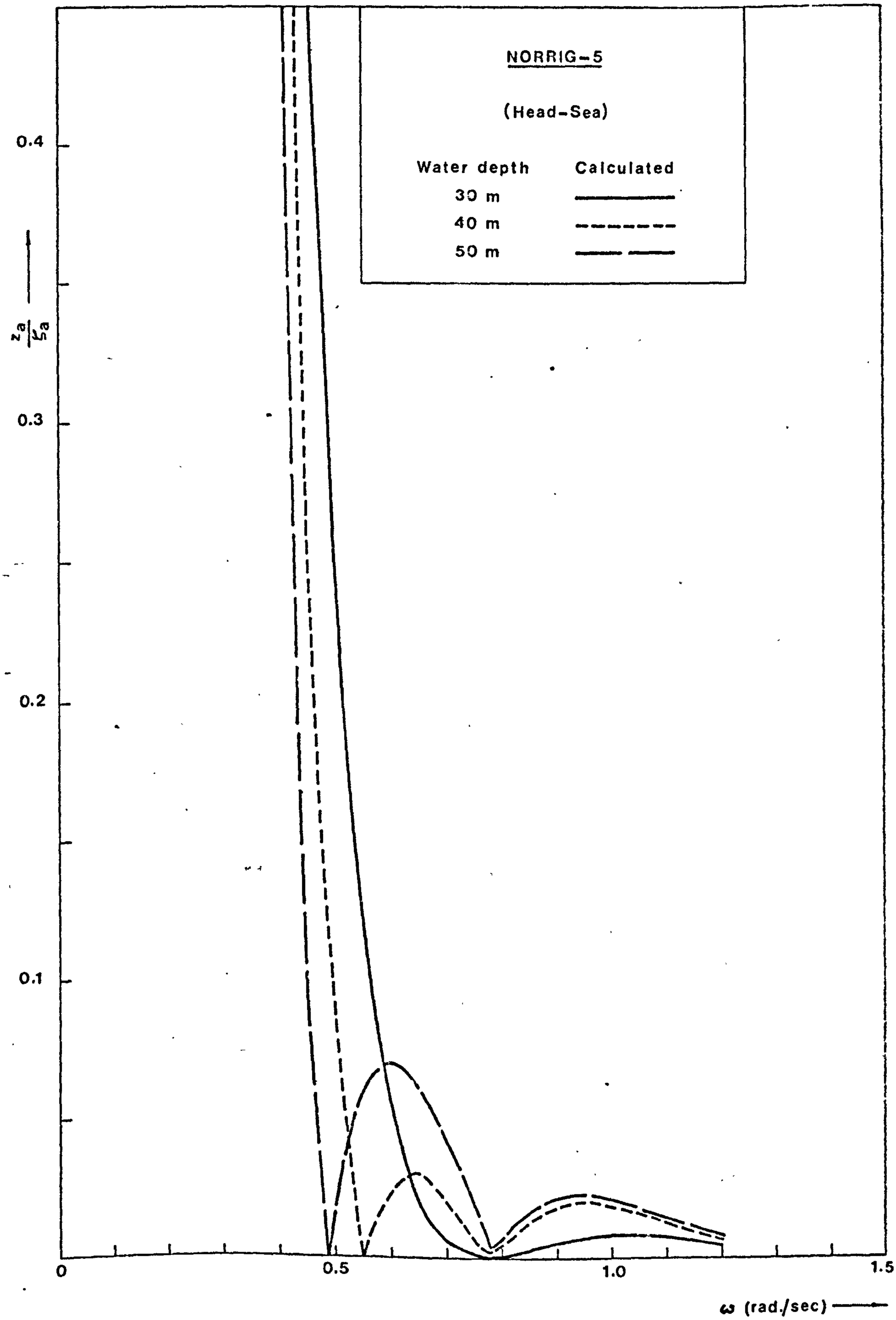

Fig. 4.10 The calculated heave response in head seas

Generally good agreement between the calculated and the measured forces is found in Figs. 4.7 and 4.8, except at the lowest frequencies where the measured forces are higher than the calculated. It should be noted that there is some differences between the theoretical results given herein and those of Hooft (Ref. 4.2) especially for 30 meters water depth. The precise reasons for this discrepancy are not known but are believed to be due to differences in the added mass values, Hooft treating each column as if it were a disc oscillating in the fluid. These differences are not large but it appears as if the present theory agrees slightly better with the measured results.

4.3 Model Tests of a Multi-Hull Platform

In order to make a more exhaustive check on the theory, calculations and model tests were carried out for a structure which on the full scale was a notional (77.16 m length x 77.16 m beam x 90.48 m depth x 76.22 m draught). It will be noted that the draught dimension is much greater than any existing semi-submersible platforms but as size increases draught will increase and it was felt necessary to check the theory at deep draughts. The model was 1/65.6 scale (1.21 m length x 1.21 m beam x 1.4 m depth). A workshop drawing of the model (using feet - inch units) is shown in Fig. 4.11.

The model had nine columns on each side of the square (total of 32 columns) and the horizontal hulls formed a square of 1.21 meters side. The complete model was fabricated from standard plumbing components and it will be noted that representation of the detailed changes in diameter it makes the calculations more complex than for the earlier comparisons. The model was tested at two draughts corresponding to 50 meters and 76.22 meters full scale and providing volume ratio of immersed column volume to total displaced volume of 0.770 and 0.836 respectively. These are very different from the ratios in Staflo and Norrig-5 and thus it is felt that this provides a more vigorous test of the theory.

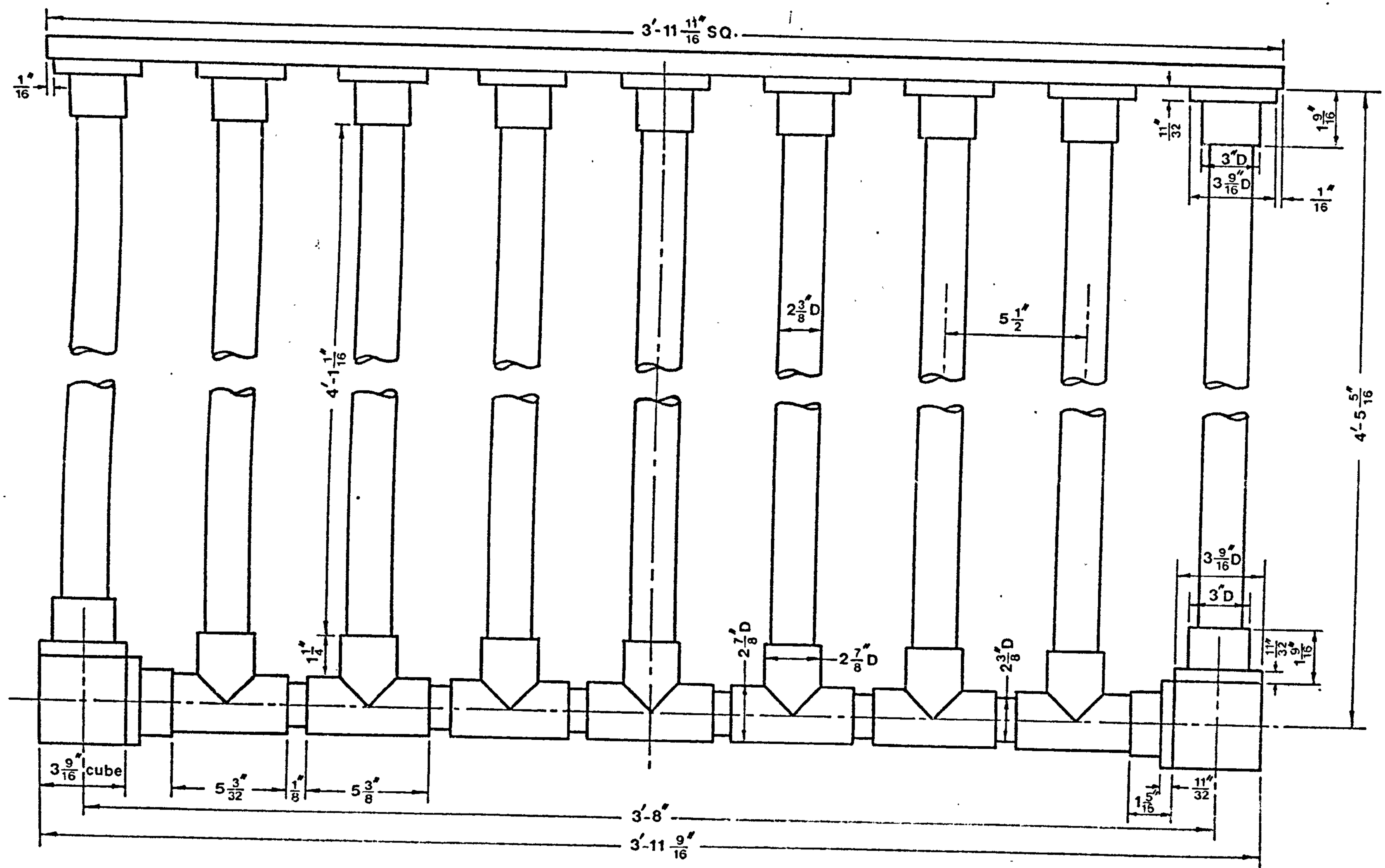

Fig.4.11 The Multi-Hull Model (Scale:1/65.6)

Experiments to measure the heave response of the model in regular waves were carried out in the Glasgow University Experiment Tank (76.22 m x 4.575 m x 2.44 m deep). The schematic arrangement of the instruments is shown in Fig. 4.12. The displacement and the metacentric height of the model at 0.762 meter (full scale - 50 meters) draught are 8.91 kg and 0.089 meter and those at 1.162 meters (full scale - 76.22 meters) draught are 124.2 kg and 0.224 meter.

The heaving motions of the model in regular waves were measured by the inductance type linear transducer capable of measuring $\pm$ 50.76 mm vertical displacement and the wave heights by the capacitance probe consisting of a 0.533 mm diameter solid copper wire loop with plastic sheath. The signals from both transducer and capacitance probe were recorded on a multi-channel ultra violet (U.V.) recorder. The capacitance probe was placed at about 0.914 meter in front of and on the fore and aft centre line of the model. The regular waves in the tank were produced by the plunger type wave making machine capable of producing waves of length 0.61 meter to 6.1 meters at heights up to 0.254 meter.

The natural heaving period and the damping coefficient of the model obtained from the experiments of free heaving of the model and the calculated natural heaving period at the two draughts are given in Table 4.1. It will be noted that the calculated and experimental natural periods agree to within 3%.

Table 4.1

Draught	50 m	76.22 m
Damping coefficient (experiment)	2.82 kg. sec/m	2.94 kg. sec/m
Natural heave period (experiment)	2.26 sec	2.56 sec
Natural heave period (calculated)	2.20 sec	2.53 sec

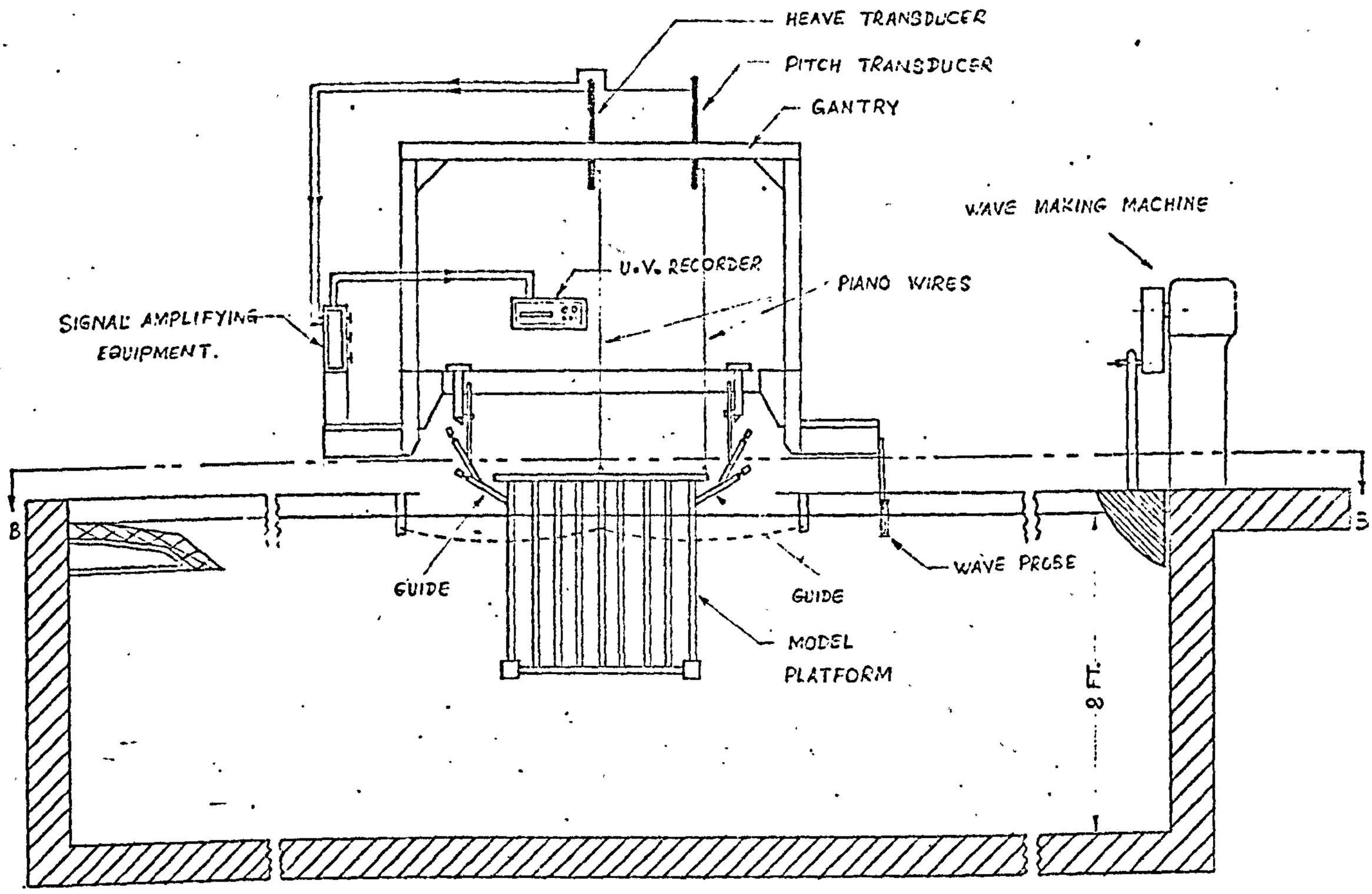

Sectional Front View
(Section AA)

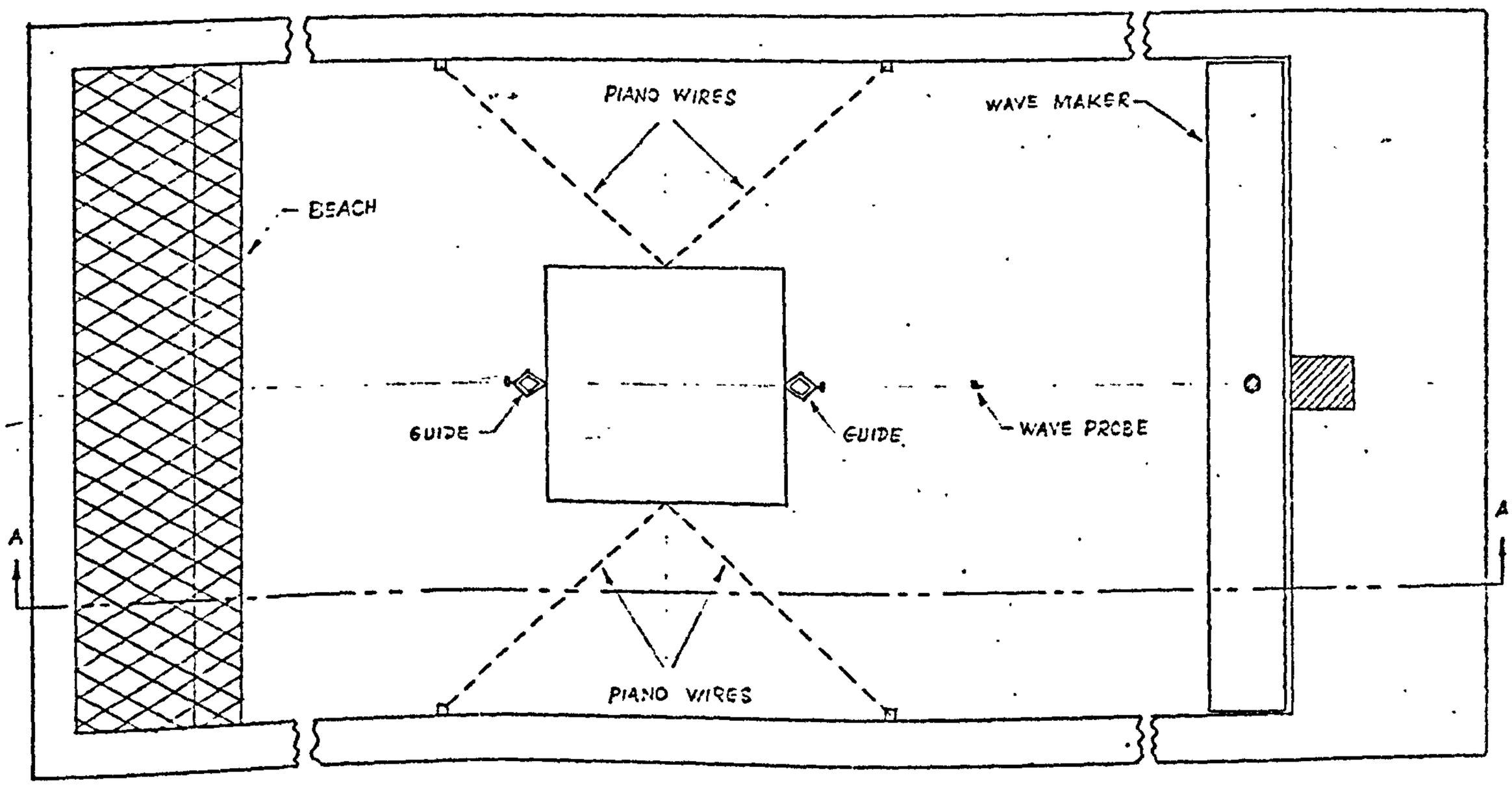

Sectional Plan
(Section BB)

Fig. 4.12 Schematic Arrangement of the Instruments

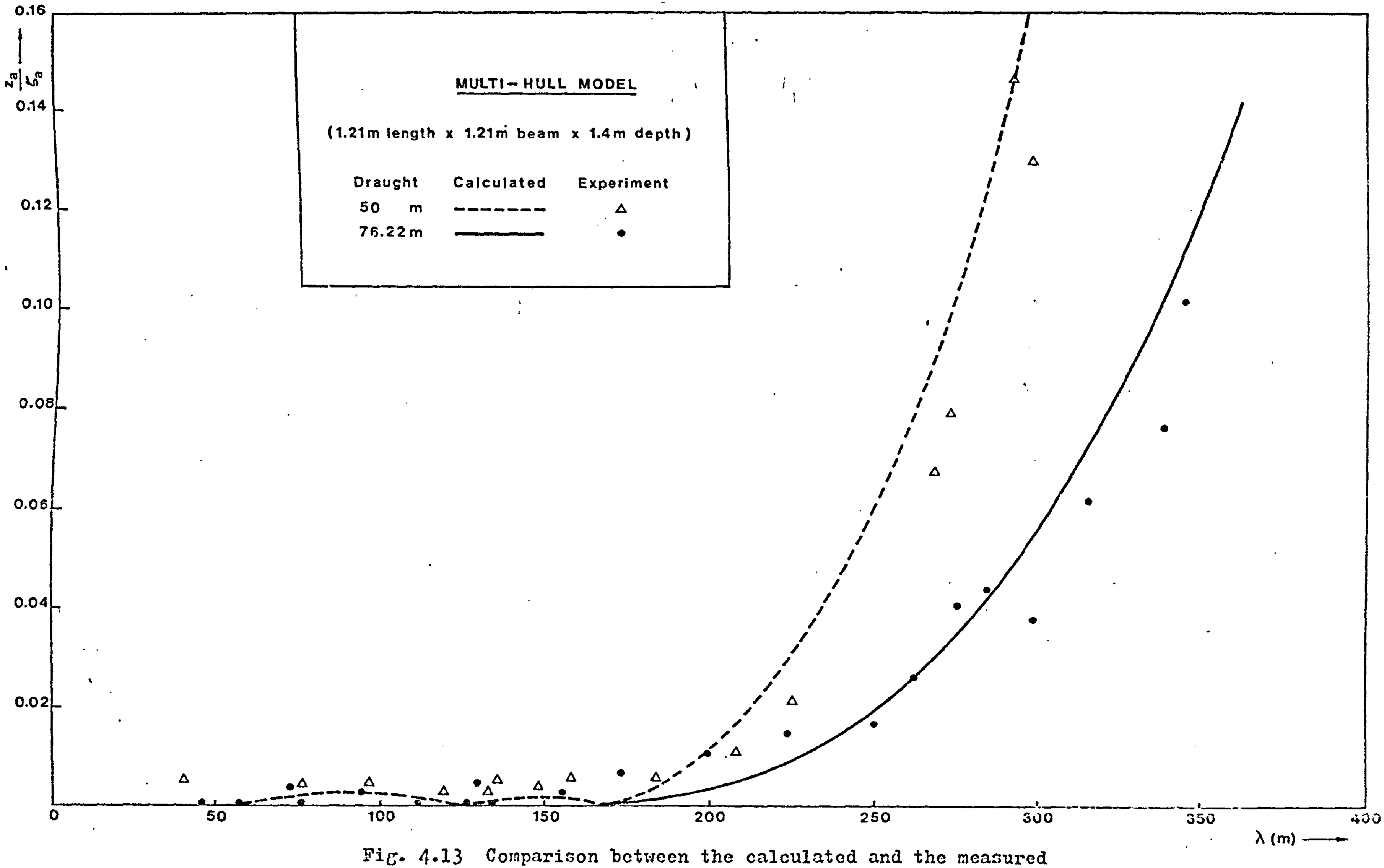

Fig. 4.13 Comparison between the calculated and the measured heave response of the multi-hull model

The comparison between the calculated and the measured heave response of the model at the two draughts is shown in Fig. 4.13 which is plotted on a base of wave length corresponding to the notional full scale. (A frequency plot compresses the data too greatly.)

Fig. 4.13 shows that the heave amplitude is less than 1 percent of the wave amplitude up to 183 meters wave length showing benefit of deep draught in this design. It can also be seen from the figure that for wave lengths up to 304.5 meters, the heave amplitude is less than 7 percent of the wave amplitude at the 76.22 meters draught and is less than 19 percent at the 50 meters draught.

According to the calculations the heave response becomes zero at 45.75 meters, 125 meters and 167.8 meters wave lengths but these zero responses were not measured in practice.

Agreement between the calculated and the measured heave response is very good in region where responses are of some magnitude but there is a tendency to overestimate at longer wave lengths.

4.4 Conclusion

The comparisons between theory and experiment which have been made above for a range of designs indicate that the present theory will give sufficiently accurate results to be used as a guide to the effect of changes in geometry or dimensions. On the whole, theory tends to overestimate response so that any errors are likely to be on the safe side.

CHAPTER 5

APPLICATIONS OF THEORY

5.1 Introduction

The theoretical method of predicting the heave response of a platform has been verified in Chapter 4. It is used in the present chapter to investigate the effect of changing the geometry or dimensions of a multi-hull semi-submersible platform on the heaving motions in regular waves and to compare the heaving motions of a multi-hull and a multi-leg platforms which have the same displacement, natural heave frequency and draught.

5.2 The Influence of the Dimensions of a Multi-Hull Semi-Submersible Platform on Heaving Motions in Regular Waves

As has been mentioned in Chapter 2, it is desirable to reduce the response amplitude operator or the heave response (i.e. heave amplitude/wave amplitude) in order to reduce the heaving motion of the platform in waves. It is believed that the heave response can be reduced when the effects of various parameters of the platform on the heave response are known.

It is extremely difficult to get a reliable basis of comparison when many factors are varied so that it was decided to assume the following data for a multi-hull platform:

(i) Number of vertical columns on each cylinder $n = 3$

(ii) Volume ratio $\frac{V_1}{\nabla} = 0.4$

(iii) Displacement volume $\nabla = 30{,}000\ m^3$

(iv) Beam $b = 60\ m$

(v) Natural heave frequency $\omega_n = 0.314$ rad./sec

These data are fairly typical of many present day designs. In order to examine the effect of these factors on the heave response, each was varied in turn while the other were maintained constant as shown in Table 5.1. The columns of h_1 and ℓ have been added to this table.

Table 5.1

		n	$\frac{V_1}{\nabla}$	∇	b	ω_n	h_1	ℓ
1	Effect of n	3 4 5 6	0.4	30,000m^3	60m	0.314 rad/sec	24.84m	73.52m 80.54 84.90 87.87
2	Effect of $\frac{V_1}{\nabla}$	3	0.4 0.5 0.6 0.7	30,000	60	0.314	24.84 33.12 42.59 53.51	73.52
3	Effect of ∇	3	0.4	20,000 30,000 40,000	60	0.314	24.84	73.52
4	Effect of b	3	0.4	30,000	50 60 70	0.314	24.84	61.27 73.52 85.78
5	Effect of ω_n (constant h_1)	3	-	30,000	60	0.349 0.314 0.286	20.00	73.52

The column h_1 shows the draught in each case and it will be noted that the draught has been maintained constant in all cases except that of changing volume ratio where it is a direct factor in the change and that of changing the natural frequency in which different value of draught was used. It was shown earlier that all the equations for heave response involve the factor e^{-Kh_1} so that increasing draught will always lead to an improved heave response and thus it is important that draught changes be avoided if other geometrical features are under investigation. Similarly two platforms can only be compared if

their natural heave frequencies are the same since the response is very dependent on the resonant condition. As well as the natural heave frequency the longitudinal and transverse metacentric height has been maintained the same for all cases. Thus the changes in number of columns and beam also involve changes in length ℓ as shown in the last column of Table 5.1. It is assumed throughout the following comparisons that the platforms can be made stable at the operating draught but clearly this may not be the case with practical weight distribution requirements but it is felt the above parameters will cover the practical range of dimensions for this order of displacement.

The natural heave frequency of the multi-hull platform given by the equation (2.4) can be rewritten in terms of the draught h_1 (i.e. submerged height of the vertical column), the total volume of the vertical columns V_1 and the total volume of the horizontal cylinders V_2 as follows:-

$$\omega_n = \sqrt{\frac{g}{h_1}} \sqrt{\frac{1}{1 + 2\alpha}} \qquad (5.1)$$

where α is the ratio of $\frac{V_2}{V_1}$. Using the equation (5.1), when α is plotted against ω_n for different values of h_1, the graph shown in Fig. 5.1 is obtained. From Fig. 5.1 it can be seen that,

(i) for a constant natural heave frequency ω_n, when the value of α (which is inversely proportional to the volume ratio $\frac{V_1}{\nabla}$) changes the draught h_1 will be changed and vice versa.

(ii) for a constant α, when ω_n changes h_1 will be changed and vice versa.

(iii) for a constant h_1, when ω_n changes α will be changed and vice versa.

Since volume ratio has been taken as one of the data of the platform, this ratio can be related to ω_n for different h_1, using the following relationship with α :

$$\frac{V_1}{\nabla} = \frac{1}{1 + \alpha} \qquad (5.2)$$

The graph of $\frac{V_1}{\nabla}$ against α shown in Fig. 5.2 is obtained from the equation (5.2).

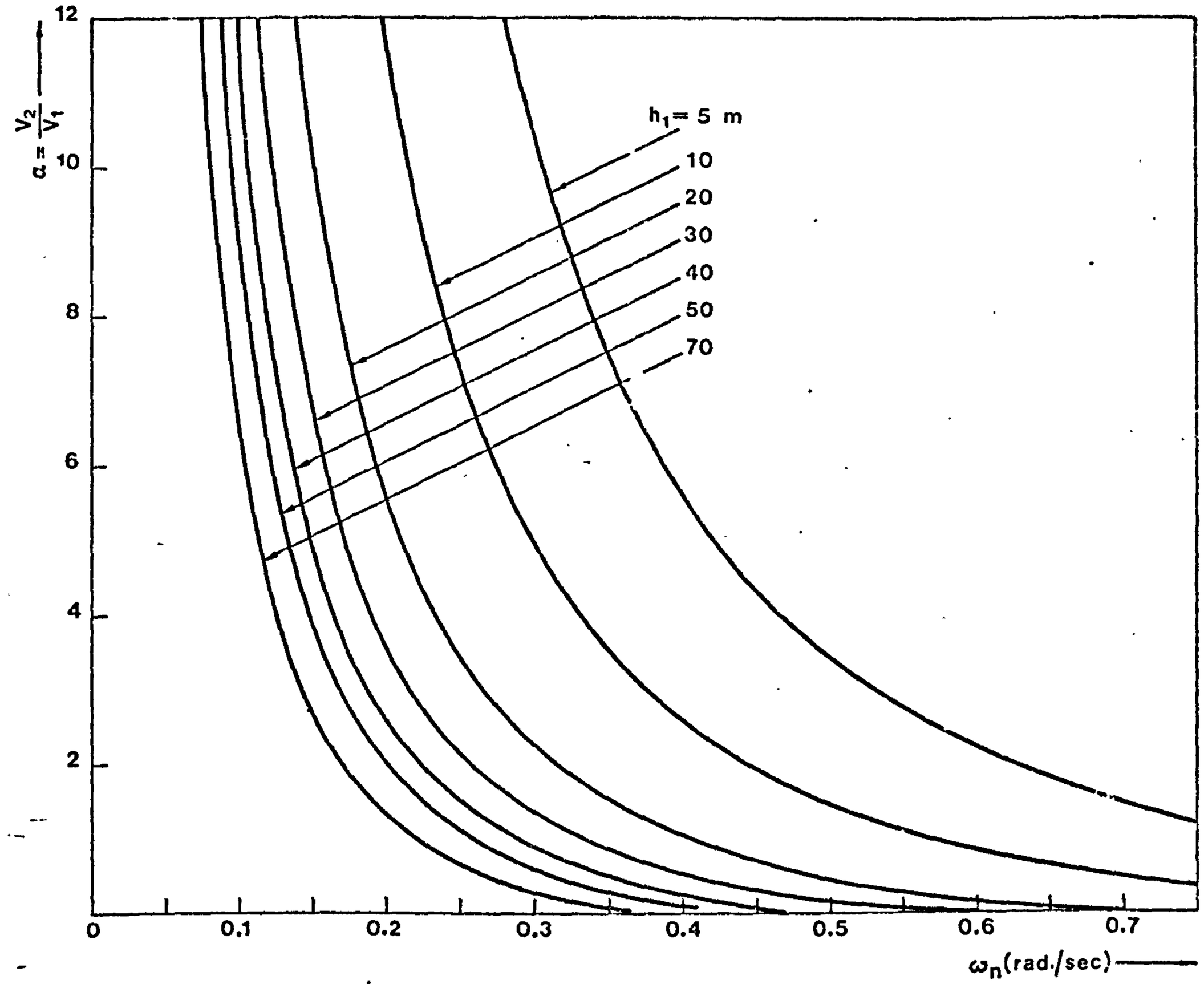

Fig. 5.1 α versus ω_n for different h_1

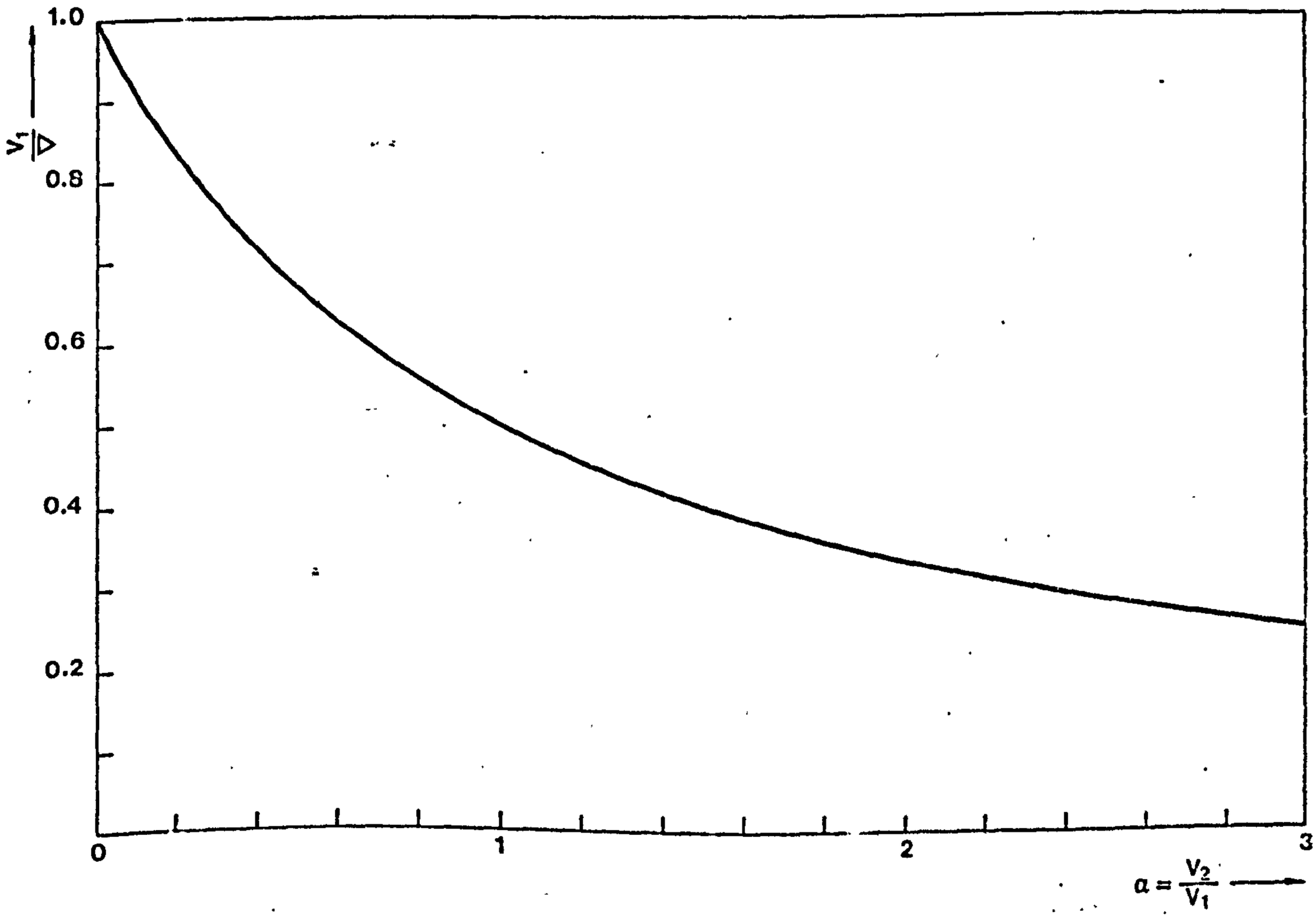

Fig. 5.2 $\frac{V_1}{\nabla}$ versus α

It will be noted that when any two of the three data, i.e. ω_n, $\frac{V_1}{\nabla}$ and h_1, are given the third can be determined immediately from the Figs. 5.1 and 5.2. For example, ω_n and $\frac{V_1}{\nabla}$ of the basic platform are given as 0.314 radian/sec and 0.4 respectively. Then the draught h_1 is obtained from the figures as follows:

Fig. 5.2

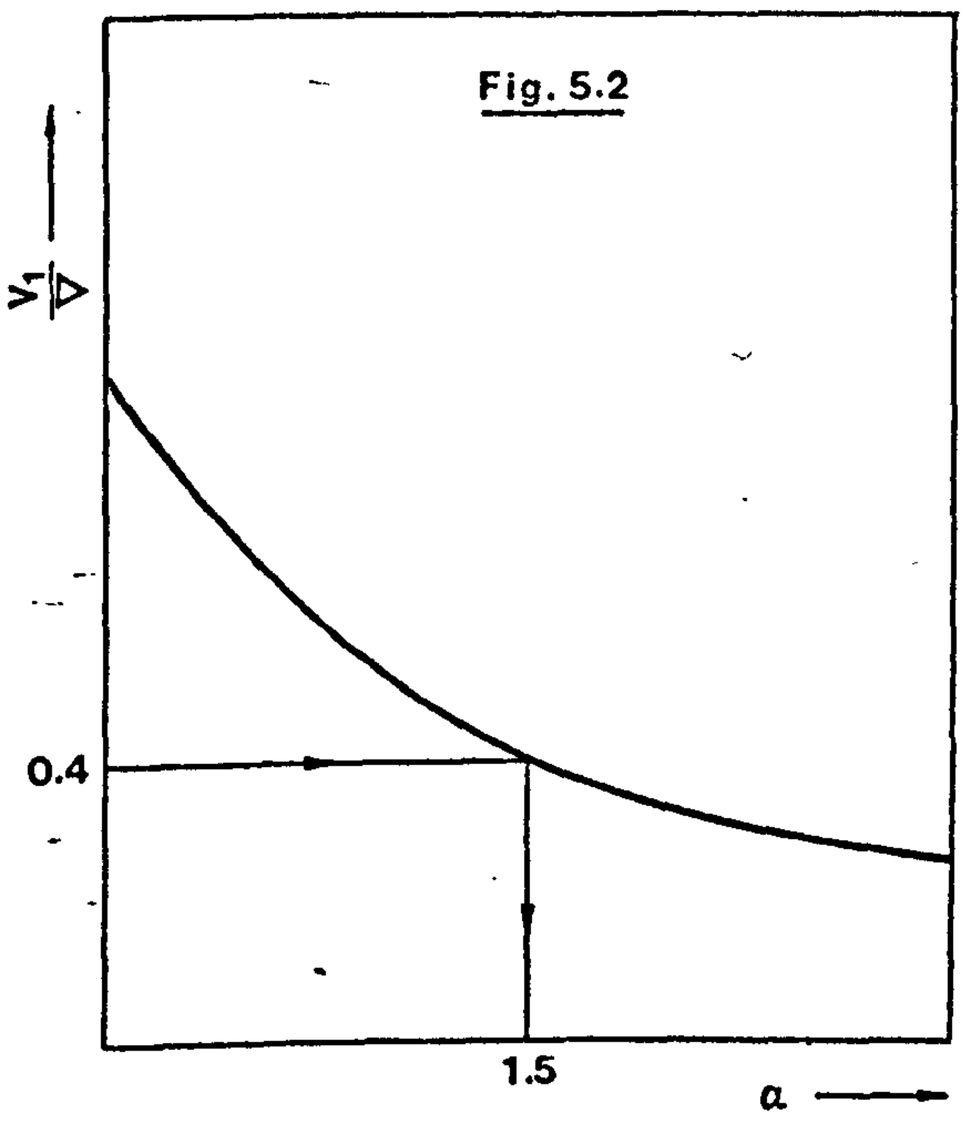

(a)

Fig. 5.1

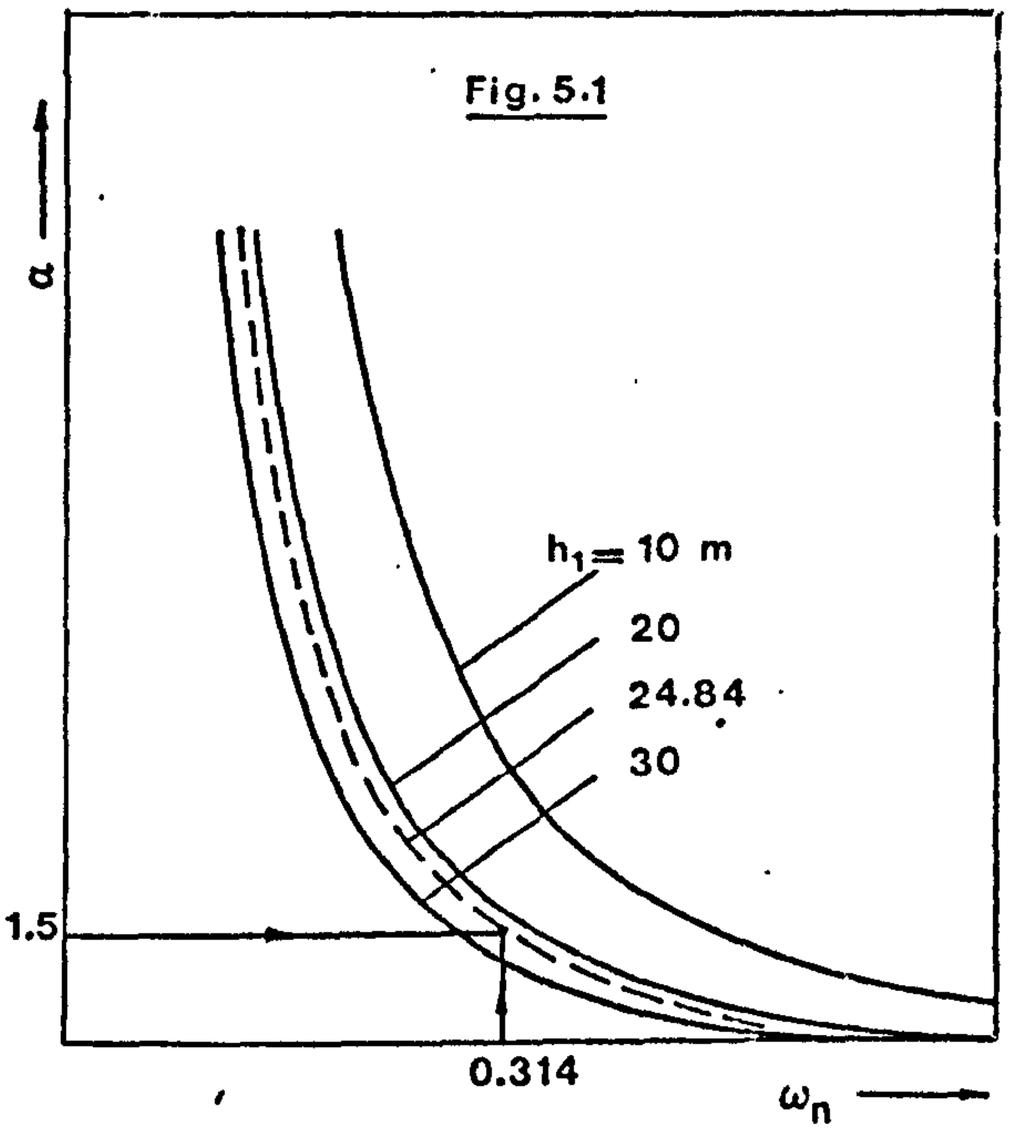

(b)

(a) α is obtained from Fig. 5.2 since $\frac{V_1}{\nabla}$ is given.

(b) h_1 is obtained from Fig. 5.1 since α and ω_n are known.

In the following investigations it is assumed that each platform can be made stable in all operating conditions but this could be difficult at extreme values of the volume ratio.

5.2.1 The effect of the number of columns of a multi-hull platform on the heave response

From Table 5.1, it can be seen that the number of columns n is varied from 3 to 6, while the following data are kept constant:

(a) $\frac{V_1}{\nabla} = 0.4$

(b) $\nabla = 30{,}000\ m^3$

(c) $b = 60\ m$

(d) $\omega_n = 0.314$ rad./sec

The procedures for determining the dimensions of the platform from the given data are as follows:-

Step 1 $\alpha \left(= \frac{V_2}{V_1}\right)$ is obtained from Fig. 5.2 since $\frac{V_1}{\nabla}$ is given.

Step 2 Draught h_1 is obtained from Fig. 5.1 since α and ω_n are known.

Step 3 Total column volume V_1 is obtained from the given $\frac{V_1}{\nabla}$ and ∇, i.e.

$$V_1 = \frac{V_1}{\nabla} \times \nabla$$

Step 4 Diameter d_1 of the vertical column is obtained from V_1 since h_1 and n are known, i.e.

$$d_1 = \sqrt{\frac{2V_1}{\pi n h_1}}$$

Step 5 Length ℓ, which is the centre distance between the two extreme vertical columns on one horizontal cylinder, is obtained from the beam-length ratio $\frac{b}{\ell}$ for a given number of columns n since b is given. The ratio $\frac{b}{\ell}$ for different values of n is given in Table 3.1, page 41.

Step 6 Overall length ℓ_2 of the horizontal cylinder is obtained from the equation,

$$\ell_2 = \ell + d_1$$

Step 7 Total cylinder volume V_2 is obtained either from $\alpha \left(= \frac{V_2}{V_1}\right)$ since V_1 is known, i.e.

$$V_2 = V_1 \alpha$$

or from the equation,

$$V_2 = \nabla - V_1 .$$

Step 8 Diameter d_2 of the horizontal cylinder is obtained from V_2 since ℓ_2 is known, i.e.

$$d_2 = \sqrt{\frac{2V_2}{\pi \ell_2}}$$

The above mentioned procedures also apply to the Sections (5.2.2), (5.2.3), (5.2.4) and (5.2.5).

The dimensions of the platform obtained for different values of n, using the above procedures are given in Table 5.2.

Table 5.2

Dimensions of the platform for different number of columns

n	d_1	d_2	h_1	ℓ_2
3	10.12 m	11.70 m	24.84 m	83.65 m
4	8.77	11.33	24.84	89.31
5	7.84	11.12	24.84	92.74
6	7.16	10.98	24.84	95.03

The vertical wave excited forces acting on the platforms having the dimensions given in Table 5.2 were calculated using the equations (3.22) and (3.34) and the results are shown in Figs. 5.3 and 5.4. The heave response of the platform was calculated using the equation (2.5) after neglecting the damping term and the results are shown in Figs. 5.5 and 5.6.

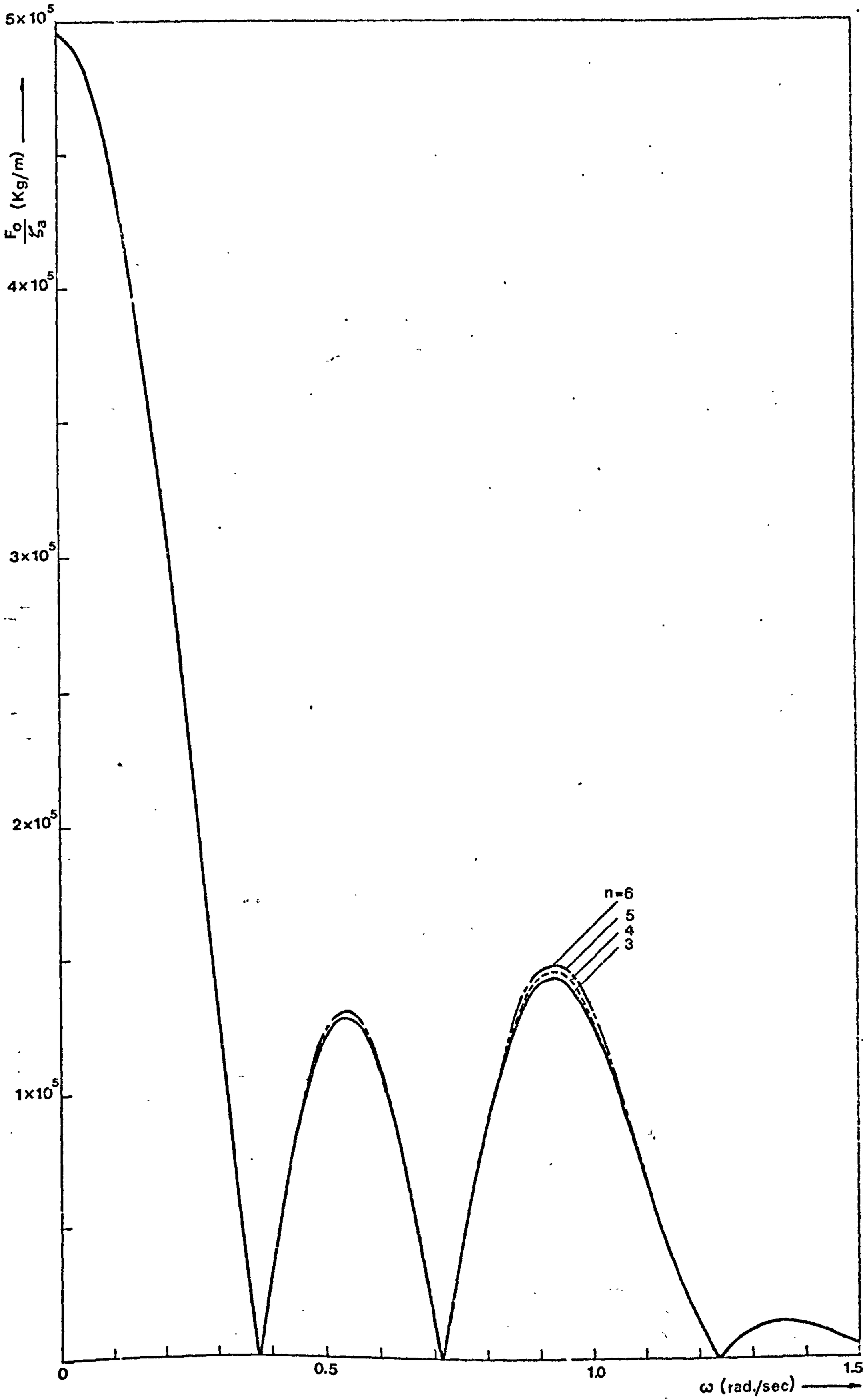

Fig. 5.3 The effect of number of columns of a multi-hull platform on the vertical wave-excited forces in beam seas

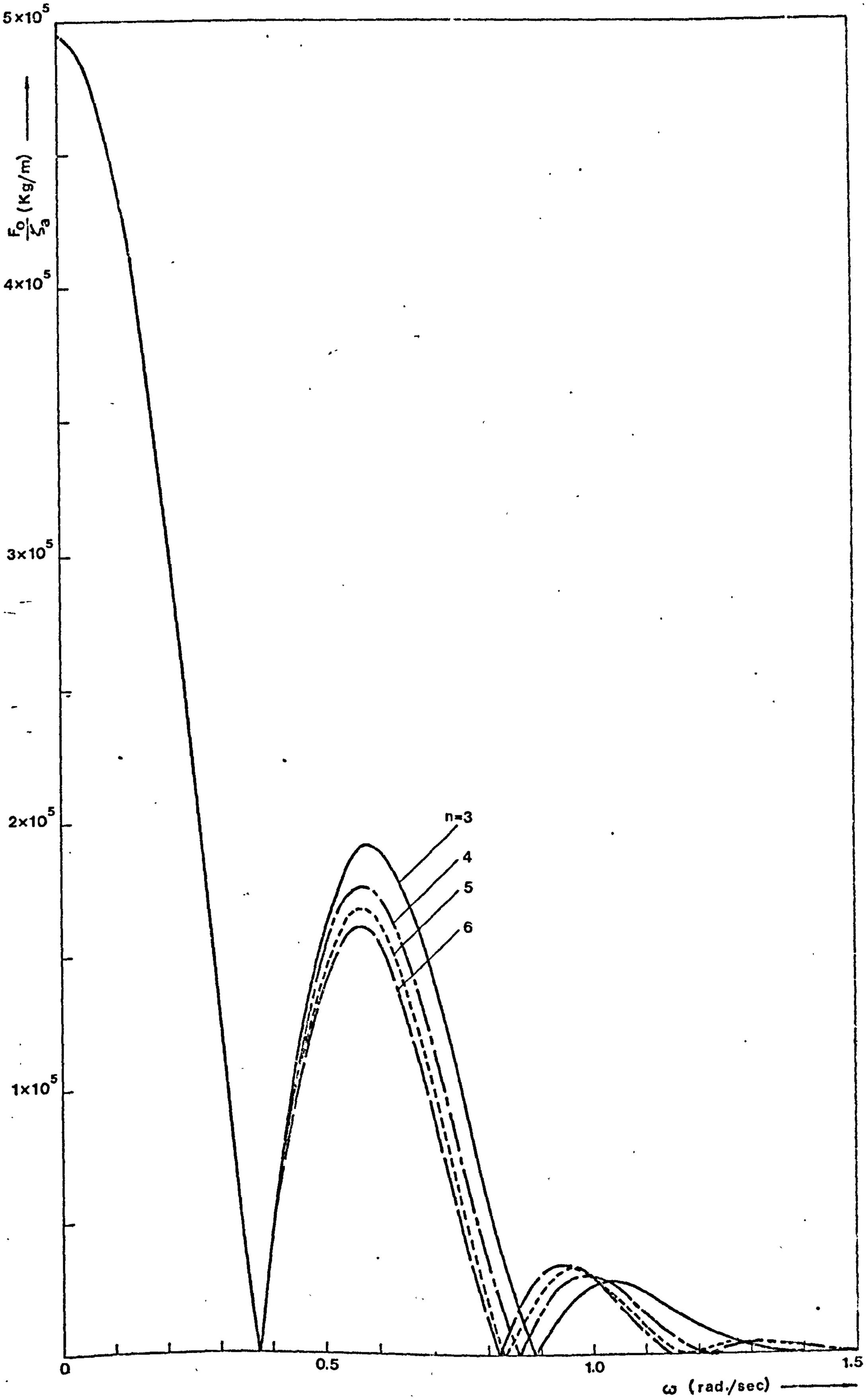

Fig. 5.4 The effect of number of columns of a multi-hull platform on the vertical wave-excited forces in head seas

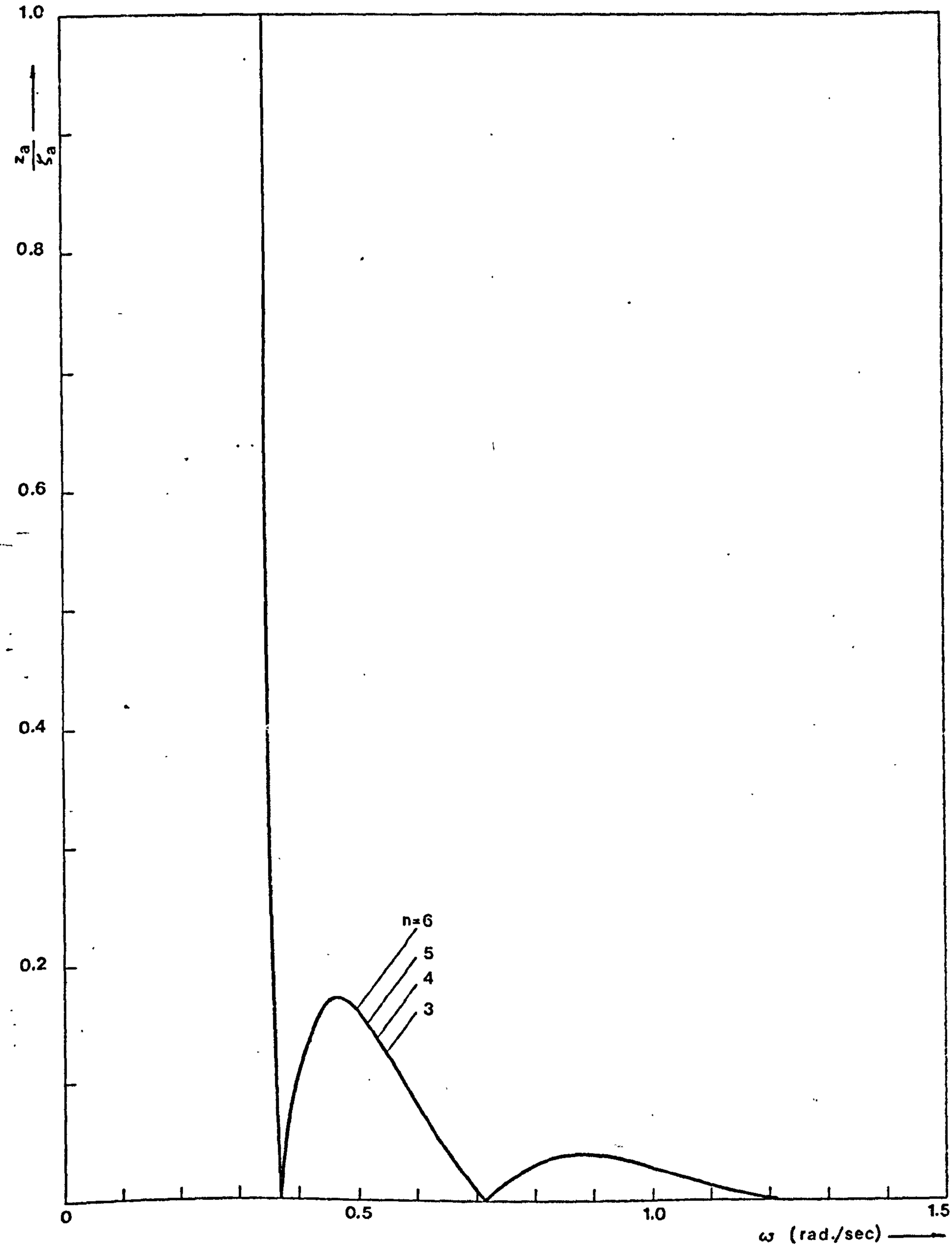

Fig. 5.5 The effect of number of columns of a multi-hull platform on the heave response in beam seas

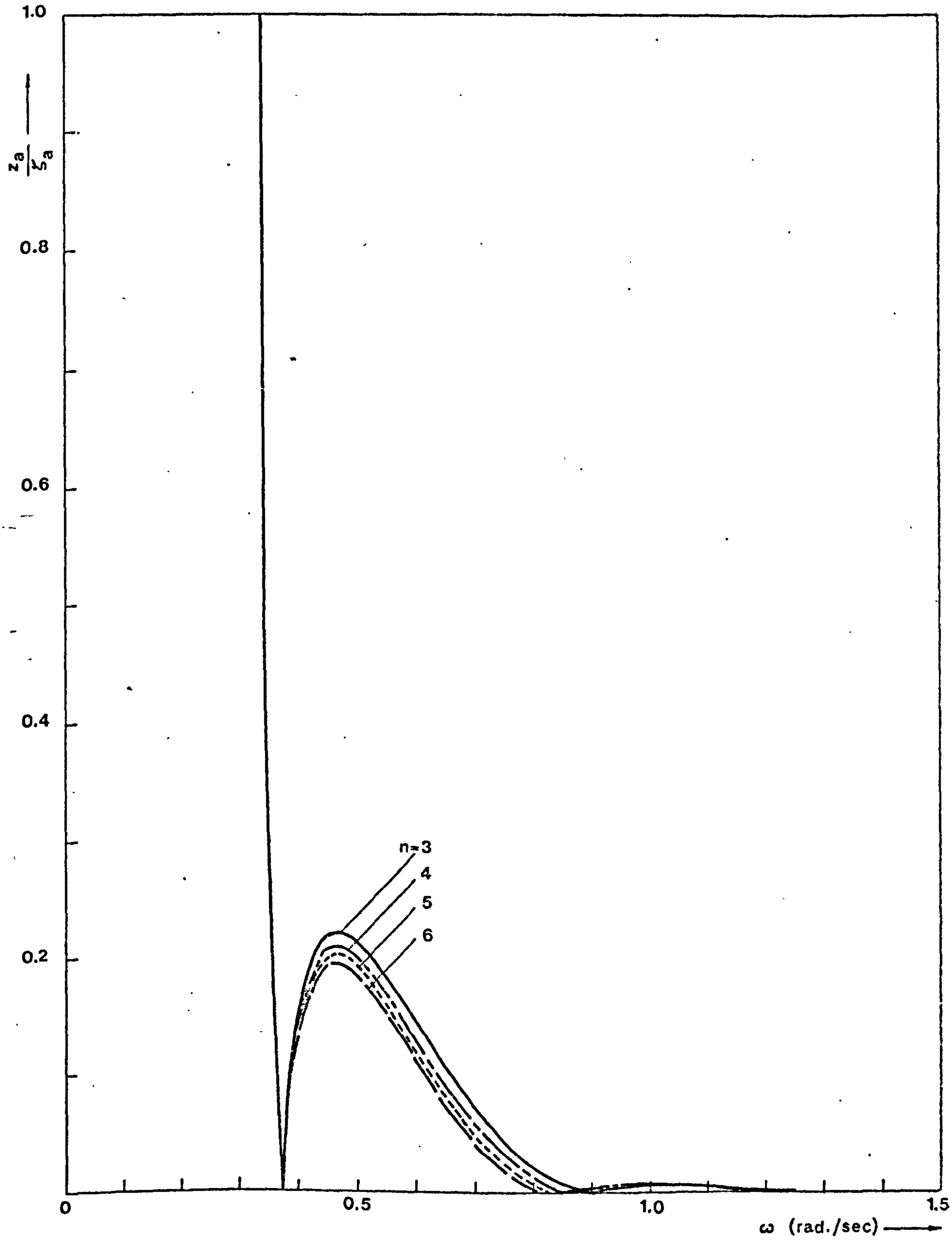

Fig. 5.6 The effect of number of columns of a multi-hull platform on the heave response in head seas

In the Figs. 5.3 to 5.6 the forces become zero at three sets of wave frequency and the heave response becomes zero at the frequencies of zero forces for both beam-sea and head-sea conditions (in the range of frequencies considered). For the beam seas, the zero force at $\omega = 0.38$ rad./sec is due to the pressure and inertia forces cancelling one another while the zeros at $\omega = 0.72$ and 1.24 rad./sec are due to the $\cos K\frac{b}{2}$ term which is outside the whole expression (see: equation 3.22). These latter frequencies can be obtained by equating

$$\cos K\frac{b}{2} = 0$$

from which

$$K\frac{b}{2} = \frac{\pi}{2}, \frac{3\pi}{2}, \frac{5\pi}{2}, - - - -$$

and taking the first two terms only, we obtained

$$\frac{\omega^2}{g}\frac{b}{2} = \frac{\pi}{2}, \frac{3\pi}{2}$$

$$\omega = \sqrt{\frac{\pi g}{b}}, \sqrt{\frac{3\pi g}{b}}$$

$$= 0.717, 1.242 \text{ rad./sec}$$

For the head seas, the zero forces at three sets of frequency are due to cancelling of the terms in the brackets (see: equation 3.34). The vertical forces and the heave response of the platform in the head seas are greater than those of the beam seas.

In general, the above mentioned observations apply to all the other cases.

From the graphs, the following can also be noted:

(a) For the beam seas, the variation of the number of columns has very little effect on the vertical forces and on the heave response.

(b) For the head seas, the maximum force and the maximum heave response of the platform decrease as the number of columns increases. The maximum response occurs at the frequency which is 1.47 times the natural frequency and is reduced by 9.64% when the number of columns is increased from 3 to 6.

5.2.2 The effect of the volume ratio of a multi-hull platform on the heave response

In this case, the volume ratio $\frac{V_1}{\nabla}$ was varied from 0.4 to 0.7 (see Table 5.1 for the other data) and the dimensions of the platform obtained by using the procedures given in the Section 5.2.1 are shown in Table 5.3 for different volume ratio.

Table 5.3

Dimensions of the platform for different volume ratio

$\frac{V_1}{\nabla}$	d_1	d_2	h_1	ℓ_2
0.4	10.12 m	11.70 m	24.84 m	83.65 m
0.5	9.80	10.70	33.12	83.32
0.6	9.47	9.59	42.59	82.99
0.7	9.13	8.33	53.51	82.65

The vertical wave excited forces on, and the heave response of the platform having the dimensions given in Table 5.3 were calculated and the results are shown in Figs. 5.7 to 5.10.

It should be noted from Table 5.3 that the draught h_1 increases with increasing volume ratio since the natural frequency is kept constant.

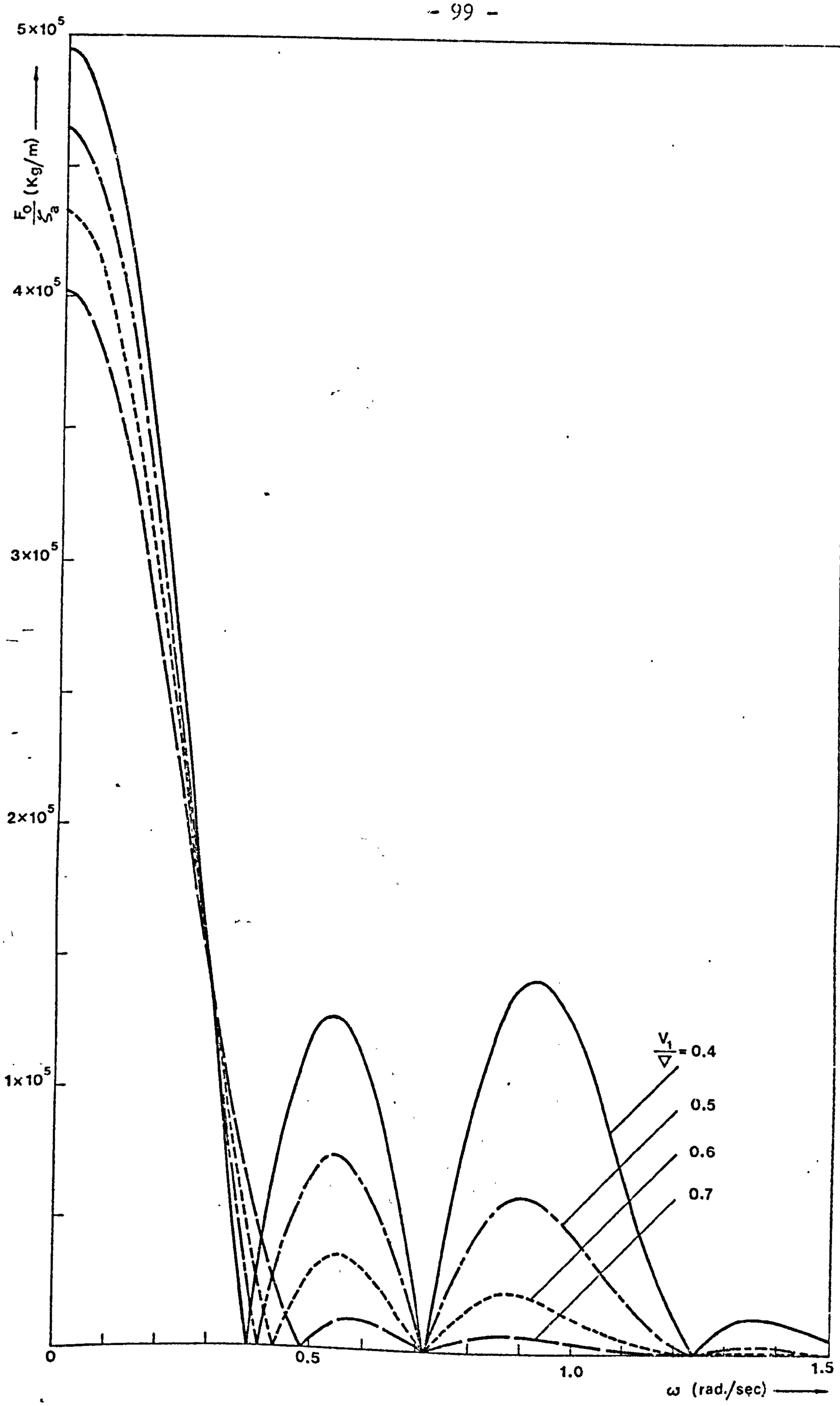

Fig. 5.7 The effect of volume ratio of a multi-hull platform on the vertical wave-excited forces in beam seas

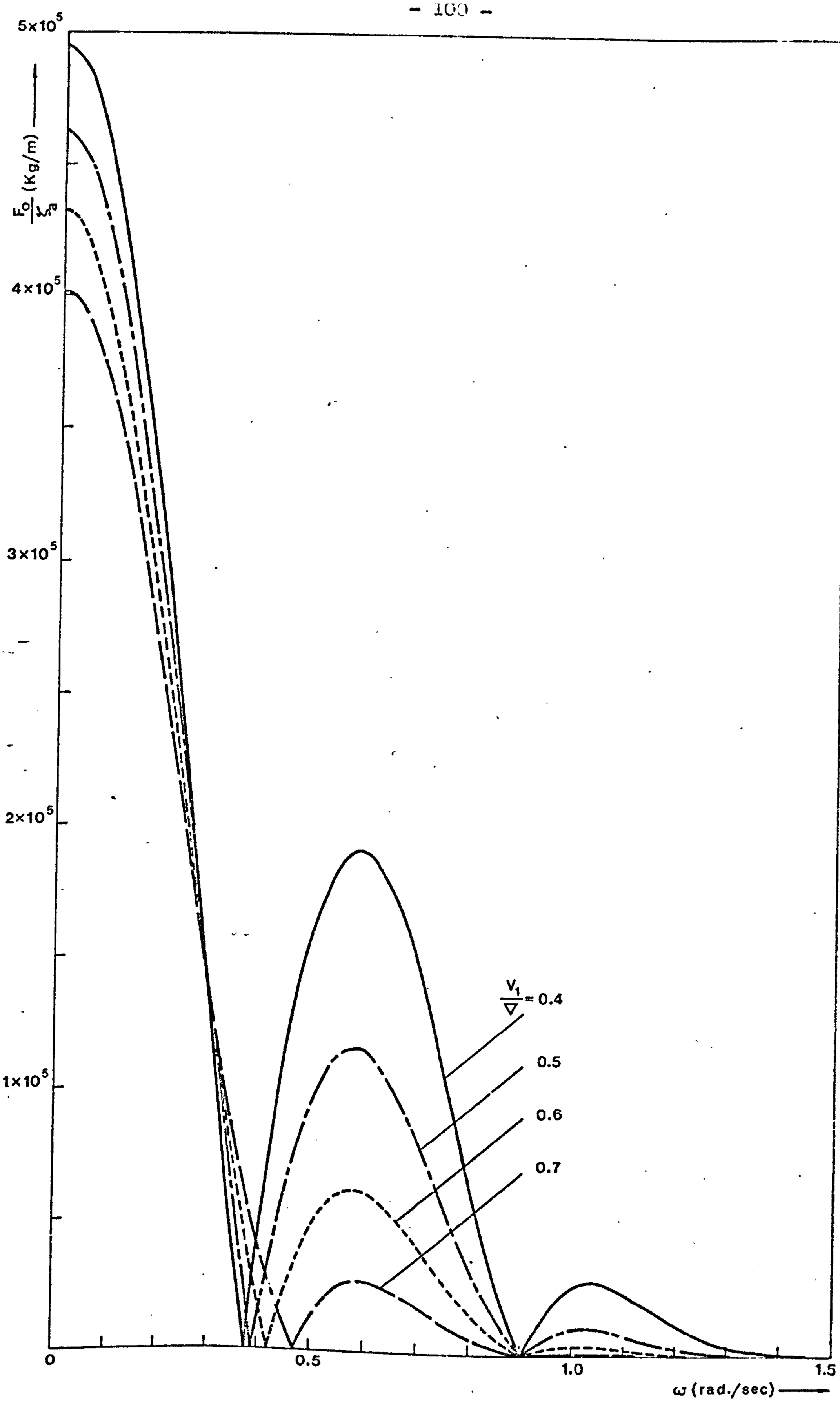

Fig. 5.8 The effect of volume ratio of a multi-hull platform on the vertical wave-excited forces in head seas

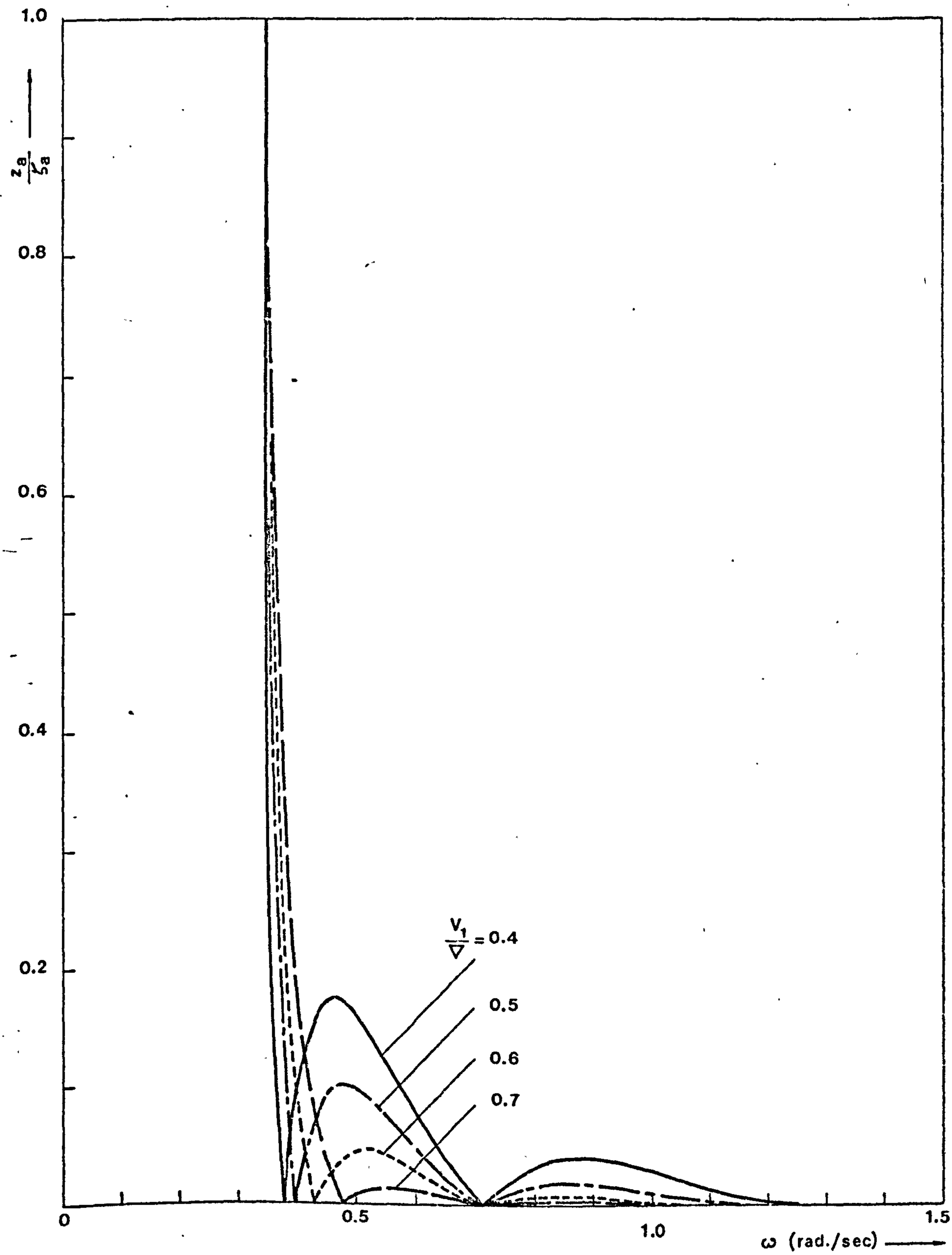

Fig. 5.9 The effect of volume ratio of a multi-hull platform on the heave response in beam seas

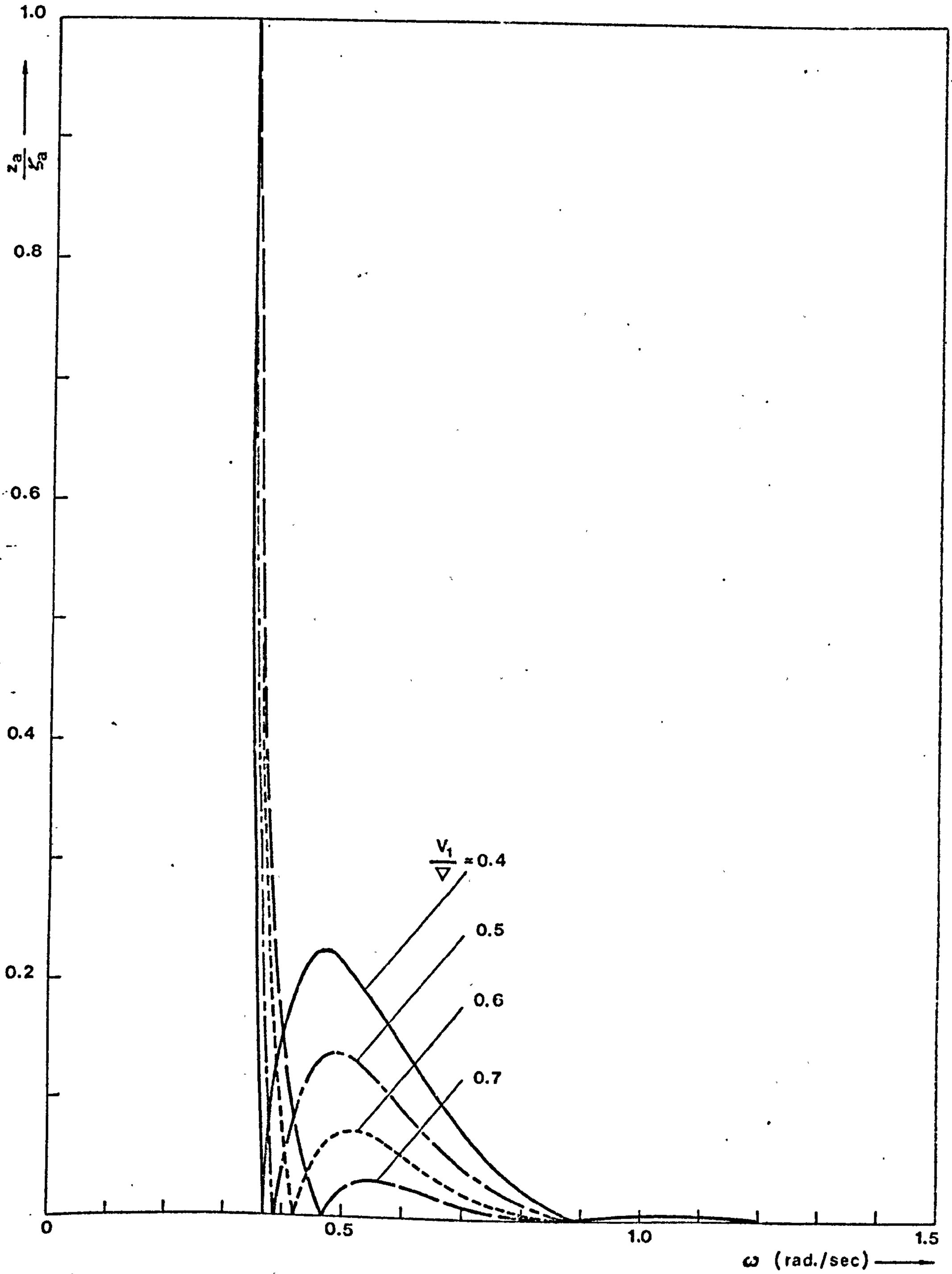

Fig. 5.10 The effect of volume ratio of a multi-hull platform on the heave response in head seas

In Table 5.3, d_2 is smaller than d_1 for the volume ratio of 0.7 and therefore this particular volume ratio will not be considered in the analysis of the results on the vertical forces and the heave response.

In the Figs. 5.7 to 5.10, it can be seen that for both beam and head seas conditions, as the volume ratio increases the forces and the heave response of the platform reduce . This effect is mainly due to the increased draught for the higher volume ratios since the pressure and acceleration in waves decrease exponentially with increasing depth from the still water level. The figures also show that the maximum heave response is reduced by 72% in the head seas and by 74.2% in the beam seas as the volume ratio is increased from 0.4 to 0.6. The heave response is proportional to the wave excited force which in turn is proportional to the term e^{-Kh_1} and when the values of e^{-Kh_1} at the frequency of maximum heave response ω_{max} are compared as shown in Table 5.4, it can be seen that the maximum response is reduced by 45% in the head seas and by 45.75% in the beam seas due to the term e^{-Kh_1} as the volume ratio is increased from 0.4 to 0.6. Thus the change in volume ratio does lead to a reduced response apart from the draught effect.

Table 5.4

$\frac{V_1}{\nabla}$	h_1	Head-Sea		Beam-Sea	
		ω_{max}	e^{-Kh_1}	ω_{max}	e^{-Kh_1}
0.4	24.84 m	0.475 rad/sec	0.564	0.47 rad/sec	0.571
0.5	33.12	0.490	0.444	0.48	0.460
0.6	42.59	0.520	0.310	0.52	0.310

5.2.3 The effect of the displacement of a multi-hull platform on the heave response

The displacement volume ∇ of the platform was varied from 20,000 m^3 to 40,000 m^3 with an increment of 10,000 m^3 while the other data were kept constant (see Table 5.1).

The dimensions of the platform obtained for different displacement volume are shown in Table 5.5.

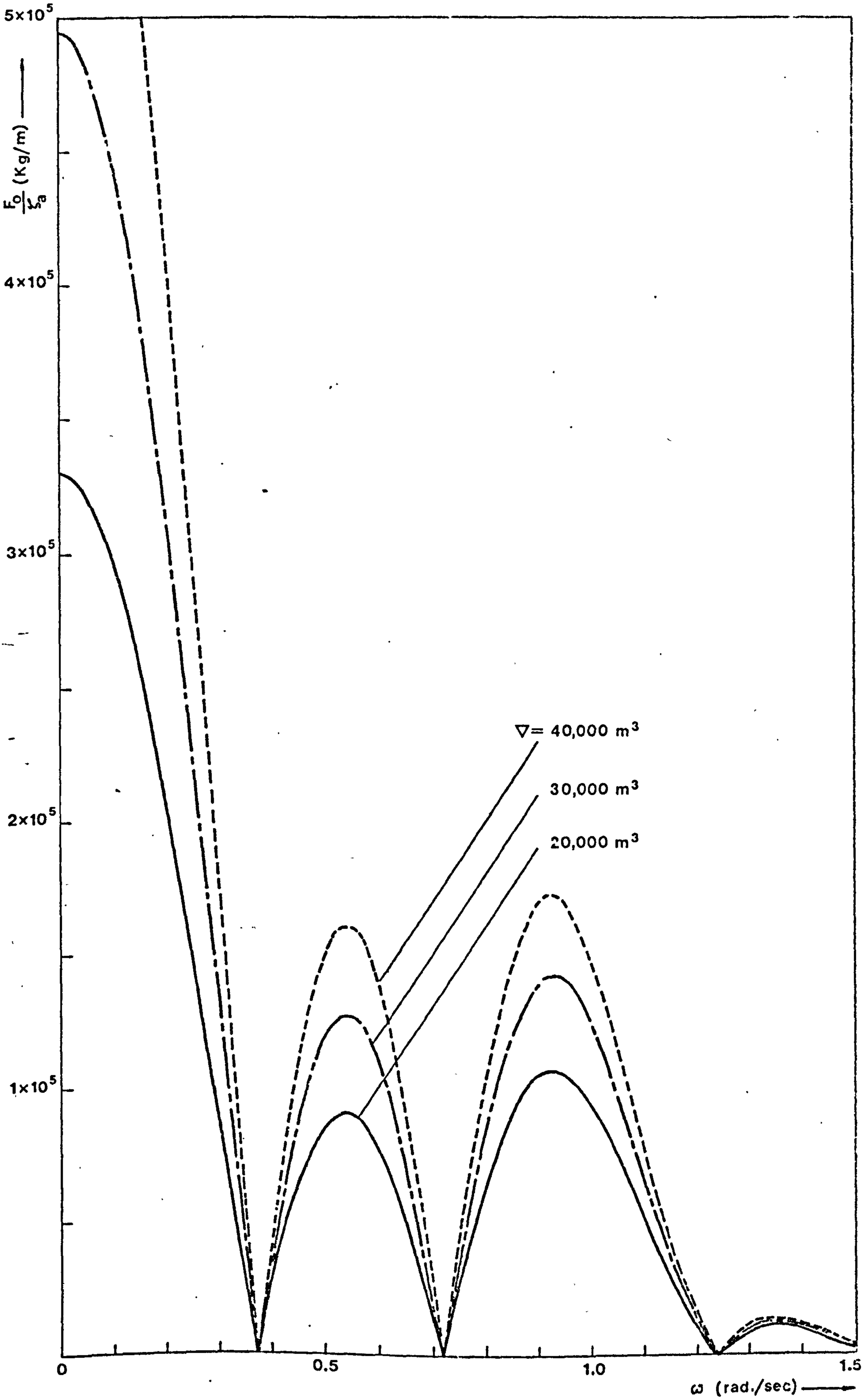

Fig. 5.11 The effect of displacement volume of a multi-hull platform on the vertical wave-excited forces in beam seas

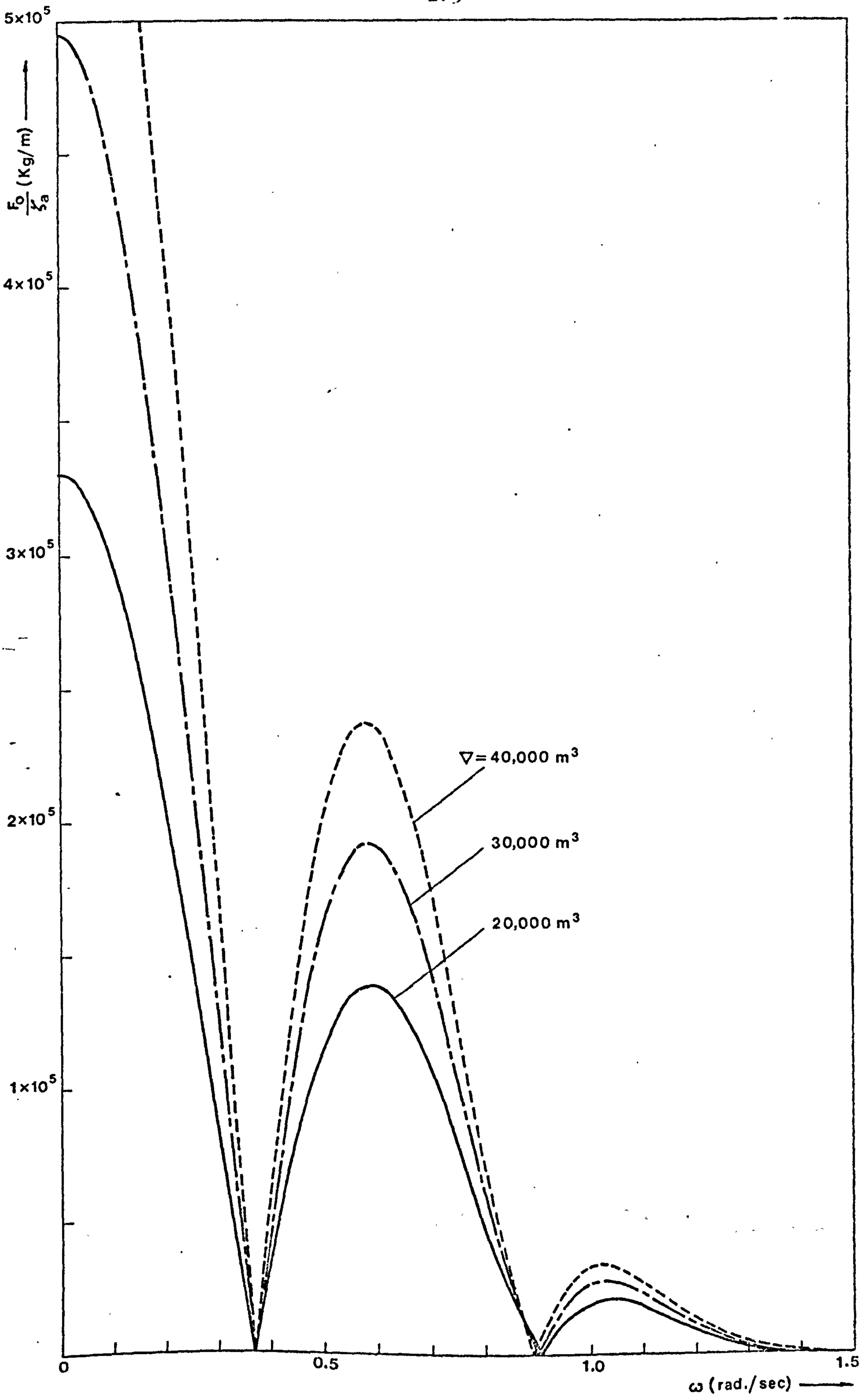

Fig. 5.12 The effect of displacement volume of a multi-hull platform on the vertical wave-excited forces in head seas

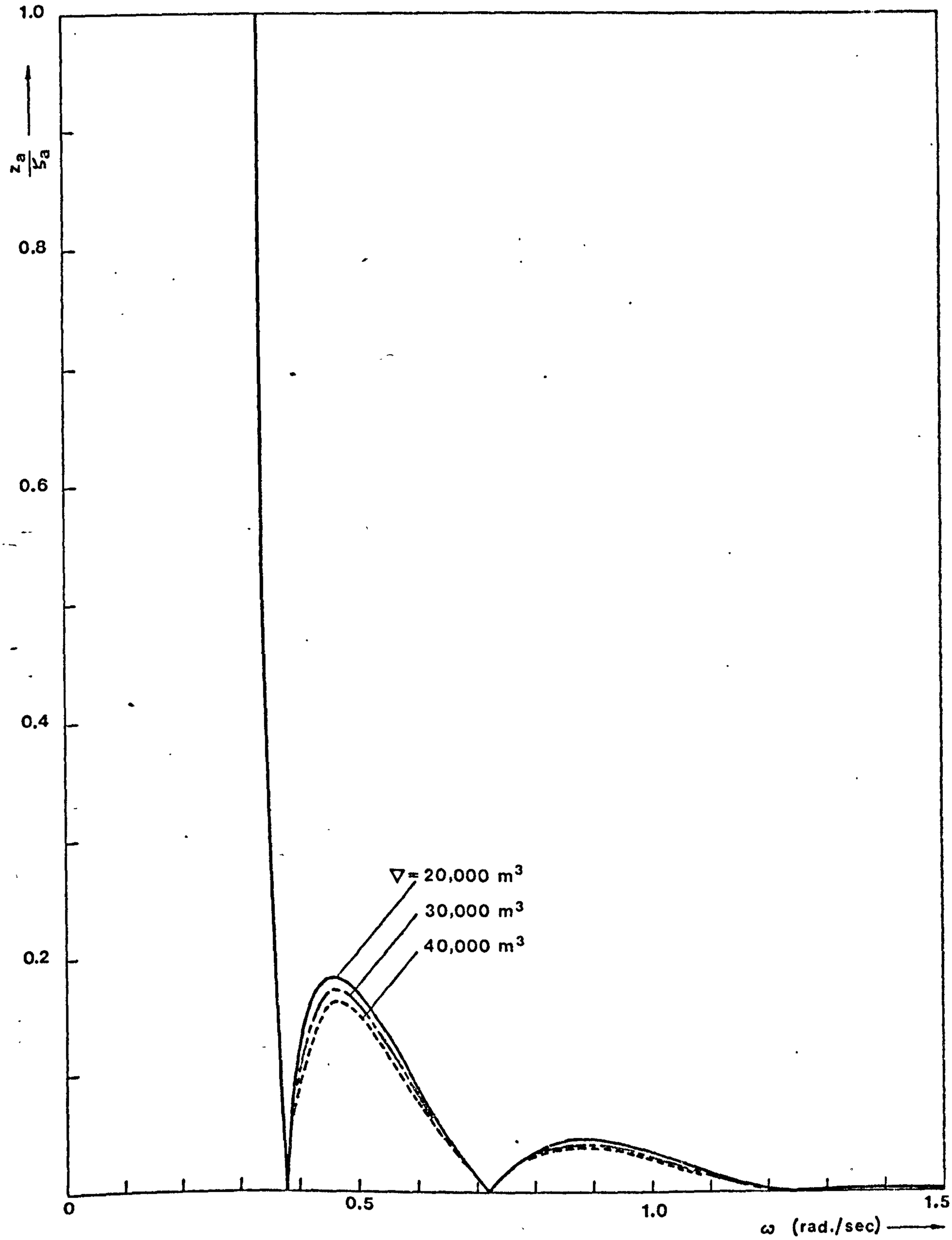

Fig. 5.13 The effect of displacement volume of a multi-hull platform on the heave response in beam seas

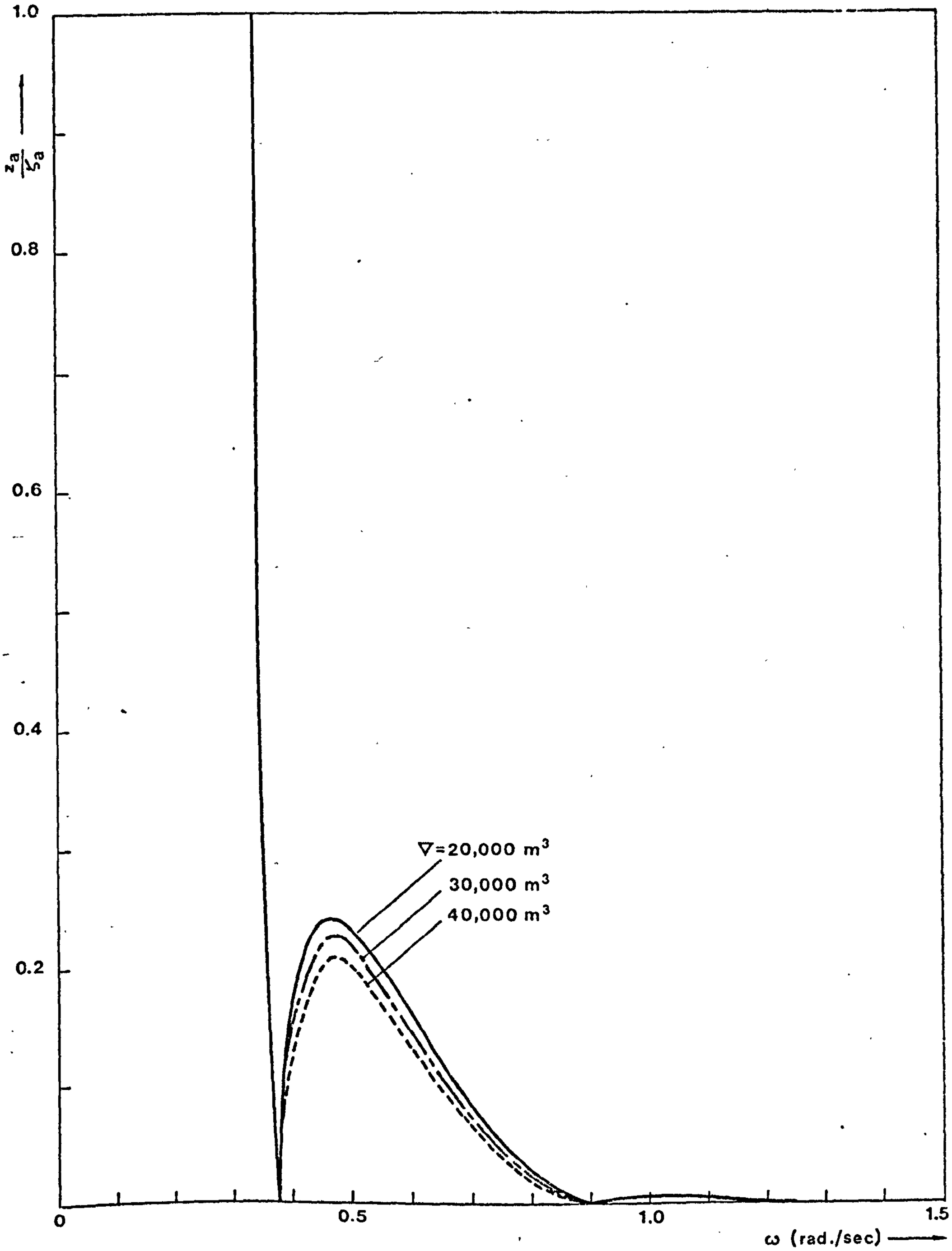

Fig. 5.14 The effect of displacement volume of a multi-hull platform on the heave response in head seas

Table 5.5

Dimensions of the platform for different displacement volume

∇	d_1	d_2	h_1	ℓ_2
20,000 m^3	8.27 m	9.66 m	24.84 m	81.79 m
30,000	10.12	11.70	24.84	83.65
40,000	11.69	13.39	24.84	85.21

The calculated vertical wave excited forces on, and the heave response of the platform are shown in Figs. 5.11 to 5.14.

From the Figs. 5.11 to 5.14, it can be seen that for both beam and head seas, the vertical forces on the platform increase as the displacement volume increases but the heave response of the platform decreases. The reduction in the response is mainly due to the increase in waterplane area i.e. spring stiffness with increasing displacement.

For the head-sea condition, the maximum heave response occurs at the frequency which is 1.49 times the natural frequency and is reduced by 12.5% when the displacement volume is increased from 20,000 m^3 to 40,000 m^3.

5.2.4 The effect of the beam and length of a multi-hull platform on the heave response

In this case, the beam b was varied from 50 m to 70 m with an increment of 10 m while the other data were kept constant (see Table 5.1). Since it is desirable to keep approximately the same period of rolling and pitching, this implies an increase in length ℓ_2 with increasing beam as shown in Table 5.6. The other dimensions of the platform for different beam are also shown in Table 5.6.

Table 5.6

Dimensions of the platform for different beam

b	d_1	d_2	h_1	ℓ_2
50 m	10.12 m	12.67 m	24.84 m	71.39 m
60	10.12	11.70	24.84	83.65
70	10.12	10.93	24.84	95.90

The calculated vertical wave excited forces and the heave response of the platform in the beam seas are shown in Figs. 5.15 and 5.16 and those of the head seas in Figs. 5.17 and 5.18.

Fig. 5.15 shows that in the frequency region of 0.38 to 0.8 radian per second, the vertical forces on the platform decrease and the frequency of maximum force moves toward a lower frequency as the beam increases.

Fig. 5.16 shows that for the beam seas, the maximum heave response of the platform occurs at the frequency which is 1.495 times the natural frequency and is reduced by 8.6% as the beam is increased from 50 meters to 70 meters.

In the Figs. 5.17 and 5.18 it can be seen that for the head seas, the maximum force decreases slightly but the maximum heave response is increased by 11.9% as the length ℓ_2 of the platform is increased from 71.39 meters to 95.90 meters.

In the beam seas the heave response reduces as the beam increases but in the head seas the response increases as the length ℓ_2 increases. Since the maximum response in the head seas is greater than that of the beam seas, an improvement in the response can be obtained by reducing the length ℓ_2.

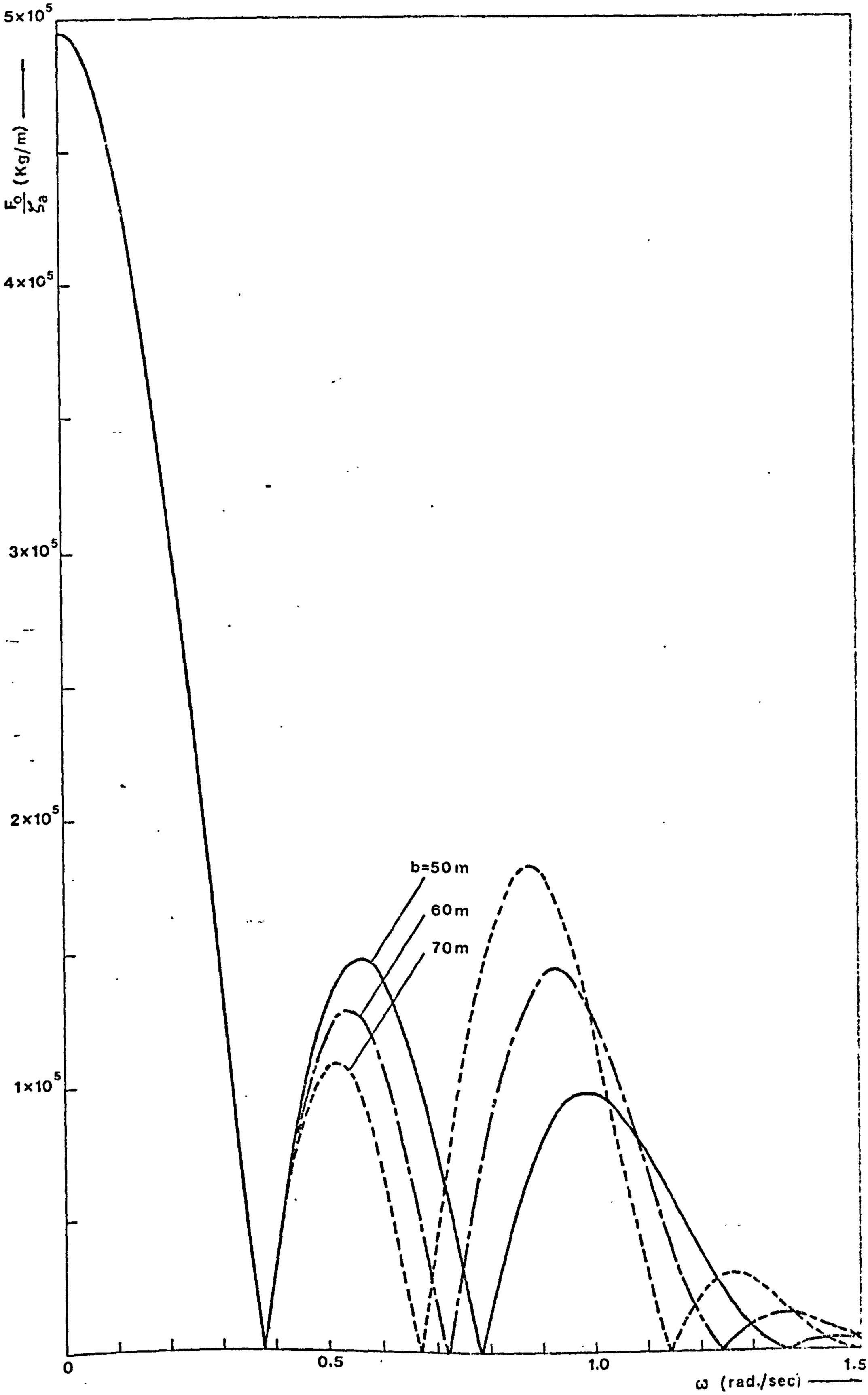

Fig. 5.15 The effect of beam of a multi-huli platform on the vertical wave-excited forces in beam seas

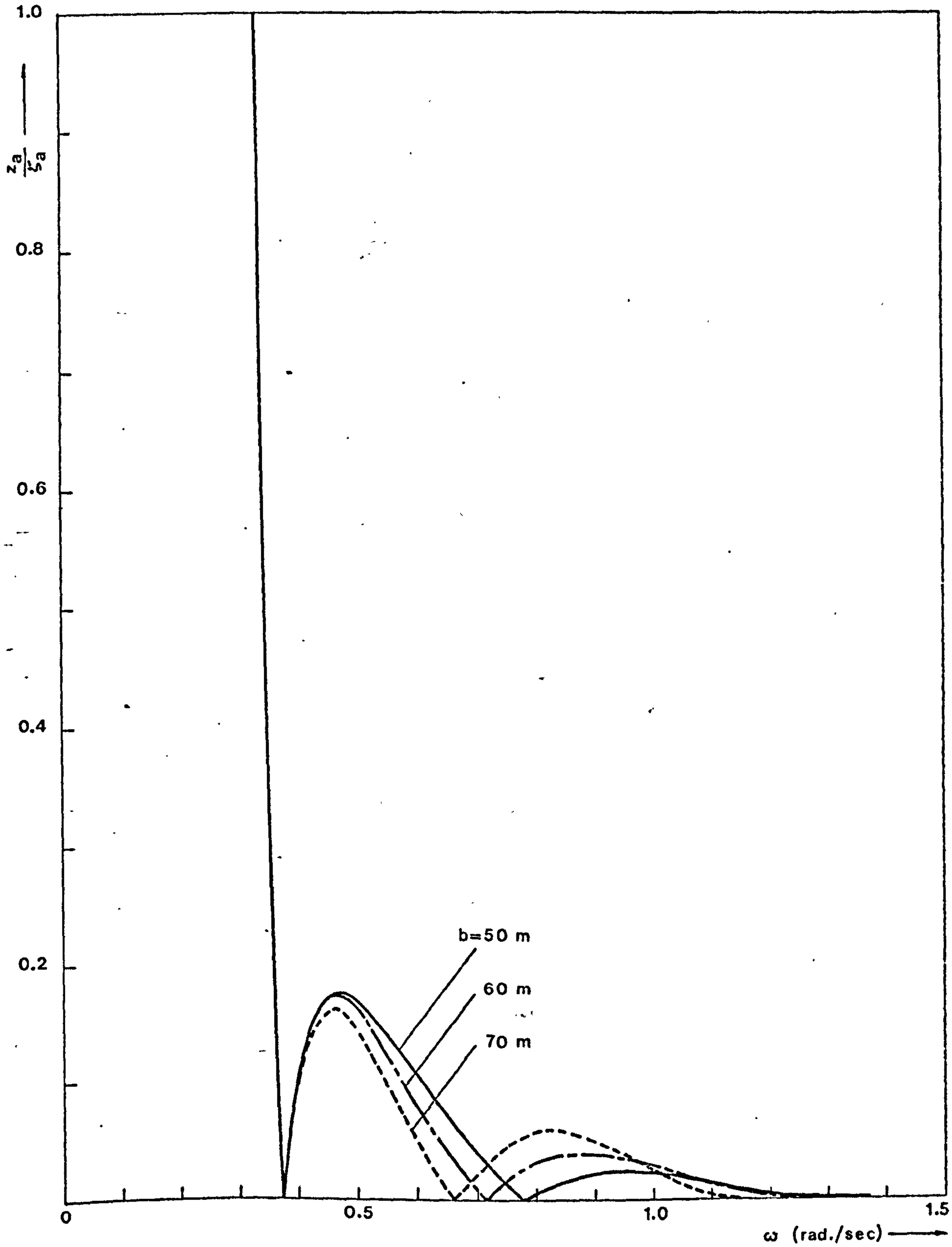

Fig. 5.16 The effect of beam of a multi-hull platform on the heave response in beam seas

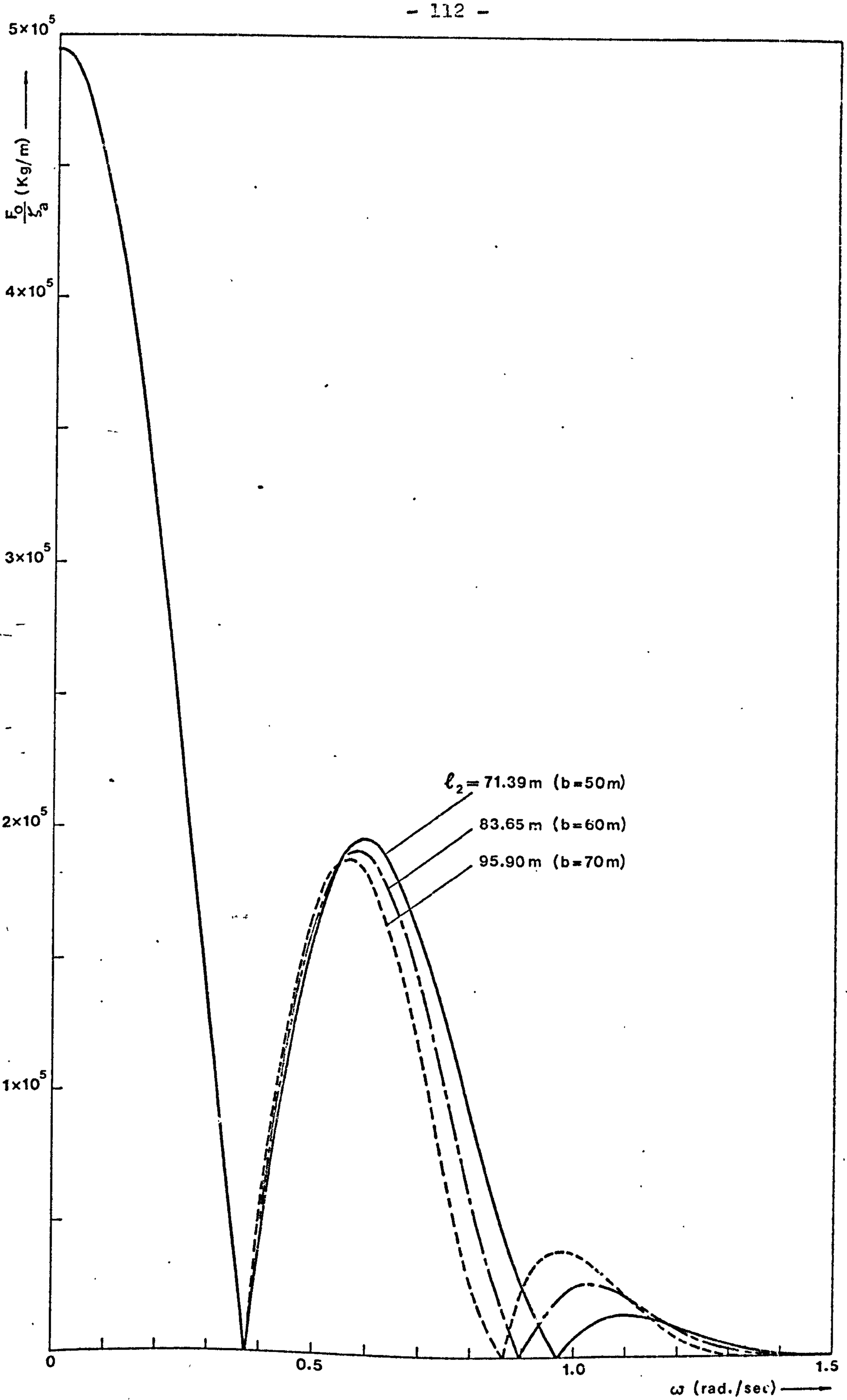

Fig. 5.17 The effect of length of a multi-hull platform on the vertical wave-excited forces in head seas

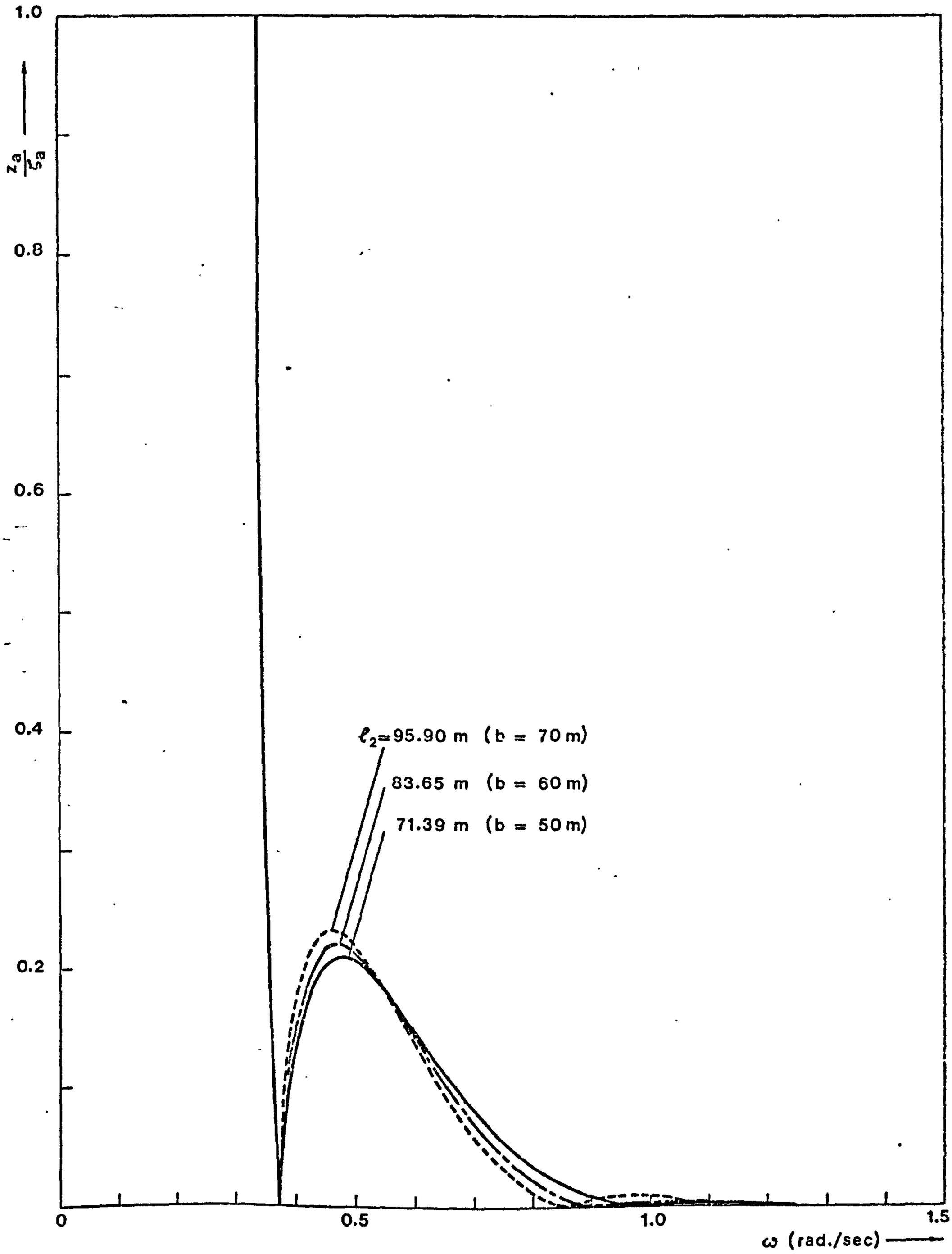

Fig. 5.18 The effect of length of a multi-hull platform on the heave response in head seas

5.2.5 The effect of the natural heave frequency of the platform on the heave response at a constant draught

In this case the natural heave frequency ω_n was varied from 0.286 to 0.349 radian per second (i.e. natural period T_Z from 22 to 18 seconds) while the draught h_1 was kept constant at 20 meters. The other data of the platform are given in Table 5.1.

The dimensions of the platform obtained for different natural frequency are shown in Table 5.7.

Table 5.7

Dimensions of the platform for different natural frequency

ω_n	T_Z	d_1	d_2	h_1	ℓ_2
0.286 rad/sec	22 sec	9.53 m	12.82 m	20 m	83.05 m
0.314	20	10.33	12.31	20	83.85
0.349	18	11.26	11.64	20	84.78

The calculated vertical wave excited forces and the heave response of the platform are shown in Figs. 5.19 to 5.22.

In the Figs. 5.19 to 5.22, it can be seen that for both beam and head seas, as the natural heave frequency increases at a constant draught the maximum wave excited forces and the maximum heave response reduce . For the head seas, the maximum response is reduced by 43.6% and the frequency of maximum response moves toward a higher frequency as the natural frequency is increased from 0.286 to 0.349 rad./sec.

Although the response can be reduced by increasing the natural frequency, it should be noted that at a higher frequency there is a risk of synchronism with high wave frequencies commonly encountered and of extremely severe response due to the synchronism.

PAGE
NUMBERS
CUT OFF
IN
ORIGINAL

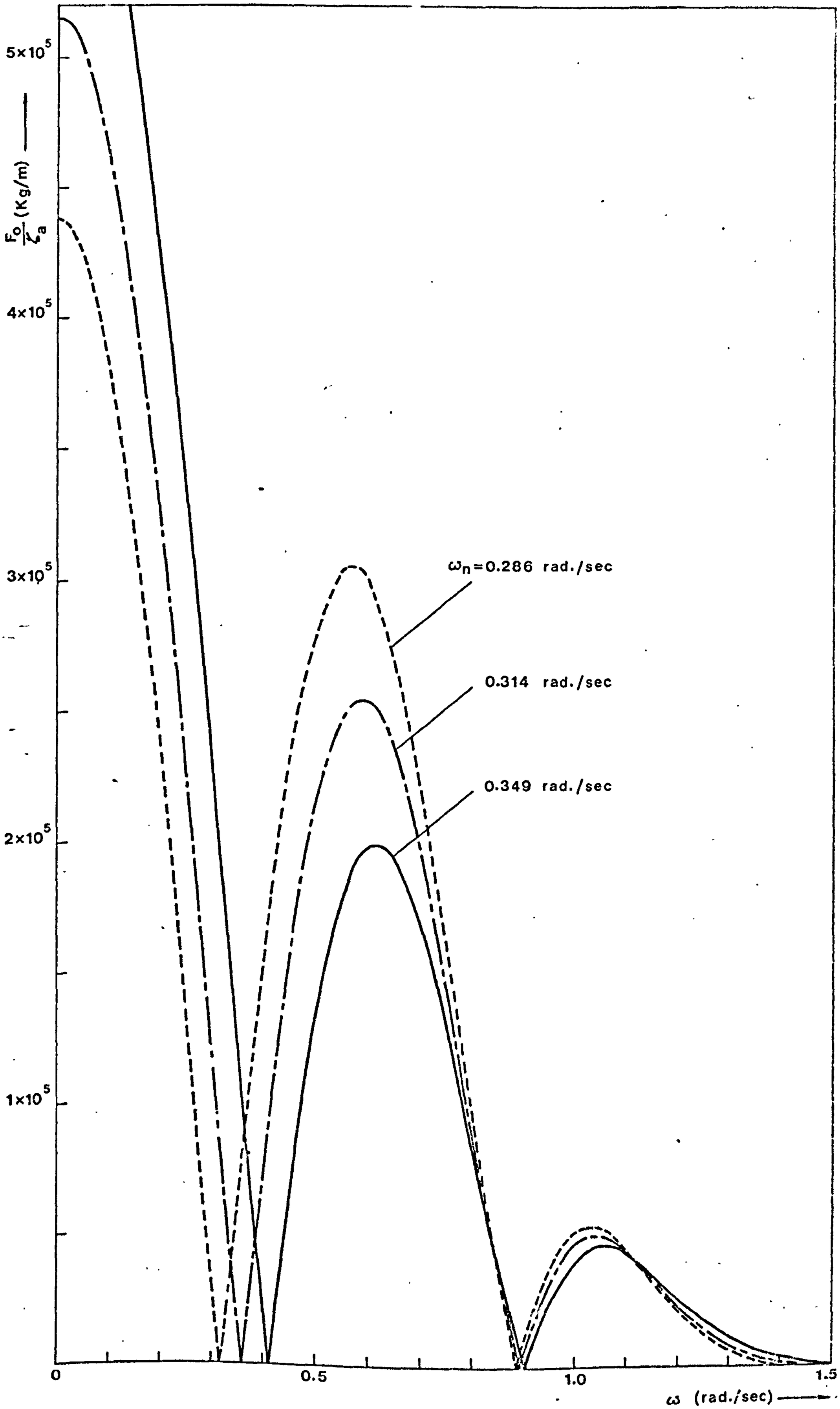

Fig. 5.20 The effect of natural heave frequency of a multi-hull platform on the vertical wave-excited forces in head seas

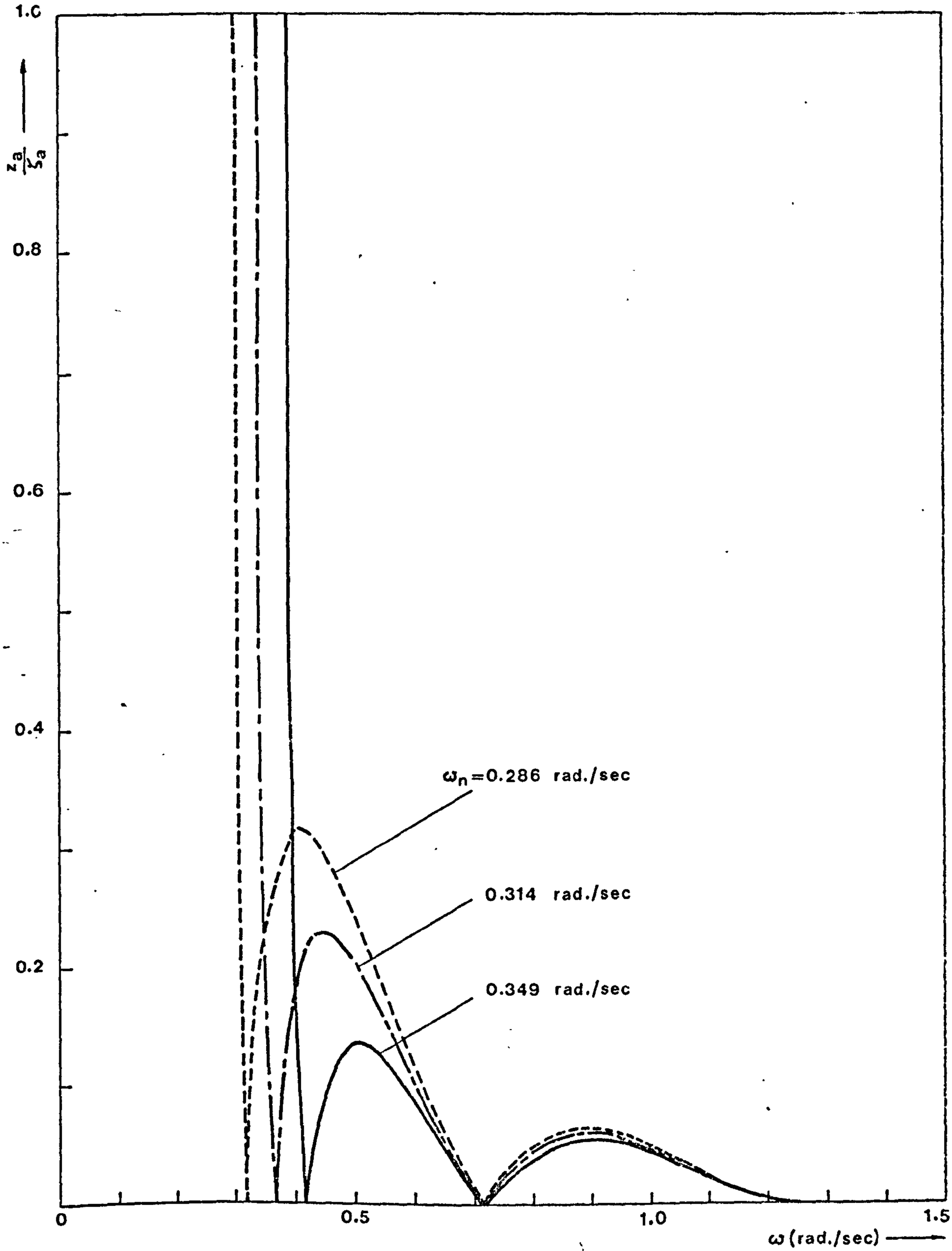

Fig. 5.21 The effect of natural heave frequency of a multi-hull platform on the heave response in beam seas

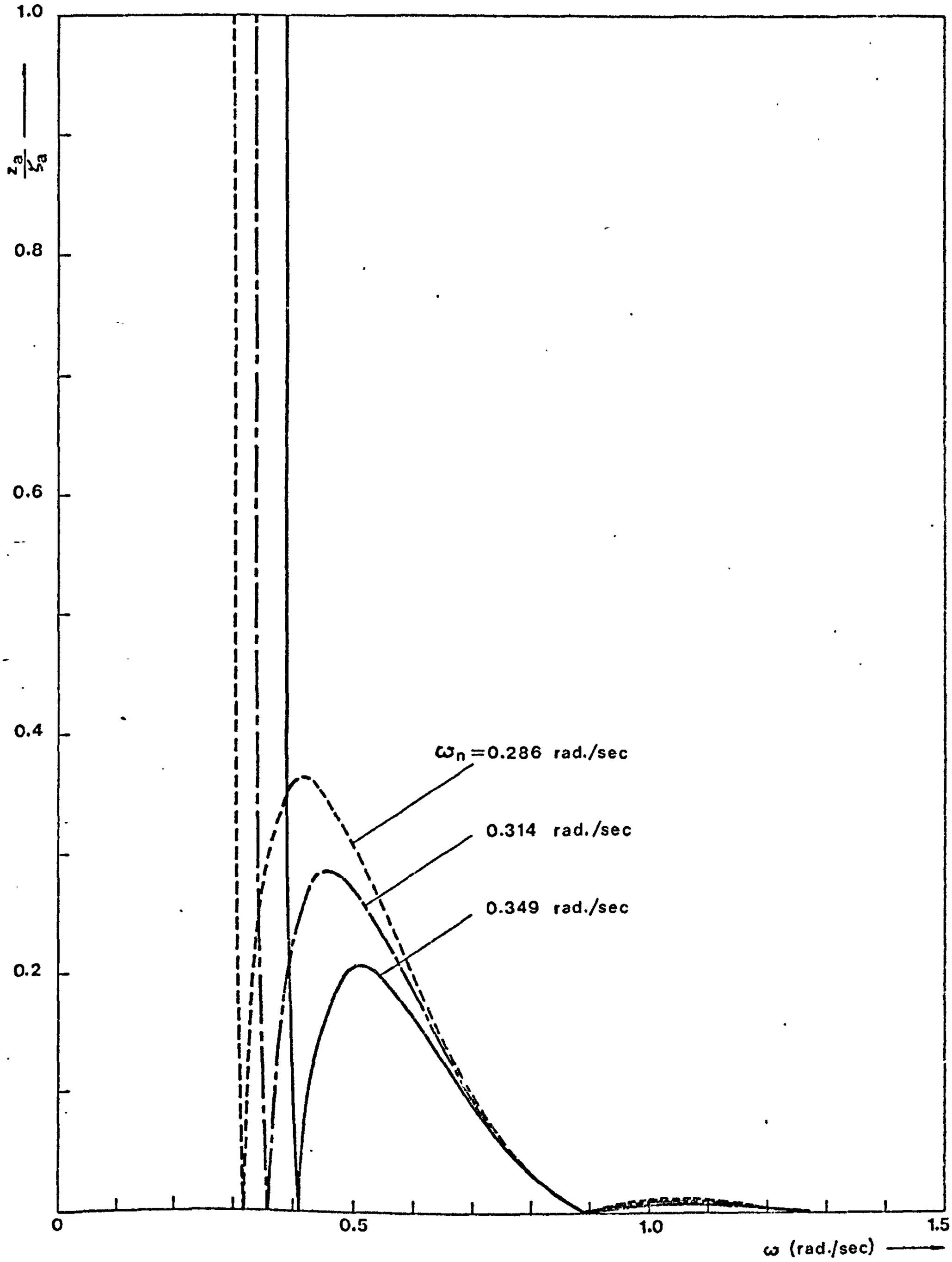

Fig. 5.22 The effect of natural heave frequency of a multi-hull platform on the heave response in head seas

5.2.6 Conclusions

The detailed effects on heaving force and heave response of each change in geometry or dimensions have been listed above and it is believed they provide sufficient guidance for a designer to evaluate the best method of improving a given initial design. Broadly speaking the heaving motion is improved with:

(a) Greater number of vertical columns,

(b) Larger volume ratio or deeper draught,

(c) Larger displacement volume,

(d) Smaller beam or length, and

(e) Larger natural heave frequency at a constant draught,

but all of these factors affect matters such as stability, water resistance, steel weight, etc., and the optimum must be selected in conjunction with an analysis of these other aspects.

5.3 Comparison Between the Heave Response of a Multi-Hull and a Multi-Leg Semi-Submersible Platform

5.3.1 The Multi-Hull Platform

The multi-hull platform (Fig. 3.1) with 3 vertical columns on each horizontal cylinder was compared with a multi-leg platform with a variable number of legs. The dimensions of the multi-hull platform were taken from Table 5.2 of Section 5.2.1. The principal data chosen for the multi-hull platform are given in Table 5.8.

Table 5.8

Displacement volume	∇ = 30,000 m^3
Natural heave frequency	ω_n = 0.314 rad./sec
Beam	b = 60 m
Volume ratio	$\frac{V_1}{\nabla}$ = 0.4
Number of vertical columns on each cylinder	n = 3
Diameter of the vertical columns	d_1 = 10.12 m
Diameter of the horizontal cylinder	d_2 = 11.70 m
Draught	h_1 = 24.84 m
Length of the horizontal cylinder	ℓ_2 = 83.65 m

The calculated vertical wave excited forces on, and the heave response of the platform were obtained from Figs. 5.3 to 5.6 for n is equal to 3.

5.3.2 The Multi-Leg Platform

The multi-leg platform (Fig. 3.4) with a variable number of legs, i.e. n is varied from 3 to 6, was chosen for comparison with the multi-hull platform described in Section 5.3.1.

In order to obtain a realistic comparison, the basic data such as the displacement volume, the natural heave frequency and the draught were kept constant for both types of platforms. In addition, the height h_2 of the circular caisson of the multi-leg platform and the diameter d_2 of the horizontal cylinder of the multi-hull platform were kept the same since the vertical wave excited forces decrease exponentially with increasing depth of submergence.

The radius R_c of the circle passing through the centres of the legs was chosen as 40 meters so that in head-sea condition, the diameter of the circle (i.e. 80 meters) would be approximately equal to the length ℓ_2 of the multi-hull platform.

The above arguments determine the following data for the multi-leg platform:-

$$\nabla = 30{,}000 \text{ m}^3$$

$$\omega_n = 0.314 \text{ rad./sec}$$

$$h_1 = 24.84 \text{ m}$$

$$h_2 = 11.70 \text{ m}$$

$$R_c = 40 \text{ m}$$

The values of radius R_1 of the vertical column and radius R_2 of the circular caisson were determined for different values of the number of legs n, by the aid of a computer programme. The values of R_1 and R_2 for different values of n are shown in Table 5.9.

Table 5.9

n	R_1	R_2
3	7.34 m	12.56 m
4	6.28	10.97
5	5.55	9.90
6	5.00	9.11

The vertical wave excited forces on the multi-leg platform were calculated using the equation (3.77) and the heave response of the platform using the equation (2.5) after neglecting the damping term.

In the calculations for head seas, the angle of orientation ϕ (Fig. 3.4) to the wave direction is zero so that one leg of the platform lies on the ξ - axis and for beam seas, ϕ is equal to $\frac{\pi}{2}$ and one leg lies on the η-axis.

If the multi-leg platform is rotated anti-clockwise from the head-sea condition, the orientation of the platform relative to the wave direction will be changed and it is necessary to consider the effect of such change in orientation on heave response. If the 3-legged platform is rotated through 60 degrees from the head-sea condition the platform will be in a mirror image position about the η-axis for the head-sea condition (see Fig. 5.23) and its response would be as for head seas. If rotated 30 degrees it is in a mirror image position about the ξ-axis for the beam-sea condition and will give the beam-sea response. If the 5-legged platform is rotated through 36 degrees the platform will be in a mirror image position about the η-axis for the head-sea condition (Fig. 5.23) and its response would be as for head seas. If rotated 18 degrees it will be in the beam-sea condition and will give the beam-sea response. If the 6-legged platform is rotated through 30 degrees the platform will be in a beam-sea condition (Fig.5.23). To obtain an orientation which will differ from the head and beam seas, the 3-legged platform has to be rotated less than 30 degrees, for the 5-legged platform less than 18 degrees and for the 6-legged platform less than 30 degrees. But for such small amount of rotation the effect of orientation would not be significant since in practice a seaway is likely to have spread of $\pm$ 30 degrees.

If the 4-legged platform is rotated 45 degrees the orientation will be different from the head and beam seas (Fig. 5.23). In 45 degrees orientation the magnitude of the forces and the frequencies of zero forces will be changed but the maximum heave response would remain the same order as those of the head and beam seas.

Comparisons between the calculated vertical wave excited forces and the heave response of the multi-hull platform and that of the multi-leg platform with variable number of legs are shown in Figs. 5.24 to 5.27.

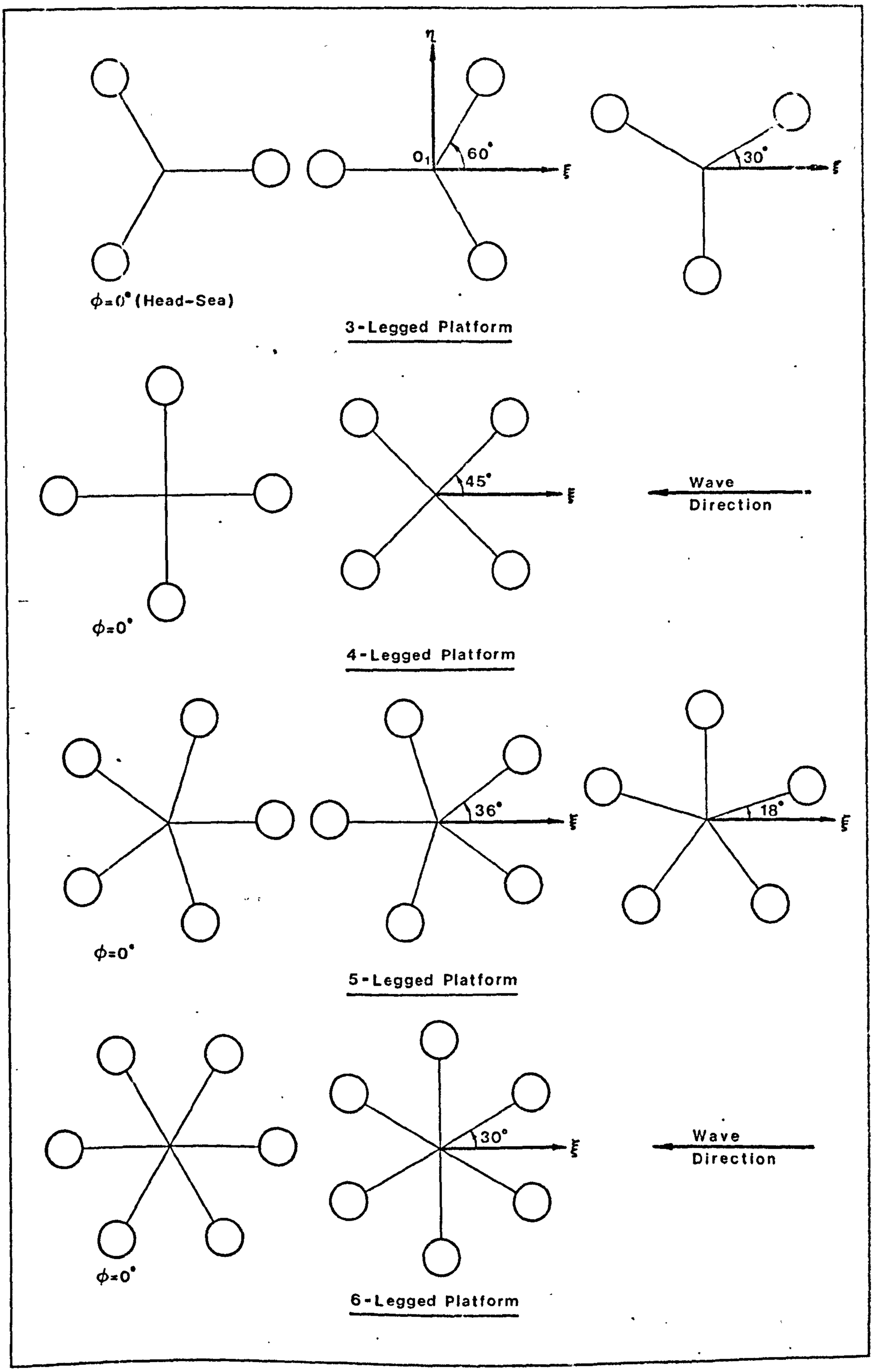

Fig. 5.23 Orientations of multi-leg platforms relative to wave direction

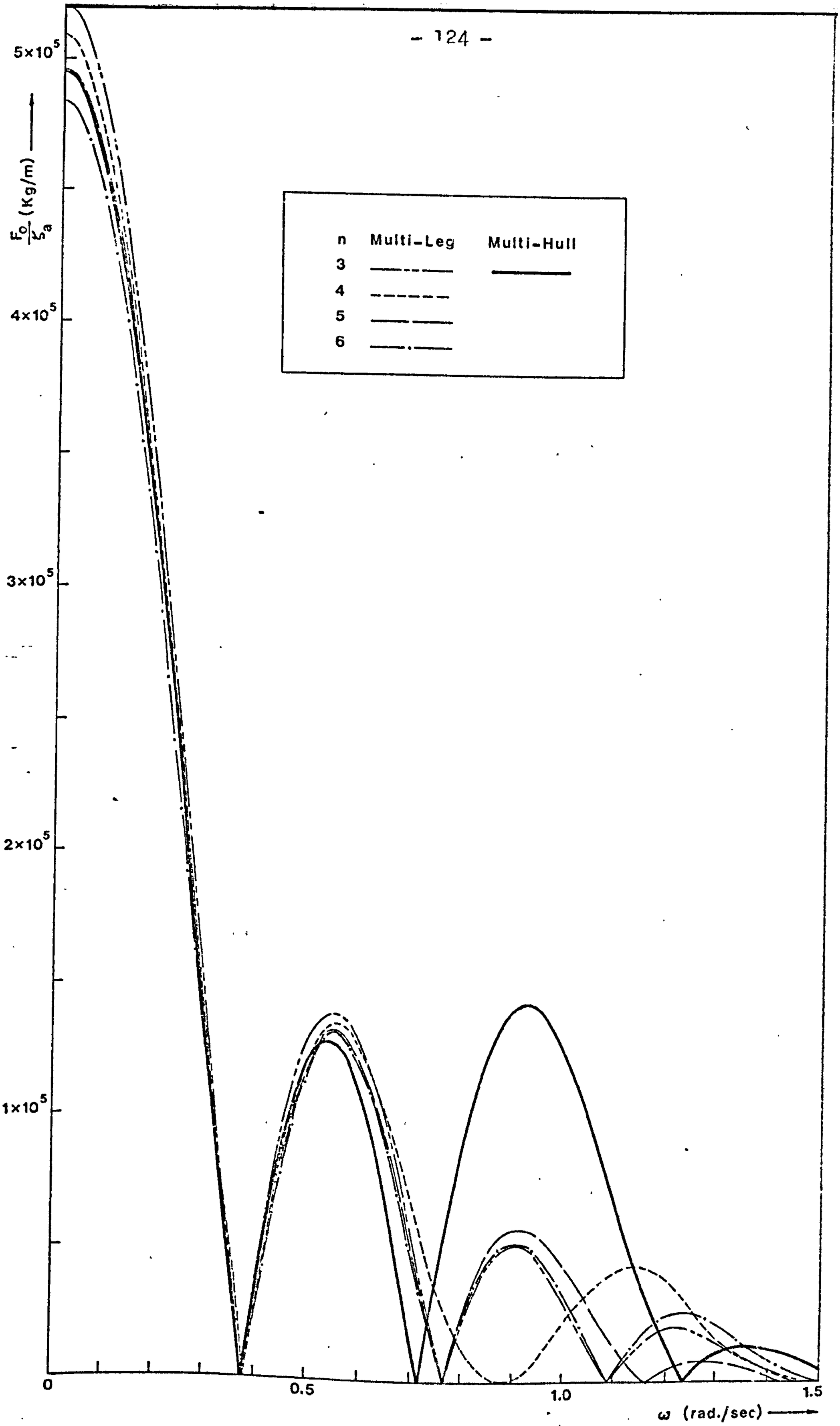

Fig. 5.24 Comparison between the vertical wave-excited forces on a multi-hull and on multi-leg platforms in beam seas

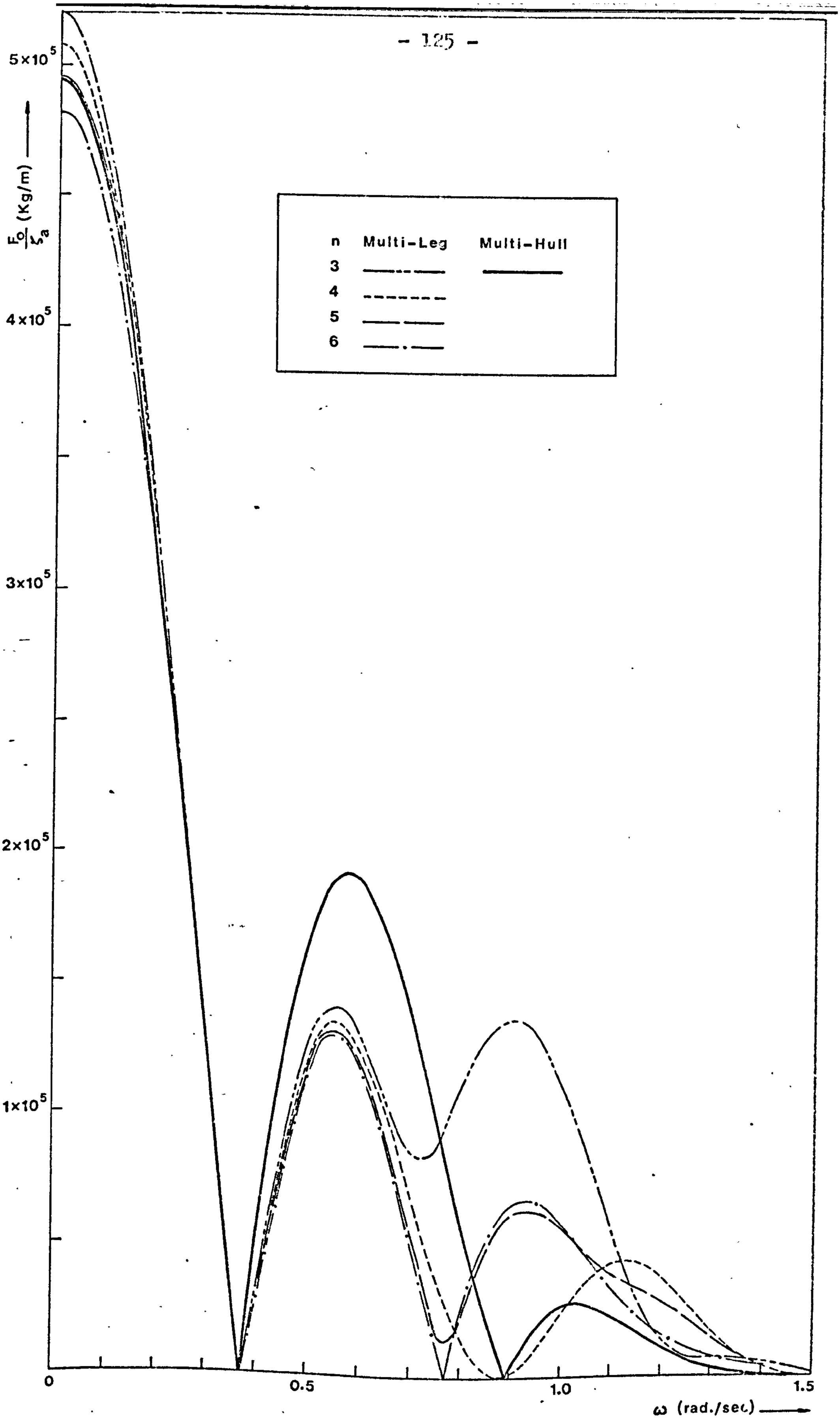

Fig. 5.25 Comparison between the vertical wave-excited forces on a multi-hull and on multi-leg platforms in head seas

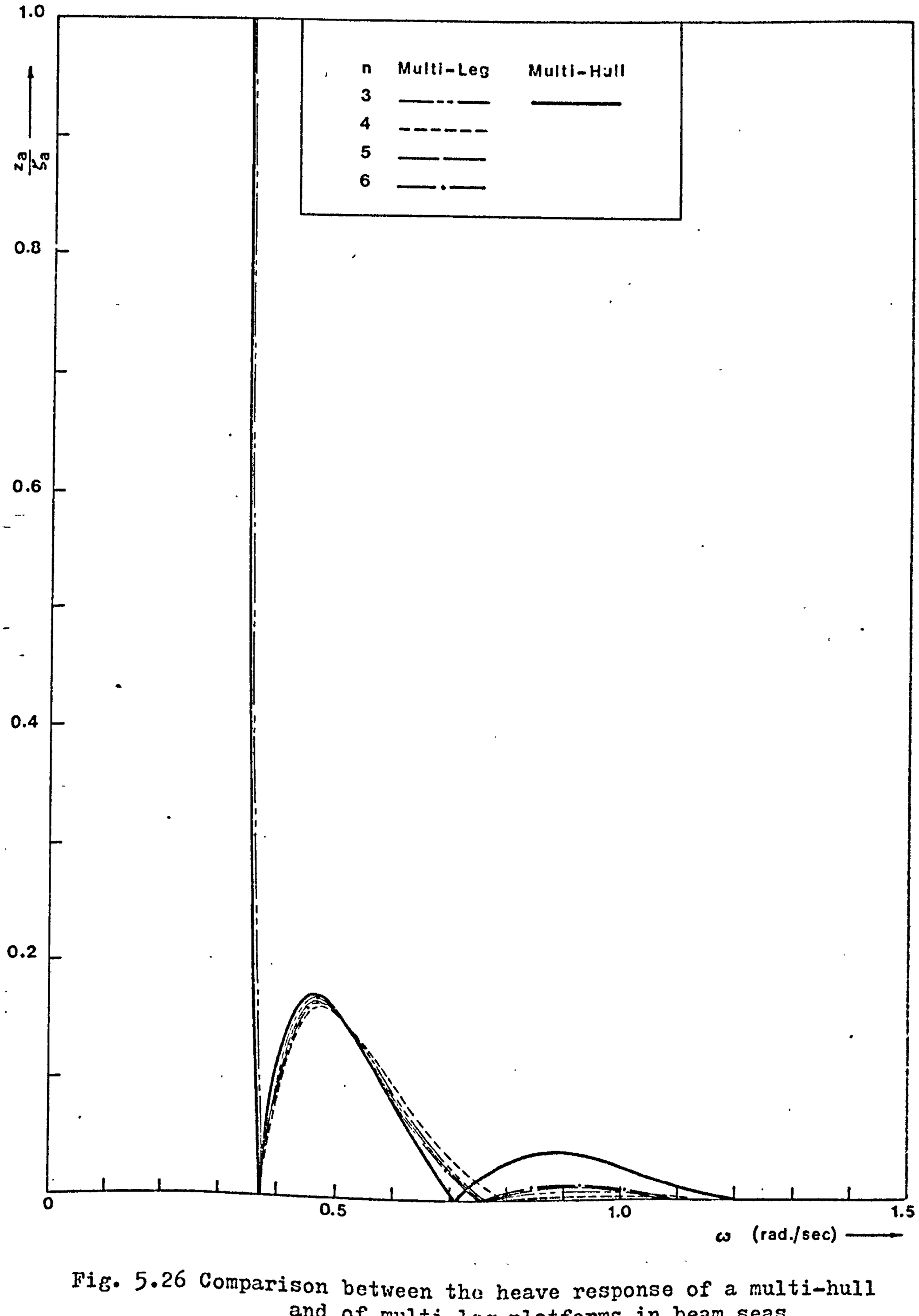

Fig. 5.26 Comparison between the heave response of a multi-hull and of multi-leg platforms in beam seas

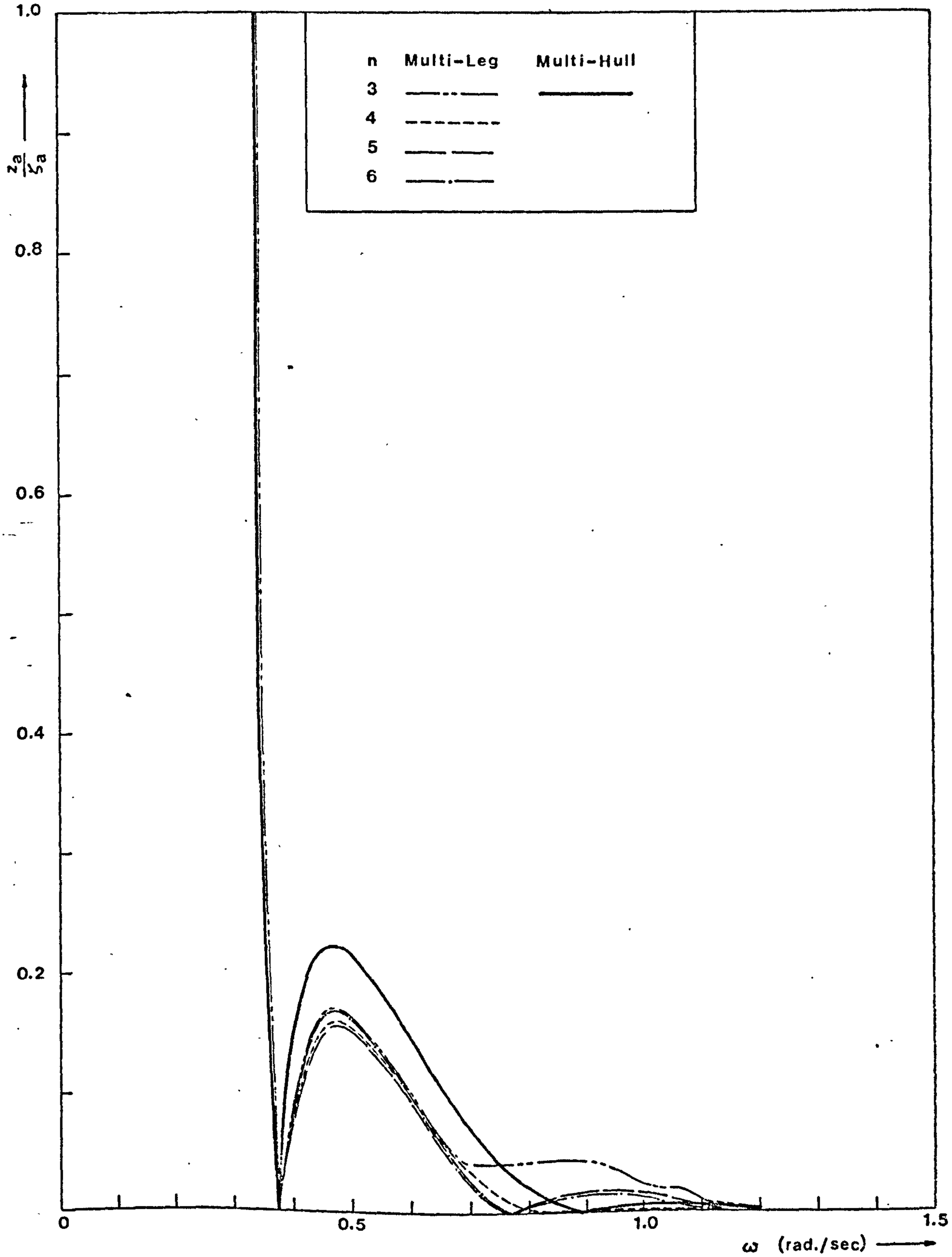

Fig. 5.27 Comparison between the heave response of a multi-hull and of multi-leg platforms in head seas

5.3.3 Discussion on the Results

Fig. 5.24 shows that in the beam-sea condition, the maximum vertical wave excited forces on the multi-hull and on the multi-leg platform with variable number of legs occur at a frequency of about 0.55 rad./sec and the magnitude of the maximum force on the multi-leg platform is about 8% greater than that of the multi-hull. The multi-hull platform has another maximum force at the frequency of about 0.93 rad./sec but this force has very little effect on the heave response since the magnification factor is small at this frequency. The forces on the multi-leg platform become zero at three values of frequencies and if we denote ω_1 for the lowest value, ω_2 for intermediate value and ω_3 for the highest value, it can be seen from Fig. 5.24 that ω_1 occurs at about 0.38 rad./sec for all number of legs. At this frequency, the pressure force and the inertia force on the platform are equal and cancel each other. The forces at ω_2 and ω_3 are zero because at these frequencies, the term $\sqrt{Q_c^2 + Q_s^2}$ in the force equation (3.77) becomes zero. Actually, in the beam-sea condition

$$Q_s = \sum_{i=0}^{n-1} \sin\left[KR_c \cos\left(\frac{2\pi}{n} i + \phi\right)\right]$$

is always zero for all values of n. Thus the forces are zero in the beam-sea condition, when

$$Q_c = \sum_{i=0}^{n-1} \cos\left[KR_c \cos\left(\frac{2\pi}{n} i + \phi\right)\right] = 0$$

For example, if the 3-legged and the 4-legged platforms are considered and the values of 40 meters and $\pi/2$ radians are substituted for R_c and ϕ respectively in the above equation, the following values of ω_2 and ω_3 are obtained:

	ω_2	ω_3
3-legged platform	0.769 rad./sec	1.09 rad./sec
4-legged platform	0.88	1.52

The values of ω_2 and ω_3 for the 5-legged and the 6-legged platforms can also be obtained in a similar way. It should be noted that there are several zero forces at the frequencies higher than ω_3 but at these high frequencies the forces and the heave response are so small that they are not significant.

From Fig. 5.26, it can be seen that in the beam-sea condition the maximum heave responses of the multi-hull and of the multi-leg platform occur at the frequency of about 0.47 rad./sec (or 1.49 times the natural frequency) and the magnitude of the maximum responses are approximately the same. For frequencies greater than 0.75 rad./sec, the heave response of the multi-hull platform is greater than that of the multi-leg platform and the heave amplitude of the former platform is less than 5% of the wave amplitude.

Fig. 5.25 shows that in the head-sea condition, the maximum vertical wave excited forces on the multi-hull platform and on the multi-leg platform occur at the frequency of about 0.56 rad./sec (or 1.78 times the natural frequency) and the magnitude of the maximum force on the multi-leg platform is 29% less than that of the multi-hull. As for the beam-sea condition the forces on the multi-leg platform become zero at the frequency of about 0.38 rad./sec for all number of legs due to the pressure force and the inertia force cancelling one another. The forces also become zero when the term $\sqrt{Q_c^2 + Q_s^2}$ is equal to zero. It should be noted that Q_c can be zero at certain frequencies for any number of legs while Q_s can be zero only for even number of legs. Thus the forces on the 3-legged and on the 5-legged platforms are not equal to zero in the frequency region from 0.7 to 0.9 rad./sec while the forces on the 4-legged and on the

6-legged platforms become zero at the frequency of 0.88 rad./sec and 0.76 rad./sec respectively. The 3-legged platform has another maximum force at the frequency of about 0.9 rad./sec.

From Fig. 5.27, it can be seen that in the head-sea condition the maximum heave responses of both multi-hull and multi-leg platforms occur at the frequency of about 0.47 rad./sec (or 1.49 times the natural frequency). The magnitude of the maximum response of the multi-leg platform is about 25% less than that of the multi-hull. In the frequency range between 0.38 and 0.75 rad./sec the heave response of the multi-leg platform is smaller than that of the multi-hull. From the frequency of 0.75 to 1.0 rad./sec, the heave response of the 3-legged platform is greater than that of the multi-hull, and the heave amplitude of the former platform is less than 5% of the wave amplitude.

5.3.4 Conclusions

From the comparison of heave responses of the multi-hull and of multi-leg platforms, the following conclusions can be made:

1. The maximum heave amplitude of the multi-leg platform which is about 16.5% of the wave amplitude is approximately the same in both beam-sea and head-sea conditions and it occurs at the frequency of about 1.49 times the natural frequency.

2. In beam-sea condition, the heave responses of the multi-hull and the multi-leg platforms are approximately the same in the frequency range from 0.38 to 0.75 rad./sec. For frequencies greater than 0.75 rad./sec, the heave amplitudesof both types of platforms are less than 5% of the wave amplitude but the heave response of the multi-leg platform is smaller than that of the multi-hull.

3. In head-sea condition, the maximum heave response of the multi-leg platform is about 25% less than that of the multi-hull and it occurs at the frequency of about 1.49 times the natural frequency. In the frequency range from 0.38 to 0.75 rad./sec, the heaving motion characteristic of the multi-leg platform is better than that of the multi-hull. For frequencies greater than 0.75 rad./sec the heave amplitude of both types of platforms are less than 5% of the wave amplitude but the heave response of the 3-legged platform is greater than that of the other platforms.

GENERAL CONCLUSIONS

A theoretical method of calculating the heave response of a semi-submersible platform in regular waves has been developed and the equations for calculating vertical wave excited forces on a multi-hull and on a multi-leg platform have been given in the foregoing chapters. Also, the calculated wave excited forces and the heave response have been compared with the experimental results of the models of different designs and compared with the full scale measurements of the multi-hull platform. The comparisons show that the theory agrees sufficiently with both the model results and the full scale measurements.

Computer programmes have been written for calculating heave response of a multi-hull and of a multi-leg platform. Using these programmes, the effects of changing dimensions or geometry of a multi-hull platform on the heave response have been investigated and the detailed effects of each change in dimensions are given in the chapter 5. In general, the heave response can be reduced with:-

(a) Greater number of vertical columns,

(b) Larger volume ratio or deeper draught,

(c) Larger displacement volume,

(d) Smaller beam or length, and

(e) Larger natural heave frequency at a constant draught.

A comparison between the heave response of a multi-hull and of a multi-leg platform with variable number of legs has also been made in the chapter 5 using the computer programmes. The comparison shows that the maximum heave response of the multi-leg platform in the beam seas is approximately the same as, and in the head seas is about 25% less than, that of the multi-hull platform in the wave frequency region of 0.38 to 0.75 radian per second.

It is believed that the results of the investigations given in the chapter 5 and the theoretical method developed in this thesis provide sufficient guidance for a designer to evaluate the best method to improve a given initial design with regard to the heaving motion.

REFERENCES (CHAPTER 1)

(1.1) "What's Ahead for Offshore Oil", Ocean Industry, January 1973, pp. 19-24.

(1.2) "1972-73 Directory of Marine Drilling Rigs", Ocean Industry, September 1972, pp. 73-120.

(1.3) Howe, R.J., "The History and Current Status of Offshore Mobile Drilling Units", Ocean Industry, July 1968, pp. 38-61.

(1.4) Macy, R.H., "Towing, Motions, and Stability Chacteristics of Ocean Platforms", Sixth Naval Hydrodynamics Symposium, Washington D.C., 1966.

(1.5) "Sedco 700 - Rig designed for the future", Ocean Industry, August 1971, pp. 44-45.

(1.6) "Sedco 135 F takes a 95 ft. wave", Ocean Industry, January 1969, pp. 21-22.

(1.7) Miller, E.R. and Scherer, J.O., "Vertical Float Platforms", Ocean Industry, April 1969, pp. 52-54.

(1.8) Werk, K.J.C., "Floating Type Production Unit", Ocean Industry, December 1972, pp. 19-21.

REFERENCES (CHAPTER 2)

(2.1) Timoshenko, S., "Vibration Problems in Engineering", D. Vanostrand Co., Inc., New York, 1955.

(2.2) "Principles of Naval Architecture", SNAME, New York, 1967, pp. 614-619, pp. 628-634.

(2.3) Korvin-Kroukovsky, B.V., "A Ship in Regular and Irregular Seas", Proceedings of Symposium on the Behaviour of Ships in a Seaway, Sept., 1957, NSMB, Wageningen, pp. 59-75.

(2.4) "Sea-going Qualities of Ships", National Physical Laboratory, Oct., 1961, pp. 13-88.

(2.5) Saunders, H.E., "Hydrodynamics in Ship Design", Vol. 3, SNAME, New York, 1965, pp. 193-200, pp. 264-275.

(2.6) Vossers, Ir.G., "Fundamentals of the Behaviour of Ships in Waves", International Shipbuilding Progress, Nov., 1959, pp. 493-512.

(2.7) Denis, M.St., "On the Reduction of Motion Data from Model Tests in Confused Seas", Proceedings of Symposium on the Behaviour of Ships in a Seaway, Sept., 1957, NSMB, Wageningen, pp. 133-144.

(2.8) Denis, M.St. and Pierson Jr., W.J., "On the Motions of Ships in Confused Seas", Trans. SNAME, Vol. 61, 1953, pp. 280-357.

(2.9) Vugts, J.H., "The Role of Model Tests and their Correlation with Full Scale Observations", Symposium on Offshore Hydrodynamics, Aug., 1971, Wageningen.

(2.10) Crandall, S.H., "Random Vibrations", John Wiley & Sons, Inc., New York, 1958, pp. 77-90.

(2.11) Crandall, S.H. and Mark W.D., "Random Vibration in Mechanical Systems", Academic Press, New York, 1963, pp. 1-64.

REFERENCES (CHAPTER 3)

(3.1) Hooft, J.P. "Oscillatory Wave Forces on Small Bodies" International Shipbuilding Progress, May 1970, pp. 127-135.

(3.2) Korvin-Kroukovsky, B.V. and Jacobs, W.R. "Pitching and Heaving Motions of a Ship in Regular Waves" Trans. SNAME, Vol. 65, 1957, pp. 590-632.

(3.3) Golovato, P. "The Forces and Moments on a Heaving Surface Ship" Journal of Ship Research, April 1957, pp. 19-26.

(3.4) Tasai, F., et al. "A Study on the Motions of a Semi-Submersible Catamaran Hull in Regular Waves" Reports of Research Institute for Applied Mechanics, Kyushu University, Vol. 18, No. 60, 1970, pp. 9-32.

(3.5) Korvin-Kroukovsky, B.V. "Theory of Seakeeping" Published by SNAME, New York, 1961.

(3.6) Hooft, J.P. "Distribution of Wave Forces on Structural Parts of Ocean Structures" Offshore Hydrodynamics Symposium, Wageningen, August 1971.

(3.7) Fujii, H. and Takahashi, T. "Estimation of Hydrodynamical Forces Acting on a Marine Structure" Mitsubishi Technical Review, Vol. 7, No. 2, pp. 97-106.

(3.8) Motora, S. and Koyama, T. "On Wave Excitationless Ship Forms" Sixth Naval Hydrodynamics Symposium, Washington D.C., 1966, pp.(14-1) - (14-19).

(3.9) Wiegel, R.L. "Oceanographical Engineering" (Chapter 11), Prentice-Hall International, Inc., London, 1965.

(3.10) Newman, J.N. "The Exciting Forces on Fixed Bodies in Waves" Journal of Ship Research, December 1962.

REFERENCES (CHAPTER 4)

(4.1) Hooft, J.P. "A Mathematical Method of Determining Hydrodynamically Induced Forces on a Semi-Submersible", Trans. SNAME, Vol.79, 1971, pp 28-70.

(4.2) Hooft, J.P. "The Behaviour of a Five-Column Floating Drilling Unit in Waves", Report No. 156 S, Netherlands Ship Research Centre TNO, November 1971.

(4.3) Wipkink, J. "Design and Development of the Semi-Submersible Drilling Platform Norrig 5", Marcon N.V., The Hague, Holland.

(4.4) Sluys, M.F. and Gie, T.S. "Experimental and Theoretical Motion Correlation of a Pipe-laying Barge", Symposium on Offshore Hydrodynamics, August 1971, Wageningen, The Netherlands.

APPENDIX 1 Derivation of the Equation of the Heaving Motion

The motion of a semi-submersible platform in regular waves and the hydrodynamical forces acting on it can be estimated approximately by using the same method as for ship motions in waves. The motions with which the ship designer is primarily concerned are oscillatory in character, viz. roll, pitch and heave. In order to understand the ship motions easily, it is best to study the heaving motion of a buoy in waves. The equation of heaving motion derived for the buoy in waves can be used as a basis for the theory of ship motions.

Consider the case of a buoy floating freely in a train of regular harmonic (sinusoidal) waves which are long in relation to the buoy. Only vertical motion is considered, though the buoy also surges as the waves pass. The vertical displacement of the buoy from the calm-water position (z) and the surface elevation of the waves (ζ) are assumed to be small so that a linearized theory can be used.

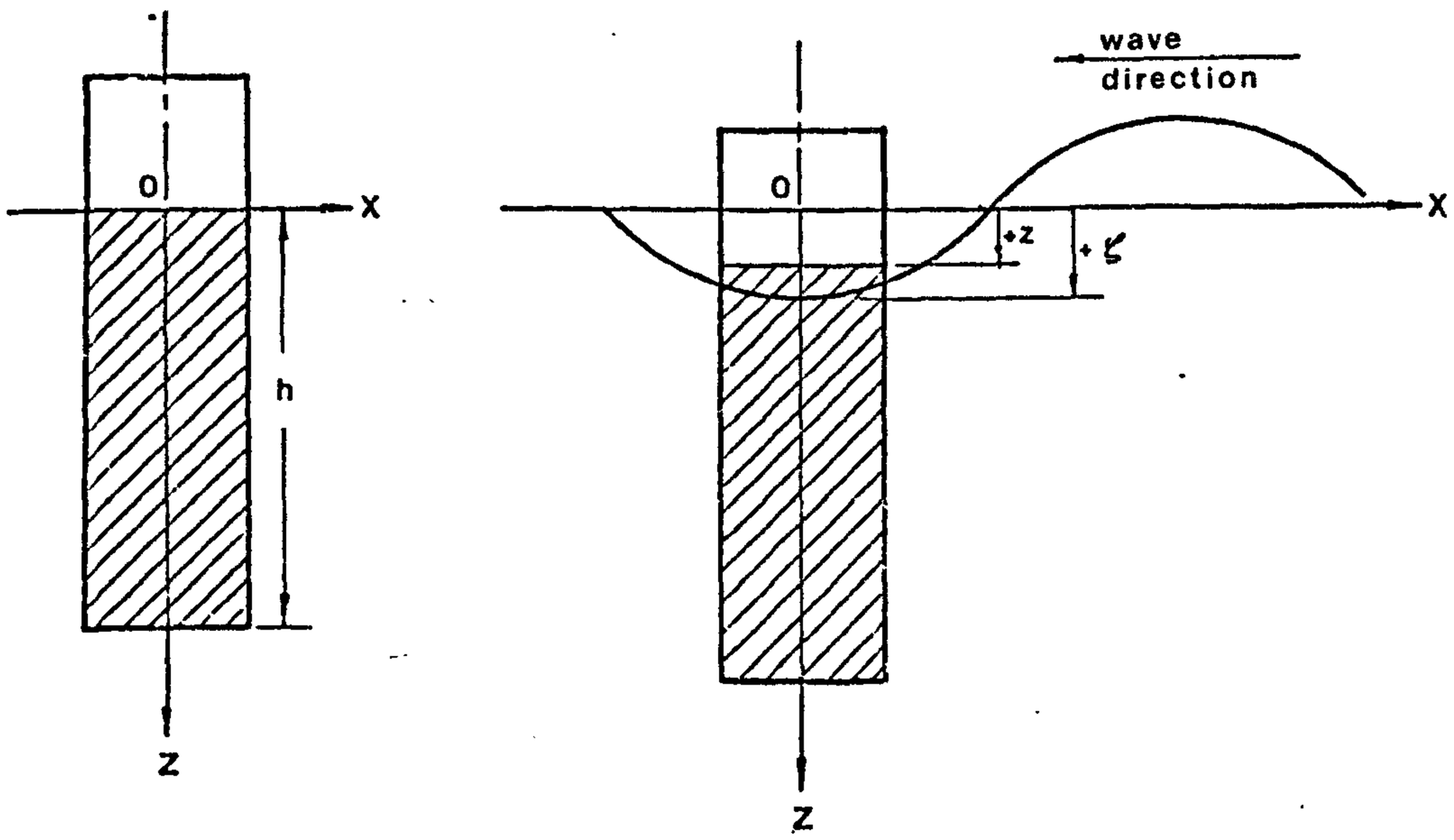

Fig. A1.1 Vertical Buoy Floating Freely in Waves.

The fundamental basis of the analytic approach is Newton's second law which is the source of the well-known relation $F = mf$, where m is the mass which is acted upon by force F and f is the linear acceleration imparted to it.

When the buoy displaced a distance (z) above or below its equilibrium position

$$F = m\ddot{z} \tag{A1.1}$$

where F is the summation of all vertical forces acting on the buoy, m is the mass of the buoy, and $\ddot{z} = d^2z/dt^2$ is the instantaneous vertical acceleration. The force F is divided into a hydrostatic and a hydrodynamic forces where the former depends only on the water level relative to the buoy and the latter depends on relative motion of the buoy and the fluid. Both act on the buoy through changes in the water pressures normal to the surface of the buoy.

When regular waves with surface elevation (ζ) above or below the calm-water level are present at the buoy, the vertical position of the buoy relative to the water surface is $(\zeta - z)$, with due regard to the signs of each (see Fig. A1.1).

In the linearized theory, the sum of all the hydrostatic and hydrodynamic forces acting on the buoy can be expressed by

$$F = \overbrace{A\,(\ddot{\zeta} - \ddot{z}) + B\,(\dot{\zeta} - \dot{z})}^{\text{Hydrodynamic}} + \overbrace{C\,(\zeta - z)}^{\text{Hydrostatic}} \tag{A1.2}$$

where the coefficients A, B and C are defined as the forces per unit relative acceleration, relative velocity and relative vertical displacement from the calm-water position, respectively. The terms $(\ddot{\zeta} - \ddot{z})$ and $(\dot{\zeta} - \dot{z})$ are relative values of acceleration and velocity, respectively, between the buoy and the wave surface. The coefficient A is also called the "added mass" or the "hydrodynamic mass" of the buoy.

If the waves are regular and of sinusoidal profile, and if the vertical motion of the buoy is assumed to be simple harmonic motion of the same period, then the relative motion terms $(\ddot{\zeta} - \ddot{z})$, $(\dot{\zeta} - \dot{z})$ and $(\zeta - z)$ are also simple harmonic, but they are not necessarily in phase.

The forces related to relative acceleration and velocity are 180 deg. and 90 deg. leading to the force related to the relative linear displacement, respectively. Therefore the forces do not attain their maximum values at the same time or in the same direction. In fact, they represent three different components of a single total force.

Substituting equation (A1.2) in equation (A1.1) and rearranging so that all unknown buoy-motion terms are on the left and all wave terms on the right, gives the differential equation of heaving motion.

$$(m + A)\,\ddot{z} + B\,\dot{z} + C\,z = A\,\ddot{\zeta} + B\,\dot{\zeta} + C\,\zeta \qquad (A1.3)$$

The left-hand side of the above equation represents the reaction forces due to the impressed vertical oscillatory motion of the buoy in calm-water while the right-hand side represents the exciting forces due to the oncoming waves when the buoy remains stationary in a vertical direction in its calm-water position.

Since all the terms on the right refer to the known wave profile and are harmonic functions with the same period, they can be replaced by the function $F_1 \cos \omega t + F_2 \sin \omega t$. When the wave profile is expressed by $\zeta = \zeta_a \cos \omega t$ where ζ_a is the wave amplitude, ω is the circular frequency of oncoming wave, equal to $2\pi/T_w$, (T_w = wave period). Taking the necessary derivatives the right-hand side of the equation (A1.3) becomes

$$A\,\ddot{\zeta} + B\,\dot{\zeta} + C\,\zeta = -A\,\omega^2\,\zeta_a \cos \omega t - B\,\omega\,\zeta_a \sin \omega t + C\,\zeta_a \cos \omega t$$

$$= \zeta_a \left[(C - A\,\omega^2) \cos \omega t - B\,\omega \sin \omega t \right]$$

Since the vertical exciting forces are acting on the bottom of the buoy, all the terms containing ζ_a must be multiplied by $e^{-\frac{\omega^2}{g}h}$ to take into account of the decrease in pressure exponentially with the distance from the still water level.

Hence,

$$F_1 = \zeta_a (C - A\,\omega^2)$$

$$F_2 = - \zeta_a (B\,\omega)$$

Alternatively, the exciting force can be represented by a single function

$$F = F_1 \cos \omega t + F_2 \sin \omega t = F_o \cos (\omega t + \sigma) \qquad (A1.4)$$

where $$F_o = \sqrt{F_1^2 + F_2^2} = \zeta_a \sqrt{(C - A\,\omega^2)^2 + (B\,\omega)^2} \qquad (A1.5)$$

$$\sigma = \tan^{-1} \left(- \frac{F_2}{F_1} \right) = \tan^{-1} \frac{B\,\omega}{C - A\,\omega^2} \qquad (A1.6)$$

where σ is the phase angle by which the force F leads the wave elevation

The equation of heaving motion of the buoy in waves is then,

$$(m + A)\,\ddot{z} + B\,\dot{z} + C\,z = F_o \cos (\omega t + \sigma) \qquad (A1.7)$$

where z = linear heaving displacement, measured from the calm-water position

$\dot{z}$ = dz/dt = heaving velocity of the buoy

$\ddot{z}$ = d^2z/dt^2 = heaving acceleration of the buoy

A = added mass of entrained water for heaving motion with a free surface

$(m + A)\,\ddot{z}$ = inertial or reactive force

$B\,\dot{z}$ = damping force

$C\,z$ = restoring force

F_o = amplitude of the wave exciting force, which is dependent on the wave frequency [see: equation (A1.5)]

The solution of the equation of heaving motion is a sum of two terms, one represents transient motion and the other represents forced oscillation of the buoy under the influence of a harmonic wave exciting force. After the transient motions have died out, the heaving motion of the buoy can be expressed in the form

$$z = z_a \cos(\omega t - \epsilon) \qquad \text{(A1.8)}$$

where z_a = amplitude of heaving motion

ϵ = phase angle by which the heaving motion lags the wave; when ϵ is negative the motion leads the wave.

The amplitude of heaving motion is given by

$$z_a = \frac{F_o}{\sqrt{\left\{C - (m + A)\omega^2\right\}^2 + (B\,\omega)^2}} \qquad \text{(A1.9)}$$

and the phase angle by which the heaving motion lags the force

$$\tau = \tan^{-1} \frac{B\,\omega}{C - (m + A)\omega^2} \qquad \text{(A1.10)}$$

We are only interested in the total phase lag angle ϵ between the motion and the wave, taking into account the positive phase angle σ of equation (A1.6). Hence, $\epsilon = (\tau - \sigma)$.

The coefficient C is a simple geometrical quantity and m is known. The coefficients A and B can be determined by experiment.

F_o can be computed readily because it depends on known wave elevation and the coefficients A, B and C as given by equation (A1.5). Then the value of the overall phase lag angle $\epsilon = \tau - \sigma$, between wave elevation and buoy motion, can be computed from equations (A1.6) and (A1.10). These vector quantities and phase angles are shown in Fig. A1.2.

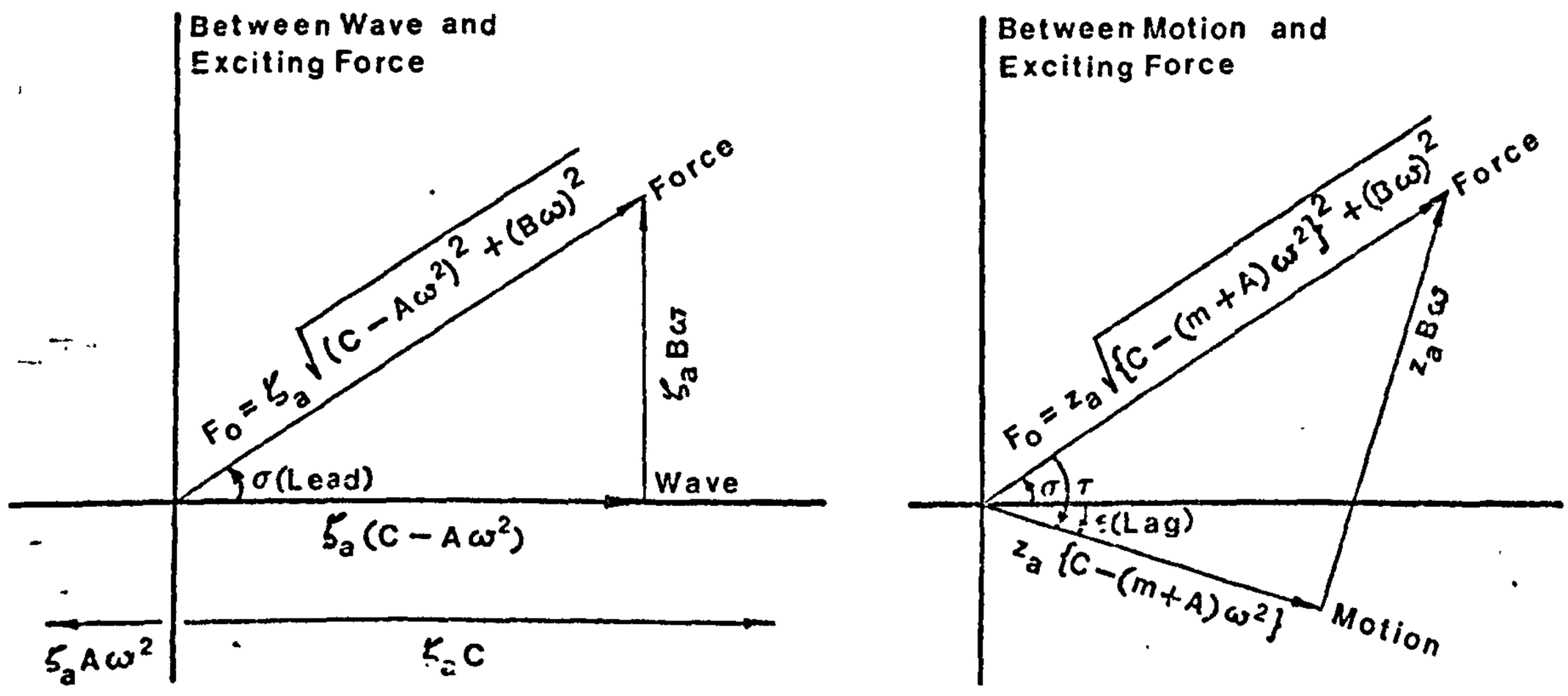

Fig. A1.2 Diagrammatic representation of vectors and phase angles for motion of a buoy in waves.

The amplitude of heaving motion given by equation (A1.9) can be rewritten as:

$$z_a = \frac{F_o/C}{\sqrt{\left\{1 - \left(\frac{\omega}{\omega_n}\right)^2\right\}^2 + \frac{B^2}{C\,(m + A)}\left(\frac{\omega}{\omega_n}\right)^2}}$$

where $\omega_n = \sqrt{\frac{C}{(m + A)}}$ = natural frequency of heaving of the buoy.

The factor F_o/C is the displacement of the buoy which the maximum

exciting force F_o would produce if acting statically and the factor

$$\frac{1}{\sqrt{\left\{1 - \left(\frac{\omega}{\omega_n}\right)^2\right\}^2 + \frac{B^2}{C\,(m + A)}\left(\frac{\omega}{\omega_n}\right)^2}}$$

takes care of the dynamical action of this force. The absolute value of this factor is usually called the magnification factor.

In mechanical system of forced vibration with viscous damping, the condition in which the damping being just sufficient to prevent vibration is known as critical damping (Ref. 2.1). Similar to the mechanical vibrating system, the critical damping of the buoy heaving in waves can be expressed as:

$$C_c = 2\,(m + A)\,\omega_n = 2\sqrt{C\,(m + A)}$$

and if the ratio between the actual value of damping to the critical value is denoted by γ, we obtain

$$\gamma = \frac{B}{C_c} = \frac{B}{2\sqrt{C\,(m + A)}}$$

Now, the magnification factor can be expressed in terms of ω, ω_n and γ, as follows:

$$\text{Magnification factor} = \frac{1}{\sqrt{\left(1 - \frac{\omega^2}{\omega_n^2}\right)^2 + (2\gamma)^2\,\frac{\omega^2}{\omega_n^2}}}$$

In most practical cases the value of γ is small. By taking $\gamma = 0$, we obtain the amplitude of heaving motion without damping.

When the values of the magnification factor for various values of γ are plotted against the values of (ω/ω_n), we obtain the graph as shown in Fig. A1.3.

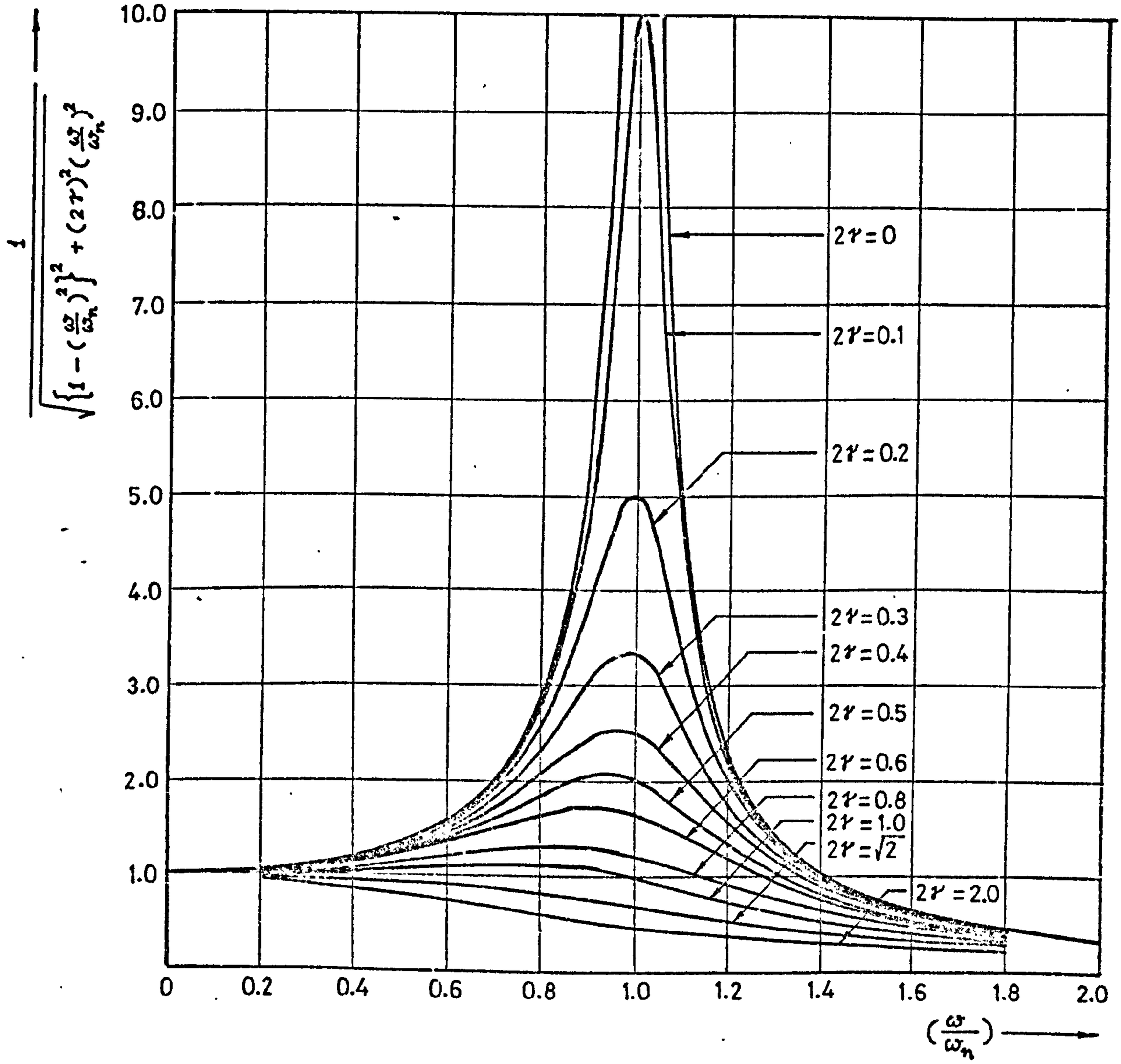

Fig. A1.3 Magnification factor for a second order linear system

From this figure, it can be seen that the magnification factor tends to unity when the frequency of wave exciting force is small and it has a very small value when the frequency of exciting force is large compared

to the natural frequency of heaving of the buoy. When the frequency of exciting force approaches the natural frequency of heaving of the buoy, the magnification factor increases rapidly and its value is very sensitive to changes in the magnitude of damping especially when this damping is small. The magnification factor reaches its maximum value at ω/ω_n values which are somewhat smaller than unity. By equating the derivative of the magnification factor with repect to ω/ω_n to zero, it can be shown that the maximum value of the magnification factor occurs when

$$\left(\frac{\omega}{\omega_n}\right)^2 = 1 - 2\gamma^2$$

Since γ is usually small, the values of frequency ω at which the amplitude of heaving motion becomes a maximum differ only very little from the natural frequency ω_n and it is usual practice to take $\omega = \omega_n$, in calculating maximum amplitudes.

The condition in which the frequency of exciting force equals the natural frequency of heaving of the buoy (i.e. $\omega = \omega_n$) is known as the state of resonance. At resonance the magnification factor will be inversely proportional to (2γ) and the amplitude of heaving motion will evidently become large and may cause overstrain in the material and consequently breakdown in the elastic member. Therefore, in the design of structures resonance must be avoided. So far we have dealt with the motion of the buoy in waves.

Now, the equation of heaving motion of a semi-submersible platform can be obtained by the same method which has been employed in the case of the buoy. When we substitute m_z, N_z and $(\rho g A_w)$ in place of A, B and C respectively, in equation (A1.7), we obtain the equation of heaving motion of a semi-submersible platform which is given by:

$$(m + m_z)\ddot{z} + N_z\dot{z} + (\rho g A_w)\, z = F_o \cos(\omega t + \sigma)$$

APPENDIX 2 Derivation of the beam-length ratio $(\frac{b}{\ell})$ as a function of the number of columns on each cylinder (n)

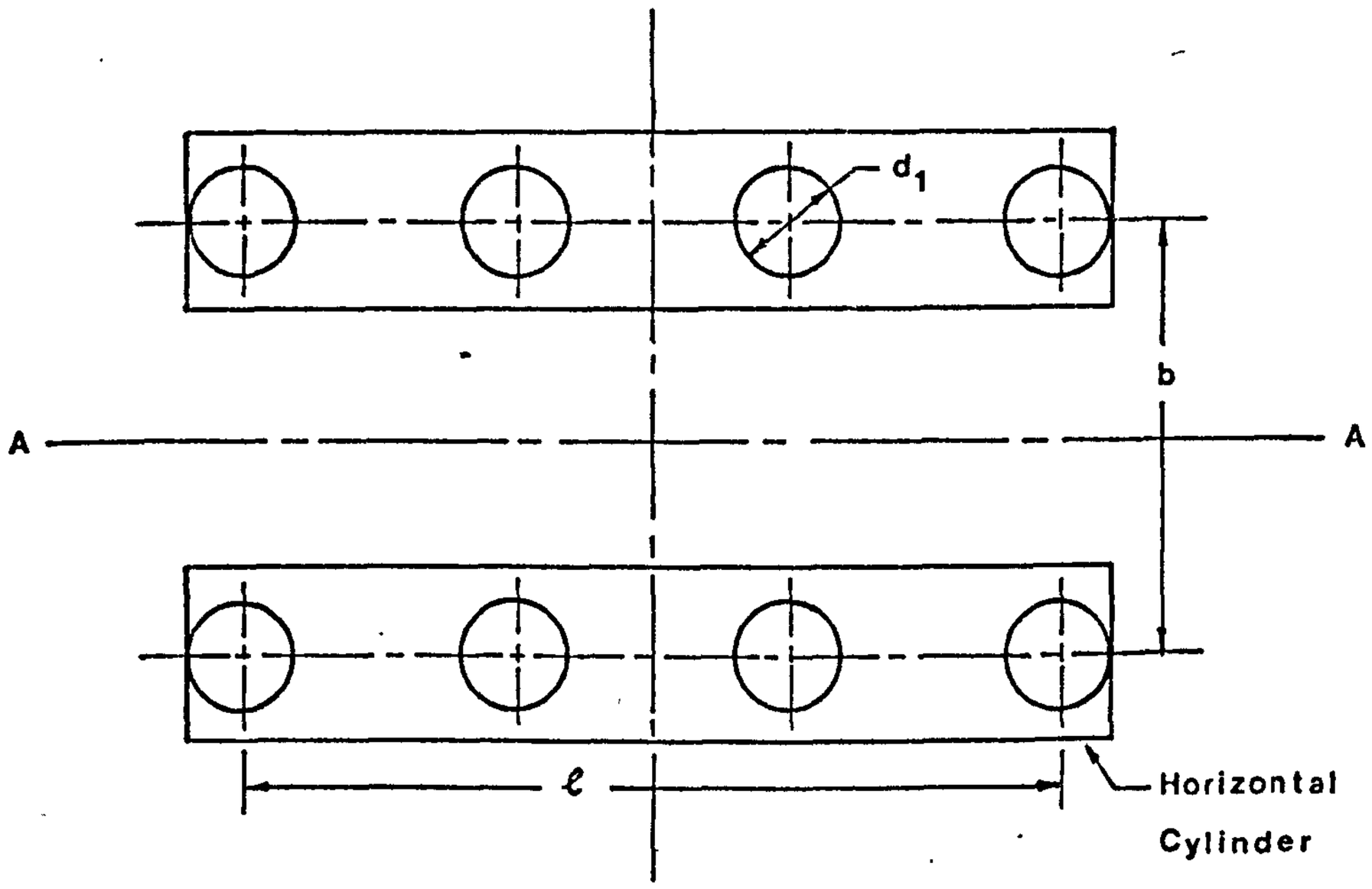

Let I_A = transverse moment of inertia

I_B = longitudinal moment of inertia

n = number of columns on one cylinder

d_1 = diameter of columns

For n = odd or even,

$$I_A = 2n \left\{ \frac{\pi d_1^4}{64} + \frac{\pi d_1^2}{4} \left(\frac{b}{2}\right)^2 \right\} \qquad (A2.1)$$

For n = odd,

$$I_B = 2n \left(\frac{\pi d_1^4}{64}\right) + 4 \left(\frac{\pi d_1^2}{4}\right) \sum_{i=1}^{(n-1)/2} \left\{ \frac{\ell}{(n-1)} \times i \right\}^2 \qquad (A2.2)$$

For n = even,

$$I_B = 2n\left(\frac{\pi d_1^4}{64}\right) + 4\left(\frac{\pi d_1^2}{4}\right)\sum_{i=1/2}^{(n-1)/2}\left\{\frac{\ell}{(n-1)}\ x\ i\right\}^2 \qquad (A2.3)$$

For n = odd, $\frac{b}{\ell}$ is obtained from equations (A2.1) and (A2.2) as follows:

$$2n\left(\frac{b}{2}\right)^2 = 4\frac{\ell^2}{(n-1)^2}\left\{1^2 + 2^2 + 3^2 + - - - + \left(\frac{n-1}{2}\right)^2\right\}$$

$$= \frac{n(n+1)\ell^2}{6(n-1)}$$

$$\frac{b}{\ell} = \sqrt{\frac{(n+1)}{3(n-1)}} \qquad (A2.4)$$

For n = even, $\frac{b}{\ell}$ is obtained from equations (A2.1) and (A2.3) as follows:

$$2n\left(\frac{b}{2}\right)^2 = 4\frac{\ell^2}{(n-1)^2}\left\{\left(\frac{1}{2}\right)^2 + \left(\frac{1}{3}\right)^2 + \left(\frac{1}{5}\right)^2 + - - - + \left(\frac{n-1}{2}\right)^2\right\}$$

$$= \frac{n(n+1)\ell^2}{6(n-1)}$$

$$\frac{b}{\ell} = \sqrt{\frac{(n+1)}{3(n-1)}} \qquad (A2.5)$$

which is the same as equation (A2.4)

APPENDIX 3 To prove that the moment of inertia of waterplane area about any axis is the same for a multi-leg platform

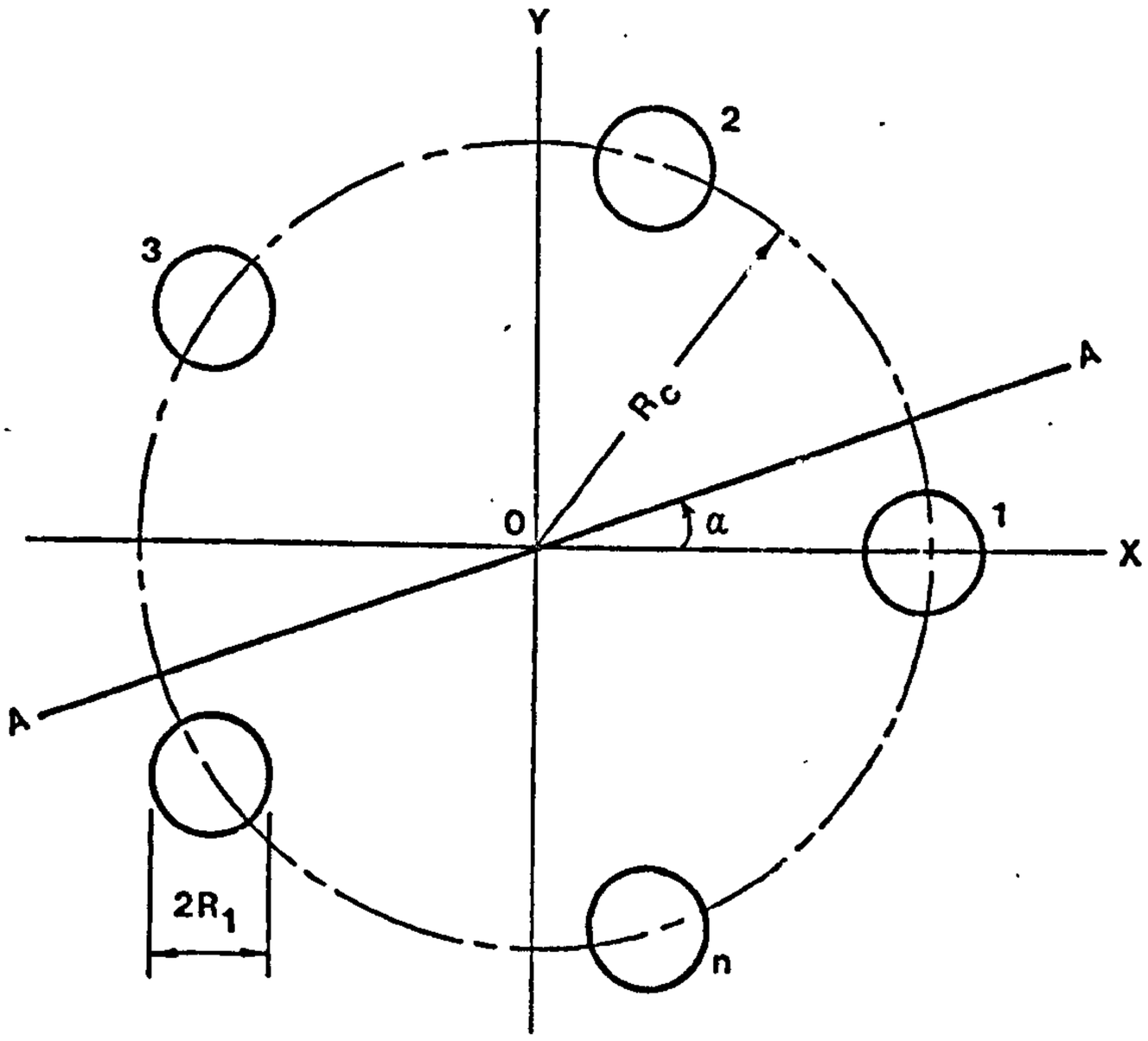

Fig. A3.1

Consider a multi-leg platform with n number of vertical columns equally spaced round a circle of radius R_c as shown in Fig. A3.1. The minimum number of columns should be three.

The moment of inertia of waterplane area about any axis AA which is inclined to the X-axis by angle α is given by:

$$I_{AA} = \frac{\pi R_1^4}{4} n + \pi R_1^2 \sum_{j=0}^{n-1} h_j^2 \qquad (A3.1)$$

in which,

$$\sum_{j=0}^{n-1} h_j^2 = R_c^2 \left[\frac{1}{2} n - \frac{1}{2} \cos 2\alpha \sum_{j=0}^{n-1} \cos \frac{4\pi}{n} j + \sin 2\alpha \sum_{j=0}^{n-1} \sin \frac{4\pi}{n} j \right] \qquad (A3.2)$$

Since,

$$\sum_{j=0}^{n-1} \cos \frac{4\pi}{n} j = 0 \quad \text{for} \quad n \geqslant 3$$

and $$\sum_{j=0}^{n-1} \sin \frac{4\pi}{n} j = 0 \quad \text{for} \quad n \geqslant 1,$$

the equation (A3.2) becomes:

$$\sum_{j=0}^{n-1} h_j^2 = R_c^2 \left(\frac{1}{2} n \right) \tag{A3.3}$$

Substituting equation (A3.3) in equation (A3.1), we obtain

$$I_{AA} = \frac{\pi R_1^4}{4} n + \pi R_1^2 R_c \left(\frac{1}{2} n \right) \tag{A3.4}$$

The equation (A3.4) is independent of the angle α and hence the moment of inertia of waterplane area is the same about any axis.

APPENDIX 4 The added virtual mass (A.V.M.) of the caisson and of the vertical column

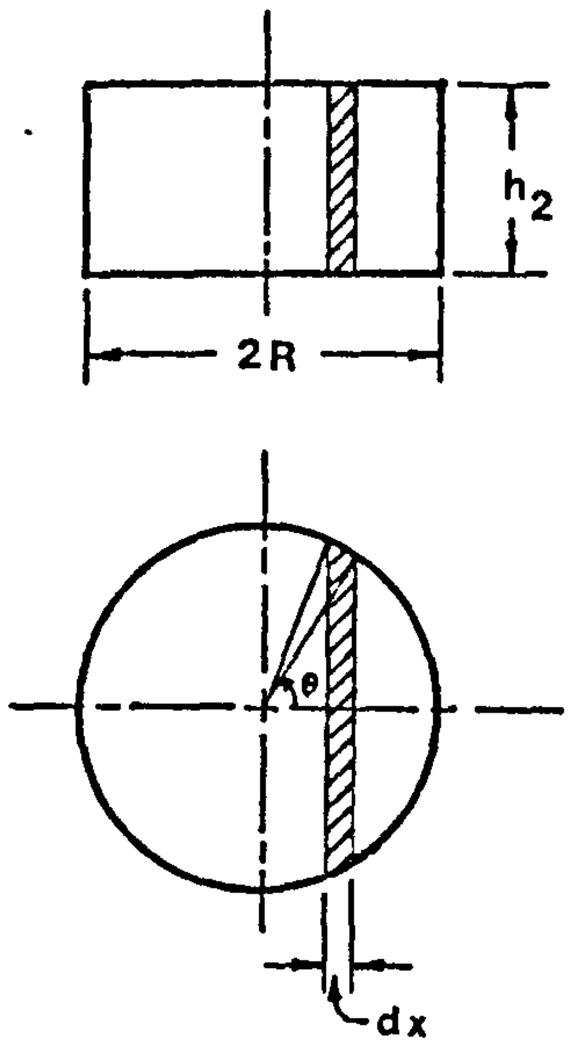

Fig. A4.1 Circular Caisson

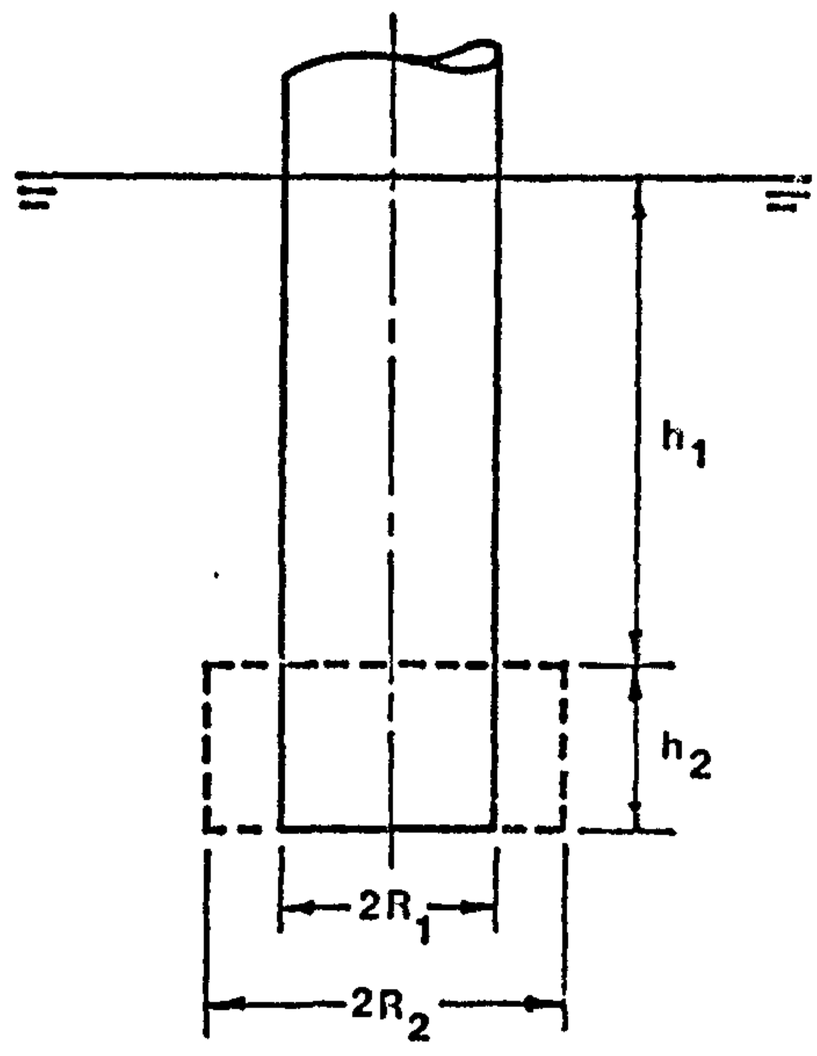

Fig. A4.2 Vertical Column

Consider a submerged circular caisson of radius R and height h_2 as shown in Fig. A4.1. The A.V.M. of the caisson is estimated as the sum of the A.V.M. of the small strips of width $(2R)\sin\theta$ and length dx along the direction of the wave. For each strip a value of C_V (i.e. added mass coefficient) could be found from data for rectangular sections with aspect ratio $(2R)\sin\theta/h_2$.

By integrating the values of A.V.M. of each strip across the diameter an expression for the total A.V.M. could be obtained. Since the analytical expression for C_V in terms of aspect ratio is relatively complicated it is proposed to use a mean aspect ratio of $\frac{\pi R/2}{h_2}$ and include a correction factor J to take account of the three-dimensional effect, i.e.

A.V.M. of the strip of width $(2R)\sin\theta$ and length dx (for one face only) $= \frac{1}{2}\rho\pi(\frac{1}{2} \times 2R \times \sin\theta)^2 (dx)\ J\ C_V$

$$= \frac{1}{2}\rho\pi J\ C_V(R \times \sin\theta)^3 (d\theta) \qquad (A4.1)$$

since $(dx) = R\,(d\theta)\sin\theta$.

Therefore, for a circular caisson of radius R the total A.V.M.

(for both faces) $= 2 \times \frac{1}{2}\rho\pi J\ C_V R^3 \int_0^{\pi} \sin^3\theta\, d\theta$

$$= \frac{4}{3}\rho\pi R^3\ J\ C_V \qquad (A4.2)$$

For a thin disc, i.e. when $h_2 \longrightarrow 0$, C_V will tend to 1.0, then

$\frac{4}{3}\rho\pi R^3 J = \frac{8}{3}\rho R^3$ (which is the exact value of the added mass coefficient for a thin disc of radius R)

$$J = \frac{8}{3} \times \frac{3}{4} = 0.635 \qquad (A4.3)$$

This value of J will be assumed throughout the work.

From equation (A4.2), A.V.M. for the caisson of radius R_2 and height h_2 is given by:

$$\text{A.V.M.} = \frac{4}{3}\rho\pi R_2^3\ J\ C_{V1} \qquad (A4.4)$$

where C_{V1} is the added mass coefficient for a mean aspect ratio of $\frac{\pi R_2/2}{h_2}$.

In the same way, A.V.M. for the caisson of radius R_1 and height h_2 is given by:

$$\text{A.V.M.} = \frac{4}{3}\rho\pi R_1^3\ J\ C_{V2} \qquad (A4.5)$$

where C_{V2} is the added mass coefficient for a mean aspect ratio of $\frac{\pi R_1/2}{h_2}$.

Again from equation (A4.2), A.V.M. for the vertical columns (see Fig. A4.2) of radius R_1 and submerged height (h_1+h_2) is given by:

$$\text{A.V.M. (for the bottom face only)} = \frac{1}{2} \times \frac{4}{3} \rho\pi R_1^3 J\, C_{V3} \qquad \text{(A4.6)}$$

where C_{V3} is the added mass coefficient for a mean aspect ratio of $\frac{\pi R_1/2}{2(h_1+h_2)}$.

From the equations (A4.4), (A4.5) and (A4.6), A.V.M. for a combination of the vertical column of radius R_1 and the caisson of radius R_2 with a hole of radius R_1 in the middle can be expressed as:

$$\text{A.V.M.} = \frac{4}{3} \rho\pi J(C_{V1}\, R_2^3 - C_{V2}\, R_1^3) + \frac{2}{3} \rho\pi J C_{V3}\, R_1^3 \qquad \text{(A4.7)}$$

APPENDIX 5 Calculation of the heaving motion of the Staflo platform in regular waves

The same coordinate systems described in the sections 3.3.2 and 3.3.3 were used for the Staflo platform in the beam-sea and head-sea conditions respectively.

The following full scale data were used in the calculations:

ρ = 104.5 kg. sec^2/m^4

g = 9.81 m/sec^2

∇ = 12,700 m^3

d_1 = diameter of the 14 vertical columns = 4.05 m

d_1'' = diameter of the 4 corner columns = 7.05 m

d_2 = diameter of the 4 horizontal cylinders = 6.03 m

d_2' = diameter of the 2 transverse horizontal tubes = 1.68 m

= diameter of the 2 diagonal horizontal tubes = 1.68 m

= diameter of the 2 vertical structural tubes = 1.68 m

h_1 = submerged height of the vertical columns = 11.97 m

h_1' = depth of submergence of the transverse and diagonal horizontal tubes = 8.02 m

b = centre distance between 2 inner cylinders = 25.91 m

b' = centre distance between 2 outer cylinders = 53.34 m

ℓ_2 = overall length of the 2 inner cylinders = 70.04 m

ℓ_2' = overall length of the 2 outer cylinders = 71.06 m

n = number of columns of diameter d_1 on one of the inner cylinders = 4

n' = number of columns of diameter d_1 on one of the outer cylinders = 3

n'' = number of columns of diameter d_1'' on one of the outer cylinders = 2

$$b_o = b' - d_1 = 49.29 \text{ m}$$

$$b_1 = b + d_1 = 29.96 \text{ m}$$

$$b_2 = b - d_1 = 21.86 \text{ m}$$

$$b_o' = \sqrt{(\ell_2' - d_1'')^2 + (b')^2} - d_1'' = 76.25 \text{ m}$$

$$b_1' = \sqrt{\left(\frac{\ell_2' - d_1''}{2}\right)^2 + b^2} + d_1 = 45.26 \text{ m}$$

$$b_2' = b_1' - 2\, d_1 = 37.16 \text{ m}$$

$$\theta = \tan^{-1}\left(\frac{\ell_2' - d_1''}{b'}\right) = 50.183 \text{ deg.}$$

The waterplane area of the platform is given by:-

$$A_w = \frac{\pi}{2}\left[d_1^2\,(n + n') + (d_1'')^2\, n'' + (d_2')^2\right] = 341 \text{ m}^3$$

The volume of the added mass of the horizontal cylinders and tubes is given by:-

$$\nabla_z = \frac{\pi}{2}\left[d_2^2\,(\ell_2 + \ell_2') + (d_2')^2\left\{(b' - 3\, d_1) + (b_o' - 2\, d_1)\right\}\right]$$

$$= 8{,}560 \text{ m}^3$$

The natural heaving frequency is given by:-

$$\omega_n = \sqrt{\frac{\rho g A_w}{m + m_z}} = \sqrt{\frac{g A_w}{\nabla + \nabla_z}} = 0.396 \text{ radian/sec}$$

$$T_z = \frac{2\pi}{\omega_n} = 15.9 \text{ sec}$$

(i) Calculation of the heaving motion in beam-sea condition

The vertical wave excited force F_Z on the platform is obtained as the sum of the forces on the four parallel horizontal cylinders, on the two transverse horizontal tubes and on the two diagonal horizontal tubes.

The vertical force on the four horizontal cylinders is given by:-

$$(F_Z)_{cyl.} = \rho g \zeta_a \frac{e^{-Kh_1}}{h_1} \left[V_1 \left(1 - e^{-K\frac{d_2}{2}} Kh_1 2a \right) \cos K\frac{b}{2} + \right.$$

$$+ V_1' \left(1 - e^{-K\frac{d_2}{2}} Kh_1 2a'\right) \cos K\frac{b'}{2} +$$

$$\left. + V_1'' \cos K\frac{b'}{2} \right] \cos \omega t \qquad \text{(A5.1)}$$

where $K = \frac{2\pi}{\lambda} = \frac{\omega^2}{g}$

$V_1 = \frac{\pi}{4} d_1^2 h_1 2n = 1{,}235 \text{ m}^3$

$V_1' = \frac{\pi}{4} d_1^2 h_1 2n' = 926 \text{ m}^3$

$V_1'' = \frac{\pi}{4} (d_1'')^2 h_1 2n'' = 1{,}710 \text{ m}^3$

$V_2 = 2 (\frac{\pi}{4} d_2^2 \ell_2) = 4{,}000 \text{ m}^3$

$V_2' = 2 (\frac{\pi}{4} d_2^2 \ell_2') = 4{,}060 \text{ m}^3$

$\alpha = \frac{V_2}{V_1} = 3.24$

$$\alpha' = \frac{V_2'}{V_1'} = 4.38$$

The vertical force on the two transverse horizontal tubes is given by:-

$$(F_Z)_{trans.} = -8\rho g\, \zeta_a \frac{\pi}{4} (d_2')^2\, e^{-K(h_1' + \frac{d_2'}{2})} \left(\sin K\frac{b_o}{2} - \sin K\frac{b_1}{2} + \sin K\frac{b_2}{2}\right) \cos \omega t \qquad (A5.2)$$

The vertical force on the two diagonal horizontal tubes is given by:-

$$(F_Z)_{diag.} = -8\rho g\, \zeta_a \frac{\pi}{4} (d_2')^2\, e^{-K(h_1' + \frac{d_2'}{2})} \left\{\sin\left(K\frac{b_o'}{2}\cos\theta\right) - \sin\left(K\frac{b_1'}{2}\cos\theta\right) + \sin\left(K\frac{b_2'}{2}\cos\theta\right)\right\} \cos \omega t \qquad (A5.3)$$

From the equations (A5.1), (A5.2) and (A5.3), the total vertical force on the platform can be written as follows:-

$$F_Z = F_o \cos \omega t \qquad (A5.4)$$

where

$$F_o = \rho g\, \zeta_a \left[\frac{e^{-Kh_1}}{h_1}\left\{V_1\left(1 - e^{-K\frac{d_2}{2}} Kh_1 2\alpha\right)\cos K\frac{b}{2} + V_1'\left(1 - e^{-K\frac{d_2}{2}} Kh_1 2\alpha'\right)\cos K\frac{b'}{2} + V_1'' \cos K\frac{b'}{2}\right\} - 2\pi(d_2')^2\, e^{-K(h_1' + \frac{d_2'}{2})}\left\{\sin K\frac{b_o}{2} - \sin K\frac{b_1}{2} + \sin K\frac{b_2}{2} + \sin\left(K\frac{b_o'}{2}\cos\theta\right) - \sin\left(K\frac{b_1'}{2}\cos\theta\right) + \sin\left(K\frac{b_2'}{2}\cos\theta\right)\right\}\right] \qquad (A5.5)$$

The vertical force versus wave frequency shown in Fig. 4.2 is obtained from the equation (A5.5).

Neglecting the damping term, the ratio of heave amplitude to wave amplitude can be obtained from the equation (2.5) as follows:-

$$\frac{z_a}{\zeta_a} = \frac{F_o/\rho g A_w}{\zeta_a \left(1 - \frac{\omega^2}{\omega_n^2}\right)} \qquad (A5.6)$$

The heaving motion versus wave frequency shown in Fig. 4.4 is obtained from the equations (A5.5) and (A5.6).

(ii) Calculation of the heaving motion in head-sea condition

The vertical wave excited force on the four horizontal cylinders is given by:-

$$(F_Z)_{cyl.} = \rho g \zeta_a \frac{e^{-Kh_1}}{h_1} \left[V_1 \left(\frac{Q_o}{n} - e^{-K\frac{d_2}{2}} 4a \frac{h_1}{\ell_2} \sin K\frac{\ell_2}{2} \right) + \right.$$

$$+ V_1' \left(\frac{Q_o'}{n'} - e^{-K\frac{d_2}{2}} 4a' \frac{h_1}{\ell_2} \sin K\frac{\ell_2}{2} \right) +$$

$$\left. + V_1'' \frac{Q_o''}{n''} \right] \cos \omega t \qquad (A5.7)$$

where $Q_o = 2 \left\{ \cos K\frac{(\ell_2 - d_2)}{2} + \cos K\frac{(\ell_2 - d_2)}{4} \right\}$

$$Q_o' = 1 + 2 \cos K\frac{(\ell_2 - d_2)}{4}$$

$$Q_o'' = 2 \cos K\frac{(\ell_2 - d_2)}{2}$$

The vertical force on the two transverse horizontal tubes is given by:-

$$(F_Z)_{trans.} = 4\rho g \zeta_a \frac{\pi}{4} (d_2')^2 e^{-K(h_1' + \frac{d_2'}{2})} K (b' - 3d_1)$$

$$\cos K\frac{(\ell_2 - d_2)}{4} \cos \omega t \qquad (A5.8)$$

The vertical force on the two diagonal horizontal tubes is given by:-

$$(F_Z)_{diag.} = -8\rho g\, \zeta_a \frac{\pi}{4} (d_2')^2\, e^{-K(h_1' + \frac{d_2'}{2})} \left[\sin\left(K \frac{b_o'}{2} \sin\theta\right) - \right.$$

$$\left. - \sin\left(K \frac{b_1'}{2} \sin\theta\right) + \sin\left(K \frac{b_2'}{2} \sin\theta\right)\right] \cos\omega t \qquad (A5.9)$$

The total vertical wave excited force F_Z on the platform in the head-sea condition is obtained by adding the equations (A5.7), (A5.8) and (A5.9) and is expressed as follows:-

$$F_Z = F_o \cos\omega t \qquad (A5.10)$$

where $F_o = \rho g\, \zeta_a \left[\frac{e^{-Kh_1}}{h_1} \left\{V_1\left(\frac{Q_o}{n} - e^{-K\frac{d_2}{2}} 4\alpha \frac{h_1}{\ell_2} \sin K\frac{\ell_2}{2}\right) + \right.\right.$

$$\left. + V_1' \left(\frac{Q_o'}{n'} - e^{-K\frac{d_2}{2}} 4\alpha' \frac{h_1}{\ell_2} \sin K\frac{\ell_2}{2}\right) + V_1'' \frac{Q_o''}{n''}\right\} -$$

$$- \pi(d_2')^2\, e^{-K(h_1' + \frac{d_2'}{2})} \left\{K(b' - 3d_1)\cos K\frac{(\ell_2 - d_2)}{4} + \right.$$

$$\left.\left. + 2\left(\sin\left(K\frac{b_o'}{2}\sin\theta\right) - \sin\left(K\frac{b_1'}{2}\sin\theta\right) + \sin\left(K\frac{b_2'}{2}\sin\theta\right)\right)\right\}\right] \qquad (A5.11)$$

The vertical force versus wave frequency shown in Fig. 4.3 is obtained from the equation (A5.11).

The heaving motion versus wave frequency shown in Fig. 4.5 is obtained from the equations (A5.6) and (A5.11).

APPENDIX 6 Calculation of the heaving motion of the Norrig-5 platform in regular waves

The same coordinate system described in the section 3.4.2 was used for the Norrig-5 platform.

The following full scale data were used in the calculations:-

n = number of legs = 5

ρ = 104.5 kg. sec^2/m^4

g = 9.81 m/sec^2

∇ = 21,039 m^3

R_1 = radius of the vertical columns = 5.1 m

R_2 = radius of the caissons = 9.5 m

R_c = radius of the circle through the centres of the columns = 38 m

h_1 = submerged height of the columns = 21.3 m

h_2 = height of the caisson = 8.7 m

C_{V1} = 1.38

C_{V2} = 1.53

C_{V3} = 2.13

J = 0.635

A_W = waterplane area = $\pi R_1^2 n$ = 408.62 m^2

The added mass of the platform is given by:- (see equation A4.7).

$$m_z = \frac{2}{3} \rho \pi J R_1^3 \left\{ 2 \left(\frac{R_2^3}{R_1^3} C_{V1} - C_{V2} \right) + C_{V3} \right\} n$$

$$= 155.44 \times 10^4 \text{ kg. } sec^2/m$$

The mass of the platform is given by:-

$$m = \rho \nabla = 219.82 \times 10^4 \text{ kg. sec}^2/\text{m}$$

The natural heaving frequency is:-

$$\omega_n = \sqrt{\frac{\rho g A_w}{m + m_z}} = 0.33 \text{ radian/sec}$$

$$T_z = \frac{2\pi}{\omega_n} = 18.81 \text{ sec}$$

The velocity potential of waves in water of any depth can be written as:-

$$\phi = \frac{g \zeta_a}{\omega} \frac{\cosh K (d-\zeta)}{\cosh Kd} \sin (K\xi + \omega t) \qquad (A6.1)$$

where d is the depth of water.

The pressure acting at any point in water is given by:-

$$p = -\rho \frac{\partial \phi}{\partial t} = -\rho g \zeta_a \frac{\cosh K (d - \zeta)}{\cosh Kd} \cos (K\xi + \omega t) \qquad (A6.2)$$

The vertical components of wave orbital velocity and acceleration of the water particles in waves are given by:-

$$\dot{\zeta}_w = -\omega \zeta_a \frac{\sinh K (d - \zeta)}{\sinh Kd} \sin (K\xi + \omega t) \qquad (A6.3)$$

$$\ddot{\zeta}_w = -\omega^2 \zeta_a \frac{\sinh K (d - \zeta)}{\sinh Kd} \cos (K\xi + \omega t) \qquad (A6.4)$$

where

$$\omega^2 = gK \tanh Kd \qquad (A6.5)$$

From the equation (A6.2), the vertical pressure force acting on the platform can be written as follows:-

$$F_{Z1} = 2\rho g\, \zeta_a\, \pi R_1^2 \left[\frac{J_1(KR_1)}{(KR_1)} \left\{ \frac{\cosh K\,(d-h_1)}{\cosh Kd} \right\} \right.$$

$$\left. - \left(\frac{R_2}{R_1}\right)^2 \frac{J_1\,(KR_2)}{(KR_2)} \left\{ \frac{\cosh K\,(d-h_1)}{\cosh Kd} - \frac{\cosh K\,(d-h_1-h_2)}{\cosh Kd} \right\} \right] x$$

$$x \sum_{i=0}^{n-1} \cos\,(K\ \xi_i + \omega t) \qquad \text{(A6.6)}$$

where ξ_i is given by equation (3.60). Since R_1 and R_2 are small compared to the wave length,

$$J_1\,(KR_1) \approx \tfrac{1}{2}\,(KR_1)$$

$$J_2\,(KR_2) \approx \tfrac{1}{2}\,(KR_2)$$

and when the above values are substituted in equation (A6.6), we obtain

$$F_{Z1} = \rho g\, \zeta_a\, \pi R_1^2 \left[\frac{\cosh K\,(d-h_1)}{\cosh Kd} - \left(\frac{R_2}{R_1}\right)^2 \left\{ \frac{\cosh K\,(d-h_1)}{\cosh Kd} - \right.\right.$$

$$\left.\left. - \frac{\cosh K\,(d-h_1-h_2)}{\cosh Kd} \right\} \right] \sum_{i=0}^{n-1} \cos\,(K\ \xi_i + \omega t) \qquad \text{(A6.7)}$$

From equation (A6.4), the vertical inertia force acting on the platform can be written as:-

$$F_{Z2} = -\rho g\, \zeta_a\, \pi R_1^2\, (\tfrac{2}{3}\, JKR_1\, \tanh Kd) \left[\left\{ \frac{\sinh K\,(d-h_1-h_2)}{\sinh Kd} + \right.\right.$$

$$\left.\left. + \frac{\sinh K\,(d-h_1)}{\sinh Kd} \right\} \left(\frac{R_2^3}{R_1^3}\, C_{V1}\, I_F - C_{V2}\, I_F\right) + \right.$$

$$\left. + \frac{\sinh K\,(d-h_1-h_2)}{\sinh Kd}\, C_{V3}\, I_C \right] \sum_{i=0}^{n-1} \cos\,(K\ \xi_i + \omega t) \qquad \text{(A6.8)}$$

Since R_1 and R_2 are small compared to the wave length, both I_C and I_F tend to unity and equation (A6.8) becomes:-

$$F_{Z2} = -\rho g \zeta_a \pi R_1^2 \left(\frac{2}{3} JKR_1 \tanh Kd\right) \left[\left\{\frac{\sinh K (d-h_1-h_2)}{\sinh Kd} + \frac{\sinh K (d-h_1)}{\sinh Kd}\right\} \left(\frac{R_2^3}{R_1^3} C_{V1} - C_{V2}\right) + \frac{\sinh K (d-h_1-h_2)}{\sinh Kd} C_{V3}\right] \sum_{i=0}^{n-1} \cos (K \xi_i + \omega t) \quad (A6.9)$$

From equations (A6.7) and (A6.9), the total vertical force F_Z acting on the platform can be expressed as follows:-

$$F_Z = F_o' \sum_{i=0}^{n-1} \cos (K \xi_i + \omega t) \quad (A6.10)$$

where

$$F_o' = \rho g \zeta_a \pi R_1^2 \left[\frac{\cosh K (d-h_1)}{\cosh Kd} - \left(\frac{R_2}{R_1}\right)^2 \left\{\frac{\cosh K (d-h_1)}{\cosh Kd} - \frac{\cosh K (d-h_1-h_2)}{\cosh Kd}\right\} - \left(\frac{2}{3} JKR_1 \tanh Kd\right) \left\{\left(\frac{\sinh K (d-h_1-h_2)}{\sinh Kd} + \frac{\sinh K (d-h_1)}{\sinh Kd}\right) \left(\frac{R_2^3}{R_1^3} C_{V1} - C_{V2}\right) + \frac{\sinh K (d-h_1-h_2)}{\sinh Kd} C_{V3}\right\}\right] \quad (A6.11)$$

The equation (A6.10) can be rewritten in the form:-

$$F_Z = F_o \cos (\omega t + \sigma) \quad (A6.12)$$

where

$$F_o = |F'_o| \sqrt{Q_c^2 + Q_s^2} \qquad \text{(A6.13)}$$

$$Q_c = \sum_{i=0}^{n-1} \cos K \xi_i \qquad \text{(A6.14)}$$

$$Q_s = \sum_{i=0}^{n-1} \sin K \xi_i \qquad \text{(A6.15)}$$

$$\sigma = \tan^{-1} \frac{Q_s}{Q_c} \qquad \text{(A6.16)}$$

From equation (A6.13), the vertical force versus wave frequency graphs shown in Figs. 4.7 and 4.8 are obtained.

The heaving motion versus wave frequency shown in Figs. 4.9 and 4.10 are obtained from the equations (A5.6) and (A6.13).